Technical Session No. 2

Biomechanics and Dummy Development

Mr. Dominque Cesari, Chairman, France

The European Communities' Programme for Promotion of Biomechanic Research

HERBERT HENSSLER
Commission of the European Communities—Brussels

THE SETTING-UP OF THE PROGRAMME

At the end of 1975 the Commission organized an international Symposium in Brussels in order to discuss the future trends in automobile regulations with all interested parties. As far as occupant safety was concerned, the need for a new generation of performance-oriented requirements was clearly defined.

Consequently, the Commission investigated the availability in Europe of the three major elements of any safety regulation: a test procedure, appropriate test tools and protection criteria based as far as possible on objective scientific data. The question of test procedures was already under discussion in the Group of automobile experts (WP 29) at the United Nations' Economic Commission for Europe (ECE) in Geneva. The interest of the EEC therefore focussed on the two other elements: the test tools, which meant essentially the availability of a test dummy, and the knowledge concerning human tolerance of accidental constraints.

The Commission did not, of course, possess the necessary expertise among its staff to deal with such specific matters. Hence, it seemed advisable to take advantage of its good relations with the European Experimental Vehicle Committee (EEVC), the European partner organisation of the United States in the Experimental Safety Vehicle Programme (ESV). A working group of this Committee had drawn the attention of the Sixth ESV-Conference, held in Washington in 1976, to the existence of considerable gaps in the knowledge of impact biomechanics and of the deficiencies of existing test dummies in side impact and car/pedestrian accident modes.

OVERALL OBJECTIVES AND FINANCING

In 1978, the first year in which a budget was made available on this subject, the Commission succeeded, with the efficient help of EEVC and its working group on biomechanics, to establish a coherent programme for the promotion of studies, investigations and experiments in the field of biomechanics.

The programme comprised the following six priority research themes:

Theme 1: Human tolerance and injury criteria concerning vehicle occupants in frontal impact;
Theme 2: Human tolerance and injury criteria concerning vehicle occupants in side impact;
Theme 3: Pedestrian injury mechanisms in impact by vehicle front structures;
Theme 4: Development of a standard dummy for side impact testing;
Theme 5: Mathematical models of impact and injury prediction;
Theme 6: Occupant behaviour and interaction during vehicle impacts.

It is important to mention that the intention of the Commission was not to set up its own spectacular research programme. The objective was to promote and accelerate, by means of decisive financial contributions, ongoing or projected research which was required to complete the necessary knowledge for future safety regulations.

It was also understood from the beginning that the programme should be limited in time in order to keep it manageable and to allow a rapid assessment of its success. Mainly for budgetary reasons, it was initially agreed to run the programme in three phases, starting with the 1978 budget year. Later it appeared necessary to add a fourth phase in order to allow the synthesis of the results of the different projects and comparative testing of the side impact dummy prototypes.

A total amount of 3.16 million of European account units (ECU) (1 ECU equals about 0.95 present US dollars) was made available by the budgetary authorities of the European Communities, divided over the budgetary years 1978 to 1981 and used as follows:

1978: 750,000 ECU; 13 projects covering themes 1 to 4
1979: 750,000 ECU; 19 projects covering themes 1 to 6
1980: 1,000,000 ECU; 28 projects covering themes 1 to 6
1981: 660,000 ECU; synthesis and dummy evaluation (6 projects)

Most of these projects covered more than one phase, so that a total of 37 different projects were promoted. The list of projects and their titles are given in the Annex.

The breakdown of the total amount for the six research themes is as follows:

Theme 1:	345,000 ECU,	7 projects*
Theme 2:	780,000 ECU,	11 projects*
Theme 3:	295,000 ECU,	7 projects*
Theme 4:	935,000 ECU,	12 projects
Theme 5:	175,000 ECU,	4 projects
Theme 6:	270,000 ECU,	2 projects
Coordination and synthesis:	360,000 ECU	

It is recalled that these figures represent only the EEC contribution to the overall costs of the different projects. This contribution was never more than 50 percent—an average of about 40 percent, in fact. It is therefore permissible to estimate the global cost of European biomechanical research for these years at essentially higher figures.

Eleven European research organisations, laboratories or institutes took contracts with the European Communities in the framework of this programme. Most of these passed on subcontracts to other institutes or adopted cofinancing partners, so that it can be assumed that all major biomechanical research bodies in Europe took part in the programme. The list of contracting institutes is also given in the Annex.

It is obvious that the management of such a programme is a tough job for an administration, even that of the European Community. We therefore looked for further help from the outside on two subjects. The scientific coordination between the different projects was assessed by a specialised institution by way of contract. It also appeared necessary to assess periodically the conformity of the current work with the objectives of the contracts and its scientific value. For this purpose a Consulting Expert Committee was created in which personalities from all participating European countries acted as members under the most efficient chairmanship of Professor Aldman from Sweden, who has earned the Commission's wholehearted thanks.

RESEARCH THEMES AND THEIR RATIONALE

As far as the six priority research themes are concerned this paper is limited essentially to a brief explanation of the reasons which caused them to be chosen. More details can be found in the scientific paper distributed later on in this session or in the numerous papers and presentations given by the institutes concerned at previous conferences and meetings.

Occupant Protection in Frontal Impact

The majority of road accidents whereby car occupants are injured occur under this impact condition. This theme is therefore of prime importance to the legislator.

Since several years specific legal requirements exist in Europe relating to occupant protection in frontal accidents, e.g., the EEC directives on approval and installation of safety belts, on interior fittings, strength of seats and headrests, behaviour of the steering system in impact, etc. These requirements have generally proved their efficiency, but they are considered to be somewhat design-restrictive. They do not allow the approval of modern passive restraint systems and thus prevent the car manufacturers from introducing such systems on the European market.

These considerations led the European legislators to envisage a global test which allows the assessment of the quality of occupant protection offered by the vehicle as a whole. The definition of such a global test requires sufficient knowledge of the tolerance of those parts of the human body which are specifically concerned by frontal impacts: head, thorax, femur.

The consultation of the experts showed, however, that despite considerable worldwide research efforts there were still important gaps in biomechanical knowledge. A major participation of the EEC in this field was highly recommended. Consequently, seven projects were promoted which referred, in general, to the demonstration, in accident reconstructions and experiments, of the specific constraints of this impact mode with the help of human substitutes and their comparison with findings of clinical investigations and autopsy of real accident victims.

Occupant Protection in Side Impact

Accidents whereby occupants are injured by lateral impact are far less frequent than front impact accidents. They are, however, of increasing interest to the legislator at a time when the first generation of legal measures related to frontal accidents becomes effective. Some of these individual measures, such as fitting of three-point belts and interior padding, also show advantages in lateral impacts. A decisive improvement of occupant protection in this case can only be expected from a pooling of different technical measures on the vehicle, e.g., structural changes. The assessment of the efficiency of such measures again calls for the definition of a global test.

The gaps in existing knowledge were relatively important and a stronger research thrust seemed necessary. Therefore a major part of the EEC's budget was allocated to this theme. The 11 projects chosen included an inves-

*2 projects cover themes 1 and 2 and 2 projects themes 1, 2 and 3.

tigation of a relevant sample of real-world side-impact accidents and comprehensive accident reconstructions where the accidental constraints of the real victims were compared with those measurable on corpses and dummies. Experimental studies concentrated on the body segments mainly concerned in this impact mode—head, thorax, abdomen and pelvis—in order to understand their injury mechanisms and consequently to allow the definition of appropriate tolerance levels.

Pedestrian Protection

Accidents between motor vehicles and unmotorized road users are traditionally of great importance in the European Community. Their proportion in accident statistics tends to increase due to the current changes in transportation habits in the present economic situation but also due to the positive effect of the legal measures relating to the protection of car occupants.

Hence it is logical that the legislator considers measures to improve this situation. As far as vehicle-related requirements are concerned, however, the scientific and technical basis does not yet seem complete enough to allow the definition of such legal measures. Consequently, the Community deemed it necessary to promote research projects most likely to fill the gaps in knowledge, mainly of the injury mechanisms of pedestrians struck by car fronts. The projects chosen were essentially focussed on the reconstruction of real accidents and on experimental investigations referring to the body segments particularly concerned: head and knee/lower leg. The possibilities for a standard pedestrian test and evaluation methodology have also been examined.

Side Impact Dummy

In contrast with the situation for frontal testing, the experts consulted by the Commission had declared that none of the available dummies could produce representative results under side impact conditions with the degree of reproducibility required for whole vehicle type-approval testing. Consequently high priority was given to this theme, which received the most important financial support of the programme.

In order to save time and costs it was never intended to conceive completely new dummy types. The six projects chosen were concentrated on the construction of dummy components which permit the reproduction of the specific constraints of car occupants in side impact accidents: neck, shoulder, thorax, pelvis and abdomen. These parts were conceived in a way to offer interfaces with the components of the Hybrid II dummy used in the US safety regulations.

Three different sets of the above-mentioned components, based on the concepts of the major contractors, were built and completed with Hybrid II parts in order to form whole dummy prototypes: Peugeot/Renault's "APROD", MIRA's "SID" and ONSER's "50". All three are presented in the exhibition related to this 9th ESV Conference.

These three prototypes, together with an HSRI prototype made available by the NHTSA, have been submitted to a comparative test programme (6 projects in Phase 4). Their performances were also compared with the draft regulatory specifications set up by an ad hoc Group of EEVC specially created for this purpose. It must be mentioned that the objective of these comparative tests was not to set up a hierarchy among the different dummy concepts. The aim was to establish realistic performance criteria with which present dummy concepts can comply at reasonable cost, and which can later be included in a standard European side impact test for type-approval of motor vehicles.

Mathematical Models

Full-scale car crash tests are invariably very expensive. Obviously, it would be advantageous both for researchers and for the car industry to have a tool at their disposal which enables them to predict the influence of the modification of individual parameters on the test results on the basis of theoretical considerations. This aspect is equally interesting for the legislator who could thus keep the costs of type-approval testing down to a reasonable level.

For this reason four projects were promoted which concerned the development of two- and three-dimensional mathematical models simulating the behaviour of car occupants in crash situations and allowing to predict their injury severity.

Occupant Behaviour Interaction

This theme is of particular interest to the European Community, as in most Member States the use of three-point belts on front seats is mandatory, whereas the occupants of other seating positions need not yet wear belts. Hence it is important to establish whether interaction of occupants occur during accidents with different impact directions and whether injury-aggravating effects are observed. The two promoted projects concerned tests with cars of different sizes occupied by Hybrid II dummies submitted to impacts of different speeds and directions. The expected results should help both the car industry and the legislators to find a solution to this problem.

CONCLUSIONS

The EEC study programme on biomechanics which has been briefly outlined in this paper has enabled the experts to compile a great amount of scientific data. It is the Commission's duty towards the citizens of the European Community whose tax money has made the execution of this programme possible to use the results of

the research work to its best advantage for the purposes of a significant mitigating of the consequences of road accidents.

The present standstill of the programme allows us to assess how close we came to the aim of making available to the legislators all relevant scientific data which they need for the definition of the next generation of safety requirements. A synthesis report is currently being made on the results of the different projects and their complementarity to the work carried out in other parts of the world.

The synthesis report as well as the conclusions of the individual projects of each study theme will be presented to the interested parties of research, industry and administrations at a seminar to be held in Brussels on 21 to 23 March 1983.

It is, of course, impossible to anticipate the conclusions of the seminar which hopefully will state a general success of the programme. A partial success can, however, already be seen today.

The EEC support, even if it was limited by budgetary and time factors, has proved to be an important encouragement for biomechanical research in Europe. Researchers from many countries have coordinated their projects, thus avoiding useless redundancy. Many projects have been carried out on a joint basis which would not have been possible on a purely national basis, at least not in such a short period of time.

We hope that this spirit of cooperation will subsist and that if, at a later stage, joint projects would again be defined, this cooperation could be extended even beyond the bounds of the Community.

ANNEXE

List of Contractors and of Study Projects of the European Community Biomechanics Programme

Contractor	Title of the Study	Reference	Phase
Bundesanstalt für Strassenwesen (BAST) Postfach 510530 D—5000 KÖLN 51	Development of a Test Dummy for Investigating Occupant Protection in the Case of Side Impacts	G 2	1
	Interaction of Car Passengers in Frontal, Side and Rear Collisions	G 3	2,3
	Methodology of Developing Accident Protection Criteria	G 4	3
	Biomechanical Investigation to determine Physical and Traumatological Differentiation Criteria, for the Maximum Load Capacity of Head and Vertebral Column with and without Protective Helmet under the Effects of Impact	G 5	3
	Proposed Standardized Pedestrian Test Methodology	G 6	3
	Lateral Dummy Comparison Testing	G 7	4
Organisme National de Sécurité Routière (ONSER)	Head tolerance to Acceleration (Brain Vulnerability from Real Accidents)	F 1	1,2,3
2, Avenue du Général Malleret-Joinville F—94110 ARCUEIL	An Experimental Study of Thorax Tolerance to Seat Belt Loads	F 2	1,2,3
	Evaluation of the Behaviour of Different Substitutes in Lateral Impact Conditions (Improvement of the ONSER 50 for Lateral Impact)	F 4	1,2,3
	Lateral Dummy Comparison Testing	F 12	4
	Scientific Coordination		1,2,3
Université libre de Bruxelles Unité de recherche de biomécanique du mouvement 28, Av. Paul Héger 1050 BRUXELLES	Characterization of Individual Bone Resistance	B 1	3
Laboratoire de Physiologie et de Biomécanique PSA/RENAULT	Tolerance of the Human Head at Impact; Reconstruction of Head Impacts observed in True Life Accidents	F 6	1,2,3
147, Av. Paul Doumer F—91500 RUEIL-MALMAISON	Development of a More Convenient Dummy than the Hybrid II Part 572 for Side Collisions by using this as a Basis	F 10	1,2,3
	Lateral Dummy Comparison Testing	F 11	4

Contractor	Title of the Study	Reference	Phase
Nederlandse Organisatie voor Toegepast Natuurwetenschappelijk *Onderzoek ten behoeve van* Nijverheid, Handel en Verkeer (Nijverheidsorganisatie TNO) Juliana van Stolberglaan, 148 NL—DEN HAAG	Development of Abdominal Injury Detection in Side Impact Dummies (Organization and Administration of Lateral Dummy Evaluations)	NL 3	2,3
	Simulation of Frontal and Lateral Collisions with Mathematical Crash Victim Models	NL 4	2,3
	Madymo-Crash Victim Simulations Optimization and Development to a General Laboratory Tool	NL 6	3
	Lateral Dummy Comparison Testing	NL 7	4
	Lateral Dummy Comparison: Theoretical Analysis	NL 8	4
	Organization and Coordination of Intercomparison Testing Programme		4
Stichting Wetenschappelijk Onderzoek Verkeersveiligheid (SWOV) Ridder Snouckaertlaan, 7 NL—VOORBURG	Development of an Injury Prediction Model	NL 5	2,3
Transport Research Delegation (TRD) Sveavägen, 166, 14 tr. S—11346 STOCKHOLM	Experimental Study of Adult Pedestrians in Frontal Impacts—Physical Simulation of Human Leg—Bumper Impacts	S 1	1,2,3
	Development of a Device for Improvement of a Standard Dummy	S 2	1,2,3
University of Birmingham P.O. Box 363 UK—BIRMINGHAM B 15 277	Investigation of a Representative Sample of Real-World Side Impacts to Cars	UK 1	1, 3
Motor Industry Research Association (MIRA) Watling Street UK—NUNEATON *CV10 OTU*	Lateral Impact Dummy Development	UK 2	1,2,3
	Lateral Dummy Comparison Testing	UK 3	4
Joint Biomechanical Research Project (KOB) Bundesanstalt für Strassenwesen Postfach 510530 D—5000 KÖLN 51	Cerebral Tolerance : Interpretation of Experimental Cerebral Injuries obtained on Cadavers	B 3/ (F 5)	2,3
	Reconstruction of Side Impacts Accidents	G 1	1
	Pelvis and Femur Human Tolerance in Side Impacts	B 2/ (F 3)	1,2,3
	The Prediction of Injuries to the Thorax by Measuring Twelve Accelerations on the Thorax Periphery	B 1/ (F 7)	1,3
	Reconstruction of Pedestrian Collisions	K 5	2
	Rib Cage Deformation in Side Impacts	K 9	2,3
	Overall Behaviour of the Animal with Respect to the Safety Belt *and* Influence of the Car Driver Posture on his Protection in Frontal Impacts	K 10	2 3
	Analysis of Frontal and Lateral Accident Reconstructions Conducted in Europe	K 11	3
	Evaluation of the Influence of Inter-Individual Differences on the Injury Level	K 12	3
	Comparative Pedestrian Test with Side Impact Dummy	K 13	3
FIAT Auto S.p.A. Corso Giovanni Agnelli, 200 I—TORINO	Development of an Occupant's Mathematical Model for a Side Impact Test	I 1	2,3
	Relationship between Occupant's Behaviour and Vehicle Characteristics in Side Collisons	I 2	2,3

Side Impact Data Analysis

R. H. EPPINGER
Head, Biomechanics Group
R. M. MORGAN
Mechanical Engineer and
J. H. MARCUS
Mechanical Engineer
National Highway Traffic Safety Administration

ABSTRACT

As part of a continuing study of thoracic injury resulting from side impact loading, the interrelationships between subject age, various kinematic parameters characterizing the impact, and injury severity were investigated in data from a series of 30 cadaver tests.

These 30 tests include, in addition to the tests previously reported by the authors, sled tests conducted by the University of Heidelberg and car crash tests performed by ONSER. These new data expand the range of subject age to 67 years.

Two propositions are examined in this analysis. The first being: Can mechanical response measures partition side impact injuries into different categories? And the second being: Can a continuous function be constructed that can accurately predict a dependent injury severity variable given the various response variables available?

With regard to the first proposition, it is shown that by using any of a number of kinematic variables the present data can be easily partitioned into two classes consisting of those injuries of an AIS 80 severity of four and greater and those of AIS 80 three and less. For the second proposition, peak acceleration of the struck side rib along with age proved the best in predicting a new injury variable, fatality rate, which is a function of two highest AIS values in the body region. Age was a needed explanatory variable in all cases.

INTRODUCTION

In 1976 Melvin reported on the results of exposing cadavers to controlled side impacts [1].* In that paper, the test conditions were 15-, 20-, and 25-mph rigid-wall impacts and 20-mph padded-wall impacts. Two years later, in a further extension of the Highway Safety Research Institute (HSRI) cadaver work, Eppinger suggested acceleration-versus-time corridors for key thoracic locations and presented a methodology for universal thoracic trauma prediction [2].

During 1979, investigations into side impact dummies and thoracic injury criteria increased. Two advanced dummies, whose design specifications are based upon biomechanical data, were introduced. They were a Side Impact Dummy (SID) designed by the HSRI [3], and the Association Peugeot-Renault (APR) dummy from France [4, 5]. Relative to injury criteria, the B parameter computed from the rib acceleration data [6], power computed from the spine acceleration data [7], and deflection of the thorax [8] were introduced. (The B parameter computed from the upper rib data on the impacted left side is denoted BLUR.)

In 1980, the APR dummy and the deflection criteria underwent further development [9]. The power and B parameter criteria were substantiated by additional cadaver data [10]. Comparisons of the SID and APR dummy began [10, 11].

Cesari [12] concluded, based on eight cadaver pendulum tests, the arm—when positioned along the side of the thorax—distributes forces on the thorax. He also found the BLUR relationship previously established not to be strictly applicable to pendulum impacts. Methods were developed [13] to allow objective judgment of a dummy's magnitude and "signature" response to a test. Ten cadaveric side impact tests under four different conditions were performed to determine the characteristic mechanical response and resulting trauma outcome [14]. A dynamic characterization of the human thorax, in the form of a digital impulsive response signature, was obtained which linked the acceleration response of the struck side with the far side of the thorax under side impact conditions [15].

Early in 1982, a paper [16] discussed the state-of-knowledge of side impact protection. The French team continued their efforts in the development of a protection criteria and introduced a bone characterization factor as an indicator of thoracic body resistance [17, 18].

DESCRIPTION OF TESTS

To date, the National Highway Traffic Safety Administration (NHTSA) has conducted or participated in 45 side impact tests utilizing cadaveric specimens. The present paper shall discuss findings based on an analysis of 30 of these tests. There are several reasons the analysis does not include 45 tests. One significant reason is that some of the tests are still being processed, i.e., the time between the actual test event and when the data becomes resident in the NHTSA computer is still considerable. With other tests, there was a loss of mechanical response data. This loss is indicative of the extremely severe environment that side impact presents not only to the specimen but also to the instrumentation.

Table 1 categorizes the 30 tests by research institution, type of test, and number of tests. As can be noted, there

*Numbers in brackets denote references cited at the end of paper.

Table 1. Data source.

HSRI	
	6 Rigid wall sled
	6 Padded wall sled
	4 Pendulum
WSU	
	1 Padded wall sled
Heidelberg	
	6 Rigid wall sled
	4 Padded wall sled
ONSER	
	1 Baseline car crash
	2 Modified car crash
30 Total Tests	

is a large variation in type of test: from lateral pendulum tests to actual vehicle tests.

In all tests, the physiological consequences were determined by autopsy after each experiment. The injuries produced in the thoraco-abdominal area were the primary focus of this analysis. An interesting dilemma exists when one classifies the observed injuries by the Abbreviated Injury Scale. That is, injuries to the thorax include the rib cage and those organs and structures above the diaphragm as seen in Figures 1 and 2. Abdominal injuries include all structures below and including the diaphragm [19], whether they are within the thoracic rib cage or not as shown in Figures 3 and 4.

Since the experimental measurements consist solely of responses of the rib cage, two types of AIS injury classifications have been made, the first, AIS thorax (AIS_T) includes only those thoracic injuries as defined by the AIS manual. The second classification, AIS hard thorax (AIS_{HT}), includes—in addition to the standard thorax injuries—those injuries of abdominal structures that lie within the rib cage, specifically the liver, spleen, and kidneys.

A third dependent injury variable was also examined

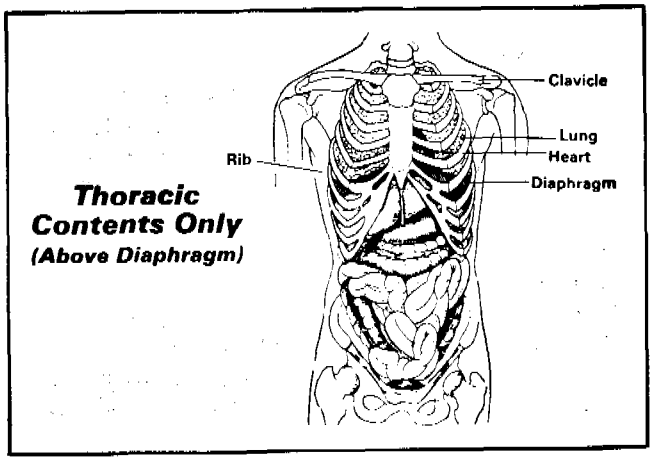

Figure 1.

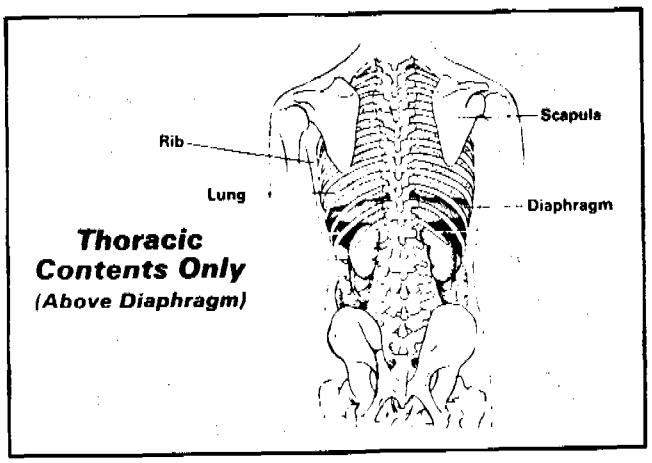

Figure 2.

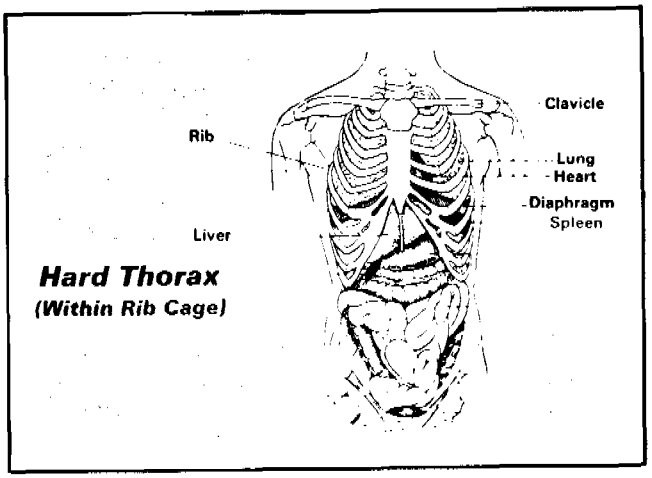

Figure 3.

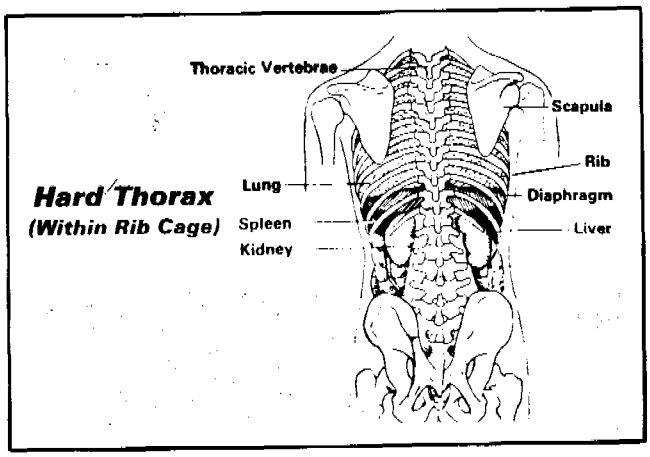

Figure 4.

Table 2. Fatality rate by (AIS1, AIS2).

(AIS1, AIS2)	Fatality rate
(0, 0)	.00000
(1, 0 -1)	.0001131
(2, 0 -1)	.00073
(2, 2)	.00456
(3, 0 -1)	.00434
(3, 2)	.00593
(3, 3)	.02174
(4, 0 -1)	.0392
(4, 2)	.04301
(4, 3)	.10526
(4, 4)	.12821
(5, 0 -1)	.28
(5, 2)	.36667
(5, 3)	.48529
(5, 4)	.58182
(5, 5)	.86364
(6, ANY)	1.00000

Table 3. Comparison of injury values.

Test type	AIS_T	AIS_{NT}	FR_{NT}	Age
Rigid wall	1	1	.0001131	80
Rigid wall	5	5	.0636	75
Rigid wall	4	4	.10526	84
Rigid wall	4	4	.12821	89
Padded wall	2	2	.00073	67
Padded wall	4	4	.04301	62
Padded wall	3	3	.00593	72
Padded wall	4	4	.0392	58
Pendulum	1	1	.0001131	63
Pendulum	3	3	.00434	60
Pendulum	1	1	.0001131	60
Pendulum	3	3	.02174	79
Rigid wall	5	5	.4853	66
Rigid wall	4	4	.1282	45
Padded wall	4	4	.1282	77
Padded wall	4	4	.10526	71
Padded wall	2	2	.00073	54
Rigid wall	1	2	.00456	27
Rigid wall	2	3	.02174	60
Rigid wall	2	2	.00073	38
Padded wall	0	1	.0001131	21
Padded wall	1	1	.0001131	26
Padded wall	0	0	.0	29
Padded wall	2	2	.00073	41
Rigid wall	0	0	.0	24
Rigid wall	4	4	.12821	57
Rigid wall	4	4	.12821	56
Baseline car	4	4	.12821	40
Modified car	2	3	.00593	43
Modified car	4	4	.12821	52

in this analysis. It is called "fatality rate" and is derived using the two highest AIS injuries observed in a particular occupant [20, 21]. That is, each possible pair of AIS values has associated with it a particular fatality rate. This fatality rate was calculated from the National Crash Severity Study by examining each AIS pair category and calculating the percentage of observed fatalities within each subgroup. Table 2 shows each AIS pair and its associated fatality rate. This table appears to allow a reversal of the process, i.e., the ability to transform from a given fatality rate back to the corresponding AIS pair. The only ambiguity to this process occurs between the (2,2) and the (3,0-1) classifications.

Applying the preceding discussion to the 30 side impact cadaver tests, Table 3 illustrates that the AIS_{HT} is higher than AIS_T in four instances and that the fatality rate is different in 17 cases where the highest AIS is the same. (The AIS values use the AIS 80 manual.)

Of the 12 accelerometer channels available [2] from the specimen tests, this analysis concentrated on examination of lateral responses observed on the fourth rib of the struck side of the rib cage and the twelfth thoracic vertebra. Parameters extracted from these signals include peak acceleration (see Appendix A for the procedure followed in preparing each signal) of the rib and spine, a synthetic relative velocity between the left and right side of the rib cage [15], and peak average power which is the maximum incremental velocity change squared divided by incremental time. Age was also utilized as an explanatory variable since a variety of studies have demonstrated the increased susceptibility of the human body to trauma with increasing age [22, 23].

ANALYSIS OF DATA

When performing an analysis of data, it is useful to know what the analysis is going to examine. This analysis examined two propositions. The first being: Can mechanical response measures partition injuries into two categories; those severe or greater (AIS $\geq$ 4) and those from minor to serious (AIS $<$ 4)? The second proposition examined was: Can a continuous function be constructed that can accurately predict the dependent injury variable given the various independent variables available?

Figures 5 and 6 indicate that indeed both peak rib acceleration and peak synthetic relative velocity (feet per second) partition the severe and greater injuries from the lesser ones quite well and—if this were sufficient—additional tests would be necessary only to gain further confidence in the partitioning line for the years from 20 to 40. (The numbers in the middle of Figures 5 and 6 denote AIS_T based on the AIS 80 manual.) For this data set, peak acceleration was found to be highly correlated with peak average power for the same anatomical location and, therefore, in the following discussion, general con-

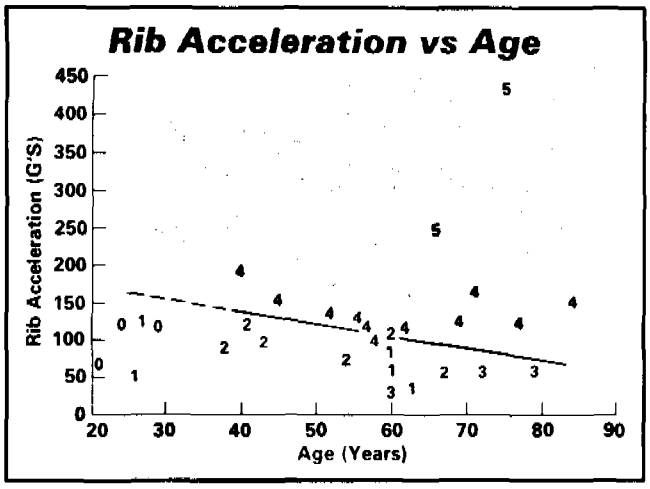

Figure 5.

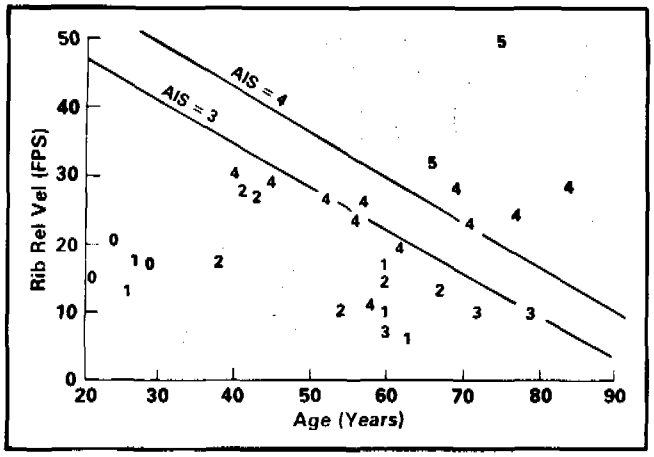

Figure 7. Constant AIS lines on data.

clusions reached relative to peak acceleration also apply to peak average power.

Efforts to predict AIS thorax gave the following results:

$$AIS_T = 0.82\Delta V + .05\ Age - 1.8 \quad R = .81 \quad (1)$$

$$S.E. = .93$$

$$AIS_T = .0089\ A_{LUR} + .049\ Age - 1.1 \quad R = .77 \quad (2)$$

$$S.E. = 1.01$$

$$AIS_T = .011\ A_{T12} + .057\ Age - 1.3 \quad R = .74 \quad (3)$$

$$S.E. = 1.03$$

For this linear regression analysis, the synthetic relative velocity (feet per second) performed the best, but just marginally. A discussion of these equations would not be complete without giving some indication of how the constant AIS lines map onto the data points. Some of the constant AIS lines from equation (1) are mapped onto the data in Figure 7. Note the AIS = 3 line goes through a number of AIS = 4 data points. It appears—due to the lack of severe injuries in the younger age bracket—that the equation has an exaggerated dependence on age. Similar results are seen when examining the other linear AIS regression equations.

Naturally, the regression equations are only good for values of the dependent variables which lie within the region covered by the original data [24]; e.g., the equations are not to be used for a 5-year-old child because children were not included in the original data set. The values of the observed variables are in Appendix B.

Linear regression on AIS hard thorax yields the following results:

$$AIS_{HT} = .081\Delta V + .044\ Age - 1.2 \quad R = .79 \quad (4)$$

$$S.E. = 92$$

$$AIS_{HT} = .0088\ A_{LUR} + .042\ Age - .5 \quad R = .74 \quad (5)$$

$$S.E. = 1.0$$

$$AIS_{HT} = .012\ A_{T12} + .049\ Age - .75 \quad R = .72 \quad (6)$$

$$S.E. = 1.0$$

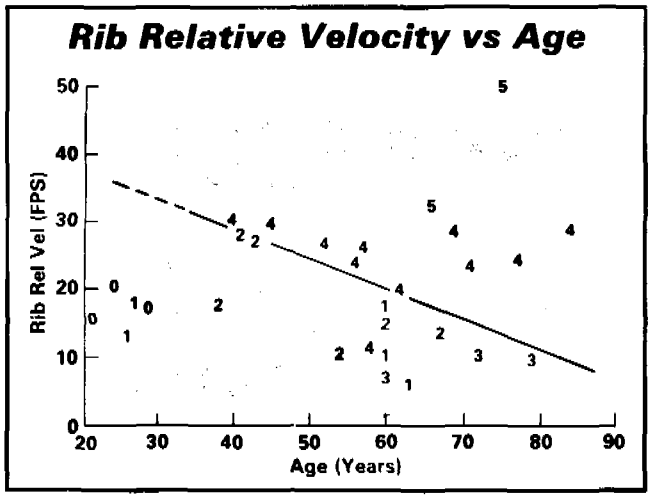

Figure 6.

So when all is said and done, adding abdominal trauma to that which lie within the thoracic rib cage had little effect on the coefficients of the linear equations other than shifting the curves by a constant term of about .6 of an AIS value. Stated another way, when considering the same impact event, the injury severity of the hard thorax is approximately one half of an AIS level greater than when considering injuries to only the thorax.

Age enters all these linear equations with roughly the same coefficient, .05. In other words, in going from 20 years to 80 years—all other things being equal—there is an AIS increase of 3. About 41% of the variation of AIS can be attributed to a linear relationship with age. Again, this appears to be an exaggerated dependence on age, and the use of these equations is not recommended.

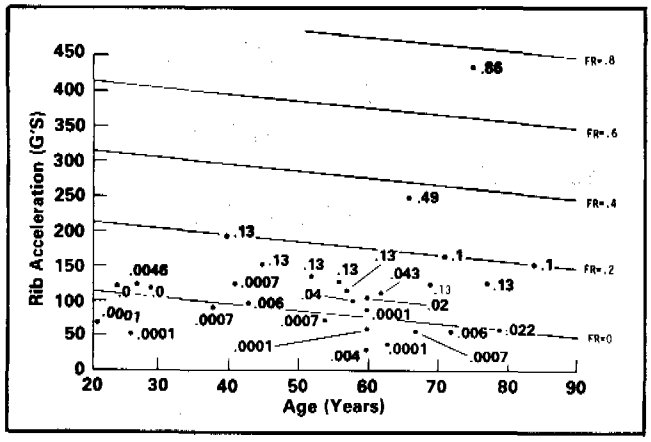

Figure 8. Constant fatality rate lines mapped onto data.

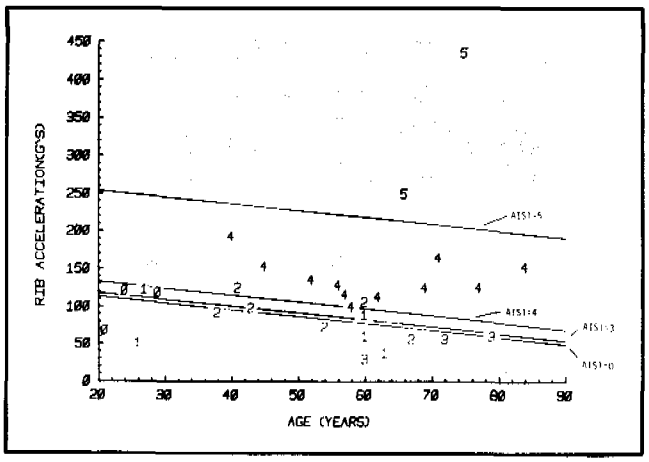

Figure 9. AIS lines derived from fatality rate regression lines.

Examining the results of predicting fatality rate based on the hard thorax injury is shown here:

$$FR_{HT} = .002\ A_{LUR} + .0018\ Age - .25 \quad R = .94 \quad (7)$$

$$S.E. = .06$$

$$FR_{HT} = .014\Delta V + .0026\ Age - .34 \quad R = .82 \quad (8)$$

$$S.E. = .1$$

$$FR_{HT} = .002\ A_{T12} + .0036\ Age - .28 \quad R = .67 \quad (9)$$

$$S.E. = .13$$

Peak acceleration along with age appears to perform the best. Here the age sensitivity is less and more consistent with the data, i.e., a 60-year increase in age reduces the required peak G's by 54 to produce the same fatality rate. This is quite consistent with the data as can be seen in Figure 8.

For completeness, the fatality rate for the thorax predictive equation with the highest correlation coefficient is presented here:

$$FR_{T} = .002\ A_{LUR} + .0018\ Age - .26 \quad R = .92 \quad (10)$$

$$S.E. = .07$$

Equation (7) is essentially identical to equation (10).

On Figure 8 the 30 data points have been plotted in fatality rate space. The number beside each data point is the observed hard thorax fatality rate. The constant fatality rate lines are the linear regression prediction based on equation (7).

Based on the family of predicted linear regression lines of Figure 8, it is possible to predict the constant AIS1 lines by using Table 2. For example, Table 2 shows that AIS1 = 3 injuries start at a fatality rate of roughly 0.00434. Substitution of FR = .00434 into equation 7 determines a line on Figure 8. This same line becomes the constant AIS1 = 3 line in the AIS injury space as shown in Figure 9.

There are a number of interesting implications in going from Figure 8 to Figure 9. For one, the linear lines in the fatality rate space (Figure 8) have become nonlinear in AIS space (Figure 9) by virtue of the transformation of Table 2. For another, the constant AIS1 = 1 and AIS1 = 2 lines have been mapped almost on top of the AIS1 = 0 line. (In fact the AIS1 = 1 and AIS1 = 2 lines are not shown in Figure 9 because they are indistinguishable with respect to the AIS1 = 0 line for the given scale.)

A further examination of these various functions was performed by posing the following question: "What injury level could be expected by a 45-year-old victim were he to experience either a 50, 100, or 150 G peak rib acceleration?" Table 4 demonstrates the results.

It can be seen that the directly calculated AIS for the hard thorax does not have as great an AIS variation due to changes in acceleration as does the AIS determined using fatality rate. In other words, the fatality rate model—because the relationship in Table 2 between FR

Table 4. Predicted injury based on three acceleration levels.

Rib Acceleration (G's)	AIS Hard Thorax	Fatality Rate Hard Thorax	AIS1 Corresponding to That Fatality Rate
50	1.83	.0	0
100	2.27	.031	3
150	2.71	.131	4
Age = 45 Years			

and AIS1 is nonlinear—rapidly moves the AIS1 through the 0, 1, and 2 levels up to AIS1 = 3 and then on to AIS1 = 4. When examining the results from these two models against the actual data in Figure 5, the latter process appears to perform the better. (The AIS1 in this example was determined by first calculating the expected fatality rate and then referring to Table 2 to find the AIS1.)

CONCLUSIONS

1. Both peak struck side acceleration and synthetic relative velocity partition injuries into AIS $\geq$ 4 and AIS $\leq$ 3 groups well.
2. Age has a statistically significant effect on injury outcome with every mechanical response parameter examined.
3. Synthetic relative velocity and age were the best predictors of AIS_T and AIS_{HT} when requiring a linear fit through the data. However, the predicted AIS has an exaggerated dependence on the age of the subject and these relationships are not suggested for use.
4. Peak struck side rib acceleration and age predicted fatality rate best.
5. Given a predicted fatality rate, one can reverse the process and determine the maximum expected AIS_{HT}. This process provided the best continuous prediction of AIS that was the most consistent with the data.

DISCLAIMER

The views presented are those of the authors and not necessarily those of the National Highway Traffic Safety Administration.

ACKNOWLEDGEMENTS

The figures which illustrate the thoracic and abdominal viscera in their normal positions are from *Kimber-Gray-Stackpole's Anatomy and Physiology*, Sixteenth Edition, published by the MacMillan Company, and are reprinted by permission of the MacMillan Company.

REFERENCES

1. Melvin, J. W., Robbins, D. H., and Stalnaker, R. L., "Side Impact Response and Injury," Sixth International Technical Conference on Experimental Safety Vehicles, October 1976.
2. Eppinger, R. H., Augustyn, K., and Robbins, D. H., "Development of a Promising Universal Thoracic Trauma Prediction Methodology," Twenty-Second Stapp Car Crash Conference, October 1978.
3. Melvin, J. W., Robbins, D. H., and Benson, J. B., "Experimental Application of Advanced Thoracic Instrumentation Techniques to Anthropomorphic Test Devices," Seventh International Technical Conference on Experimental Safety Vehicles, June 1979.
4. Fayon, A., Leung, Y. C., Stalnaker, R. L., Walfisch, G., Balthazard, M., and Tarriere, C., "Presentation of a Frontal Impact and Side Impact Dummy, Defined from Human Data and Realized from a 'Part 572' Basis," Seventh International Technical Conference on Experimental Safety Vehicles, June 1979.
5. Stalnaker, R. L., Tarriere, C., Fayon, A., Walfisch, G., Balthazard, M., Masset, J., Got, C., and Patel, A., "Modification of Part 572 Dummy for Lateral Impact According to Biomechanical Data," Twenty-Third Stapp Car Crash Conference, October 1979.
6. Robbins, D. H., and Lehman, R. J., "Prediction of Thoracic Injuries as a Function of Occupant Kinematics," Seventh International Technical Conference on Experimental Safety Vehicles, June 1979.
7. Burgett, A., and Hackney, J. R., "Status of the National Highway Traffic Safety Administration Research and Rulemaking Activities for Upgrading Side Impact Protection," Seventh International Technical Conference on Experimental Safety Vehicles, June 1979.
8. Tarriere, C., Walfisch, G., Fayon, A., Rosey, J. P., Got, C., Patel, A., and Delmas, A., "Synthesis of Human Tolerance Obtained from Lateral Impact Simulations," Seventh International Technical Conference on Experimental Safety Vehicles, June 1979.
9. Fayon, A., Tarriere, C., Walfisch, G., Duprey, M., and Balthazard, M., "Development and Performance of the APR Dummy (APROD)," Eighth International Technical Conference on Experimental Safety Vehicles, October 1980.
10. Morgan, R. M., and Waters, H. P., "Comparison of Two Promising Side Impact Dummies," Eighth International Technical Conference on Experimental Safety Vehicles, October 1980.
11. Mellander, H., and Bohlin, N., "A Comparison Between Different Dummies in Car-to-Car Side Impacts," Eighth International Technical Conference on Experimental Safety Vehicles, October 1980.
12. Cesari, D., Ramet, M., and Bloch, J., "Influence of Arm Position on Thoracic Injuries in Side Impact." Twenty-Fifth Stapp Car Crash Conference, September 1981.
13. Morgan, R. M., Marcus, J. H., and Eppinger, R. H., "Correlation of Side Impact Dummy/Cadaver Tests," Twenty-Fifth Stapp Car Crash Conference, September 1981.
14. Kallieris, D., Mattern, R., Schmidt, G., and Eppinger, R. H., "Quantification of Side Impact Responses and Injuries," Twenty-Fifth Stapp Car Crash Conference, September 1981.

15. Eppinger, R. H., and Chan, H. S., "Thoracic Injury Prediction via Digital Convolution Theory," Twenty-Fifth Stapp Car Crash Conference, September 1981.
16. Burgett, A., and Brubaker, W., "The Role of the Side of the Motor Vehicle in Crash Prediction." SAE Publication No. 820245, International Congress and Exposition, Detroit, Michigan, February 1982.
17. Walfisch, G., Chamouard, F., Lestrelin, D., Fayon, A., Tarriere, C., Got, C., Guillon, F., Patel, A., and Hureau, J., "Tolerance Limits and Mechanical Characteristics of the Human Thorax in Frontal and Side Impact and Transposition of these Characteristics into Protection Criteria," IRCOBI Conference, Cologne, Germany, September 1982.
18. Sacreste, J., Brun-Cassan, F., Fayon, A., Tarriere, C., Got, C., and Patel, A., "Proposal for a Thorax Tolerance Level in Side Impacts Based on 62 Tests Performed with Cadavers Having Known Bone Condition," Twenty-Sixth Stapp Car Crash Conference, October 1982.
19. "The Abbreviated Injury Scale 1980 Revision," American Association for Automotive Medicine, Morton Grove, Ill. 60053.
20. Eppinger, R. H., and Partyka, S. C., "Estimating Fatality Reductions Associated with Safety Improvements," Eighth International Technical Conference on Experimental Safety Vehicles, October 1980.
21. Partyka, S. C., "A Comparison of AIS and ISS Predictions of Fatality on NCSS," Twenty-Fourth Conference of the American Association for Automotive Medicine, October 1980.
22. Eppinger, R. H., "Considerations in Side Impact Dummy Development," Seventh International Technical Conference on Experimental Safety Vehicles, June 1979.
23. Neathery, R. F., Kroell, C. K., and Mertz, H. J., "Prediction of Thoracic Injury From Dummy Responses," Nineteenth Stapp Car Crash Conference, November 1975.
24. Draper, N. R., and Smith, H., "Applied Regression Analysis," Second Edition, John Wiley and Sons, Inc., New York, 1981, pg. 8.

APPENDIX A

Data processing of the accelerometer signal closely followed that in Reference 2. The steps included: (A) electronic filtering to appropriately band limit the response and minimize aliasing in the A/D process, (B) analog to digital conversion (1600 Hz sampling rate), and (C) digital filtering with a finite impulse response filter having the following characteristics; pass band frequency = 100 Hz, stop band frequency = 189 Hz, pass band ripple = 0.0225 dB, and stop band gain = − 50 dB.

APPENDIX B
Injury Data and Parametric Value Summary

Test No.	Test Velocity (mph)	Test Type	Age (Years)	Sex	Weight (kg)	Height (cm)	Testing Organization	Test No.	$AIS1_T$	$AIS2_T$	$AIS1_{HT}$	$AIS2_{HT}$	NFR	Peak Rib Synthetic Relative Velocity (fps)	Peak Rib Acceleration (G's)	Peak Spine (T12) Acceleration (G's)
76T003	15	RW	60	M	102.1	180.5	HSRI	76T003	1	0	1	0	1	16.7	88.	---
76T009	25	RW	75	F	44.1	155.5	HSRI	76T009	5	5	5	5	20	49.7	435.	207.
76T010	20	RW	84	M	87.8	162.2	HSRI	76T010	4	3	4	3	13	28.6	153.	106.
76T011	20	RW	69	M	74.9	170.2	HSRI	76T011	4	0	4	4	17	28.3	125.	167.
76T029	15	PW	67	M	62.5	167.1	HSRI	76T029	2	0	2	0	3	13.5	56.	54.
76T034	20	PW	62	M	59.	183.5	HSRI	76T034	4	2	4	2	18	19.8	112.	---
76T039	20	PW	72	M	73.9	186.8	HSRI	76T039	3	2	3	2	9	10.3	56.	40.
76T042	25	PW	58	F	64.5	177.7	HSRI	76T042	4	0	4	0	15	11.3	99.	67.
76T065	9.5	P	63	M	94.7	178.9	HSRI	76T065	1	0	1	0	0	6.3	38.	12.
77T071	9.5	P	60	M	80.7	172.2	HSRI	77T071	3	1	3	1	0	7.1	30.	14.
77T074	9.5	P	60	M	54.	176.9	HSRI	77T074	1	0	1	0	1	10.0	61.	15.
77T077	13.6	P	79	M	73.7	175.5	HSRI	77T077	3	3	3	3	3	9.7	60.	20.
77T089	20	RW	66	M	55.1	173.5	HSRI	77T089	5	3	5	3	9	32.0	249.	88.
77T092	20	RW	45	F	58.3	176.7	HSRI	77T092	4	4	4	4	21	29.3	153.	79.
77T095	20	PW	77	M	92.8	183.2	HSRI	77T095	4	4	4	4	11	24.4	125.	59.
77T098	20	PW	71	M	59.	168.2	HSRI	77T098	4	3	4	3	13	23.1	165.	98.
WSU484	15	PW	50	M	78.4	164.	Wayne State	WSU484	2	1	2	1	8	---	---	51.
WSU487	20	PW	54	F	54.4	165.	Wayne State	WSU487	2	1	2	1	5	10.6	73.	57.
WSU488	17	RW	58	M	97	183.	Wayne State	WSU488	4	2	4	2	7	---	---	69.
WSU490	15	RW	50	M	49.9	185.	Wayne State	WSU490	2	1	2	1	10	---	---	38.
H80011	15	RW	27	M	89	180.	Heidelberg	H80011	1	1	2	2	1	17.8	123.	93.
H80014	14	RW	60	F	84	169.	Heidelberg	H80014	2	0	3	3	3	15.0	106.	146.
H80017	15	RW	38	M	70	175.	Heidelberg	H80017	2	0	2	0	6	17.6	92.	76.
H80018	19	PW	21	M	61	166.	Heidelberg	H80018	0	0	1	1	0**	15.3	69.	61.
H80020	19	PW	26	F	67	167.	Heidelberg	H80020	1	1	1	1	3	13.4	52.	---
H80021	20	PW	29	M	63	180.	Heidelberg	H80021	0	0	0	0	0	17.5	118.	56.
H80023	20	PW	41	F	82	159.	Heidelberg	H80023	2	0	2	0	8	27.9	125.	86.
H80024	20	RW	24	M	65	176.	Heidelberg	H80024	0	0	0	0	0	20.2	121.	134.
H81002	20	RW	57	M	65	165.	Heidelberg	H81002	4	2	4	4	14	25.9	116.	130.
H81004	20	RW	56	M	80	165.	Heidelberg	H81004	4	1	4	4	16	23.7	128.	135.
BMD001	40*	BC	40	F	69	167.	ONSER	BMD001	4	1	4	4	11	30.1	193.	138.
BMD002	40*	MC	43	M	70	175.	ONSER	BMD002	2	2	3	2	11	27.1	98.	57.
BMD003	40*	MC	55	M	74	174.	ONSER	BMD003	4	2	4	4	12	26.7	135.	49.

* Velocity of deformable side impact moving barrier.

P = Pendulum
RW = Rigid Wall
PW = Padded Wall
BC = Baseline Crash
MC = Modified Vehicle Crash

AIS values in terms of 1980 manual.
NFR = Number of Fractured Ribs.

Signals processed according to Appendix A.

Synthetic Relative Velocity discussed in Reference 15. The numbers here are slightly changed from Reference 15 due to a slight change in the transfer function.

**Incorrectly reported in Reference 13 as 6 fractured ribs.

Human Head Tolerance to Lateral Impact Deduced from Experimental Head Injuries Using Primates

ATSUMI KIKUCHI, KOSHIRO ONO
Japan Automobile Research Institute, Inc.

NORIO NAKAMURA
Department of Neurosurgery
Jikeikai University

ABSTRACT

Impacts were applied to temporal regions of 23 subhuman primates, while controlling 1) impact velocity, 2) impactor elasticity and 3) impact stroke. Such impacts were repeatedly applied to test primates until they showed symptoms of brain concussion or other brain injuries. As a result, the range of head accelerations, in which brain concussion and pathological brain injuries such as subdural hemorrhage, brain stem hemorrhage, etc. were likely to occur, was clearly indicated on the coordinates represented by the averaged resultant head acceleration and its duration of impact.

This provided a clear indication of thresholds of severe pathological brain injuries as well as the threshold of brain concussion of subhuman primates against lateral impacts. Based on the experimental results using subhuman primates, the extrapolation was done of human head acceleration and its duration, and thresholds of human brain concussion and severe pathological brain injuries were deduced. From results thus obtained it was estimated that the tolerances to brain concussion and severe pathological brain injuries for humans and subhuman primates were higher for lateral impacts than those of frontal or occipital impacts and that the hemorrhage of callosal, cortical and subcortical was often involved at time of occurrence of brain concussion by lateral impact on the head. According to the above, it was concluded that it should be appropriate to determine the tolerance threshold of the lateral impact, using slight skull fracture, minor subarachnoid hemorrhage or other similar head injury for reference.

INTRODUCTION

Doctors who actually engage in clinical treatment feel that a certain pattern exists among head traumas, and there are clearly some rules concerning the relationship between the direction of force and area of brain injury. Nevertheless, only a few quantitative analyses of the relation between the impact region, injury and impact magnitude have been done, (1,2,3) and the tolerance of each region of the head against impacts has not been clearly developed, whereas relatively more qualitative analyses have been performed.

Gurdjian et al. reported the Wayne State Tolerance Curve (WSTC) regarding tolerance thresholds against frontal impacts in 1965, based on data obtained from a number of animal tests, skulls, cadavers, volunteers and clinical cases. (4,5,6) Since then the WSTC has been used extensively not only as a criterion for motor vehicle safety but also as an index to safety against head impacts. The author et al. recently extrapolated the threshold of human brain concussion against frontal or occipital impacts from the results of head impact tests performed using subhuman primates, (7,8,9) which was reported as the JARI Human Head Tolerance Curve (JHTC) (10,11). As a result, it was confirmed that the WSTC developed by Gurdjian et al. employed injuries similar to brain concussion in terms of severity as the index to tolerance thresholds.

In recent years, safety measures for motor vehicle side collisions have been attracting the attention of people concerned, but safety thresholds of head, thorax, pelvis, etc. against lateral impacts are not recognized yet. The author et al., therefore, carried out lateral impact tests using subhuman primates, in an attempt to clarify tolerance thresholds against lateral impacts through the extrapolation of human brain concussion threshold according to experimental results.

EXPERIMENTAL SUBJECTS

Twenty-three subhuman primates which were morphologically, anatomically and physiologically analogous to humans were used as test subjects. The primates were classified as follows; 7 Macaca fuscatas (Japanese monkeys), 12 Macaca mulattas (Rhesus monkeys) and 4 Macaca fasicularises (crab eating monkeys) consisting of 21 male monkeys and 2 female monkeys. Their weights ranged from 4 to 13 kg, presumed ages from 3 to 9 years old.

EXPERIMENTAL APPARATUS AND IMPACT METHOD

The impactor ejection apparatus shown in Figure 1 was used as the test equipment to apply impacts to temporals of test monkeys. The posture of each test monkey was held by subject restraint device shown in Figure 2. The impactor ejection apparatus was capable of colliding the piston, accelerated by the compressed air, against the impact shaft located at the front end of the cylinder, for ejection of the impact shaft. The impact stroke was con-

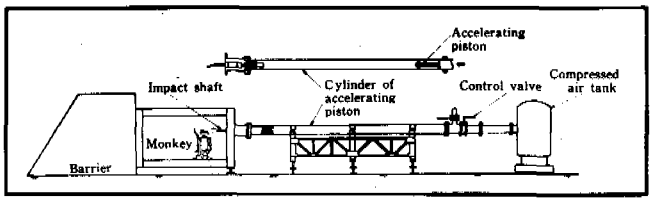

Figure 1. Impactor ejection apparatus.

trolled by the impact shaft stopping position. The maximum capability of the impactor ejection apparatus was 50 m/s where the weight of the impact shaft was 13 kg. The impactor head was made of a solid rubber block of 120 × 80 × 100 mm, and the degrees of hardness of the rubber block were 20, 30 and 70. Elastic characteristics of each impactor head are shown in Figure 3. Each test monkey under light anesthesia was seated on the subject restraint device with its chin held by a urethane foam block, while impacts were applied. The impact direction was vertical to the sagittal plane of the head, with the Frankfurt line of the monkey's head held horizontal (Figure 4). The upper region of the zygomatico arch was selected as the area of impact in order to avoid fracturing of the zygomatico arch. The magnitude of impact was controlled by 1) impactor ejection velocity, 2) impact stroke and 3) impactor head elasticity. After applying impacts, the test monkey's head was held by the supporting net so as to avoid the hyperextension of the neck. At the same time when the body fell against the supporting net, the net started to tilt by 30 to 60° while reducing the velocity, then stopped. Owing to the braking function of the supporting net, the test monkey stopped moving while avoiding secondary collision. At that time, the chair on the subject restraint device did not travel.

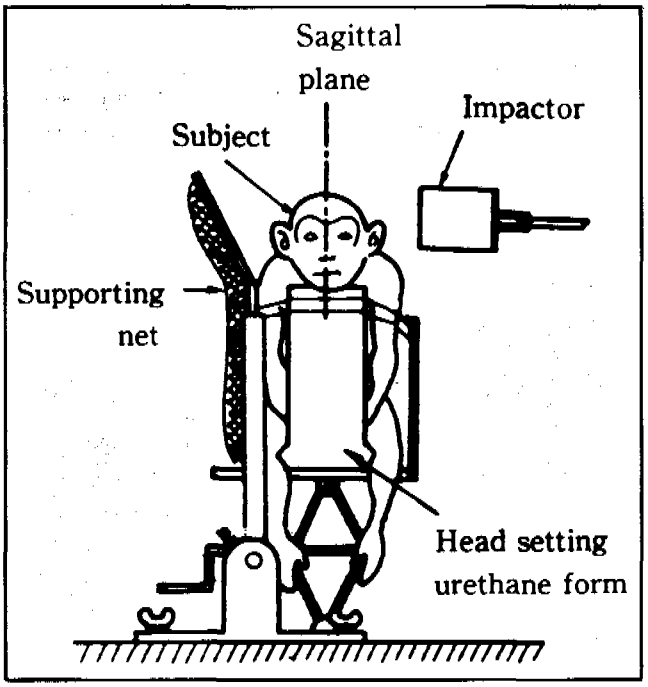

Figure 2. Subject restraint device.

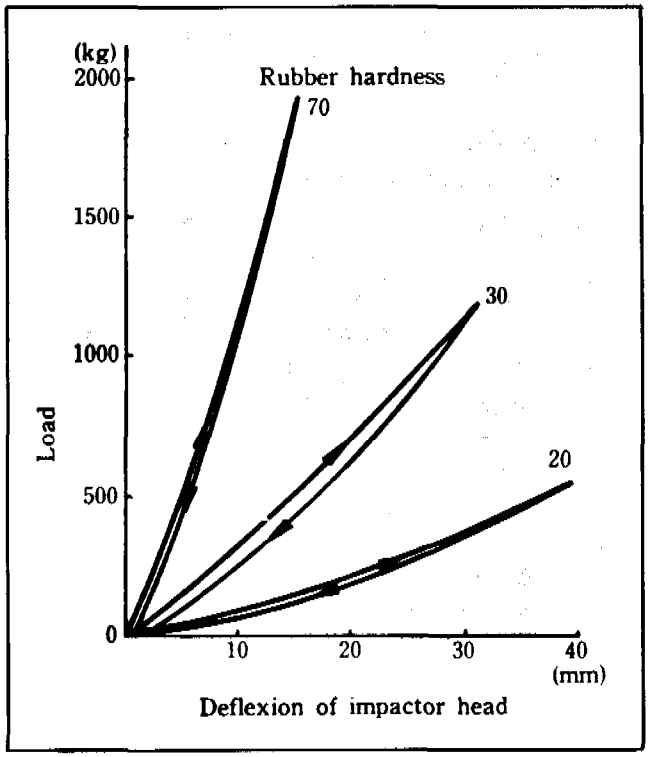

Figure 3. Load-deflexion curve of impactor head.

PHYSICAL MEASUREMENTS AND BIOLOGICAL OBSERVATION

Ketamin hydrochloride for anesthesia was injected into the muscles of each test monkey about 2 hours prior to the test. Under the anesthesia, the test monkey's physical dimensions and weight were measured and various trans-

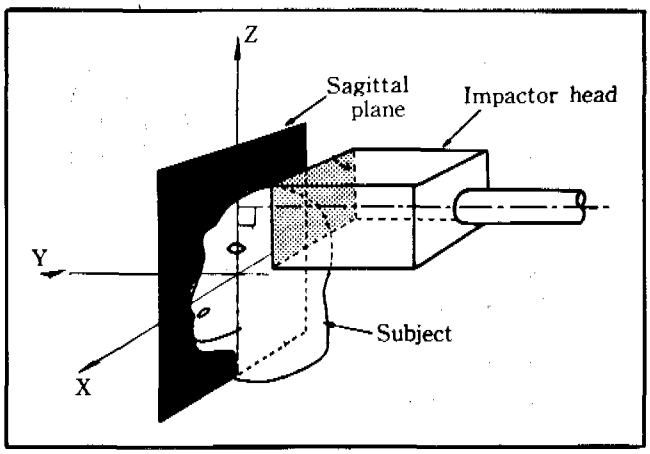

Figure 4. Impact direction; impact direction was set vertical to the sagittal plane, with the Frankfurt line set horizontal.

ducers, electrodes, etc. were installed onto specified locations. The coordinate reference frame of the subject's head was set at the left-hand system. X-axis was set in parallel to the Frankfurt line, while Y and Z axes were set vertical to the X-axis. Head acceleration of each axis was measured by the accelerometer of semiconductor strain gauge type (AH-2000, ST). Values measured by such accelerometers were analyzed and processed through low-path filters by means of a data processing system (NOVA Nihon Minicon). Velocity of impactors was measured optically by laser beams and phototransistors. Behaviors of test monkeys were photographed by high speed cameras at 4000 frames per second (HYCAM, Pedlake) from the direction of X-axis on the head, and the results were studied by a film analyzer (Motion Analyzer, Nack). Electroencephalograms (EEGs) were induced from right and left sides of the frontal-temporal and the parietal scalp, while electrocardiograms (ECG) were induced from the front chest. Respiration measurements were made by means of thermistor-type respiration meters (MTR-2TIS, Nihon Koden). The foregoing biological data were recorded on an electroenceparagraph (EEG-4109, Nihon Koden) and pen-type oscilloscope (RTG-3034, Nihon Koden). Before and after each impact, pupillary light reactions, ciliary reflexes, winks, occular movements, spontaneous movements, etc. were repeatedly observed from time to time. X-ray tests were also done on the head and neck before and after impacts, and skull dimensional measurements were performed and fractures checked, etc. Autopsies were made immediately after death for fatal cases, while surviving monkeys were subjected to euthanasia using nembutal sodium solution 1 hour to 7 days after the impact test, and then given an autopsy. After autopsy, fracture of the skull and cervical vertebra was examined first and extra-intradralle hemorrhage was investigated next. Finally the brain, the cervical spinal cord and upper portion of the thoracic spinal cord were taken out in one, and the skull base duramater was opened to check skull base fractures. After taking photographs and weighing, the brain and spinal cord were held in 10% formalin solution. After 4 weeks or so, they were dissected and studied under an optical microscope.

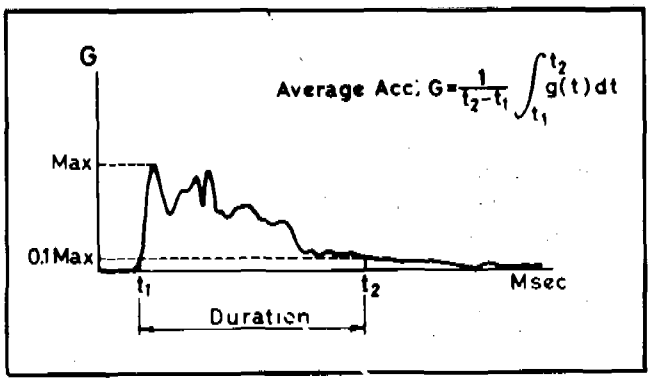

Figure 5. Duration of acceleration; time interval t_1 -t_2 at 10% level of max. acceleration is assumed as acceleration duration.

EVALUATIONS OF IMPACTS AND INJURIES

Magnitudes of impacts on the head were evaluated by head acceleration and its duration, while brain injuries were evaluated by the extent of damage to brain concussion and pathological brain injuries. The methodology and criteria are given in the following.

Magnitude of Impacts

The magnitude of impact from the impactor to the test monkey head is judged by the averaged resultant head acceleration and its duration.

The resultant acceleration is expressed by the absolute value of the sum of vectors of accelerations on X, Y and Z axes. The resultant acceleration is obtained by equation (1), while the duration of the resultant acceleration is expressed by 10% level interval against the maximum of the resultant acceleration (Figure 5).

$$G_R(t) = \sqrt{G_X^2(t) + G_Y^2(t) + G_Z^2(t)} \qquad (1)$$

where, G_R : resultant acceleration
G_X : X-axis acceleration
G_Y : Y-axis acceleration
G_Z : Z-axis acceleration

The averaged value of the resultant acceleration is the value obtained by the integral value of accelerations within the duration by the duration.

Criteria of Brain Concussion

The extent of damage of brain concussion is judged mainly by 3 indices of 1) disappearance of ciliary reflex, 2) apnea and 3) bradycardia, while making reference to test results of neurological reflex and physiological response.

Criteria:

a. Ciliary reflex disappears for 20 seconds or longer after impact
b. Apnea continues for 20 seconds or longer after impact
c. According to the degree and duration of bradycardia, bradycardia is classified by "none", "slight" and "severe", and judged as "severe".

The degree of brain concussion is classified into 3 grades as listed below, according to the criteria mentioned above.

Brain concussion grade 0: does not fall under either one of a, b or c.
Brain concussion grade I: falls under either one of a, b or c.

Brain concussion grade II: falls under two out of a, b and c.

Brain concussion grade III: falls under all of a, b and c.

Criteria of Pathological Changes

Pathological brain injuries differ greatly according to the area and contents of injury. Although it is difficult to make a general classification and grading of pathological brain injuries in terms of morphology, the location of injury, etc., grading is given in this report as listed on Table 1 for injuries found by this experiment. Consequently, pathological brain injuries were classified into 4 grades, including the grade of "intact".

RESULTS OF EXPERIMENT

Impacts were applied 1 to 5 times per test monkey, which totaled 75 times for 23 monkeys, with impactor velocity of 10 to 27 m/s, impact strokes of 20 to 80 mm and impactor head rubber hardnesses of 20 to 70. As a result, significant brain concussions (grade II and III) were found 12 times (16%) out of total impacts of 75 times, some degrees of pathological brain injuries were found in 18 monkeys (78%) out of 23 monkeys, and skull fractures were found in 6 monkeys (26%).

Head Behaviors

According to results of high speed film analysis, details of head behaviors upon impact differ from impact to impact according to differences in impact conditions. For macroscopic behaviors of test monkeys, however, the following common sequential behaviors were found starting from the moment when the monkey head contacted the impactor to the moment when the monkey head stopped.

(1) Initiation of impact: The impactor head surface contacted the temporal region while keeping itself parallel to the sagittal plane of the test monkey. As the impact progressed, the monkey head started moving toward the direction of impact, while crushing into the impactor head.

(2) Progression of impact: As the impactor further progressed, the monkey head started falling to one side with the neck acting as the fulcrum, while crushing further into the impactor head.

(3) Impactor stop: The impactor stopped with the preset stroke. In some cases, the monkey head was accelerated due to the rebound of the impactor after its stopping, while in other cases the head was not accelerated.

(4) Termination of impact: Even after the monkey head left the impactor head, it fell sidewise further with the neck still acting as the fulcrum, then stopped as the inclination angle became 90° to 100°, and was held by the side net.

(5) Finale: The body fell toward the direction of impact as it was pulled by the head through the neck, then held by the side net. The side net in turn inclined by 60° or so while braking down the speed, then stopped. As mentioned above, nearly reproducible macroscopic head behaviors were obtained throughout the experiment.

Table 1. Classification of pathological brain injury of no-fractural case.

Injury Severity	Injury
0	Intact
I	Subarachnoid hemorrhage
II	Cortical or Subcortical Hemorrhage Callosal hemorrhage Thalamus or Basal ganglia hemorrhage
III	Brain stem hemorrhage Subependymal hemorrhage Subdural hemorrhage

Head Accelerations

Measurements of effective head acceleration for all of X, Y and Z axes were obtained in 56 cases. In the 56 effective measurement cases, accelerations occurred in all directions of X, Y and Z axes. For the processing of acceleration data, a low-pass filter with a cut-off frequency of 1650 Hz was used. Typical examples of time histories of head accelerations are shown in Figure 6. In every impact, the Y-component head acceleration which coincided with the direction of impact showed the maximum acceleration. In case of the time history of Y-component head acceleration, the standard pattern of waves was that a triangular wave with a sharp peak appeared initially, and was followed by a half sine wave or flat wave. The peak value of the sharp triangular wave which appeared first tended to become greater as the impactor velocity increased or the impactor head hardness become harder, ranging from 190 G to 2800 G. The head acceleration wave of Y component that followed the first sharp wave varied its form according to impact conditions. Under conditions where the impactor was soft (rubber hardness 20) and the impact stroke was long (60 to 80 mm), the duration of head acceleration tended to become long, while the duration of head acceleration tended to become shorter where the impactor head was hard (rubber hardness 70) and the impactor strokes were short (20 mm).

Head accelerations of X and Z component were smaller than the Y-component acceleration, but the duration of acceleration was longer for the Z component in most cases. This was due to the rotation of the head around the X axis centering about the neck, and the Z component acceleration continued even after the head had left the impactor head. The acceleration of the X component was smaller than Y and Z components in every case.

The wave form of the resultant acceleration obtained from each component of acceleration in X, Y and Z axes

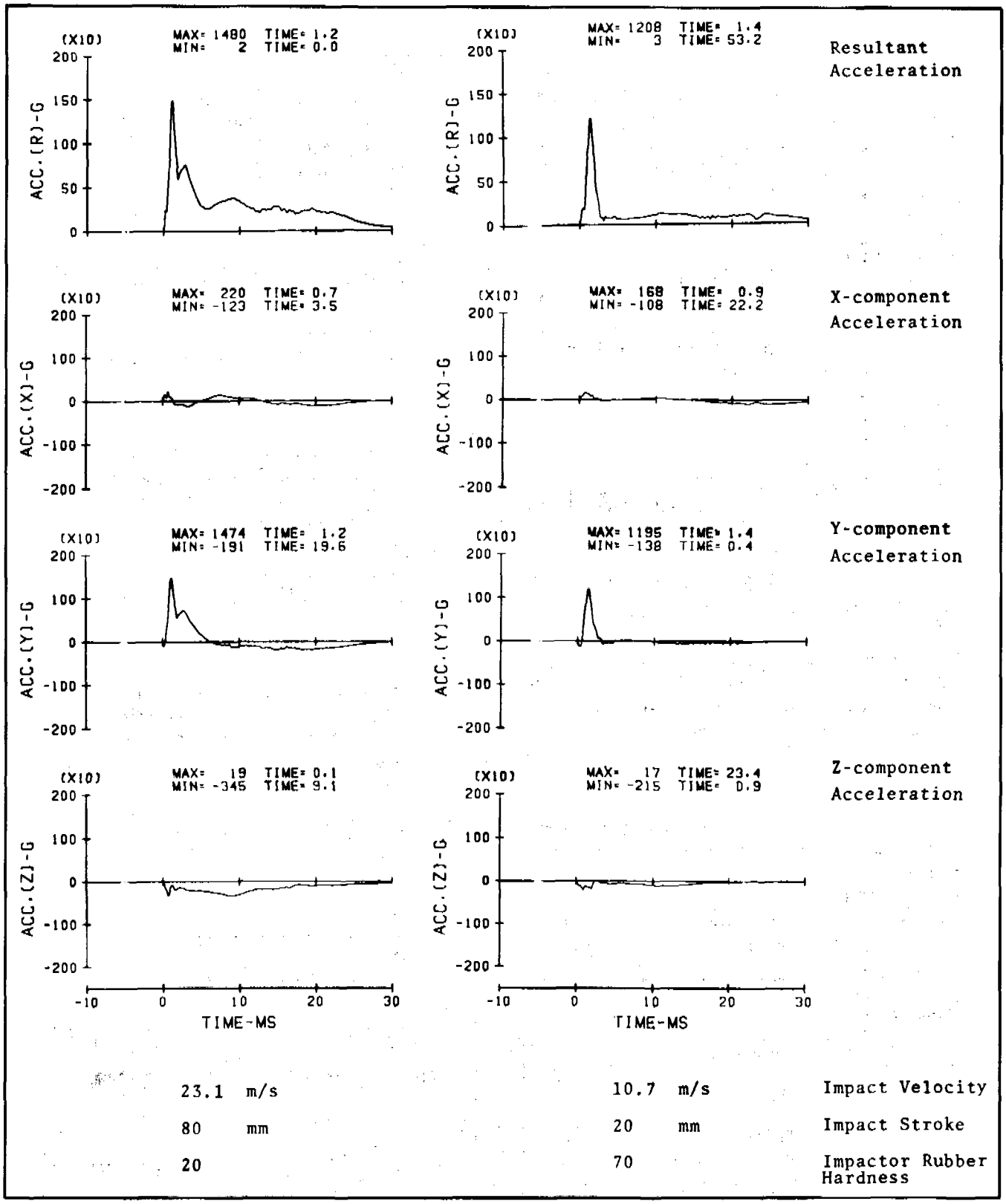

Figure 6. Time histories of head acceleration.

had wave form approximate to the sharp peak wave of the acceleration of the Y component which was the principal component, and it also appeared in the initial stage of impact, and the effect of the Z component on the duration of the resultant acceleration was significant. The averaged resultant head acceleration of 56 effective measurements ranged from 70 to 1310 G, and the duration was in the range of 2.2 to 43.0 ms.

Head Injuries

Physiological and neurological observations: Some physiological and neurological changes were observed in every case. Respiration stopped initially after impact, then resumed as time went by in many cases. In cases where the injury was slight, however, the respiration cycle hardly changed, whereas test monkeys died without recovering from apnea in cases of severe injuries, showing significant variations in respiration. Nevertheless, respiration patterns may be roughly classified into the following 5 types (Fig. 7).

a. No changes in respiration cycle
b. Respiration stopped initially rapidly resumed after a certain time
c. Respiration stopped initially resumed gradually
d. Stopped respiration was initially resumed but deteriorated again
e. Stopped respiration was not resumed

Of 5 types listed above, cases that fell under b and d often showed irregular an weak breathing, but all of them were considered as recovered cases. Therefore, out of 56 effective head acceleration measurements, cases that required more than 20 seconds (a criterion for brain concussion) to recover from apnea were 12, and 10 cases of no-skull fractures were found.

Correlationship was found between blood pressure and heart rate. That is, in many cases, the greater the blood pressure fluctuation, the greater became the variation in heart rate. Blood pressure variation patterns after impact may be classified into the following three types, as shown in Figure 8. Normally, during the fluctuation of blood pressure, bradycardia also appeared, and as the blood pressure resumed its original level, bradycardia also disappeared. Therefore, bradycardia was nearly nil or slight when the blood pressure fluctuation was Type I, but it became more significant for Type II and Type III. The case with the most significant bradycardia showed Type III blood pressure fluctuation and the R-R interval on the ECG was 0.5 sec before impact and 5.6 sec after impact, showing an increase rate of 11 times or so, the original interval then resuming within 5 minutes or so. The recovery time in most cases was between 1 and 5 minutes. Damages appearing in heart rate were judged as "none", "slight" and "severe" using R-R interval and its duration as criteria. Consequently, 17 cases out of 56 impacts of head acceleration effective measurements were judged as "severe", which means that at least one of our criteria for brain concussion, out of 15 cases of non-skull fractures, was found. In most cases ciliary reflex and light reaction were found to be lost, and cases in which ciliary reflex was resumed within 10 sec amounted to 17 cases out of 56, accounting for 30% of the total effective measurements, and those which recovered within 20 sec accounted for 70% or so. The longest recovery time was 154 sec. As for light reaction, on the other hand, 16% were less than 10 sec, and 57% less than 20 sec, with the longest recovery time being 190 sec. The number of cases requiring more than 20 sec (a criterion for brain concussion) for the recovery of ciliary reflex was 17, out of which 12 cases had no-skull fractures.

Using respiration, heart rate and ciliary reflex mentioned in the foregoing as indices, brain concussion judgments for the 56 effective head acceleration measurements were done as follows; brain concussion 0: 30 cases, brain concussion I: 16 cases, brain concussion II: 6 cases, and III: 4 cases. Thus significant brain concussion was observed in 10 cases (18%), out of which 3 monkeys had skull fractures.

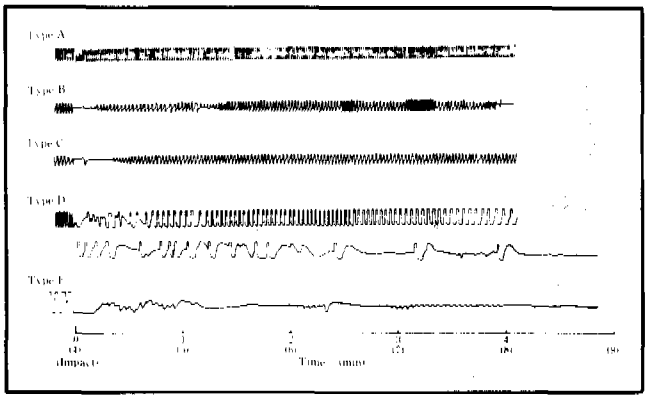

Figure 7. Respiration pattern after impact.

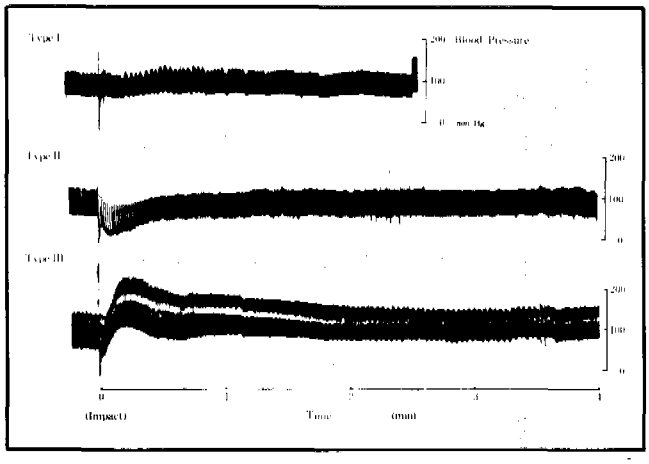

Figure 8. Blood pressure pattern after impact.

Pathological observations: Skull fractures were found in 6 monkeys, out of which one monkey did not have pathological brain injury due to the fact that the fracture was only orbital. The remaining 5 monkeys had skull base fractures, all of which except one were comminuted depressed fractures. This type of fracture caused very serious injuries of brain contusion, brain crush, subdural hemorrhage, etc. as compared with non-fracture cases, and such monkeys died within 15 minutes. Neurological reflex and physiological response of two monkeys of the above resumed within 1 minute, but two other monkeys resumed neither of them.

Of 17 monkeys that had no-skull fracture, on the other hand, one died within 15 minutes and two others died in 6 to 7 days. The 15 minute fatal case had extensive subdural hemorrhage and subarachnoid hemorrhage, and judged as "brain concussion III". Two fatal cases that died in 6 to 7 days did not show any visible injuries, and their brain concussions were below "brain concussion I". Pathological brain injuries of total 18 monkeys consisting of 17 no-fracture cases and 1 case of orbital fracture without any effect to the brain are shown on Table 2. Of the above, subarachnoid hemorrhage was found in 9 monkeys and callosal hemorrhage in 9 monkeys. Cortical hemorrhage and subcortical hemorrhage were also found in 10 monkeys, respectively. Brain stem hemorrhage was observed in 4 monkeys, and subdural hemorrhage was observed in 5 monkeys, out of which 1 fatal case occurred. Moreover injuries were both to the impact side and opposite side of impact, in combinative or separately. No-cortical contusion was found directly beneath the impact.

The classification of pathological brain injury to such no-skull fracture is as follows, according to the injury grades shown on Table 1; pathological injury severity (abbreviated to patho. injury severity) 0: 5 monkeys, severity I: 0, severity II: 7 monkeys and severity III: 6 monkeys. Of these monkeys, effective measurement cases of head acceleration were 3, 0, 4 and 6 monkeys, respectively.

Table 2. Pathological brain injuries no-fractural cases.

monkey No. / Patho brain injury	1	2	3	4	5	6	7	8	9	10	11	12	13	14	15	16	17	18
injury severity	0	II	III	II	III	II	III	0	II	0	III	III	0	III	II	0	II	II
subarachnoid hemorrhage			B.L.	B.L.	B.L.		B.L.		B.L.		B.L.	B.L.			B.L.		B.L.	
cortical hemorrhage		B.L.	B.L.		B.L.	B.L.			B.L.						B.L.		B.L.	B.L.
subcortical hemorrhage			B.L.	B.L.	B.L.	B.L.			B.L.		B.L.				B.L.			B.L.
callosal hemorrhage			B.L.	B.L.	B.L.	B.L.			B.L.		B.L.			B.L.	B.L.			B.L.
hemorrhage of thalamus or basal ganglia											B.L.							
brain stem hemorrhage			B.L.		B.L.		B.L.				B.L.							
subependymal hemorrhage			B.L.		B.L.													
subdural hemorrhage			B.L.		B.L.						B.L.	B.L.		B.L.				

I.L.: ipsilateral to the impact side, C.L.: contralateral to the impact side, B.L.: bilateral

DISCUSSION

Since the mechanism of injuries accompanying skull fractures differs substantially from that of no-fractural cases, the relationship between severity of the no-fractural head trauma and the magnitude of impact will be discussed in this report.

Head Acceleration and Brain Concussion

Assuming that the case of orbital fracture is a no-skull fracture, impacts that did not produce skull fracture were 70 cases, of which 53 cases were effective head acceleration measurements. For the 53 cases, relationship between head acceleration/duration and the severity of brain concussion is shown in Figure 9.

The head acceleration is represented by the mean of the resultant acceleration of X, Y and Z components, while the brain concussion is expressed as brain concussion grades of 0 (intact), I (slight) and II or III (significant). In Figure 10, concussion grades 0 and I incidence, and concussion grades I and II or III incidence distributions are partially overlapped, but respective regions of brain concussion grades 0, I and II or III are nearly clarified. In particular, incidence regions of concussion grade 0 and II or III are clearly separated by the boundary which is approximate to the hyperbolic curve, without any overlap. The inclination of the boundary is nearly approximate to inclination of the brain concussion threshold curve on the frontal impact or occipital, and furthermore, the boundary also constitutes approximately the center of the incidence region of brain concussion grade I. From the foregoing findings, it may be deduced that it is necessary to have greater acceleration/duration than the boundary between concussion grade 0 and II or III shown in Figure 9, in the head of a subhuman primate subject to lateral impact in order to induce significant brain concussion in them. It may thus be said that the boundary between brain concussion grades 0 and II or III is the threshold of brain concussion against lateral impact for subhuman primates.

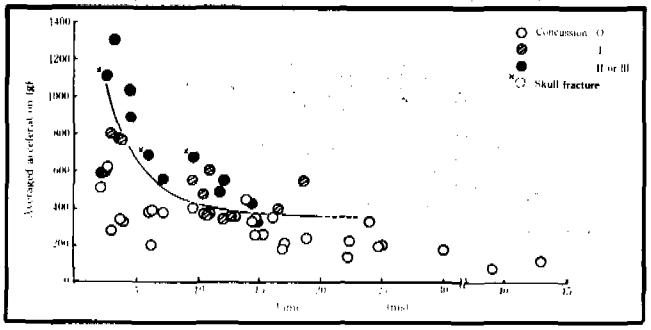

Figure 9. Correlation between averaged head acceleration-duration and grade of concussion in lateral impact.

Head Acceleration and Pathological Brain Injuries

The relationship between the head acceleration/duration and pathological brain injury was investigated, assuming that organic injuries had occurred in impact in which the neurophysiological responses had been the severest in a series of impacts for the same monkey (Fig. 10). In most cases, the severest damage was observed in the final impact. Cases of no-fractural injuries for which head acceleration measurements were effective are as follows; pathological injury severity 0, 4 monkeys; severity I, none (0); severity II, 3 monkeys; and severity III, 6 monkeys, totaling 13 monkeys. As the severity of injury declines from severity III to II and 0, the level of head acceleration/duration also tends to drop. At less than 15 ms of head acceleration's duration in Figure 10, as well as the case of concussion, the pathological injury severity 0 and III incidence distributions are not overlapped, but the underpart of pathological injury severity III incidence and grade II incidence distributions are overlapped. According to the above, the incidence lower limit of pathological injury severity III in Figure 10 which is obtained from these experiment results is the threshold of the subdural hemorrhage, the brain stem hemorrhage and the subependymal hemorrhage, and this threshold is higher than that of the brain concussion by lateral impact on the head as well as the case of frontal and occipital impact. However, it is suggested that the threshold of patho. injury severity II which is the hemorrhage of callosal, cortical or subcortical nearly agrees with or is lower than the threshold of brain concussion.

Extrapolation to Humans

In order to deduce the relationship between the impact and injury of human heads from the relationship between the impacts and injuries of subhuman primates stated above, the dimensional analysis method employed by Stalnaker et al. was applied to extrapolate human brain con-

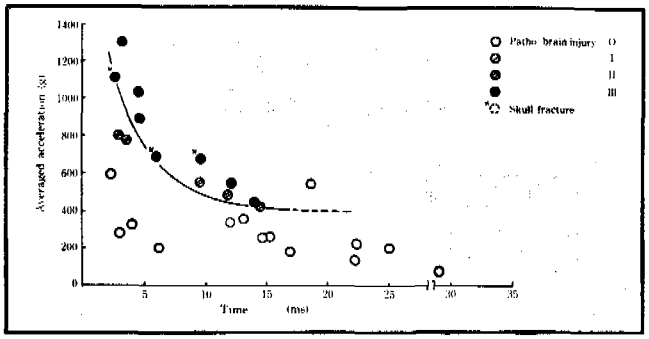

Figure 10. Correlation between averaged head acceleration-duration and grades of pathologica brain injury in lateral; on the patho. brain injury severity O, datas of all impact other than final impact of same subject were contained.

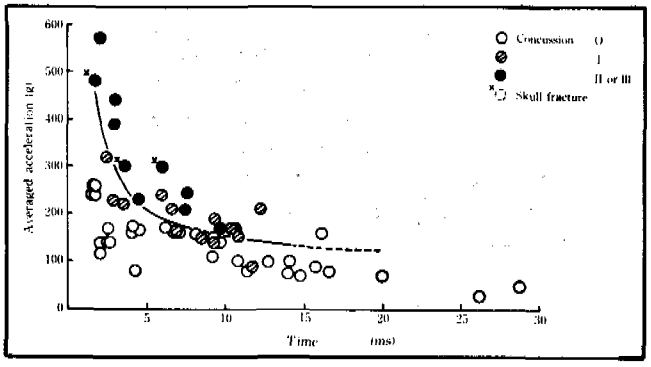

Figure 11. Threshold of concussion in human extrapolated from averaged acceleration-duration by dimensional analysis in lateral impact of the monkey head.

cussion threshold and pathological brain injury threshold. Assuming, therefore, that shapes of subhuman primates and human heads were analogous, and further that physical characteristics of biological tissues of their brains, skulls, etc. are the same, the head acceleration and duration, which would cause human head injuries equivalent to those of subhuman primates upon lateral impacts, were extrapolated. Parameters necessary for the dimensional analysis were the following five items: 1) head acceleration, a; 2) head acceleration duration, t; 3) impact speed, v; 4) average radius of skull, ℓ and 5) average thickness of skull, h.

Non-dimensional quantity π is expressed as $\pi_1 = 1/h$, $\pi_2 = vt/h$ and $\pi_3 = a \cdot h/v^2$. The relationships among π_1, π_2 and π_3 were determined by using the data (12,13) Stalnaker et al. obtained from subhuman primates of various sizes (sucioroid monkeys, Macaca mulattas, chimpanzees, etc.). The ratio between the average radius and average thickness of human heads in expressed at ℓ /h, and the average weight is assumed to be 1.35 kg.

Human head acceleration and its duration extrapolated from 54 cases of effective measurements of conversion parameters upon lateral impacts of subhuman primates are listed together with the relationship between brain concussion and pathological brain injuries in Figures 11 and 12. Similar to the case of subhuman primates, regions of brain concussions of grades 0 and II or III are also separated for humans, and brain concussion threshold based on grade II or III is also clearly indicated. This brain concussion threshold is represented by the hyperbola passing through 400 G — 2.2 ms and 160 G — 10.0 ms.

Lateral Impact Tolerance Threshold

It was believed from clinical experience, etc. that lateral impact tolerance was lower than the frontal and occipital impact tolerances. However, a comparison between the brain concussion threshold of subhuman primates obtained through this experiment and the results of frontal

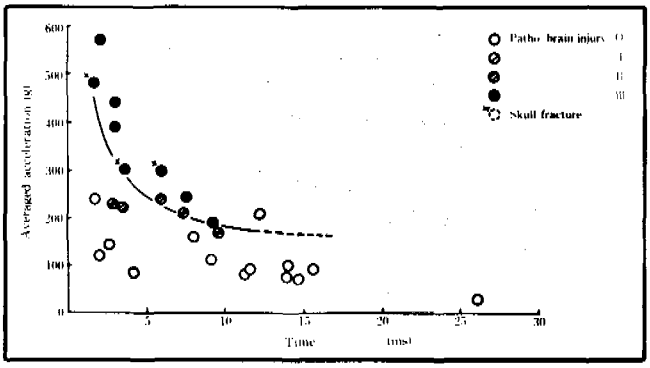

Figure 12. Threshold of pathological brain injury in humans extrapolated from averaged acceleration-duration by dimensional analysis in lateral impact of monkey head.

impact or occipital impact experiment previously reported by the author et al. reveals that the former has markedly higher tolerance than the latter. Gurdjian et al. suggested the WSTC employing brain concussion as the index to the human frontal impact safety threshold, while the author et al. reported the JHTC as the human brain concussion threshold upon frontal or occipital impact, extrapolated from subhuman primates. The comparison between the brain concussion threshold upon frontal or occipital impact indicated by the WSTC and the JHTC and the human brain concussion threshold extrapolated from the results of this experiment shows a clearly high tolerance for lateral impacts.

As regards the threshold of pathological brain injuries, a comparison was also made between the results of frontal or occipital impact already reported by the author et al. and the results of this experiment, which show that the tolerance is higher for the latter as compared with the former similar to the case of brain concussion stated above. According to the results of this experiment described so far, the temporal blow has much higher impact tolerance than the frontal and occipital in terms of brain concussion as well as pathological brain injuries, which agrees with the report published by McElhaney et al., (14) which stated that the impact tolerance to lateral impacts is much higher than that of occipital, according to a head impact experiment performed on primates using the criterion of "whether after effects would remain or not" as the indicator. McElhaney et al., however, reported at the same time that the frontal impact tolerance was higher than the lateral impact tolerance.

As for indices for frontal or lateral impact tolerance threshold, brain concussion is often used as the indicator, as in the JHTC cases and the WSTC. The reasons are that: 1) brain concussion is a transitory and recoverable injury, and 2) brain concussion is likely to occur at the lowest impact level as compared with brain injuries upon frontal or occipital impact. Impacts in the vicinity of the JHTC were such that "at most, subarachnoid hemorrhage might occur (15) (patho. injury severity I)", and it would have been necessary to apply more intense impact to produce skull fracture, subdural hemorrhage, brain stem hemorrhage, etc. (patho. injury severity III). However, the following symptoms were observed upon occurrence of brain concussion of subhuman primates by lateral head impact: 1) subarachnoid hemorrhage (patho. injury severity I) was found in nearly all cases, 2) cortical hemorrhage, subcortical hemorrhage, etc. (patho. injury severity II) were found in more than half the monkeys, and 3) even the concurrence of severe injuries such as subdural hemorrhage, brain stem injury (patho. injury severity III) was found in some cases.

On the other hand, it is reported that the lateral bone fracture load is lower than the frontal bone fracture load according to the studies on skull fracture by head impact, and that lateral bone fracture load is approximately 50 to 80% of the frontal bone fracture load according to a number of experiments. (14,16,17) It is thus deduced, from those studies and skull fracture threshold on frontal or occipital impact as shown in the appendix, that the skull fracture threshold of lateral head impact for humans is the impact level equivalent to or below those of WSTC or JHTC; also it is lower than the threshold for brain concussion on the lateral head impact.

From findings mentioned so far, it was deduced that the thresholds of subdural hemorrhage, brain stem hemorrhage and subependymal hemorrhage (patho. injury severity III) were highest, followed by brain concussion (grade II or III) and cortical hemorrhage and subcortical hemorrhage, etc. (patho. injury severity II) were next, while the threshold of subarachnoid hemorrhage and skull fracture were the lowest for lateral impact, different from frontal or occipital impact. This deduction agrees with a clinical fact that skull fractures are likely to occur in many cases by lateral impacts". Furthermore, this is considered to be one of the reasons for the common belief that the lateral impact tolerance is lower than the frontal impact tolerance due to the difference in the orders of thresholds of injuries as compared with frontal or occipital

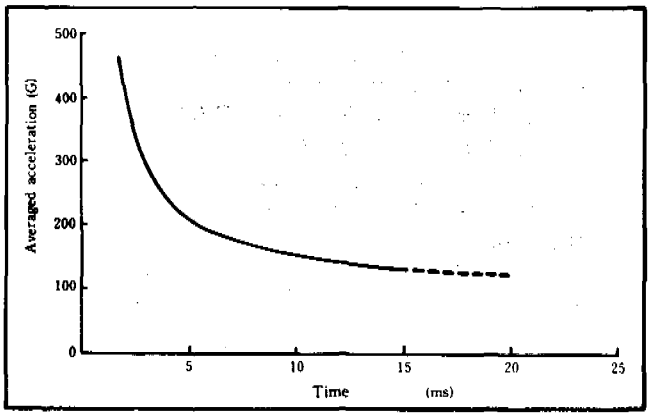

Figure 13. Human brain concussion threshold curve of lateral impact on the head.

impact. The human brain concussion threshold curve of lateral impact on the head extrapolated by the result of this experiment is shown in Figure 13. This is one indicator of judgment on lateral head impact safety. However it was estimated by this experiment that cortical and subcortical hemorrhages and callosal hemorrhage were often involved at time of the occurrence of brain concussion by lateral impact on the head. Consequently it is considered appropriate to determine the safety threshold of lateral impact by referring to skull fractures or subarachnoid hemorrhage of which the tolerance level is deduced to be lower than the tolerance level of brain concussion, brain stem hemorrhage, subdural hemorrhage, etc.

SUMMARY AND CONCLUSIONS

1) In order to clarify thresholds of brain concussion and pathological brain injuries, impacts were applied 75 times to temporals of 23 subhuman primates under various conditions. Of 56 cases of effective measurements, averaged resultant head accelerations of 70 to 1310 G with durations of 2.2 to 43.0 ms were produced, and brain concussion (grade II and III) was found in 10 cases. Of 23 test monkeys, some pathological brain injuries were found in 18 monkeys.

2) For skull fracture cases, the relationship between the head acceleration and brain concussion, and the relationship between head acceleration and pathological brain injury were investigated in order to clarify brain concussion threshold and thresholds of subdural hemorrhage, brain stem hemorrhage, etc. upon application of lateral impact. Extrapolation was also made from data of subhuman primates to humans.

3) Brain concussion threshold of lateral impact, and thresholds of subdural hemorrhage, brain stem hemorrhage, etc. for humans and primates showed higher values than those of frontal or occipital impact.

4) In lateral impact on the head, threshold for hemorrhage of brain stem, subependymal and subdural is higher than that of concussion, and threshold for hemorrhage of cortical, subcortical and callosal nearly agrees with or is lower than the threshold of brain concussion. Comparing these thresholds with JHTC and the skull fracture threshold it is deduced that the threshold of skull fracture is lower than the threshold of brain concussion and cortical hemorrhage, etc.

5) It has been believed from the clinical point of view in craniocerebral injury that the tolerance to lateral impact is lower than the tolerance to frontal impact. It is deduced that one of the reasons for the above concept is that the relationship of skull fracture threshold, brain concussion and various pathological brain injuries threshold differs between the case of frontal or occipital impact and the case of lateral impact.

6) Various pathological brain injuries are often involved at time of occurrence of brain concussion by lateral impact on the head. Therefore slight skull fracture or subarachnoid hemorrhage is an adequate indicator of tolerance by lateral impact on the head.

ACKNOWLEDGEMENTS

The authors received generous assistance from many research and laboratory staff members of the Neurosurgery Departments of the Tokyo Jikeikai University School of Medicine, the University of Tokyo, and Tokyo Women's Medical College and Engineering Department of the University of Tokyo.

REFERENCES

1. K. Sano, N. Nakamura, K. Hirakawa, H. Masuzawa, et al.; Mechanism and dynamics of closed head injuries (preliminary report). Neurol. Medicochir. (Tokyo) 9:(1967)
2. C. B. Courville; Coup-contrecoup mechanism of craniocerebral injuries. Some observations. Arch. Surg. 45:(1942)
3. R. Hooper; Patterns of Acute Head Injury. Edward Arnold Ltd., London (1969)
4. E. S. Gurdjian, H. R. Lissner and L. M. Patrick; Protection of the head and neck in sports. JAMA 182:(1962)
5. E. S. Gurdjian, V. R. Hodgson, W. G. Hardy, L. M. Patrick and H. R. Lissner; Evaluation of the protective characteristics of helmets in sports. J. Trauma 4:(1964)
6. L. M. Patrick, H. R. Lissner and E. S. Gurdjian; Survival by design-----Head protection. Proc. 7th Stapp Conference 7:(1965)
7. H. Sekino, N. Nakamura, A. Kikuchi, K. Ono, et al.; Experimental Head Injury in Monkey Using Rotational Acceleration Impact. Neurologia medico-chirurgica Vol. 20, No. 2: 1979 (Japanese)
8. H. Kohno, N. Nakamura, M. Matuno, et al.; Experimental Head Injury and Concussion—Morphologic Change and Pathophysiologic Following Translational Acceleration in Primates. Neurologia medico-chirurgica Vol. 19, No. 8; 1979 (Japanese)
9. R. Kanda, N. Nakamura, A. Kikuchi, K. Ono, et al.; Experimental Head Injury in Monkeys-Concussion and its Tolerance Level. Neurologia medico-chirurgica, Vol. 21, No. 7:1981
10. K. Ono, A. Kikuchi, M. Nakamura, H. Kobayashi, N. Nakamura; Human Head Tolerance to Sagittal Impact Reliable Estimation Deduced from Experimental Head Injury Using Subhuman Primates and Human Cadaver Skulls. Proc. 24th Stapp Conference 24: 1980

11. A. Kikuchi, K. Ono, H. Kobayashi, N. Nakamura, M. Nakamura; Evaluation of Head Tolerance to Sagittal Impact by Head Acceleration and Duration, and Head Velocity, JSAE Review, No. 3:1980
12. R. L. Stalnaker, V. L. Roberts and J. H. McElhaney; Side Impact Tolerance to Blunt Trauma. Proc. 17th Stapp Conference 17:1973
13. R. L. Stalnaker, J. H. McElhaney, R. G. Snyder and V. L. Roberts; Door Crashworthiness Criteria. U. S. Dept. of Transportation Report No. HS-800-S34; 1971
14. J. H. McElhaney, V. L. Roberts and F. Hilyard; Handbook of Human Tolerance. Japan Automobile Research Institute, Inc.: 1976
15. H. Sekino, N. Nakamura, et al.; Brain Contusion Detected by CT Scan in Minor Head Injury. Neuro Traumatology: 1979
16. J. W. Melvin and P. M. Fuller; Effect of Localized Impact on the Human Skull and Patella. SESA Paper No. 70-491: 1970
17. A. M. Nahum, J. D. Gatts, C. W. Gadd and J. Danforth; Impact tolerance of the skull and force. Proc. 12th Stapp Conference 12: 1968

APPENDIX

It is a figure that shows the threshold of concussion and cadaver skull fracture in human on frontal or occipital impact. (10)

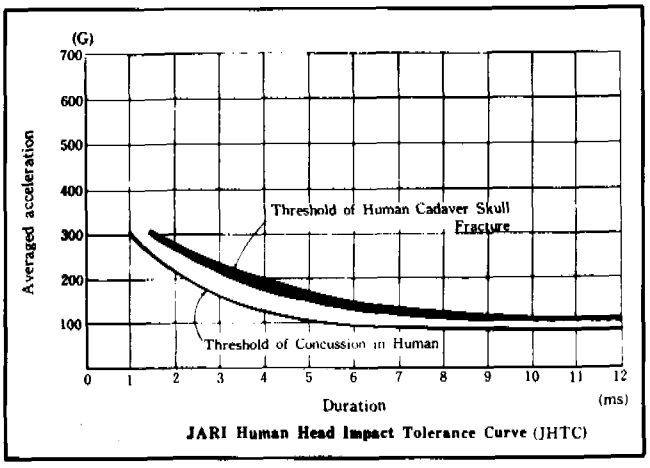

Tolerance of Human Pelvis to Fracture and Proposed Pelvic Protection Criterion to be Measured on Side Impact Dummies

D. CESARI, M. RAMET and R. BOUQUET
O.N.S.E.R. France

INTRODUCTION

<3675>

The problems of side impact protection have been extensively analysed in several countries in the world.

To make the evaluation of protection offered by cars against side impact, proposals of side impact tests using a mobile deformable barrier have been made as well in the United States (1) as in Europe (2).

The evaluation of car behaviour in side impact would be made through the values of injury parameters recorded on dummies. These injury parameters would be related to injury mechanisms of real side impact accidents.

This paper analyses the results of 60 cadaver tests conducted to determine the pelvis tolerance and to propose a protection criterion of pelvis in side impact.

TEST METHODOLOGY

All the tests were performed using a device especially designed to reproduce impacts similar to those observed in real accidents. The procedure we used has been described in a previous paper (3) but it is briefly described hereafter. The device is made of a fixed frame and a mobile impactor, horizontally guided in order to hit a human subject seated on a rigid seat locked with the frame end.

The mobile part is propelled by rubber extensible springs and the system is tightened through a small trolley guided on the same axis as the impactor and attached to a steel cable. It is possible to pull on the cable through a winch and then to move the trolley and the impactor back by tightening the rubber extensible springs. A bolt located between the trolley and the impactor releases the impactor which is then accelerated by the rubber extensible springs and hits the human subjects.

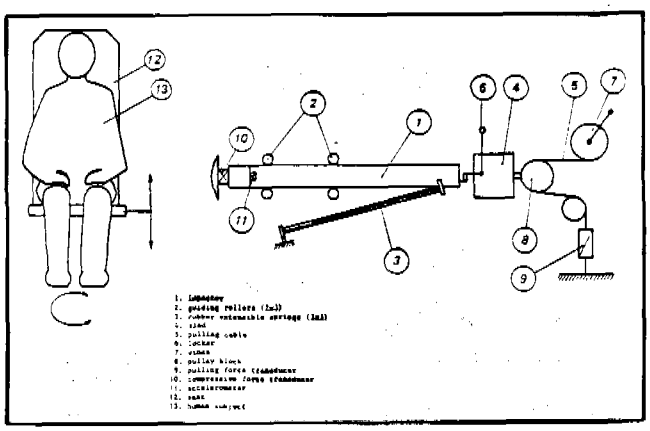

Figure 1. Impactor diagram.

The impactor mass is 17.3 kg and the impacting system is the portion of a sphere (r = 600 mm, R = 175 mm). The impact force and impact acceleration are measured on the mobile system through transducers.

All the tests were performed with fresh human cadavers. They were incised along the iliac crest to expose the internal face of the wing of ilium. Three strain gauges were applied on this internal face : 2 below the iliac crest and 1 behind the acetabulum. These gauges were plastic sheathed, which made their fitting simpler.

Then, the incision was sutured. A fourth gauge was placed on the same side on the upper face of the ilio-pubic ramus. Then, the cadaver was dressed up, weighted, measured and placed on the seat. The seat was centered on the trochanter major tuberosity.

The seat used gave the cadaver a posture identical to that of a car driver. The subject was unbelted and without lateral support.

In order to reach the pelvic fracture at a level as close as possible to the tolerance, several tests at increasing impact speed were conducted on the same cadaver. However, we performed only one impact test on 5 cadavers because the fracture happened at this first test. The results of these 5 tests would also allow to verify the influence of following tests on the same cadaver.

An X ray picture is taken after each test to verify whether it produced a fracture or not. Moreover, an X ray picture is taken before the tests to verify that there was no previous fracture or important osseous decalcification.

We decided to perform tests with unbelted subjects, because the analysis of car-to-car collisions shows that the safety belt is generally not solicited in lateral impact, at least during the main phase of the impact.

Sixty impact tests on pelvis were performed for this study, using 22 cadavers. All the tests, excepted five which were performed with a padded impactor, were conducted using a rigid impactor described previously. Additional static tests have been conducted on five half pelvis in order to determine the force distribution inside the pelvic bone. Cortical area and inertia momentum of the two rami have been calculated for the pelvis of 10 cadavers.

RESULTS

The results of impactor tests reported here are analysed in different directions:

—Injuries found by the autopsy,
—Dynamic test results,
—Static test results and bone mechanical properties.

Table 1.

Test N°	AIS	Injuries
A4	3	Fracture of the right ilio + ischio-pubic rami sacro iliac disjunction non complete fracture of sacrum
B3	3	Fracture of the right ischio-pubic ramus Fracture of the right femoral neck and collapse of the femoral head
C4	3	Fracture of the right iliac wing Fracture of the right femoral shaft
D2	3	Fracture of the right ilio and ischio-pubic rami, fracture of the right femoral neck, sacro iliac disjunction
E2	3	Fracture of ilio and ischio-pubic rami Sacro iliac joint disjunction
H4	2	Right femoral shaft fracture
I5	2	Fracture of the right iliac wing
J3	3	Fracture of the right ilio and ischio-pubic rami. Pubic symphisis disjunction
M3	2	Fracture of the right iliac wing
N7	3	Fracture of the right iliac wing. Fracture of the right ilio and ischio-pubic rami. Right sacro iliac disjunction
O6	3	Fracture of the right ilio and ischio-pubic rami and right sacro iliac disjunction
R5	2	Fracture of the sacrum
S4	3	Collapse of the head of the right femur through the acetabulum. Fracture of the right and left ilio and ischio-pubic rami
T2	3	Fracture of the right acetabulum. Fracture of the right ilio and ischio-pubic rami
V2	3	Multiple fracture of the right ilio and ischio-pubic rami. Fracture of the right femoral neck
W2	2	Fracture of the right femoral shaft
X2	3	Fracture of the right and left ilio and ischio-pubic rami. Bilateral sacro iliac disjunction
Y2	2	Fracture of right ilio and ischio-pubic rami
Z2	3	Fracture of the right ilio and ischio-pubic rami. Right sacro iliac disjunction

RESULTS CONCERNING THE INJURIES

The injuries sustained by the cadavers during the impactor tests were carefully recorded by an autopsy made after the tests. During this autopsy the pelvis was removed and the pelvic fractures carefully analysed. This procedure allows us to set up a complete list of pelvic injuries sustained by the cadavers during the tests. The injuries recorded during autopsies are listed on Table 1.

Pelvic injuries sustained in side impact real accidents are not generally described in details; however, an in-depth study of pelvic fractures in side impact accidents gives a description of injuries sustained by impacted side accident victims (4). The distribution of these injuries and those recorded on cadavers are listed in Table 2.

Comparison of accident and test injuries shows a good correlation with nevertheless some minor differences. In both samples the fracture of pelvic rami is the most frequent injury (13 among 19 in tests and 12 among 14 in accidents). However the pelvic rami fractures are mainly on one side in tests whereas they involve both sides in accidents: these differences seem to depend from the severity of impact; the tests were made at increasing speed until a pelvic injury was found, which limits the extension of injuries, whereas in accidents the energy dissipated by the impact between the occupant and the side parcel can be higher than the energy necessary to produce injuries, and then this impact can make extensive fractures.

The pubic rami fractures seem to be a typical injury of direct lateral impact in the sitting position (which corresponds to the position of car occupants). In tests conducted in similar conditions, but with cadavers having legs in line with the torso, i.e., like in standing posture, (5) the injuries found were completely different: they were mainly acetabulum (hip) fractures: but the energy to produce these injuries was in the same order of magnitude as the energy amount necessary to produce side impact pelvic injuries.

The other differences concern mainly the number of femoral neck fractures and of sacroiliac disjunctions.

The femoral neck fractures are very rare even if we have found more in tests than in accidents. The femoral neck mechanical resistance decreases with age (the spontaneous femoral fracture of elderly is well known) and the cadavers used in these tests were older than the victims of car accidents.

The sacroiliac disjunctions seem also more frequent in tests than in real accidents. These injuries have never been found isolated, but always associated with pubic rami fractures.

In two tests these disjunctions were very minor and were not found by X ray pictures analysis but only at the autopsy; such injuries could be forgotten on human living.

In a general way cadavers sustained on an average, less pelvic injuries than human people involved in side accidents (51 pelvic injuries for 19 cadavers against 47 injuries for 14 accident victims). This increasing of the number of injuries can be associated with the higher severity of impacts in accidents compared to the tests.

Table 2.

Location	Number of fractures	
	Tests (19)	Accidents (14)
Femoral shaft	3	4
Femoral neck	3	1
Acetabulum	2	1
Iliac wing	5	3
Pubic symphisis	1	1
Sacro-iliac symph.	6	3
Sacrum	1	1
One ramus	1	1
Two rami	10	5
Three rami	0	3
Four rami	2	3
Pelvic crush	1	1

DYNAMIC TEST RESULTS

For the purpose of this study 60 tests have been conducted: 55 of them were performed with a rigid impactor and 5 with a padded impactor. For all the tests the impactor was centered on the right great trochanler. They are analysed separately in this paper.

RIGID IMPACTOR TESTS

The results of the 55 tests performed with a rigid impactor are listed in Table 3. These tests were made with 19 cadavers. Six of them are female cadavers whose age varies from 59 years old to 84 years old with an average value of 71 years old. The age of the 13 male cadavers varies from 54 years old to 85 years old with an average value of 72 years old.

The cadavers used in this study were carefully selected according to their antecedents and the medical treatment that they followed; however, one cadaver (M) had very poor bone conditions, and the results of this cadaver should be cancelled.

Analysis of results shows that there is a large scatter of the results. The 3 ms impact force corresponding to pelvic fracture varies from 4880 N to 12920 N for male cadavers and from 4440 N to 8200 N for female cadavers.

If we consider the tests in which injuries occurred, i.e., tests with an AIS 2 and AIS 3, the average value of the 3 ms impact force is 5600 N for female cadavers and 8600 N for male cadavers. This value of 8.6 KN is higher than the acceptable limit proposed by TRRL to be measured on a side impact dummy (the proposal was 6 KN) (6). The tentatives to correlate the impact force with other parameters did not give interesting results except the correlation between the impact force and anthropometric parameters such as cadaver height or weight. The an-

Table 3.

Test N°	Speed KM/H	Force Peak/3MS N	Accel. 3MS g	Impulse N.s	AIS
A1	21	4170/3355	—	63	0
A2	25.3	5800/4355	—	122	0
A3	30.0	6960/5220	—	163	0
A4	41.0	11140/8200	—	209	3
B1	21.0	5100/3240	—	71	0
B2	30.0	6260/5575	—	131	2
B3	34.9	8120/6200	—	161	3
C1	25.6	5620/5375	—	113	0
C2	32.0	10120/8070	—	136	0
C3	39.4	10140/8080	—	162	2
C4	47.5	13780/12920	—	232	3
D1	25.0	4410/3330	34	88	0
D2	30.8	5240/4720	45	115	3
E1	25.2	5520/4330	45	88	0
E2	31.1	5520/4440	34	112	3
F1	28.3	5610/4430	33	89	0
F2	31.1	3890/3330	24	90	0
F3	35.0	5610/4430	24	110	0
H1	25.5	6620/6390	27	82	0
H2	30.2	10760/10000	42	99	0
H3	34.6	11110/10440	40	128	0
H4	38.2	12690/10555		140	2
I1	25.5	10210/7330	39	77	0
I2	30.2	11040/7890	49	97	0
I3	35.5	11590/8440	49	115	0
I4	39.8	12690/8780	35	139	0
I5	40.1	13240/8935	80	157	2
J1	25.5	7730/6835	34	79	0
J2	30.6	6440/6110	30	124	0
J3	35.5	8270/6945	62	131	3
K1	25.0	5520/4665	34	73	0
K2	30.8	7170/4720	35	85	0
K3	35.0	8280/6720	40	102	0
L1	29.7	8330/8220	60	118	0
L2	35.0	11660/10275	60	130	0
L3	39.6	13330/11330	80	142	0
L4	44.6	15550/12770	120	174	0
M3	22.1	4330/3780	32	79	2
N5	33.0	8610/8390	59	110	0
N6	37.7	10000/9500	62	148	0
N7	41.1	10278/9580	72	163	3
O4	32.9	5695/5580	48	126	0
O5	37.8	6140/5890	51	142	0
O6	42.2	6830/6670	53	151	3
R1	36.5	9440/9280	68	163	0
R2	39.6	10694/10440	74	166	0
R3	43.4	10972/10750	81	168	0
R4	47.1	11806/11580	90	173	0
R5	50.6	12306/12080	95	177	2
S2	36.1	7083/6640	54	126	0
S3	40.7	6670/6500	60	137	0
S4	44.4	7140/6890	65	143	3
T2	34.6	4611/4445	33	107	3
V2	27.7	5740/4880	40	75	3
W2	30.0	7490/7165	56	98	2
X1	45.7				
X2	53.2	7620/7220	52	172	3
Y2	53.9	11130/10750	65	225	2
Z1	45.5	7360/7150	25	158	0
Z2	52.0	9120/8760	79	180	3

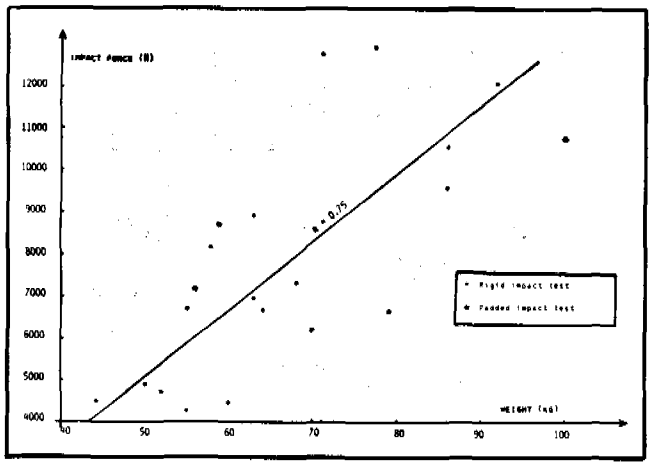

Figure 2. Cadaver weight versus 3 ms injury producing impact force.

thropometric parameters are correlated with bone sizes: taller and stronger persons have bigger bones, and the correlation found between impact force and height and weight seems to indicate a possible correlation between impact force and pelvic bone dimensions.

Figure 2 gives the value of 3 ms fracture producing impact force.

The corpulence of the subjects can be evaluated by the use of the Livi index which is defined by:

$$\text{Li} = 10\,\frac{\sqrt[3]{\text{Weight}}}{\text{Height}}$$

with weight in kg and height in m.

Based on statistical data the corpulence is defined as follows:

Li $\leq$ 22 : the subject is very thin,
22 $<$ Li $\leq$ 23 : the subject is thin
23 $<$ Li $\leq$ 24 : the subject is normal
24 $<$ Li $\leq$ 25 : the subject is stout
Li $>$ 25 : the subject is obese.

The values of Li are listed in Table 4.

These values can be used to correct the values of weight of cadavers. The proposed correction is:

$$W_c = W_a\,\frac{23.5}{\text{Li}}$$

in which W_c is the corrected weight, W_a is the actual weight, Li is the actual value of the Livi index. The coefficient 23.5 is the value of Livi index for a normal person.

The values of weight corrected according to Livi index values are also listed in Table 4.

If we draw the relationship between the 3 ms impact force of fracture producing tests, and the corrected weight we find a better linear correlation than with actual weight values, as indicated on Figure 4.

The correlation coefficient is .89 instead of .75 on Figure 3.

This better correlation confirms that the pelvic tolerance depends on the bone geometry which is linked to the anthropometry.

The value of impact force as a function of weight is given by the formula: impact force = 193.85 weight − 4710.6.

Table 4.

Cadaver	Sex	Age	Height cm	Weight kg	Livi Index	Corrected Weight kg
A	F	70	167	58	22.9	59.5
B	F	84	154	70	26.4	62.3
C	M	69	173	78	24.3	75.4
D	F	63	160	52	23.0	53.0
F	F	59	152	55	24.7	52.3
H	M	69	175	86	24.9	81.0
I	M	65	181	63	21.7	68.2
J	M	75	177	63	22.2	66.7
K	M	75	171	55	21.9	59.0
L	M	71	175	85	25.1	79.6
M	M	68	165	62	24.0	60.7
N	M	54	184	86	24.0	84.2
O	M	70	160	79	26.8	69.5
R	M	80	180	82	25.1	86.1
S	M	79	164	64	24.4	61.6
T	F	79	144	44	23.7	43.6
V	M	61	162	50	22.7	51.8
W	M	85	170	68	24.0	66.6
X	F	54	162	56	23.6	55.8
Y	M	74	175	100	26.5	88.6
Z	M	67	167	58	23.2	58.8

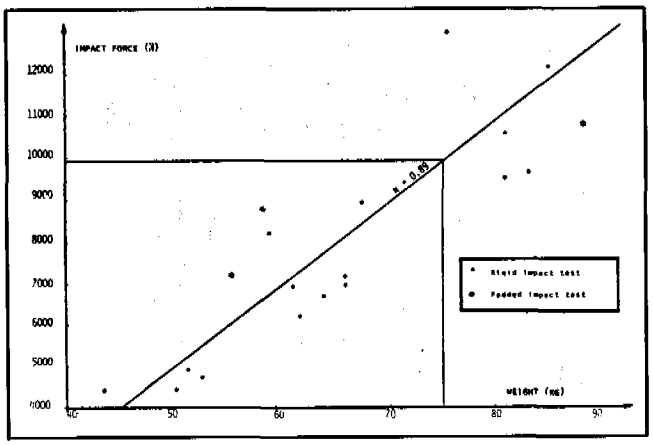

Figure 3. Corrected cadaver weight versus 3 ms injury producing impact force.

The value of impact force calculated for a weight of 75 kg, which is the weight of the 50th percentile male, is 9830 N, which is higher than the mean value for the cadavers used in this study.

During the test we recorded also pelvic acceleration; the values of 3 ms pelvic acceleration are listed in Table 2. All the values recorded are low and much under the proposed tolerance of 100 g's (7). This is probably due to the test methodology: in the impactor test only the pelvis is impacted and no other part of the body is restrained, whereas in drop tests and in sled or car tests, several areas of the body are involved by the impact.

The value of impact speed necessary to produce fractures is in the same order of magnitude as the door velocity change in car-to-car tests in which pelvic fractures occur (8). In these tests, the impact speed producing pelvic injuries varies from 22 km/h to 50 km/h.

Nineteen cadavers sustained following impacts at increasing speed, until five of them got a pelvic fracture at the first impact. Comparison of results shows that several following tests at increasing speed do not change the capability of the cadaver to sustain impacts: the traces of recorded parameters are not changed after the first impact. The value of impact force always increases until the fracture occurs, and, in fact, the value of fracture impact force was lower for cadavers which sustained only one impact than for cadavers which got a pelvic fracture after several tests.

PADDED IMPACTOR TESTS

Five tests with a padded impactor were performed on three cadavers. For these tests the impactor extremity was covered by a polyurethane foam parallelepipedic block (14.5 cm thick, 24.7 cm long, 14.5 cm wide, density 130 kg/m^3). These blocks were developed by APR as paddings for side impact protection. Two of them sustained an AIS 3 pelvic fracture after the second test, whereas the third one sustained only one test which produces an AIS 2 injury. The impact force values recorded on the impactor were in the same order of magnitude as those recorded during rigid impactor test. But the impactor speed necessary to produce pelvic fracture is undoubtedly increased by the padding; all the cadavers in padding tests sustained more than 52 km/h whereas the average value of impact speed in rigid impactor tests in which the injuries occurred in 37.1 km/h. These results are summarized in Table 5.

Table 5.

	Rigid	Padded	Gain
Average impact speed (km/h)	37.1	52.6	40%

PELVIC BONE CHARACTERISTICS

For 10 of the 22 cadavers used in impactor tests, we have determined the value of parameters related to the bone structure. For this we have cut a slice of the 2 rami of half a pelvis. We took macro pictures of these bone slices and from the scaled pictures we determined the total and cortical bone sections and the inertia momentum of these sections.

This was made with a computer which was used to digitize the outlines of the section and to make the calculations. The results of these parameters are included in Table 6.

The pubic rami are mainly involved in a bending process during a lateral impact; the stress at the fracture is defined by:

$$\sigma = \frac{P.L.Y}{Ix}$$

in which P is the force applied to the ramus, L the length of the ramus, Y the distance between the center of mass and the external surface of the ramus, and Ix the inertia momentum of the cortical area. As P is proportional to the impactor force and the variation of L is small the stress and the fracture could be written:

$$\sigma = KF\frac{Y}{Ix}$$

and then it would exist a linear relationship between F and $\frac{Y}{Ix}$. This relationship is drawn on Figure 4 which shows a good correlation.

However the values of geometrical parameters of the iliopubic ramus of the 50th percentile male have to be known to determine the human tolerance of this percentile. The geometry of human pelvis have been measured recently (9). The specific points for which coordinates

Table 6.

TBF	Ramus	S_t mm2	S_c mm2	I_x mm4	I_y mm4	Ymini mm	I_x Ymini mm3
C	ilio	311.5	98.6	3349.8	4946.7	8.41	398
	ischio	281	85.3	1417.6	7175.7	5.64	251
H	ilio	250.2	86	2145.4	3193.3	7.32	293
	ischio	136.4	47.6	417.7	1713.4	4.30	87
K	ilio	217.5	66.7	1306.7	3048.9	5.65	231
	ischio	160.1	42.6	359.8	2615.5	3.58	100
N	ilio	256.5	96.7	2286.2	4496.2	7.82	292
	ischio	202.4	65.2	564.8	1170.6	5.59	101
O	ilio	159.3	53.3	1199.8	1530.4	6.32	190
	ischio	112.3	32.4	248.2	1013.3	3.44	72
S	ilio	265.8	66	1748.2	3505.4	8.32	210
	ischio	165.6	43.3	687.5	1466.03	5.66	121
T	ilio	139.9	45.5	672.1	1105.3	5.91	115
	ischio	100.2	32.7	193.2	1093.4	3.20	60
X	ilio	178.4	61.7	1166.9	1722.3	5.91	204
	ischio	148.7	43.4	381.8	1856.7	3.32	115
Y	ilio	248.4	94.5	2450.4	4284.8	7.93	309
	ischio	137.1	49.7	600	1288.1	5.66	106
Z	ilio	225.9	67.3	1790.5	3006.1	6.86	261
	ischio	167.3	44.9	761.6	2382.3	4.82	159

were measured were on the exterior surface and thus it is not possible to determine the inertia momentum of the ramus section but by comparing the external dimensions, the inertia momentum of the iliopubic ramus cross section can be evaluated. The found value is Ix = 2300 mm^4 and the distance between the center of mass and the external surface y = 7,8 mm, for the 50th percentile. The corresponding value of Ix/y would be 295 mm^3, which corresponds to approximately 10 kN for the 3 ms impact force.

PROPOSED PROTECTION CRITERION

On the basis of the test results described behind the tolerance for a cadaver weighing 75 kg would be about 10 KN 3 ms impact force. This value would be the base for a protection criterion applied to a 50th percentile dummy. The use of such a protection criterion implies that the side impact dummies are able to be fitted with a pelvic lateral force transducer. At the present time only one side impact dummy type, manufactured by the MIRA, is fitted with pelvic force transducers.

This pelvis is equipped with 3 force transducers needing 5 measurement channels and the use of this dummy in several test environments (car-to-car tests, sled tests, impactor tests) have shown the feasibility of the measurement of pelvic lateral force in side impact; but as most of the injuries are located on the pubic rami it seems possible to simplify the force measurement device, and to use only one force transducer located in the anterior part of the pelvis.

CONCLUSIONS

Analysis of these test results allows to conclude as follows:

- —impactor tests reproduced realistic pelvic injuries at realistic impact speed
- —these injuries are mainly impacted side ischio and ilio-pubic rami fractures
- —the impact force seems more correlated to injury than other parameters
- —the value of the tolerable impact force varies greatly with anthropometry
- —there is a correlation between the geometry of the ischio pubic ramus cross section and the tolerable impact force
- —the use of a padding can protect efficiently by increasing the acceptable impact speed. A gain of 40% has been found
- —the value of the tolerance is close to 10 KN of 3 ms impact force for the 50th percentile male subjects
- —a protection criterion for pelvis based on the 10 KN tolerance could be used on a dummy fitted with a pelvic lateral force transducer.

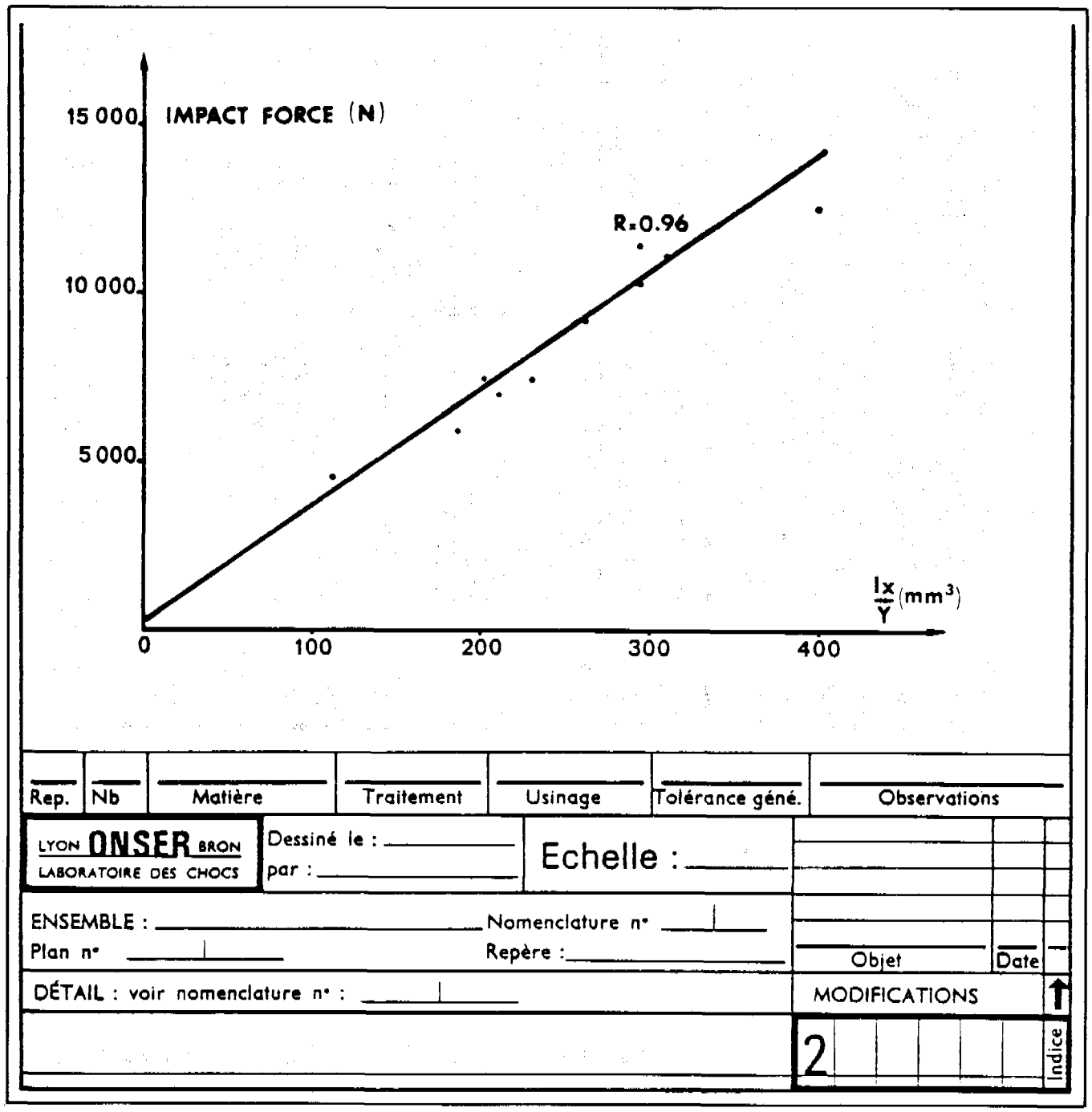

Figure 4. Injury producing impact force versus Ix/y of the ilio-pubic ramus.

REFERENCES

1. Davis, S., Ragland, C. Development of a deformable side impact moving barrier 8th International Conference on ESV, Wolfsburg 1980.
2. EEVC WG7 report-structures. Improved side impact Protection in Europe. 9th ESV Conference Kyoto—Nov. 1982.
3. Cesari, D., Ramet, M., Clair, P. Y. Evaluation of pelvic fracture tolerance in side impact 24th Stapp Car Crash conf., 1980.
4. Dejeammes, N. Fractures du bassin au cours des chocs latéraux automobiles. Thèse LYON 1978.
5. Creyssel, J., Schnepp, J. Fractures tanscotyloïdiennes du bassin, MASSON Ed, 1961.
6. Harris, J. The design and use of the TRRL side impact dummy 20th Stapp Car Crash conf. Oct. 18–20, 1976, 77–106.

7. Joint biomechanical research project KOB. Unfall-und Sicherheitsforschung Strassenverkehr. N° 34, BAST 1982.
8. Cesari, D., Ramet, M., Herry-Martin, D. Injury mechanism in side impact. 22nd Stapp Car Crash conf. Oct. 24–26, 1978, 429–448.
9. Reynolds, H. M., Snow, C. C., Young, J. W. Spatial Geometry of the Human Pelvis. Unpublished.

Intracranial Deformation Patterns Due to Impulsive Loading—A Model Study

B. ALDMAN
C. LJUNG
L. THORNGREN
Department of Traffic Safety, Chalmers University of Technology, Göteborg, Swedish National Institute for Testing, Borås, Sweden

3676

ABSTRACT

Presently used head injury criteria have lately been questioned for several reasons, and there is much evidence to show that a deeper understanding of the injury-producing mechanisms is needed. It is discussed what kinds of research are needed, and a specific model study is described. The model is intended to provide a better understanding of the skull-brain system when subjected to different kinds of trauma, thus facilitating the planning of research specifically aimed at producing better tolerance criteria.

A series of progressively more refined models of the skull-brain system has been used to qualitatively study the effect of different head impact directions and locations. The model can be subjected to sudden linear and/or angular accelerations. Localized trauma to the head resulting in local compression of the brain can be simulated by means of sudden injections of fluid. Observables are normally internal relative displacements. High speed cinematography is used to capture the motion of markers at different depths in the transparent model. So far only two-dimensional studies have been performed but based on results from earlier two- or three-dimensional mathematical models the validity of results can be judged.

INTRODUCTION

Over the years a great number of investigations in the field of brain injury research have demonstrated the importance of sudden motions of the head. These could be caused by either direct impact to the head or by forces transmitted to the head through the neck region, but it is widely agreed that the latter situation is hardly likely to produce brain injury before extensive injury to the neck occurs. At direct impact to the head the brain tissue is obviously sustaining a multitude of mechanical excitation including local compression of brain matter due to the deformation of the skull bone at the impact site, pressure waves travelling through the brain and deformations of the brain inertially produced through the acceleration of the head. It is still a topic of considerable bewilderment how brain injury, reversible or irreversible, is produced. It is indeed probable that all the above mentioned mechanisms do participate in injury production, and in order to provide a better knowledge of means to prevent injury, methods to determine the relative importance of different mechanisms are of interest. The present study on a physical model of the skull-brain system is meant to provide a better qualitative understanding of deformation pattern development in the brain. It is intended to make progressively more refined models of the skull-brain system, but so far attention has been focussed on how rotational accelerations to the head develop strains within the brain matter. It has an advantage over mathematical models of the brain in that fairly complex geometries and materials can be studied, whereas the main disadvantage is the limited number of observables in each experiment. Like in other fields of complex dynamic systems it would seem feasible to combine experimental and mathematical modelling in the future.

ROTATIONAL CEREBRAL INJURIES

As mentioned earlier it was decided to restrict attention to pure rotational motion to begin with. The ability of rotational head accelerations to produce brain injury has been demonstrated clinically by the nature of post mortem findings by, among others, Lindenberg and Freytag (1), Unterharnscheidt and Higgins (2), and Voigt et al., (3). It has also been demonstrated experimentally by, e.g., Ommaya et al. (4), Ommaya and Hirsch (5), Löwenhielm (6), Ljung (7), and Ono et al. (8). The experimental work suggests that angular accelerations can produce cerebral concussion and brain injuries if the angular velocity change exceeds a certain value. In human volunteer tests performed by Ewing et al. (9) no obvious damage occurred at angular accelerations up to 1,700 rad/s^2 resulting in

angular velocities of 32 rad/s. However, Ommaya claims that angular acceleration greater than 1,800 rad/s^2 and change in angular velocity above 60–70 rad/s will result in cerebral concussion and Löwenhielm suggests tolerance levels of 4,500 rad/s^2 and 50–70 rad/s for bridging vein rupture. Hypotheses put forth to explain the mechanical reactions of various parts of the brain have been examined in physical and mathematical models, but so far authenticated explanations to the mechanisms of injury have been offered for just a few, albeit common, injury types. The mechanisms of concussion has, for example, not been possible to explain, probably due to the fact that the geometry in the vicinity of the brain stem is particularly complex. It is a specific purpose of this paper to shed some light on the motion of the central parts of the brain under rotational acceleration.

A thorough understanding of brain injury can of course not be obtained without studies on the cellular level. Only by piecing together information from different kinds of research will it be possible to gain an insight into the relations between outer load, inner mechanical events and cellular damage.

ASSESSMENT OF MATERIAL PROPERTIES

To enable studies of the influence of anatomical structures during linear and angular motions it appeared advantageous to have a model material which was transparent and in which the material properties could easily be changed within certain limits. After a series of tests it was found that a silicone gel (Dow Corning dielectric gel Q3 6527) best fitted the requirements. The gel is produced by mixing two components and cures in about 24 hours at room temperature. By varying the proportions of the two components the material properties change within certain limits.

A series of cylindrical vessels with tight fitting lids were made of acrylic plastic in such a way that they could easily be fastened on a rotor. The radius of the vessel, 95 millimetres, was chosen to be not too far from that of the skull in different planes. The height of the vessel was 80 or 120 millimetres.

For the assessment of the material properties the two components of the gel were mixed and poured into the vessel to cure at room temperature. A few hours before the curing was completed photographic targets—consisting of confetti-like pieces of black paper—were carefully placed in a straight line on the surface of the gel. When cured, the gel sticks to the sides and the bottom of the vessel. The distance from the surface to the bottom—90 millimetres—was chosen big enough to ensure that the influence from the bottom on the displacement of the targets under angular acceleration of the vessel was negligible. In order to prevent the gel from getting in contact with the lid during rotation the vessel was filled up with water and closed in a careful way so as to avoid having air bubbles trapped under the lid.

The rotor used in these experiments consisted of a circular wooden table fixed to a hub and brake drum taken from the front wheel of a motor car. The brake drum was connected to an electric motor by a belt and the brake could be actuated by a pneumatic cylinder. Accelerometers were fitted under the wooden table and via a slip-ring device and cables connected to amplifiers, the signals were recorded on tape. The vessel could be rotated at a pre-chosen velocity and stopped by applying the brake. The deceleration pulse used was a ramp function which from the peak rapidly dropped to zero. The film from a high-speed camera operating at 500 f/s and placed vertically above the center of the vessel was analyzed with respect to the tangential displacement of the targets relative to the surrounding vessel. The set-up is shown in Figure 1.

In a previous study by Ljung (7) mathematical models were developed for a Kelvin-Voigt viscoelastic material contained in cylindrical and spherical rigid shells subjected to sudden rotational motion. The two material parameters of a Kelvin-Voigt material are in such cases shear modulus and kinematic viscosity. In order to determine those parameters for brain tissue, experiments were performed using brain matter from human cadavers. The temporal lobe was inserted in a cylinder which was then subjected to an angular acceleration of a magnitude which ascertained that the experiment was realistically simulating an injurious situation. The two material parameters of the mathematical model were then chosen so as to minimize the model and experiment displacement response differences in a least squares sense.

In the present investigation the above procedure has been repeated in the opposite direction. Given the material properties of brain matter (as expressed by shear modulus

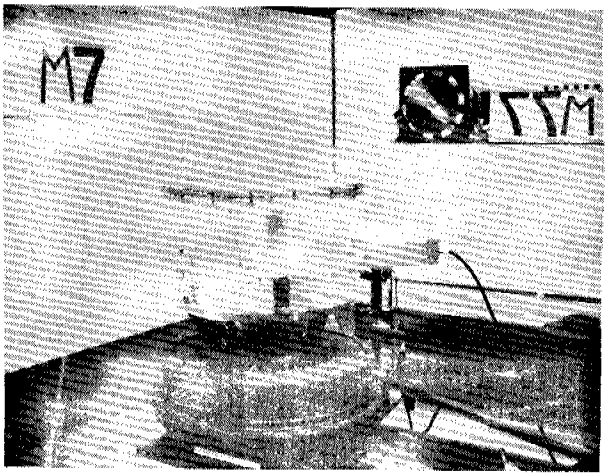

Figure 1. The cylindrical vessel containing silicone gel and water fitted on the rotor for the assessment of the material properties of the gel.

and kinematic viscosity), the correctly mixed silicone gel is sought by comparison of experiment and model displacement responses. An example of the kind of responses obtained is shown in Figure 2, where the deformation pattern of the gel is reproduced from the high-speed films.

It is true that in this way care is only taken to ensure that material properties of brain matter and silicone gel match in problems of rotational symmetry where shear modulus and kinematic viscosity suffice in describing the material. It is, however, maintained that the comparison of material properties made will give a reasonable result for the present study. The material properties of the brain under rotational motion have been studied previously by Schuck and Advani (10) and at West Virginia University (11), and in the latter report is also suggested possible substitute materials for experimental use. The determination of material properties were, however, made under sinusoidal excitation, a fact which casts doubts on the applicability of the data to transient problems. One has to bear in mind that if a simple material model is employed, its field of application does not extend far away from the circumstances under which it was established.

PROCEDURE

The deformation of the gel at angular deceleration was studied by recording the displacement of strategically arranged photographic targets by high-speed cinematography. The targets were not placed on top of the gel but in the substance itself at approximately the same distance from both horizontal surfaces. They were placed in a pattern which was thought to give the best information about the deformation of the simulated brain substance in each test.

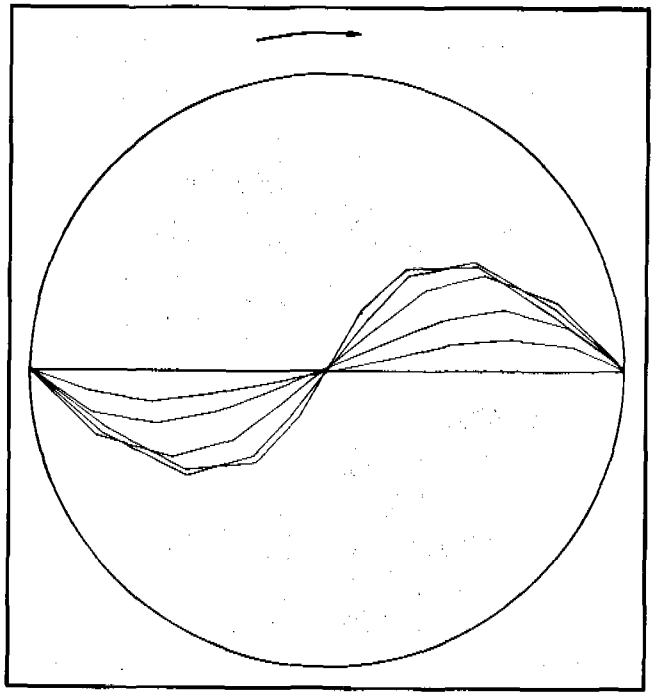

Figure 2. The initially straight line across the cylindrical model is deformed in several stages as a result of the sudden rotation of the cylinder in the direction of the arrow.

For practical purposes it seemed better to decelerate the model from a preset angular velocity by actuating the brake rather than to accelerate it to the desired velocity. The rotation about the centre of the cylindrical vessel in these tests would roughly represent rotation about the centre of gravity of the head in the projections chosen. Two different velocities were chosen for these experiments: 30 rad/s and 60 rad/s. Two pressure levels, 3 and 5 bar, in the pneumatic cylinder resulted in approximately the following peak values of deceleration at 30 rad/s: 1,500 rad/s^2 and 2,600 rad/s^2 and at 60 rad/s: 2,200 rad/s^2 and 4,700 rad/s^2. These values were used throughout these tests since they range from well below and up to what has been suggested as injury producing levels.

In a previous investigation of oblique impacts of a dummy head wearing different types of approved crash helmets by Aldman et al. (12) peak angular accelerations ranging from 4,500 to 14,500 rad/s^2 and peak angular velocities from 20 to 55 rad/s were recorded during the impact sequence in drop tests. The vertical velocity component in these tests was 5.18 m/s (drop height 1.37 m), the horizontal velocity component 8.33 m/s (30 km/h) and the helmeted dummy head impacted different types of simulated road surfaces. In these tests the peak linear accelerations ranged from 90 to 135 g's and peak angular and linear accelerations occurred simultaneously.

It would seem therefore that the angular accelerations used in these experiments are not unrealistically high but could occur in many accident situations.

THE EVOLUTION OF THE MODEL

It was decided early in the planning of these experiments that one essential feature of the series should be a step-wise refinement of the model, such that it would always be possible to distinguish the contribution of the latest model change. For the same reason it is then of interest to briefly relate the history of the model.

A cylindrical vessel like the one used for the assessment of material properties was divided in two halves by rigidly fitting a plate of acrylic plastic across the center. Each half cylinder would then roughly resemble a lateral projection of a middle portion of the skull where the flat plate represented a straight approximation of the skull base and the tentorium. The resulting pattern of deformation is shown in Figure 3. The displacement now takes place round a new centre situated approximately half way between the cylinder wall and the newly inserted plane wall. The extent to which the gel is sheared can be judged from the local slope of the lines as compared to their

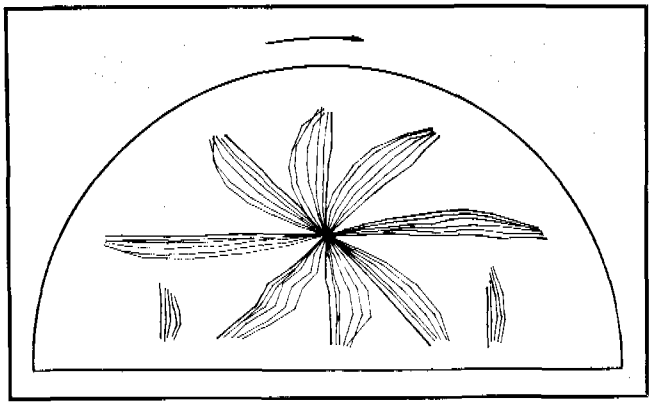

Figure 3. Resulting deformation pattern after insertion of a plane wall roughly simulating the skull base and the tentorium.

original position. The shear deformation is obviously most pronounced along the symmetry line of the half cylinder.

In one of the two half cylinders a shorter plate was fitted to the concave wall at approximately right angles to the longer plate. This new plate was intended as a simulation of the falx cerebri in a frontal projection of the skull. The two quadrants joined in their central parts could then approximately represent cross sections of the two cerebral hemispheres and the mid brain. The resulting pattern of deformation is shown in Figure 4. This time motion occurs round two distinct centres, and the motion will be directed in opposite directions each side of the sagittal plane. Obviously then, local strains could become very high in this region, but the number of markers is not big enough to get a detailed picture.

It would also be of interest to simulate displacements in the brain matter in a horizontal plane (x-y). In order to do so a rigid plastic mould and three soft and transparent vinyl bags were made to fit the base of the skull. The rigid mould was secured inside a cylindrial acrylic vessel by means of a rigid polyurethane foam. The three soft vinyl bags were placed inside the rigid mould. In the inner bag a transparent tentorium and parts of the falx cerebri were welded in position. It was then filled with silicone gel which was left to cure when photographic targets had been placed in the cerebellar as well as in the cerebral parts. These were in both of these structures placed in a middle plane which means at two different levels. The spaces between the rigid mould and the vinyl bags were then filled with water, air bubbles removed and the acrylic lid fitted on top of the cylindrical vessel.

In this horizontal projection of the brain deformation of the model brain material occurred in a similar pattern (cf. Figure 5) at both levels. Thus, large displacements of the targets were seen in the forward half and the rearmost part of the mould, while little or no displacement was recorded in the brain stem area. It should be pointed out, however, that the simulated parts of the falx in this experiment were not fixed to the mould at their upper ends but could move a little with the vinyl bag containing the gel.

With the exception of the last simulation of deformations occurring in a horizontal plane, all studies performed have been two-dimensional in the following sense. Motion is studied in one plane only and the distance of this plane to the bottom and lid of the container was big enough to make sure that they did not disturb the pattern.

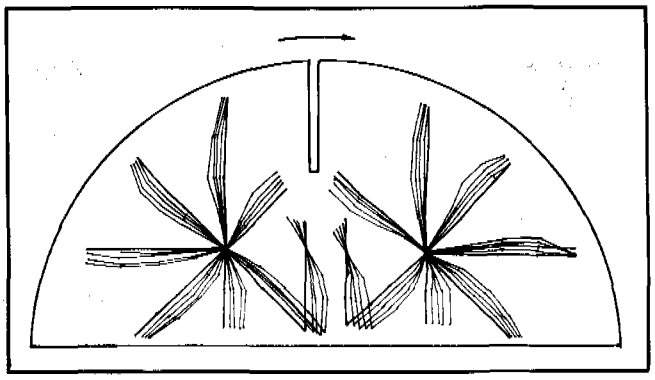

Figure 4. Deformation pattern in a model roughly simulating a frontal section through the skull. The projection at right angles to the cylindrical wall represents the falx.

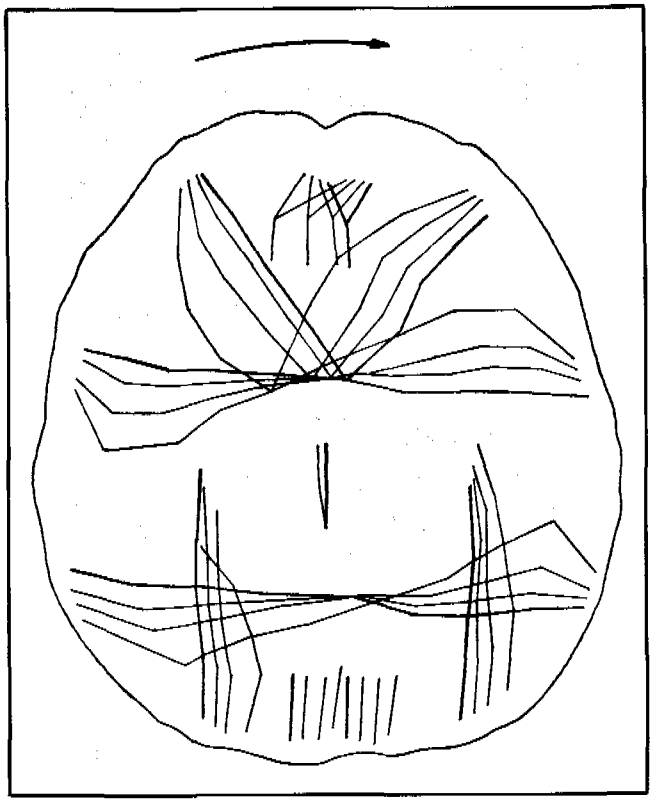

Figure 5. Deformation pattern in a horizontal projection of the head. The back of the head is pointing downwards in the figure which means that the foramen magnum is situated very close to the apparent centre of deformation at this level.

Mathematical simulations of this problem have been performed previously by Ljung (9). The next section deals with a more refined, but similarly two-dimensional model of a lateral projection of the brain.

REFINED LATERAL VIEW MODEL

In this step a more elaborate system of plates was fitted in a cylindrical vessel in order to simulate a mid-sagittal section including brain, brain stem, cerebellum and upper spinal cord. The skull base and the tentorium are still represented by an approximately straight plane but with an opening simulating the tentorial opening. The geometry of the model can be seen in Figure 6 which also shows the resulting deformation pattern in one of the last experiments. Earlier experiments have been presented in greater detail by Aldman et al. (13) and will be only briefly mentioned here.

A comparison has been made between the deformation patterns if the gel sticks to the side walls of the container or if the outer surface of the gel can move freely relative to the wall. In the human skull the brain is anchored more firmly to the dura with age, a fact also reflected in the kind of injury produced (Voigt et al. (3)). The only significant change in pattern between the two experiments was, however, that the direction of rotation of the gel below the tentorium was reversed. This is probably a result of little consequence, since the deformations are quite small in this region anyway. The overall pattern of deformation is otherwise the same although it seems as if the more relaxed conditions in the latter case permit larger displacements to occur. Throughout the series of experiments with this model high values of shear can be detected in the vicinity of the tentorial opening.

In the last experiments the gel was again allowed to stick to the walls and an attempt was made to simulate the influence of the ventricles, since it was anticipated that the reduced shear stiffness of the ventricular fluid could permit greater deformations to develop especially in the vicinity of the tentorial opening. For this purpose a pocket in the gel, approximately 10 mm high, 40 mm long and 40 mm deep, was filled with liquid paraffin. The pocket was terminated above and below with a gel layer so that the paraffin was completely enclosed in gel. Thus, no substantial volume changes were to be expected. The deformations in the model were recorded in a plane situated approximately at the middle of the pocket, far enough from its ends to ensure that the idea of looking at a two-dimensional problem was not disturbed.

In reality the geometry of the ventricles is very complicated and far from two-dimensional, but it is still believed that the essence of the ventricles is maintained in this crude model. The resulting deformation pattern is shown in Figure 6. It is interesting to note the change of shape in the fluid-filled pocket. This means that although

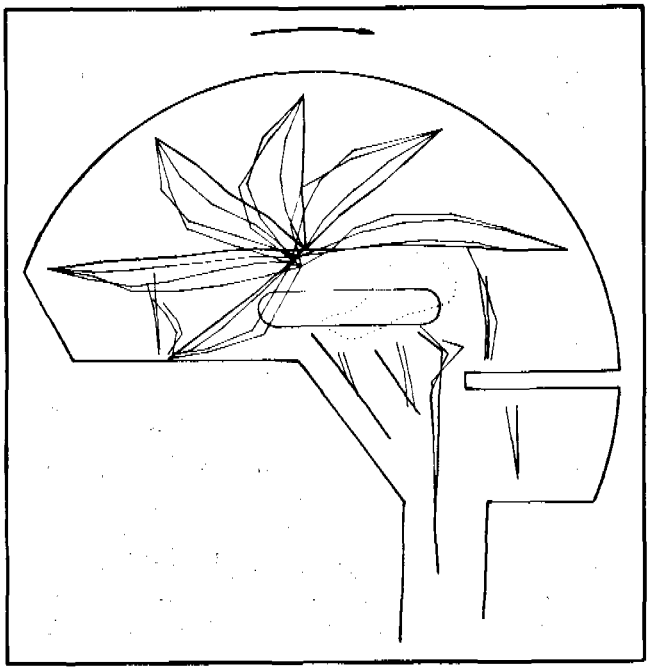

Figure 6. Pattern of deformation in a lateral view model incorporating simulated ventricles. The dotted shape represents the ventricles at maximum deformation.

the overall deformations, as measured by the markers, is not very much changed in relation to the earlier experiments, there may still be significant local changes in the shear strains.

CONCLUDING REMARKS

There is not any dramatic change in the deformation pattern present in the series of experiments with the lateral view model. This gives rise to several conclusions regarding future research.

First of all, the overall pattern of deformation is quite well described by the model at its present stage of development. This means that it might be feasible to try to formulate mathematical models for small parts of the brain, where the overall behaviour of the model coincides with the results found here.

Secondly, the methods for analysis have to be refined for future experimental work with this model. Markers must be placed in such a way as to permit a direct evaluation in terms of local shear strain for example. Once this is achieved further studies in the influence of material inhomogeneities can be made, e.g., studies using simulated brain matter of different stiffness at different sites. It would also be interesting to see the effect of allowing some motion of the upper spinal cord in the direction of the spine.

A more rugged aluminium model is being constructed presently. This model has the same principal features as

the lateral view model and is intended to be used in experiments where translational accelerations are also present. It is obviously of great interest to see if the deformations will be changed to any significance when translational accelerations are introduced. It is also intended to make pressure measurements in the gel in these experiments.

Finally, in order to be able to express the results in quantitative form the two-dimensional approach has to be abandoned and methods for building and studying three-dimensional models are being investigated.

REFERENCES

1. Lindenberg, R. and Freytag, E. (1960). The mechanisms of cerebral contusions. Arch. Path. 69, 440-469.
2. Unterharnsheidt, F. and Higgins, L. S. (1969). Traumatic lesions of brain and spinal cord due to non-deforming angular acceleration of the head. Tex. Rep. Biol. Med. 27, 127-166.
3. Voigt, G. E., Löwenhielm, C. G. P. and Ljung, C. B. A. (1977). Rotational Cerebral Injuries near the Superior Margin of the Brain. Acta neuropath. (Berl.) 39, 201-209.
4. Ommaya, A. K., Yarnell, P., Hirsch, A. E. and Harris, E. H. (1967). Scaling of Experimental Data on Cerebral Concussions in Sub-Human Primates to Concussion Threshold for Man. Proceedings of 11th Stapp Car Crash Conference Oct. 10-11, 1967. SAE, N.Y. USA.
5. Ommaya, A. K. and Hirsch, A. E. (1971). Tolerances for Cerebral Concussion from Head Impact and Whiplash in Primates. Journal of Biomechanics, 4, 13, 1971.
6. Löwenhielm, P. (1975). Brain Susceptibility to Velocity Changes. Relative and absolute limits for brain tissue tolerance to trauma and their relation to actual traumatic situations. Proceedings of an International Interdisciplinary Symposium on Traffic Speed and Casualties held at Gl Avernaes, Funen, April 22-24, 1974, Denmark.
7. Ljung, C. (1975). A Model for Brain Deformation due to Rotation of the Skull. J. Biomechanics, 1975, Vol 8, pp 263-274.
8. Ono, K., Kikuchi, A., Nakamura, M., Kobayashi, H. and Nakamura, N. (1980). Human head tolerance to sagittal impact reliable estimation deduced from experimental head injury using subhuman primates and human cadaver skulls. 24th Stapp Car Crash Conf. Troy, Mich., Oct. 1980, 101-160.
9. Ewing, C. L., Thomas, D. J., Lustick, L., Becker, E., Willems, G. and Muzzy, W. H. (1975). The Effect of the Initial Position of the Head and Neck on the Dynamic Response of the Human Head and Neck to $-G_x$ Impact Acceleration. Proceedings of the 19th Stapp Car Crash Conference, November 17-19, 1975, SAE, Warrendale, USA.
10. Schuck, L. Z. and Advani, S. H. (1977). Rheological response of human brain tissue. ASME paper 72-WA/BHF-2 presented at ASME Winter Annual Meeting, 1972.
11. West Virginia University (1970). Determination of the physical properties of tissues of the human head. Report from the Biomechanics Laboratories. College of Engineering, West Virginia University, Morgantown, West Virginia.
12. Aldman, B., Lundell, B., and Thorngren, L. (1978). Oblique Impacts—A Parametric Study in Crash Helmets. Proceedings of the 3rd International IRCOBI Meeting 1978, Lyon, France.
13. Aldman, B., Thorngren, L., and Ljung, C. (1981). Patterns of deformation in brain models under rotational motion. Consensus Workshop on Head and Neck Injury Criteria, NHTSA, Washington, March 1981.

3677

Automotive Neck Injuries

A comparative study of neck injury mechanisms in frontal collisions in the U.S. and in the Federal Republic of Germany

AYUB K. OMMAYA, M.D., S. BACKAITIS, W. FAN, and S. PARTYKA
National Highway Traffic Safety Administration

K. LANGWIEDER, Ph.D.
HUK-Verband

In an earlier report by K. Langwieder et al. we presented the results of coordinated studies on neck injuries in which it was shown that it was possible to obtain useful information by such comparative evaluation of two large scale accident files in two different countries. (1) Similar proportions of accident types and distributions of injuries to car occupants with a few differences related to data sampling techniques were found. Thus the U.S. data set (NCSS file) contained a higher proportion of uninjured people compared to the German (HUK-Verband) data set because the NCSS data are based on tow-away of at least one of the involved accident vehicles whereas the HUK data are based on the presence of at least one minor injury to accident victims. This and other differences could be controlled by techniques described in the above referenced report. In this paper we summarize our pre-

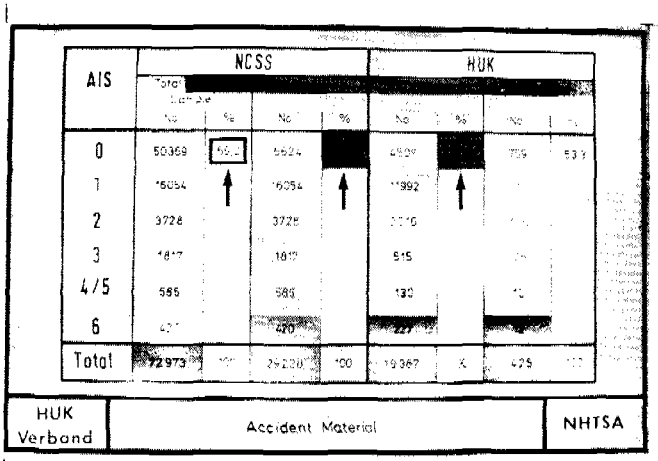

Figure 1. Accident material.

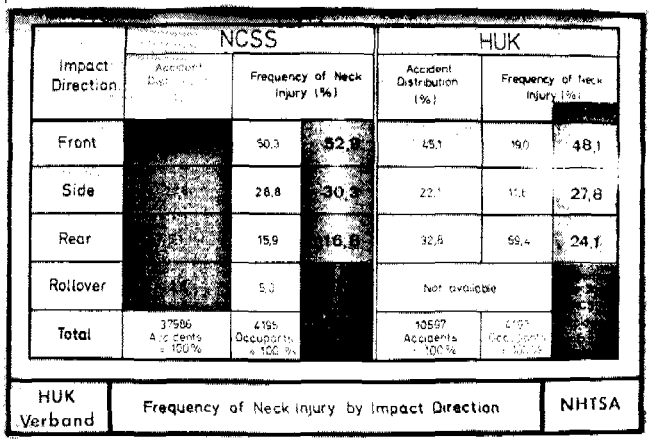

Figure 3. Frequency of neck injury by impact direction.

vious findings and present the results of that analysis combined with a review of the files of 222 cases of AIS-3 to -6 injuries which constitute all of the more severe neck injuries in the N.C.S.S. files with adequate medical data. Although the vast majority of automotive neck injuries are of the minor cervical strain, "whiplash" or hyper-extension/ flexion variety, the more disabling minority of cases produce devastating consequences in terms of human, social and economic costs. In recent studies by Smart and Sanders it was estimated that 5500 cases of AIS-5/6 occurred in 1974 of which 3000 died at the accident site due to the neck injuries and 2500 were admitted to hospitals. Of these only 133 made functional recoveries, 1091 remained quadriplegic and the remainder died. Since automotive neck injuries constitute over 50% of all neck injuries the mounting annual costs are highly significant. (2) It should also be emphasized that even the approximately 95% of all neck injury cases at the AIS-1 and -2 levels often entail loss of work and medical care costs which are out of proportion to the seeming "lesser" severity of these injuries.

The accident material is summarized in Figure 1 which shows a comparison of the weighted and normalized samples from the NCSS file (unrestrained) with the cases from the HUK file for varying levels of the AIS. Note that when the NCSS data are normalized by reducing the uninjured category that the percentages of injured and uninjured necks at the various AIS levels are fairly comparable. The numbers of neck injuries in the two data sets related to different impact directions are shown in Figure 2. Note the greater number of more severe neck injuries in the NCSS file data with more comparable numbers at AIS-1 to -3 levels. The frequency of neck injury by impact direction distribution is more clearly seen in Figure 3. Note the clear predominance of frontal impacts with side and rear collisions following in a similar sequence in both data sets.

The severity distribution of neck injury between minor (AIS-1), moderate (AIS-2 and -3) and severe (AIS-4 to -6) is shown with reference to impact direction in Figure 4. This clearly brings out the fact that although frontal impacts produce neck injuries most frequently, AIS-1 or whiplash type injuries are more often due to rear end collisions.

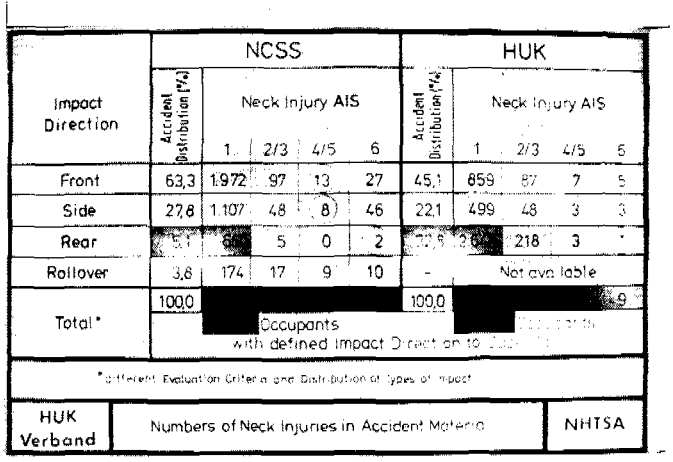

Figure 2. Numbers of neck injuries in accident material.

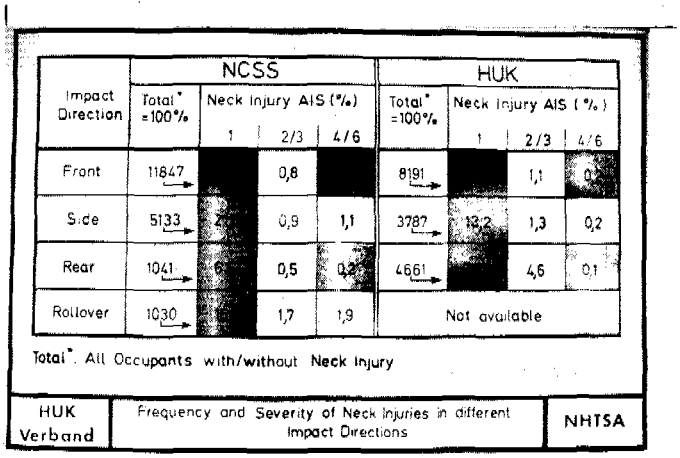

Figure 4. Frequency and severity of neck injuries in different impact directions.

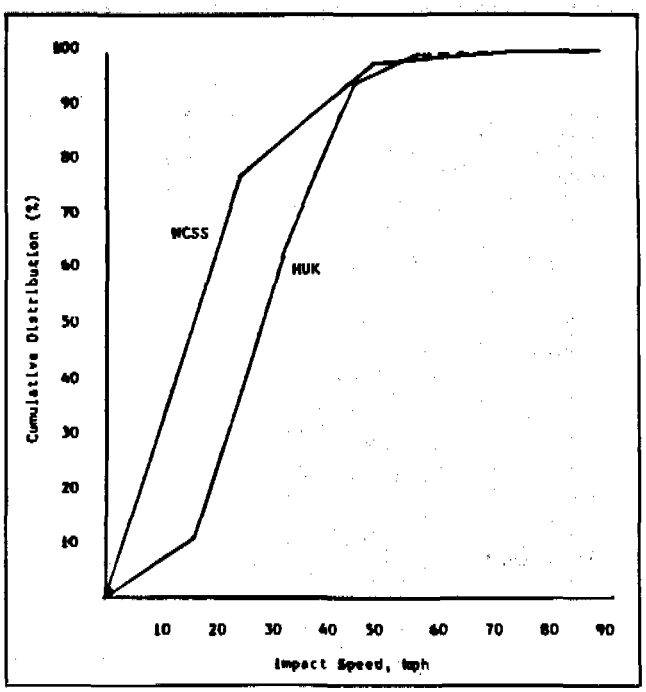

Figure 5. Cumulative distribution of occupants involved in frontal collisions versus change in impact speed (ΔV).

EFFECT OF SEX AND AGE ON NECK INJURY

This study confirmed previous observations by Langwieder on HUK data that females are at a higher risk for AIS-1 and -2 neck injuries (but at equal risk with men for AIS-3 and above injuries) and that children up to 10 years old have about 1/6 the risk of neck injuries as compared to adults. This finding was also supported by the observation made in both NCSS and HUK data in this study that shorter people (below 152 cm/5 ft) have a risk of neck injury about 40% less than taller occupants. Significantly higher risk also exists for occupants aged 30 + as previously also shown in HUK data. (3,4,5)

NECK INJURY AS A FUNCTION OF DELTA V

Although both data sets begin to converge above 20 mph for increasing risk of neck injuries in frontal collisions, a clear limit of speed change above which severe injuries (AIS-3 to -6) would occur cannot be set. Thus 18 of the severe injuries in these data occurred at < 15 mph ΔV. Figure 5 shows the cumulative distribution of occupants with neck injuries (frontal collisions) versus ΔV. Critical and fatal neck injuries (AIS-5/6) do seem to occur, however, above a threshold of 20-25 mph ΔV. These data support the idea that unfavorable occupant kinematics, relation of head and neck to car interior surfaces and its intrusions and the characteristic of contact surfaces all play a role in neck injury causation in addition to accident severity (ΔV). This conclusion is further supported by the finding that no neck injury of severity > AIS-3 occurred in any restrained occupant in the NCSS data at any impact speed. Only 2 such cases were found in the HUK data, most probably related to vehicular structural failures rather than ΔV.

VEHICLE CONTACT AREAS FOR HEAD AND NECK IMPACTS CAUSING NECK INJURIES

Figure 6 illustrates the distribution of contact areas versus neck injury severity for all the frontal collision cases. These include 1569 cases with known contact and injuries at all AIS levels of which 973 were related to 6 main contact areas, i.e., windshield, steering wheel, instrument panel, A-Pillar, Mirror-Sunvisor and glove compartment/hardware. Critical and fatal neck injuries were related primarily to the A-Pillar contacts.

RESTRAINT EFFECTS ON NECK INJURY OCCURRENCE

The majority (82.6%) of neck injuries to unrestrained occupants do not involve direct impact to the neck although 58.2% of these are related to *head* impacts leaving only 30.4% caused by inertial forces on the neck. Figure 7 shows the overall frequency of neck injuries related to head contacts in belted and unbelted occupants in frontal collisions. These data clearly indicate how restraints apparently reduce the frequency of head contact related neck injuries. The distribution of neck injury severity for belted occupants in both the NCSS and HUK data is shown in Figure 8. Note the absence of AIS-4 through -6 injuries in the NCSS data and only 2 injured drivers in the HUK data. The interaction between restraint systems and presence or absence of head contact in the NCSS data is shown in Figure 9. The majority (88.6%) of neck injuries

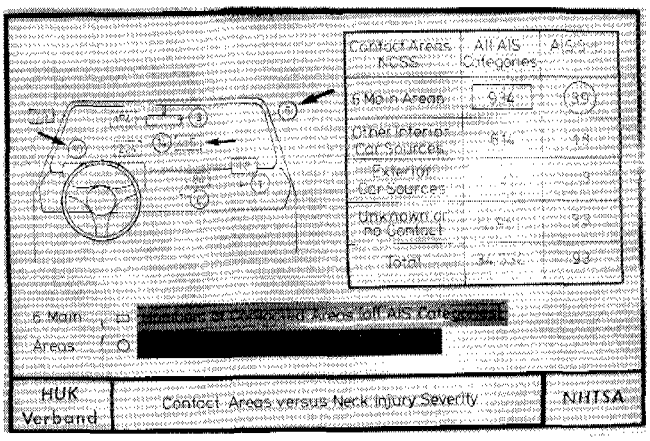

Figure 6. Contact areas versus neck injury severity.

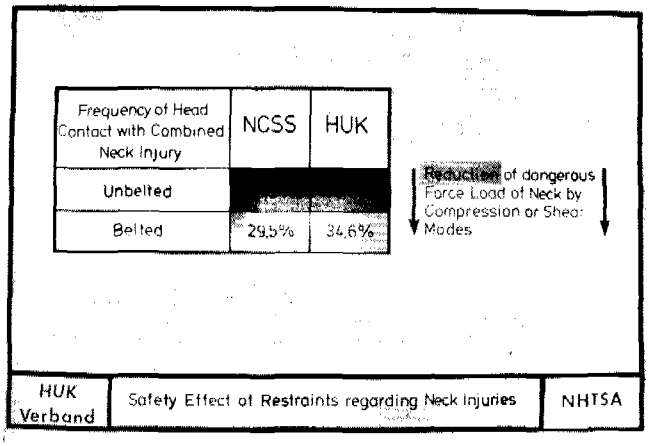

Figure 7. Safety effect of restraints regarding neck injuries.

to *unrestrained* occupants do not involve neck impacts. Of these 58.2% are produced by direct head impacts and 30.4% by inertial forces. Only 11.4% of all neck injuries occur via direct neck contact. For *restrained* occupants the rate of neck injury is reduced because of lower incidence of head impacts. However the rate of neck injury via direct neck contact is doubled and inertial force injury rate increases by 50%. However, no injuries higher than AIS-3 occurred in the restrained occupants and neck injury rates for unrestrained occupants at the AIS-2 and -3 levels are more than twice that of restrained persons. Only at the AIS-1 level do restrained occupants show a slightly larger proportion of neck injuries. These data are very similar to the HUK data shown in Figure 10. In this data set most of the serious neck injuries are combined with an independent head injury for unrestrained occupants, further supporting the conclusion that the most frequent type of severe neck injury (AIS-3 and above) for unbelted occupants consists of an initial force loading the head by contact which results in compressive and shear strains followed by severe flexion or extension of the cervical spine. This figure shows a nearly 3-fold reduction of combined head/neck injuries when they occur with

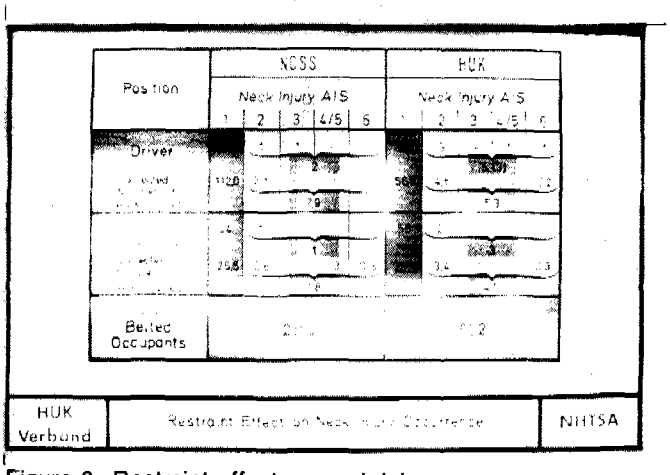

Figure 8. Restraint effect on neck injury occurrence.

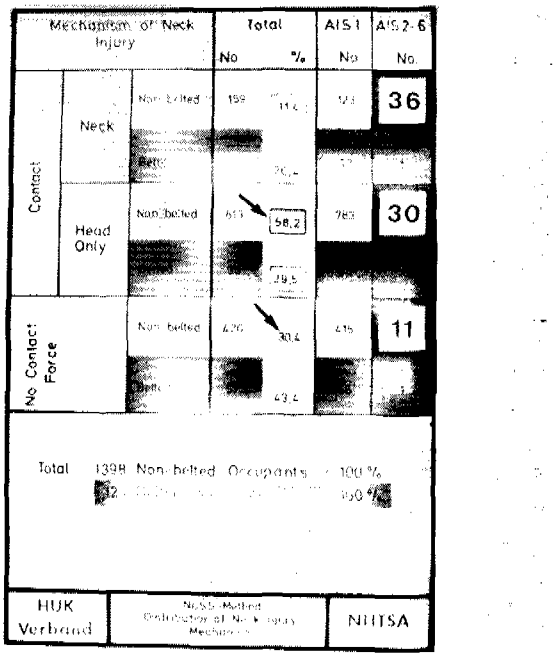

Figure 9. NCSS-Method distribution of neck injury mechanism.

concussion with or without soft tissue damage in 5.2% belted versus 16.5% unbelted occupants. This protective effect of restraints is not seen when more serious head injuries occur (2.6% versus 2.9%) most probably because of structural intrusions into the occupant compartment. In sum, both data sets show a more than 2-fold decrease of occupant injury rates at the AIS-2 and -3 levels by the use of seat belts and a significant decrease of injury at

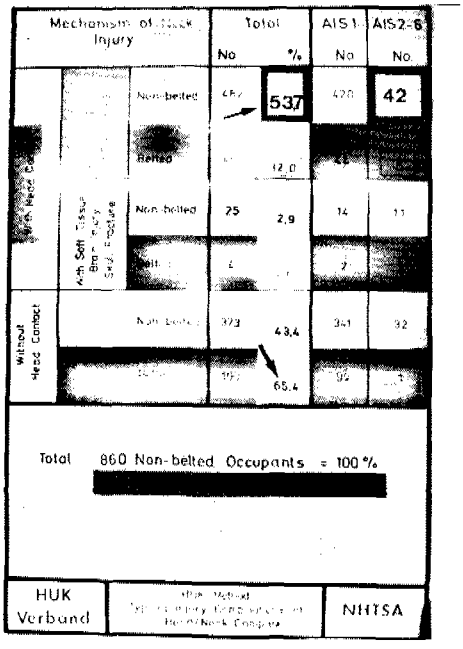

Figure 10. HUK-Method typical injury combinations of head/neck complex.

the higher AIS levels. Only AIS-1 injuries increase in the restrained occupants.

MECHANISMS OF NECK INJURY

A computer search of the NCSS data file revealed 222 cases with AIS-3, -4, -5, and -6 injuries to the neck in which adequate medical data were available. The distribution of these cases between these AIS levels is of considerable interest. Thus the majority of cases were distributed almost equally between AIS-3 (= 86) and AIS-6 (= 93) cases with a much smaller proportion falling into the AIS-4 (= 15) and AIS-5 (= 28) categories. Because significant neural damage to the spinal cord begins at AIS-5 there appears to be a fairly abrupt transition at the AIS-4 level between the less severe and the most severe cases. These transition data are very reminiscent of the findings collected by NHTSA staff member J. Marcus from two sources[6,7] which showed that if the putative levels of injurious moments (M) at the occipital condyles in flexion are listed for increasing severity of neck injury, a sharp transition is seen between AIS-2 injuries at 140 ft lb and AIS-5 injuries at 150 ft lb. This small moment increase for catastrophic neck injuries could be due to methodologic causes, but it is certainly supported by the accident date reviewed above.

Statistical study of NCSS and HUK files shows that a major cause of critical and fatal neck injuries in frontal collisions are head impacts with the interior surfaces of the vehicle. Inertial loading of the head and neck without head impact is significantly less noxious. With head impact, the compressive and/or shear loading of the neck and its subsequent failure in flexion or extension is the putative mechanism for severe neck injuries causing quadriplegia. Without head impact, flexion/extension (whiplash) caused by inertial loading is the injury mechanism observed, which, fortunately, is not a cause of major injury. The close association of head and neck injuries is well supported by these data and the role of restraint systems in reducing both types of injuries by preventing head impact is clearly brought out. The in-depth analysis of the case reports establishes the following points for further study:

1. Insights into injury mechanisms require a greater sophistication of medical data in accident investigation studies.
2. Such studies should optimally be designed as prospective research with careful attention to adequate comparability of impacts to assure that the cases used to establish the statistical profile truly reflect the claimed injury mechanisms.
3. Further clinical studies must be supplemented with experimental work to extend the knowledge of neck injury criteria from the currently accepted data which provide information on only 3 of the 9 criteria required; e.g., data on flexion and extension, bending moments and axial compression are available, but horizontal and lateral shear, torsion, lateral bending and axial-tension data are nonexistent.

The results and the conclusions of this study should not be considered definitive for neck injuries, but they do confirm the fact that neck injury characteristics in both continents are nearly identical and that similar countermeasures could produce significant injury reductions.

BIBLIOGRAPHY

1. Langwieder, K., Backaitis, S., Fan, W., Partyka, S., and Ommaya, A. K. Comparative Studies of Car Occupants in Frontal Collisions in the United States and the Federal Republic of Germany. Proc. 25th Stapp Car Crash Conference. S.A.E. 1981.
2. Smart, C. N. and Sanders, C. R., "The Costs of Motor Vehicle Related Spinal Cord Injuries." Insurance Institute for Highway Safety, Washington, D.C. 1976.
3. Langwieder, K. Dissertation. Techisches Universitatet TU Berlin 1975.
4. Langwieder, K. et al. "Kinderversicherunger in PKW." IRCOBI Proceedings. Lyon, France 1974.
5. Langwieder, K. et al. Comparisons of Passenger Injuries in Frontal Car Collisions with Dummy Loading in Equivalent Simulations. Proceedings 23rd Stapp Car Crash Conference. San Diego, Cal. 1979.
6. Mertz and Patrick. "Strength and Response of the Human Neck." 15th Stapp Car Crash Conference.
7. Monthly report for Feb. 1982. Contract No. DOT-HS-7-01792. Wayne State University (R. Morgan, NHTSA Contract Manager).

Development of Neck Injury Tolerance Criteria in Human Surrogates. I. Static Tensile Loading in the Baboon Neck: Preliminary Observations

3678

JOHN B. LENOX, RICHARD L. STALNAKER, CURTIS D. WHITE, GARY T. MOORE, ORIN M. ANDERSON, RALPH R. SCHLEICHER, H. HERBERT PEEL, SUSAN S. MARTIN, GERALD D. DRISCOLL
Southwest Research Institute

HOWARD W. HUNTINGTON
The University of Texas Health Science Center at San Antonio

K. DEE CAREY
Southwest Foundation for Research and Education

MARK P. HAFFNER and AYUB K. OMMAYA, M.D.
National Highway Traffic Safety Administration

ABSTRACT

Currently available biomechanical data are insufficient for determining the neck loads required to produce cervical injuries in automotive accidents. The purpose of this study was to initiate a series of experiments required for identifying injury mechanisms and to develop criteria suitable for representing the spectrum of significant functional and structural neck injuries that could be sustained by car crash occupants. The first test conducted was a static neck tension test performed on an anesthetized, 12.2-kg baboon (*Papio hamadryas*). A state of muscle paralysis was maintained throughout neck loading to mimic the flaccid muscle tone present in fresh human cadavers. Tensile neck loading was increased at a rate of 20.2 N every five minutes until definitive structural failure (atlas-occipital subluxation) occurred at the 1170 N load level. Neurophysiological testing in the anesthetized animal demonstrated that cervical spinal cord function was seriously impaired at the 595 N load level, i.e., at 51 percent of the structural failure load. The potential implications of this finding are discussed, relative to the understanding of injury mechanisms. In addition, a strategy is presented for deriving functional neural tissue impairment thresholds, from fresh human cadaver data, that may apply in real accident victims.

INTRODUCTION

The primary objective of this study was the initiation of an experimental series for identification of a set of neck injury criteria suitable for representing serious neck injuries sustained by car crash occupants. Pursuing this objective meant considering the full spectrum of medically significant structural (skeletal-ligamentous) and functional neural tissue (spinal cord) injuries that could be sustained due to indirect neck loadings occurring during automotive crash events. (1-17)

Cervical spinal injuries have been studied (18-23) and some injury threshold data for static and dynamic neck loads already exist. (6,24-26) However, injury thresholds have not been experimentally established for static or dynamic head loaading that induces combined atlas-occipital tensile and shear loads and torques.

The first test of an initial static neck loading test series has been conducted in this program; specifically, a neck tension test of an anesthetized, 12.2-kg, eight-year-old female baboon (*Papio hamadryas*) is reported. A state of muscle paralysis was maintained throughout neck loading, for several reasons. First, the experiment provided a living-equivalent muscle tone state that mimicked the state of flaccid muscle tone present in fresh cadaver test subjects, in contrast to the varying muscle "tone" present either in embalmed cadavers or in cadavers that are not fresh. Second, injury thresholds derived represented worst-case, static, tensile neck loading, since the flaccid muscles could provide only minimal protection. Third, the plan was to achieve test conditions that were more reproducible than could be achieved by attempting to maintain muscle tone at levels that can only be poorly defined. Fourth, the state of flaccid muscle paralysis enhanced the physical significance of having elected to equivalently characterize neck loading by a resultant force, acting at that skull-fixed point defined by the intersection of the animal's mid-sagittal plane with the flexion-extension axis of the atlas-occipital joint, and a torque (that was essentially zero for the first test).

METHODOLOGY

Medical

Animal Care. The *Papio hamadryas* used as the experimental study model for this program was purchased from

a United States Department of Agriculture (USDA)-approved commercial animal dealer. The baboon was brought to Southwest Research Institute (SwRI) and quarantined according to established procedures for baboons. The quarantine included five weeks of strict isolation from other nonhuman primates and a specific tuberculin testing and disease monitoring regime during this period. Upon release from quarantine the baboon was maintained in an individual cage in a controlled atmosphere until used for testing. The SwRI Laboratory Animal Medicine Program and Facilities are approved by the American Association for Accreditation of Laboratory Animal Care and the USDA. Approval by these organizations is based on guidelines from the Animal Welfare Act of 1970 and the Guide for Care and Use of Laboratory Animals. In addition to these approvals all protocols involving animal care and testing are subjected to a review by the SwRI Animal Care Committee. This program was reviewed and approved by the SwRI Animal Care Committee.

Test Day Regime. On the morning of the test day, the animal was anesthetized, shaved and prepped, and a set of shape and size body measurements was recorded. Surgery was then performed to: (1) insert an endotracheal tube; (2) introduce a Millar combination blood pressure transducer and arterial blood sampling catheter into a femoral artery, placing it in the abdominal aorta at the level of the xyphoid; (3) implant right and left occipital average evoked response (AER) skull electrodes; (4) perform the minimum cutdown required to apply a Michel clip adjacent to the spinous process of the first thoracic (T1) spinal vertebra, for X ray verification reference (just prior to initiating neck loading, the T1 extender hemostat was clamped between the T1 and seventh cervical (C7) spinous processes); and (5) place an indwelling urethral catheter into the bladder.

A deep state of anesthesia was maintained throughout the test day by the veterinary anesthesiologist until death occurred. Chloralose anesthesia was utilized during loading to accentuate the far field AERs. A state of complete flaccid muscle paralysis was maintained by administering curare in divided doses prior to and throughout the loading phase. Ventilation was maintained by an abdominal respirator that was monitored and adjusted in accordance with pneumotachometer readings and arterial blood gas values.

Medical Data. Instrumentation was provided for monitoring and recording:

(1) Blood pressure (B.P.) (systolic, diastolic and mean; recorded continuously)
(2) Heart rate (H.R.) (recorded continuously)
(3) Electrocardiogram (ECG) (Lead II recorded continuously)
(4) Rectal temperature (recorded continuously)
(5) Right- or left-sided far field somatosensory and auditory AERs (implanted skull and C1 electrodes; recorded once per five-minute loading cycle midway between load increases)
(6) Ventilation rate and depth (pneumotachometer coupled to the endotracheal tube; recorded continuously)
(7) Arterial blood gases (pO_2, pCO_2 and pH measured periodically)

B.P. and H.R. were both recorded on a multichannel strip chart recorder and digitized for digital display and storage. The data stored in digital form were processed post-test to provide compact trend analysis graphs. AERs were stored on computer disks, for post-test retrieval and analysis of AER data.

Radiology. Whole body and cervical X rays were taken of the animal on test day prior to surgery and at the end of the loading phase, immediately after removal of the animal from the potted torso and head containers. In addition to repeating the standard set of pretest X rays, lateral and ventrodorsal X rays were taken of the cervical spine during reapplication of a tensile neck load estimated to be in the range of 300 N.

Post-Test Regime. Post-test, the custom-potted torso and head containers, when coupled together rigidly with linkages, provided a secure litter for transporting the neck-injured animal (without further injuring the neck) to the X ray laboratory and later to the necropsy laboratory. Following the post-test X rays, and up until one hour prior to necropsy, the test animal was kept refrigerated at 4°C. A complete necropsy was performed 36 hours post-test. The necropsy findings were thoroughly documented in writing and via medical photographs. The brain and spinal cord were then preserved in 10 percent buffered formalin for microscopic neuropathological examination.

Bioengineering

Torso and Head Constraint. Stereotaxic alignment and restraint of the head within the head container was achieved by clamping to a custom-fitted dental appliance, and butting the caudal surface of the animal's occiput and mandible up against the firm rubber grommet covering the custom-sized and shaped exit neck opening (see Figure 1). With the dental appliance in place and the mouth taped firmly shut, the occiput was pushed snuggly up against the neck hole. A four-degree-of-freedom linkage grasping the dental appliance extension pipe was then adjusted and locked to achieve maximum flexion of the head within the head container and mandibular contact with the head container, and to align the skull squarely within the head container.

Stereotaxic alignment and restraint of the torso within the torso container was achieved by using a detachable torso alignment and restraint frame. This frame had adjustable shoulder clamps for positioning and restraining the upper thorax symmetrically about the animal's mid-

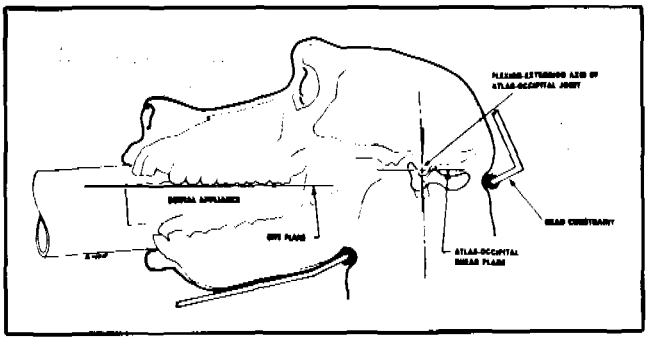

Figure 1. Head constraint, dental appliance, flexion-extension atlas-occipital axis of rotation, and definition of atlas-occipital shear plane

sagittal plane in an erect, shoulders-back, posture. In addition, this alignment-restraint frame had right and left thoracic supports, right and left pelvic/leg supports, and provisions for holding the animal in place with cephalic and caudal thoracic straps and a mid-abdominal strap. The caudal thoracic strap and the mid-abdominal strap were fastened over the abdominal respirator bell. Once the animal was secured to the alignment-restraint frame, this frame was then bolted in place in the torso container. The neck exited the torso container through a custom-sized, circular opening. The neck hole edge was covered with a firm rubber grommet for protection.

Both the head and torso containers were comprised of separate right (lower) and left (upper) halves, with provision for fastening them together in the mid-sagittal plane of the animal. The four-degree-of-freedom linkage to which the dental appliance extension pipe was secured, and the torso alignment and restraint frame, were designed to facilitate release of the head and torso after they had been potted in place with structural polyurethane foam.

Head and torso container dams were custom-shaped, using an adjustable, two-dimensional template, to conform to the mid-sagittal planar contours of the animal. These dams were inserted in duplicate between the right and left halves of the head and torso containers. In addition, custom-shaped right and left dams were also used to seal the torso container at the thoraco-abdominal junction.

Twenty-four hours prior to testing, all interior surfaces of the head and torso containers were coated with latex liquid rubber. Just prior to placing the animal in these containers, the head was covered with a latex hood and the torso and upper arms were covered with a latex jacket. The latex rubber covering on the animal, the inside of the containers, and internal stereotaxic container parts facilitated post-test release of the animal from the structural foam and the foam from the container itself.

The structural polyurethane foam was then injected and poured into the head and torso containers. Exit holes in the containers were provided for excess foam, to prevent either shifting of the head and torso within the containers or injury to the test animal as a result of overcompression of vital tissues.

Abdominal Respirator. A plaster casting had been made of the test animal's abdomen prior to test day. A fiberglass abdominal respirator bell had been fabricated with the bell opening custom-shaped to contact the animal's abdomen from just cephalad of the symphysis pubis to just cephalad of the xyphoid and along the ventro-lateral margins of the thoracic cage and walls of the abdomen. The opening of the bell was covered and sealed with a Neoprene® diaphragm that had its resting shape "domed" to match the domed shape of the abdomen. The maximum positive (expiratory) and negative (inspiratory) pressure of the ventilator could be adjusted, along with the respiratory rate.

T1 Extender. The T1 vertebral body extender consisted of a 12.7-cm straight hemostat modified by adding (1) two pins for piercing the interspinous ligaments, to minimize artifactual rotation of the hemostat; and (2) two crossbars to the handle, to serve as X-ray targets and supports for photographic targets.

Biomechanical

Head Attitude for Tensile Neck Testing. The skull-fixed shear plane of the test animal's atlas-occipital joint was defined as being normal (perpendicular) to the long axis of the thoraco-cervical spinal column when the animal's bite plane was also perpendicular to the long axis of the thoraco-cervical spinal column (see Figure 1). This definition of atlas-occipital shear plane was selected, based upon: (1) assessment of the natural, neutral position of this baboon's head, relative to the torso; (2) assessment of a contrived, human-equivalent, "eyes front" neutral position of the head, relative to an erect thorax held in a shoulders-back posture of attention; (3) X-ray flexion-extension range-of-motion studies of the head; and (4) actual study of *Papio hamadryas* cadaver atlas-occipital joint articular surfaces.

The biomechanical goal for this first tensile neck loading experiment was to position the head, relative to a shoulders-back, erect, torso posture, such that the animal's bite plane (atlas-occipital shear plane) was perpendicular to the long axis of the cervical spine. For the first test, this goal was nearly achieved with the head versus torso orientation having been set at 3.5° of head extension. Thus, a pure tensile load applied to the head by means of a load pin effectively colinear with the flexion-extension atlas-occipital axis would induce an atlas-occipital ventral shear load equal to 6 percent of the induced atlas-occipital tensile load (sine 3.5° × 100). The 3.5° of head extension could not be eliminated for this test, because the already short chin-chest clearance of baboons was further reduced by the requirement to hold the mouth open with the dental

appliance that provided clearance for the endotracheal airway.

Skull Location of Shaft (Load Pin) Transmitting Load from Head Container Translation Platform to Head Container (Skull). Prior to performing neck loading, the head container was radiographically positioned to ensure that the animal's flexion-extension axis of rotation was coincident with the vertical load pin axis. This positioning maneuver was accomplished in two iterations and confirmed by the third X ray, at which time the optical axis of the X ray beam, the flexion-extension atlas-occipital axis and the load pin axis were all essentially coincident (see Figure 2). Theoretically, when the load pin and the flexion-extension atlas-occipital axis are coincident, tensile loading of the neck by the skull can be equivalently characterized, by analyst's choice, as: (1) one resultant atlas-occipital force that can be resolved into tensile and shear components, and (2) zero applied external torque. Induced torque applied to the head by the neck, by ligamentous imbalance occurring during loading, was recorded and resisted with essentially zero rotary displacement by a rotary torque transducer that coupled the head container and head translation platform.

T1 Extender. By utilizing two visual/X-ray targets on the T1 extender and by tracking (via the overhead television video and 35 mm cameras) the "X-Z" torso container coordinates of these targets as a function of load, a full three-degree-of-freedom analysis of T1 vertebral body displacement could be performed. This provided the means for tracking translation of the T1 vertebral body centroid, even as significant T1 vertebral body rotation was occurring.

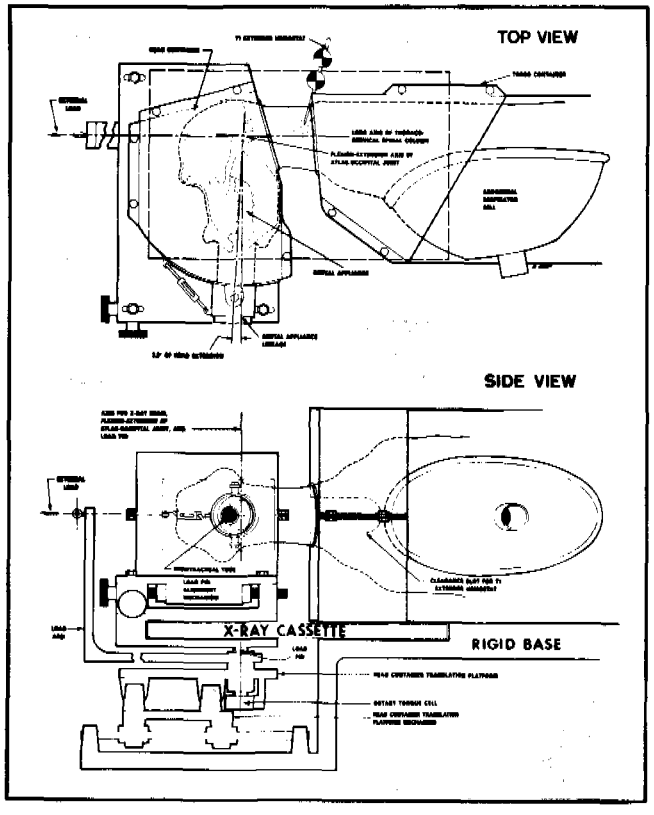

Figure 2. Static neck loading fixture setup.

X-Rays. Radiographs taken for biomechanical purposes included:

(1) Cervical spine during loading (at every fifth load level and at the last load level of 1170 N when structural failure occurred)
(2) Location of load pin versus atlas-occipital axis
(3) Location of T1 extender hemostat versus T1 vertebral body
(4) Cephalic (superior) thoracic spine (torso aligned and restrained in torso container)
(5) Caudal (inferior) thoracic spine (torso aligned and restrained in torso container)
(6) Maximum head extension (erect torso posture)
(7) Maximum head flexion (erect torso posture)

Test Configuration. Neck tension testing was conducted with the anesthetized test animal lying on its right side on a static neck testing fixture. The torso container remained fixed, while the head container was free to translate within the horizontal plane (the animal's sagittal plane) as loading was applied (see Figure 2).

Load Application Rate. Loading was applied to the head platform in 20.2 N increments at five-minute intervals. A load transducer measured the tensile load applied to the head platform (i.e., to the neck). The line-of-force of the load applied to the head platform was aligned parallel with the long (head-to-tail) axis of the thoraco-cervical vertebral spinal column of the test animal.

Engineering Data. The following engineering data were recorded continuously throughout the loading phase of the test:

(1) Tensile neck load versus time
(2) Neck torque applied to the head
(3) "Z" (cephalic) head translation (analog and manual)
(4) "X" (ventral) head translation (analog and manual)
(5) Real-time load versus head displacement plot (for monitoring during loading)
(6) Black and white photographs (one exposure per load increment midway between load increases; optical axis of camera set perpendicular to animal's sagittal plane and intersecting ventral T1 vertebral body extension target)
(7) Color television video coverage (15 seconds prior to, during and following each load increase; optical axis of camera set nearly perpendicular to animal's sagittal plane and intersecting C5 vertebral body when the neck was unloaded).

General

The described methods provided the means for applying large tensile loads to the neck without introducing

artifactual injuries more serious than minor, integument contusions or abrasions to the occiput, mandible and shoulders. Atlas-occipital loading involving predominately pure ventro-dorsal shear loading could have been induced, instead of tensile atlas-occipital loading, by adjusting the line-of-force of the applied load to be perpendicular to the long axis of the thoraco-cervical vertebral spine. However, it should be emphasized that the method currently used for computing the atlas-occipital forces and torque will not apply if the head container makes contact with the torso container.

RESULTS

Engineering

External Load Versus Time. Induced tensile neck load was increased every five minutes until the 51st load level. Death had occurred at the 50th load level. The load increments were continued every two minutes until definitive, ligamentous structural failure (definitive increase in skull displacement) occurred at the 56th load level (see Figure 3).

Neck Torque Versus Load. The neck torque magnitude varied throughout loading but never exceeded 0.45 N·m of torque.

Head Displacement, Relative to Torso Body Block, Versus Load. The total displacement of the head container, relative to the torso container, at 1150 N tensile neck loading (just prior to definitive structural failure) was 106 mm. This represented an average displacement-load ratio of 0.091 mm/N. The final total displacement at 1170 N was 115 mm. This final displacement of 9 mm exhibited a displacement-load ratio of 0.45 mm/N, a value that was 4.9 times higher than the average displacement-load ratio.

T1 Vertebral Body Displacement, Relative to the Torso Container, Versus Load. Translation of the T1 vertebral body centroid, relative to the torso container, was confined to positive Z (cephalic) displacement along the long axis of the cervical spinal column, since essentially zero X (ventro-dorsal) displacement occurred. The Z displacement of the T1 vertebral body centroid plateaued at a maximum of 6.55 cm at a tensile load of 1050 N (see Figure 3).

T1 vertebral body displacement involved left-handed rotations about a leftward-directed (Y) axis, in progressively diminishing increments, until the 20th load level of 433 N. A maximum total rotation of 16° was reached at the 20th load level. T1 vertebral body orientation did not change further at higher load levels.

Neck Length and Neck Elongation Versus Load.* The neck elongation at the tensile load level of 1150 N (just prior to the neck undergoing structural failure) was 64 percent of the initial neck length (see Figure 3).

Medical

Physiological. The mean blood pressure declined and heart rate increased until the 655 N level was reached, at which point the mean blood pressure and heart rate both fell steadily. Death occurred at the 1040 N level (see Figure 3).

Neurophysiological. The somatosensory (wrist-to-brain) far field AER test results, that provided an electrophysiological measure of cervical spinal cord and brain integrity, remained essentially normal and unchanged for the first 115 minutes of tensile neck loading, until the 24th load level of 514 N. At this 514 N level the somatosensory AER primary peak amplitude fell 50 percent and the somatosensory AER transmission time latency period had begun to increase significantly (see Figure 3). By the 27th load level of 575 N, the somatosensory AER latency time

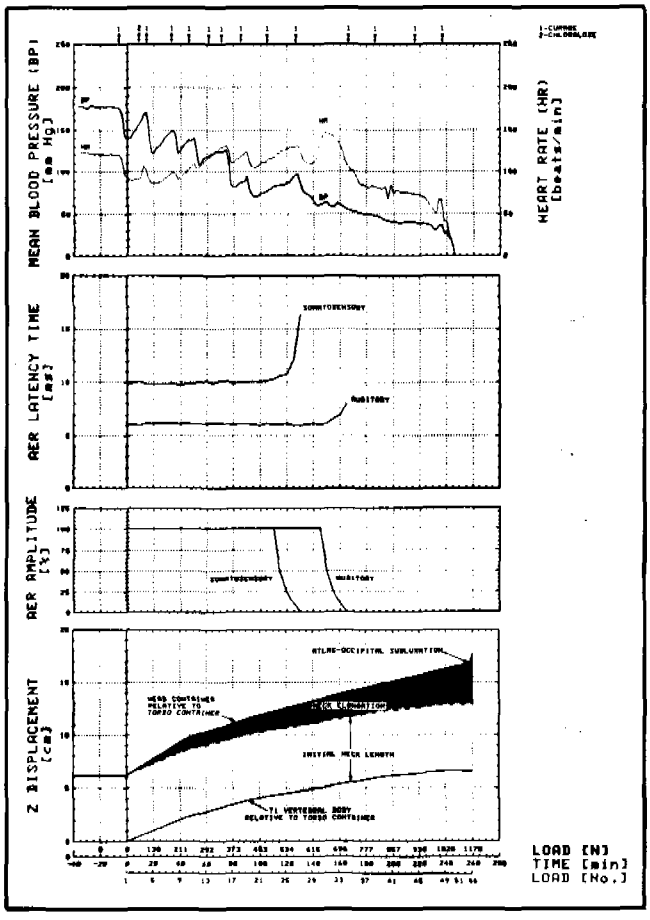

Figure 3. Mean blood pressure, heart rate, somatosensory and auditory far field average evoked response (AER) latency time and principal peak amplitude, and neck elongation versus tensile neck load.

*Neck length was defined as the perpendicular, mid-ssgittal planar distance from the centroid of the T1 vertical body to the flexion-extension axis of the atlas-occipital joint.

had increased by 60 percent from 10 to 16 ms. By the 28th load level of 595 N no somatosensory AER could be detected.

The auditory (ear-to-brain) AER test results, that provided an electrophysiological measure of brain integrity, remained essentially normal and unchanged for the first 150 minutes of tensile neck loading, until the 31st load level of 655 N. At this 655 N level the auditory AER primary peak amplitude fell by 50 percent while the auditory AER transmission time latency period remained unchanged (see Figure 3). By the 34th load level of 716 N, the auditory AER latency time had increased by 33 percent from 6 to 8 ms. By the 35th load level of 736 N no auditory AER could be detected.

Radiological. Post-test, tensile, stress x-rays of the cervical spine revealed marked caudal displacement of the atlas (C1 vertebral body) relative to the occiput.

Gross Pathological. There was severe subluxation of the atlas-occipital joint, with laceration of the dura on the dorsal aspect of the spinal cord. The ventral dura was not torn. There was complete separation of the spinal cord at the junction of the medulla, although there was little evidence of hemorrhaging along the separated margins of the spinal cord and medulla. There was massive basilar subarachnoid hemorrhage, covering all surfaces of the basal meninges and extending as far ventrally as the optic chiasm.

The ventral cervical strap muscles had torn away from the occiput. The ventral atlas-occipital (C1 vertebral body-skull) ligaments were completely severed. The dorsal atlas-occipital ligaments were intact but appeared to be stretched. The atlas-occipital joint capsule was torn with severe hemorrhage into the joint space. The atlas-axis (C1 vertebral body-C2 vertebral body) joint capsule was hemorrhagic, with severe hemorrhage into the joint space.

Neuropathological. Microscopically, the edges of the separated cervical spinal cord and the medulla showed definite, acute parenchymal hemorrhage, extending several millimeters into the adjacent tissue, although no actual hematomas could be found at these margins.

DISCUSSION

Injury Thresholds for Static Neck Tension Test

Neural Function Threshold. Extinction of the somatosensory AERs, in the presence of normal auditory AERs, provided evidence for a putative site of interference with electrical signal transmission and processing between the wrist and the cerebral cortex. It appears reasonable to hypothesize that this site of traumatic blockage of transmission was at the level where complete separation of the spinal cord and medulla eventually occurred, i.e., at the spino-medullary junction. It is known that signal transmission at this level of the spinal cord comprises a critical threat to life. In fact, if respiration had not been sustained mechanically by the abdominal respirator, it appears certain that death would have resulted. Because of the large difference between the neck loads for AER blockage and for structural failure, it is reasonable to hypothesize that normal cervical spinal cord function might have been completely, or partially, restored had the static tensile neck loading been immediately removed following extinction of somatosensory AERs (i.e., at 51 percent of the structural failure load). Alternatively, once a given load level, above the threshold load level for extinction of somatosensory AERs, had been reached, injuries sustained by the cervical spinal cord might well be irreversible. Only further experiments can resolve this question.

Functional Versus Structural Thresholds. At the 595 N tensile load level there was neurophysiological evidence that transmission of electrical signals through the cervical spinal cord had been interrupted. Thus, a functional neural injury impairment of critical clinical significance had been sustained at 51 percent of the neck tensile load level required to induce structural failure in the neck tissues. It should be noted that progressive, static tensile neck loading in the anesthetized animal resulted in death at the 1040 N level. Loading was continued on this fresh cadaver until structural failure occurred at the 1170 N load level. For comparison, Sances (24) found that the cervical spinal column of an anesthetized, 12.0-kg monkey (*Macaca mulatta*) failed at a static axial tensile load of approximately 1100 N. In addition, Sances found that the afferent and efferent average evoked responses significantly decreased well before the cervical spinal column failed.

Injury Mechanisms

Cervical Spinal Cord. Although there was evidence of some fresh parenchymal bleeding, there was a remarkable paucity of blood along the separated margins of the spinal cord and medulla. This would suggest that: (1) the animal was essentially without blood pressure at the time that structural failure (subluxation of the atlas-occipital junction) occurred; and (2) the actual separation of the spinal cord occurred as a late event. Regardless, the parenchymal hemorrhage that was present would suggest that there had been severe pressure on this region of the spinal cord, perhaps from compromise of the spinal canal that had occurred with marked stretching of the atlas-occipital ligaments.

The massive basilar subarachnoid hemorrhage could only have occurred at a time when the animal had blood pressure higher than intracranial cerebrospinal fluid pressure. It is possible that the basilar or intracranial vertebral arteries high in the neck tore early in the sequence of

events as a result of tensile strains transmitted intracranially. Direct evidence of cervical vertebral artery tearing was not detected during the gross necropsy for this first tensile neck loading test. Methods suitable for detecting the source of hemorrhage associated with neck loading will be utilized in future studies.

Structural. The high cervical ligamentous, joint capsular, spinal cord dural and muscular injuries occurred, no doubt, as a result of predominately tensile loading to each of these structures. These lesions were all high in the neck, implying that the atlas-occipital and atlas-axis joints and surrounding structures must be weaker and more vulnerable to injury than the lower cervical joints. Whether disruption or tearing occurred ventrally or dorsally would have been dependent upon the relative degree of head flexion or extension present during tensile loading, along the long axis of the thoraco-cervical spinal column.

SCALING FRESH HUMAN CADAVER DATA TO PROVIDE SOFT TISSUE INJURY THRESHOLDS FOR LIVING HUMANS

No data currently exist for directly scaling *Papio hamadryas* data to predict either structural or functional neural tissue injury thresholds for neck loading in fresh human cadavers or in living humans. Although the *P. hamadryas* is one of the more human-like nonhuman surrogates available, relative to many important shape and size considerations, existing differences in structural and material properties make it nearly impossible to directly derive most human injury threshold relationships from baboon data. However, a reasonable assumption might be that the ratios of injury threshold load values for inducing neural functional failure versus structural failure, in the necks of living *P. hamadryas* and humans, are approximately the same.

Continued experimentation with *P. hamadryas* under other types of static and dynamic loading should demonstrate (for each given type of neck loading) that the threshold loading value for inducing an impairment of cervical spinal cord function can be approximated by some experimentally determined percentage of the threshold loading value for inducing structural failure of the neck. This same experimentally determined percentage value could be used in interpreting the data obtained in matched experiments with fresh human cadavers that have sound structures. Then, threshold loading values for inducing functional failure of neural, cervical spinal cord tissues in living humans may also be deduced. Such additional experimentation with *P. hamadryas* must provide for more realistic values of muscle tone in order to further refine the scaling ratios derived for predicting the values for neural tissue functional failure in living humans from the threshold loading values for structural failure in fresh human cadavers. Such functional versus structural injury scaling relationships for the necks of living humans could, perhaps, be further validated from data analysis on selected crashes and suitably paired accident reconstructions.

CONCLUSIONS

A static tensile loading experiment performed on an anesthetized *Papio hamadryas* produced neurophysiological evidence that cervical spinal cord function had been seriously impaired at 51 percent of the load subsequently required for the occurrence of structural failure (subluxation of the atlas-occipital joint). It appears likely that dynamic neck loading experiments will confirm that serious functional impairment of the neck can be produced at load levels well below those that cause structural failure of the neck.

Existing anthropomorphic automotive test dummies have generally been developed based upon biomechanical data generated from testing performed on human cadavers. This biomechanics data base should be expanded, so that future, advanced test devices can provide realistic measures of the functional impairments sustained by automotive crash victims.

ACKNOWLEDGEMENTS

The technical contributions made by the following project participants are gratefully acknowledged: biomedical engineering—Billy L. Carpenter, Victor C. Graham, Menan C. Hanz, Samuel R. McFarland, Guy N. Phillips, Houston D. Smith, Walter G. Switzer; computer science—Arthur F. Muller; dental science—Thomas B. Aufdemorte; editorial—Barbara J. Alexander, Sylvia V. Alvarado, Judy L. Brandle, Wilma B. Sloan, Lorna L. Wilson, SwRI Editorial staff; instrumentation—William H. McGinnis, M. Eugene Locke, John P. Prudhomme, Maurice C. York; mechanical design—A. Robert Nye, J. Wray Fogwell; SwRI Machine Shop staff; SwRI Photography staff; veterinary anesthesiology—Samuel J. Tomlinson, Sr.; veterinary care—J. Juan Cano, Plutarco Zertuche; veterinary medicine—Edward E. Dean; and veterinary pathology—Ned R. Zamora. In addition, the consultative support provided by the following individuals is gratefully acknowledged: biomechanics—Rolf H. Eppinger, Roger P. Daniel, Harold J. Mertz, Priyaranjan Prasad; manuscript critique—C. William Hall; and neurophysiology—Edwardo Eidelberg.

This research was sponsored by the National Highway Traffic Safety Administration, U.S. Department of Transportation, under contract DTNH-22-80-C-07165.

REFERENCES

1. Huelke, D. F., O'Day, J., Lawson, T. E., Barhydt, W. H. and Mendelson, R. E. Cervical Injuries in Automotive Crashes. Report No. UM-HSRI-80-40, HSRI, University of Michigan, Ann Arbor, 1980.
2. Portnoy, H. D., McElhaney, J. D., Melvin, J. W. and Croissant, P. D. Mechanism of Cervical Spine Injury in Auto Accidents. *Proceedings of 15th Conference of American Association for Automotive Medicine*, 1971.
   The Human Neck-Anatomy, Injury Mechanisms and Biomechanics. Publication No. SP-438. Society of Automotive Engineers, 400 Commonwealth Drive, Warrendale, PA 15096. March, 1979. Includes articles (3–6) by:
3. Huelke, D. F. Moffat, E. A., Mendelson, R. A. and Melvin, J. W. Cervical Fractures and Fracture Dislocations—An Overview. (HS-026-181).
4. Huelke, D. F., Mendelson, R. A., States, J. D. and Melvin, J. W. Cervical Fractures and Fracture Dislocations Sustained Without Head Impact (HS-026-182).
5. States, J. D. Soft Tissue Injuries of the Neck (HS-026-185).
6. Melvin, J. W. Human Neck Injury Tolerance (HS-026-186).
7. Ommaya, A. K., Bakaitis, S., Partyka, S., Langwieder, K. and Fan, W. Automotive Neck Injuries—Comparative Studies in the United States and in the Federal Republic of Germany. *Proceedings of the 9th International E.S.V. Conference*, Kyoto, Japan, November, 1982.
8. Levy, L. M. An Unusual Case of Flexion Injury of the Cervical Spine. *Surgical Neurology* 17(4): 255–259, 1982.
9. Kiesel, T. M., Frerichs, R. L. and Seljeskog, E. L. Cervical Spine Injuries. *Proceedings of 13th Conference of American Association of Automotive Medicine*, 1969.
10. Neurosurgical Aspects of Traffic Accidents: Report of a Subcommittee of the Canadian Neurosurgical Society. *Canadian Medical Association J.* 97: 1364, 1967.
11. Norton, W. L. Fractures and Dislocations of the Cervical Spine. *J. Bone Joint Surgery* 44A: 115–139, 1962.
12. Roaf, R. A. Lateral Flexion Injuries of the Cervical Spine. *J. Bone Joint Surgery* 45B: 36–38, 1963.
13. Rogers, W. A. Fractures and Dislocations of the Cervical Spine. An End Result. *J. Bone Joint Surgery* 39A: 341–376, 1957.
14. Schneider, R. C. and Kahn, E. A. Chronic Sequelae of Spine and Spinal Cord Trauma. I. The Significance of the Acute "Teardrop" Fracture. *J. Bone Joint Surgery* 38A; 985, 1956.
15. Schneider, R. C., Livingston, K. E., Cave, A. J. E. and Hamilton, G. Hangman's Fracture of the Cervical Spine. *J. Neurosurgery* 22: 141–154, 1964.
16. Taylor, A. R. and Blackwood, W. Paraplegia in Hyperextension Cervical Injuries with Normal Radiographic Appearances. *J. Bone Joint Surgery* 30B: 245–248, 1948.
17. Voight, G. E. and Wilfert, K. Mechanisms of Injuries of Unrestrained Drivers in Head-On Collisions. *Proceedings of 13th Stapp Car Crash Conference*, 1969.
18. Roaf, R. A. A Study of the Mechanics of Spinal Injuries. *J. Bone Joint Surgery* 42B: 810–823, 1960.
19. Burstein, A. H., Otis, J. C. and Torg, J. S. Mechanisms and Pathomechanics of Athletic Injuries to the Cervical Spine. *Mechanisms and Pathomechanics of Cervical Spine Injury*. (J. S. Torg, ed.) Lea and Feiberger, Philadelphia, 1982.
20. Brauze, R. J. and Ardran, G. Experimental Production of Forward Dislocation in the Human Cervical Spine. *J. Bone Joint Surgery* 60B: 239–245, 1978.
21. Beatson, T. R. Fractures and Dislocations of the Cervical Spine. *J. Bone Joint Surgery* 45B: 21–35, 1963.
22. Davis, D., Boylman, H., Walker, A. E., Fisher, R. and Robinson, R. The Pathological Findings in Fatal Craniospinal Injuries. *J. Neurosurgery* 34: 603–613, 1971.
23. Holdsworth, F. W. Fractures, Dislocations, and Fracture-Dislocations of the Spine. *J. Bone Joint Surgery* 45B: 6–20, 1963.
24. Sances, A., Jr., Myklebust, J., Cusick, J. F., Weber, R., Houterman, C., Larson, S. J., Walsh, P., Chilbert, M., Prieto, T., Zyvoloski, M., Ewing, C., Thomas, D. and Saltzberg, B. Experimental Studies of Brain and Neck Injury. Paper 811032, *Proceedings of 25th Stapp Car crash Conference*, 1981.
25. Culver, R., Bender, M. and Melvin, J. W. Mechanisms, Tolerances and Responses Obtained in Neck Injury by Superior-Inferior Head Impact. Report No. UM-HSRI-78-21, HSRI, University of Michigan, Ann Arbor, 1978.
26. Mertz, H. J. and Patrick, L. M. Strength and Response of the Human Neck. Paper 710855, *Proceedings of 15th Stapp Car Crash Conference*, 1971.

Part Two: Dummies

Description and Basis of a Three-Year-Old Child Dummy for Evaluating Passenger Inflatable Restraint Concepts

M. J. WOLANIN, H. J. MERTZ,
R. S. NYZNYK, J. H. VINCENT
General Motors Corporation

ABSTRACT

A primary concern in the development of a passenger inflatable restraint system is the possibility that a child could be in the path of the deploying cushion either due to initial position at the time of an accident or due to precrash braking accompanying an accident. Previous studies by General Motors and Volvo have indicated that serious injuries to children are possible if the cushion/child interaction forces are not controlled by system design. This paper describes an instrumented child dummy which was developed to provide measurements of the various cushion/child interaction forces. An analysis is given describing the types of injuries which could be associated with the various types of interaction forces. These results were used to develop appropriate dummy instrumentation for indicating the severity of the cushion/child interaction. A description of the modifications made to an existing three-year-old child dummy are described. The usefulness and limitations of the measurements made with the child dummy are discussed. While the measurement techniques were developed for evaluating inflatable restraint system performance, some of the response measurements are appropriate for estimating child responses when restrained by a lap/shoulder belt or unrestrained.

INTRODUCTION

When General Motors started its development of a second generation passenger inflatable restraint, the interaction of the out-of-position child with the deploying cushion was identified as a topic requiring further study. In previous inflatable restraint development programs by General Motors Corporation (1) and Volvo (2), animals have been used as child surrogates to evaluate potential injury hazards to children who may be in the path of the cushion during its deployment. The General Motors' program which was conducted at Wayne state University used baboons and chimpanzees as surrogates while the Volvo study conducted at Chalmers University in Sweden used pigs. Significant brain, heart, liver and spleen injuries were noted during the courses of these development programs. It was also apparent from these programs that significant neck injury might occur if the animal was positioned so that the interaction forces produced large head to torso motion. Unfortunately, neither program provided any objective correlations between the observed animal injuries and the inflatable restraint system design factors, nor was any attempt made in either program to develop a test device to aid in understanding the relationships between the observed injuries and the forces exerted by the deploying cushions which could be used to guide the development of future inflatable cushion systems. Consequently, when General Motors initiated the development of its second generation passenger inflatable restraint system, it concurrently undertook the development of a child dummy which would provide measures of the various deployment interaction forces thought to be associated with injuries observed or inferred from previous animal test programs.

An extensive child dummy development program was considered impractical because such a program would not result in a child dummy soon enough to be used to support the passenger inflatable restraint development program. To be useful, a child dummy had to be developed in a relatively short time frame and had to provide measures of the types of forces and acelerations which were thought to be associated with the types of animal injuries observed in the previous inflatable restraint development programs.

A two-phase child dummy development program was formulated. For the first phase, instrumentation was added to an existing child dummy to improve its measuring capabilities. Due to time constraints, modifications to improve impact response characteristics were kept to a minimum. For phase two, the child dummy was further modified to improve impact response characteristics and to eliminate any major deficiencies noted while using the first phase dummy. This paper describes the child dummies (Design 1 and Design 2) developed in Phases 1 and 2, respectively.

DESIGN 1 DUMMY

Analysis of Child/Cushion Interaction Forces

To gain an insight as to what types of measurements should be made with the child dummy, the kinematics and kinetics associated with possible child/cushion interactions were analyzed.

During the initial stage of deployment, the cushion and cover material are accelerated rearward relative to the vehicle. If the child is close enough to the system he will be impacted by this mass when it is in a relatively dense, concentrated form. The center of gravity of this mass will be decelerated by the part of the child's body being impacted. This interaction force is termed "onset impulsive force".

A second type of force is developed on the out-of-position child when a sufficient volume of gas has been generated to produce a positive gage pressure in the cushion resulting in the cushion material becoming taut. Prior to this point in the deployment cycle, the cushion is unfolding and its volume is increasing in response to the gas filling it. A large positive gage pressure cannot be developed unless the cushion material is prevented from unfolding, thus restricting its volume expansion. During the unfolding phase of the deployment cycle, the forces on the out-of-position child are relatively small. However, when sufficient gas has been generated to make the cushion material taut, the cushion gage pressure will begin to increase and the child will be accelerated rearward as the remainder of the gas is generated. The forces applied to the child during this phase of the deployment cycle are called "membrane forces" since they depend on biaxial tensile forces being developed in the cushion material. The magnitude of these membrane forces is dependent on the difference in the volumes of the undeformed and deformed air cushion, the envelopment geometry, the rate at which the remaining gas is generated, the gas leakage from the cushion and the elasticity of the air cushion material.

A third type of force is applied to the child when he impacts the seat after being accelerated rearward by the air cushion. These forces are called "rebound" forces. The magnitude of the rebound forces are dependent on the relative velocity at which the child strikes the seat, and the shape and stiffness of the seat structure involved in the impact. The relative impact velocity is dependent on the magnitude of the membrane forces and the velocity of the seat structure at the time of impact.

Since injuries can be produced by any of these different types of forces, the first priority in the Phase I program was to identify techniques to measure the effects of these types of forces.

Techniques to Measure Effects of Onset Impulsive Forces

The magnitude of the impulse associated with the onset impulsive force is proportional to the product of the impact velocity and the mass of the cushion/door which contacts the child. The peak of the onset impulsive force will be large and the time to peak will be short because the mass of the cushion/cover contacting the child will be quickly decelerated to the velocity of the surface of the child which it impacts. Of importance in terms of possible serious injuries are the onset impulsive forces applied to the head and torso of the child.

The severity of the onset impulsive forces applied to the head can be measured by accelerometers mounted at the center of mass of a dummy's head since the head structure is quite rigid and will transmit short duration loads. Measurement of torso contact force is more difficult because accelerometers mounted to the spine of the dummy are not sensitive to the onset impulsive force due to the lack of transmissibility of the chest structure to short duration impulses applied to the front surface. However, an array of accelerometers attached to the front surface of the torso would be sensitive to onset impulsive forces and would give an indication of their distribution over the torso surface. The technique required to make these measurements and corresponding torso modifications are described in detail under the section on Torso Modifications.

Techniques to Measure Effects of Membrane Forces

The child can be injured in two ways by membrane forces. If large membrane forces are developed, the child will be rapidly accelerated rearward. Since the internal organs will be accelerated as well, forces will be applied to them through their internal attachments and/or through contact with neighboring organs. If these internal forces are large enough, injury to the organs and/or attachments can occur. The magnitude of these internal forces will be dependent on the magnitude and direction of the acceleration of the body segment containing the organs of interest. Injuries to the brain and the organs of the torso such as the heart, lungs, liver, spleen and kidneys are of particular concern. Measurement of the potential for injury to these internal organs due to membrane forces can be obtained from whole body accelerations. Techniques to measure whole body accelerations are discussed under the sections on Head and Torso Modifications.

A second way the child can be injured by membrane forces is by one body segment being accelerated at a different rate than an adjacent segment, resulting in high interaction forces in the connecting tissues. Of specific concern is injury to the neck area if the head is accelerated at a different rate than the torso. A load transducer inserted between the dummy's head and neck can be used to measure internal neck loads. Analysis of such loads can be used to predict the potential for neck injury. A technique to measure internal neck loads is discussed in detail under the section on Head Modifications.

Techniques to Measure the Effects of Rebound Forces

Injury to the internal organs can occur if the rebound forces are too large, as well as injury to connecting tissues if the relative motion between adjacent body segments is too great. Since these are the same injury concerns noted for the membrane forces, no additional dummy instrumentation was considered necessary to assess the severity of the rebound forces.

Mainframe Selection

In order to have a child dummy available for use in GM's Inflatable Restraint System Development Program,

an existing dummy mainframe was chosen for Design 1. At the time of this work, child dummies were being manufactured by both American and European companies. General Motors had test experience with American-made three-year-old and six-year-old child dummies manufactured by Sierra Engineering Co. and Alderson Research Laboratories, Inc. (ARL). Since Sierra was phasing out of the dummy manufacturing business, only the ARL three-year-old and six-year-old dummies were selected as possible candidates for the mainframe for the Design 1 dummy.

After weighing many considerations, the ARL VIP-3C was selected as the mainframe for the Design 1 dummy for the following reasons:

i) Due to precrash braking, more younger children would be expected to be near the instrument panel and thus involved with a deploying cushion. The three-year-old child dummy would be more representative of these size children.
ii) A greater range of possible child positions and postures could be evaluated with a smaller, three-year-old child dummy.

The ARL VIP-3C dummy is shown in Figure 1. The head is a urethane casting covered with a removable vinyl skin and is joined to the upper torso by means of a monolithic natural rubber neck. A foam-filled, molded urethane rib cage and steel weldment form the upper torso segment. The lumbar spine is a monolithic natural rubber cylinder connecting the upper torso and pelvis assemblies. A bronze casting and aluminum weldment form the pelvis which incorporates spherical sockets at the femur joints. The limbs are constructed of steel tubing covered with foam and a vinyl skin. Primary joints for the shoulder, elbow, wrist, knee and ankle are of a clevis design with adjustable joint friction.

Twist joints which are incorporated in the arms and legs utilize a rod and sleeve design with clamping friction adjustment. Spherical joints with adjustable friction characteristics are employed in the shoulder to clavicle and the femur to hip joints.

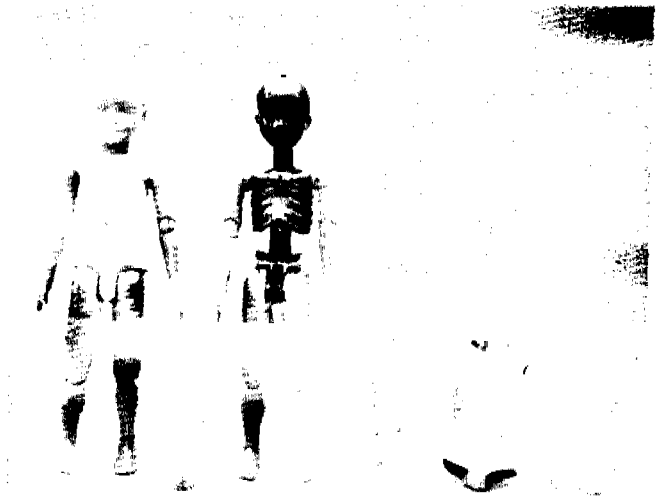

Figure 1. ARL VIP-3C three-year-old child dummy.

Head Modifications

Previous test experience with the ARL VIP-3C dummy indicated that the thin vinyl head covering frequently failed at the zipper. This vinyl skin also interacted with the head and neck in a somewhat variable manner during both neck flexion and extension bending. To improve both durability and repeatability, the vinyl skin was discarded in Design 1, resulting in a slight reduction in overall head size.

The head cavity was modified to mount five linear accelerometers; three accelerometers to measure the three components of linear acceleration of the head's mass center and two accelerometers to measure head angular acceleration in the sagittal plane (Figure 2). The acceleration of the head's mass center is measured by three Endevco linear accelerometers orthogonally mounted on an alu-

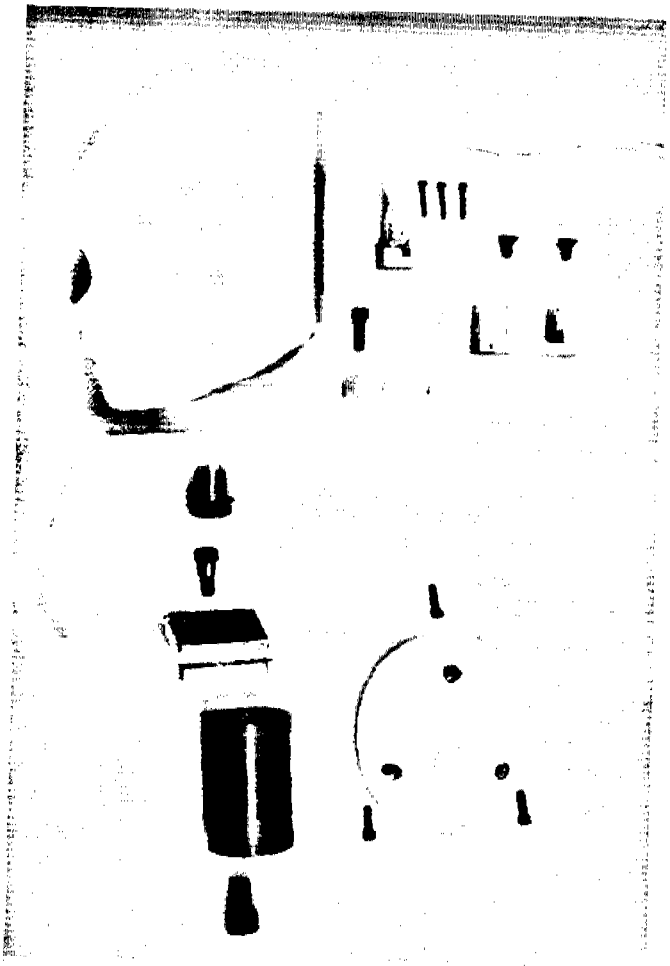

Figure 2. Exploded view of the design 1 head and neck assembly showing the various head accelerometers and neck load transducer which were added to the VIP-3C head and neck.

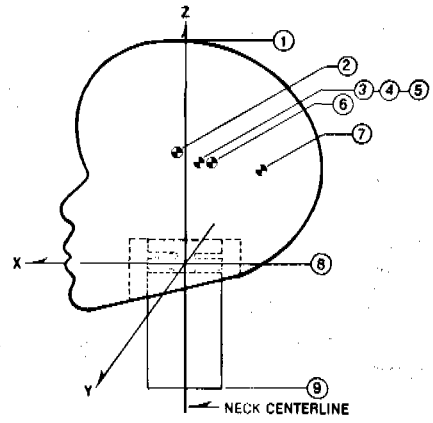

REF. PT.	DESCRIPTION	X	Y	Z
1	TOP OF HEAD	0.0	0.0	146.5
2	ANTERIOR HEAD ANGULAR ACCELEROMETER	4.5	15.9	76.6
3	LATERAL HEAD ACCELEROMETER	-10.2	-10.0	67.5
4	VERTICAL HEAD ACCELEROMETER	-10.2	-1.0	66.7
5	HEAD CENTER OF GRAVITY	-10.2	0.0	67.0
6	LONGITUDINAL HEAD ACCELEROMETER	-18.6	0.0	67.5
7	POSTERIOR HEAD ANGULAR ACCELEROMETER	-52.5	15.9	63.0
8	NECK TRANSDUCER GAGE PLANE	0.0	0.0	0.0
9	BASE OF NECK	0.0	0.0	-84.0

ALL DIMENSIONS GIVEN IN mm

Figure 3. Sensitive element locations for the instrumentation used in the design 1 head and neck.

minum block. The center of the accelerometer cluster is located at the mass center of the unmodified ARL VIP-3C head and neck. Angular acceleration is measured by two Endevco linear accelerometers mounted on a horizontal plane with their sensitive axes vertical. One accelerometer is forward of the head's mass center and the other accelerometer is rearward of the head's mass center. The outputs of these two accelerometers are subtracted to obtain sagittal plane angular acceleration. Figure 3 shows the seismic mass locations for each of the five head accelerometers.

A major modification to the base of the VIP-3C head was required to accommodate the neck load transducer while maintaining the overall height of the head and neck assembly. To house the neck transducer, a 76 mm diameter pocket was cut into the base of the VIP-3C head to the depth of the steel insert which was then removed and discarded. The deletion of this steel insert not only provided physical space for the neck transducer, but also tended to compensate for the additional mass of the neck transducer. Attachment of the head to the neck was accomplished by clamping the remaining urethane base of the head to the top of the neck transducer. The clamp was formed by the accelerometer mount adapter and screw which are shown in Figure 2.

The neck transducer used was a four axes load cell capable of measuring axial forces, anterior-posterior shear forces, and lateral shear forces up to 9000 Newtons and sagittal plane bending moments up to 70 Newton-metres. The neck load cell was mounted to the top of the neck since high cervical neck injuries have more severe consequences than injuries to the lower cervical area. No modification was made to the ARL VIP-3C neck structure and the overall dimension from the base of the neck to the top of the head was maintained at the ARL VIP-3C value.

Torso Modifications

The technique chosen to measure the effects of onset impulsive forces on the torso was to suspend a series of small masses near the surface of the torso and measure the accelerations of these masses as they responded to the onset impulsive forces. A uniaxial accelerometer was mounted to each mass and its sensitive axis was oriented perpendicular to the torso surface.

To mount these instrumented torso surface masses, extensive torso modifications were required. The existing ARL VIP-3C thoracic and lumbar spine structures and the foam torso were discarded. A rigid, two-piece backbone was fabricated. It was attached at its lower end to the pelvic structure and at its upper end to the neck and shoulder pivots (Figures 1 and 4). The length of the

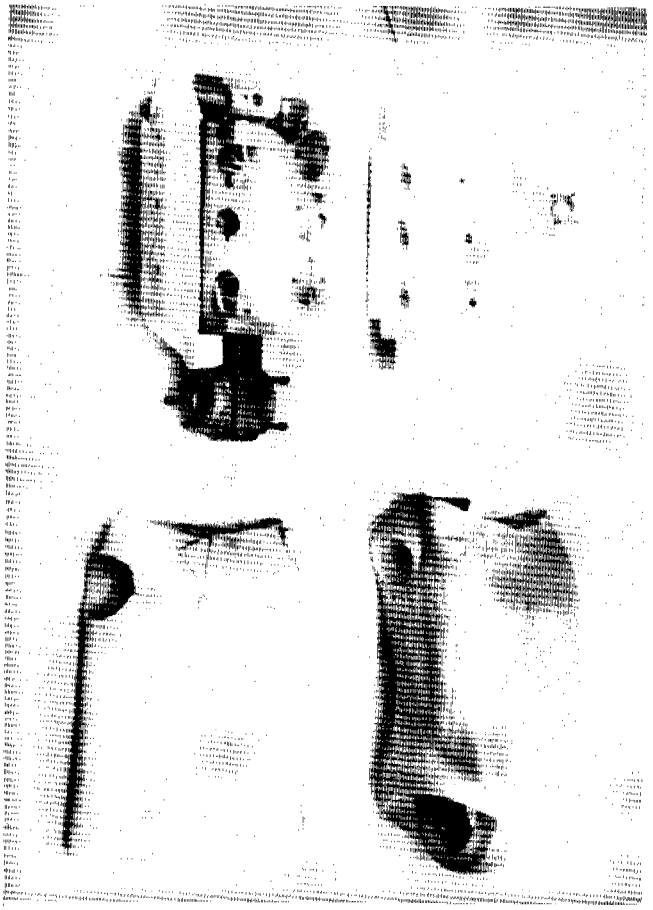

Figure 4. Exploded view of the torso used in both designs 1 and 2 showing the rigid skeletal structure, compliant foam chest structure, spine accelerometers, instrumented surface masses, and skin coverings.

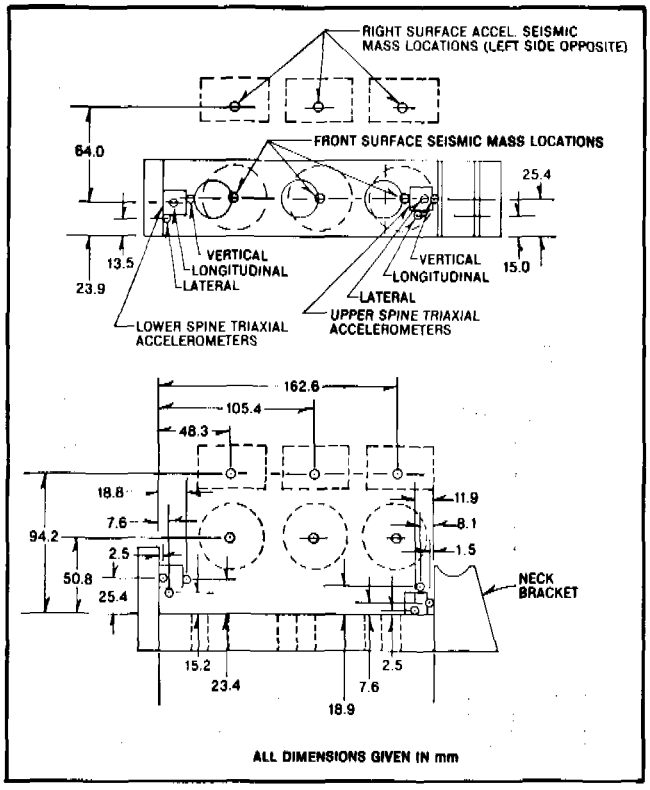

Figure 5. Seismic mass locations of the various torso accelerometers used in designs 1 and 2.

backbone was selected to maintain the torso length of the ARL VIP-3C. Closed cell foam pads were used to fabricate the torso shape. Holes were cut in the foam to accommodate the instrumented surface masses (Figure 4). Provisions were made to mount nine such masses; three in mid-sagittal plane of the front surface (upper, mid and lower torso), and three in each side. The instrumented surface masses were made of aluminum and weighed 92 grams each including the accelerometer.

The primary purpose of the torso foam was to suspend the instrumented surface masses. No attempt was made to develop a human like force-deflection characteristic for the torso because biomechanics data on child torso response characteristics were not available, and the time constraints did not allow for such a development program. Foam stiffness was not considered critical for the assessment of the effect of short duration onset impulsive forces because the instrumented surface masses will undergo only small displacements during the time required for the onset impulsive forces to reach their peak values resulting in only small amounts of foam compression during this time period. This implies that the foam resisting force will be quite small compared to the peak onset impulsive force. Thus, the peak acceleration of the instrumented surface mass should give a good indication of the peak onset impulsive force applied to the mass.

To measure the effects of membrane and rebound forces applied to the torso, triaxial clusters of uniaxial accelerometers were mounted to each end of the backbone (Figure 4). Seismic mass locations for all the accelerometers mounted in the torso are shown in Figure 5.

The torso was encased in a 1/16 inch thick, oaktanned leather jacket shown in Figure 4. Darts were sewn in the upper chest area for contouring. Brass grommets were inserted in the rear to facilitate lacing the jacket with a nylon cord. The existing ARL VIP-3C vinyl torso skin with added gussets was used to cover the torso. A 50 mm wide hook and loop tape fastener was sewn on the back to replace the zipper.

The modifications that were made to the torso resulted in a 35 mm increase in chest circumference; however, torso mass remained the same. No changes were made to the arms and legs. The complete Design 1 dummy is shown in Figure 6.

Component Response Documentation

The following response data only document the responses of the various components of the Design 1 dummy. They should *not* be construed as being representative of a child's responses.

Head Drop Test—The impact response characteristics of the head of the Design 1 dummy were documented by dropping it onto a rigid steel plate. The impact point was the forehead and the drop distance was 376 mm. A typical acceleration response is shown in Figure 7. Note the low frequency resonance which reflects the low stiffness and damping of the urethane used to mold the head.

Neck Bending Test—Dynamic neck bending tests were conducted to document the response characteristics of the Design 1 neck structure in forward flexion and rearward extension. The pendulum test fixture specified for measuring neck response characteristics in Part 572 (3) was

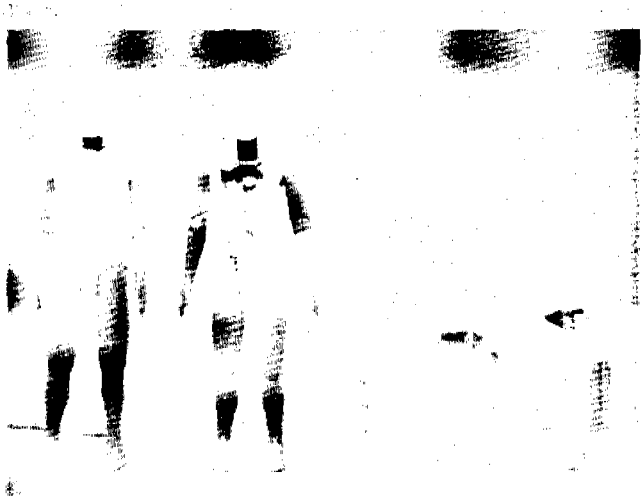

Figure 6. GM design 1 three-year-old child dummy.

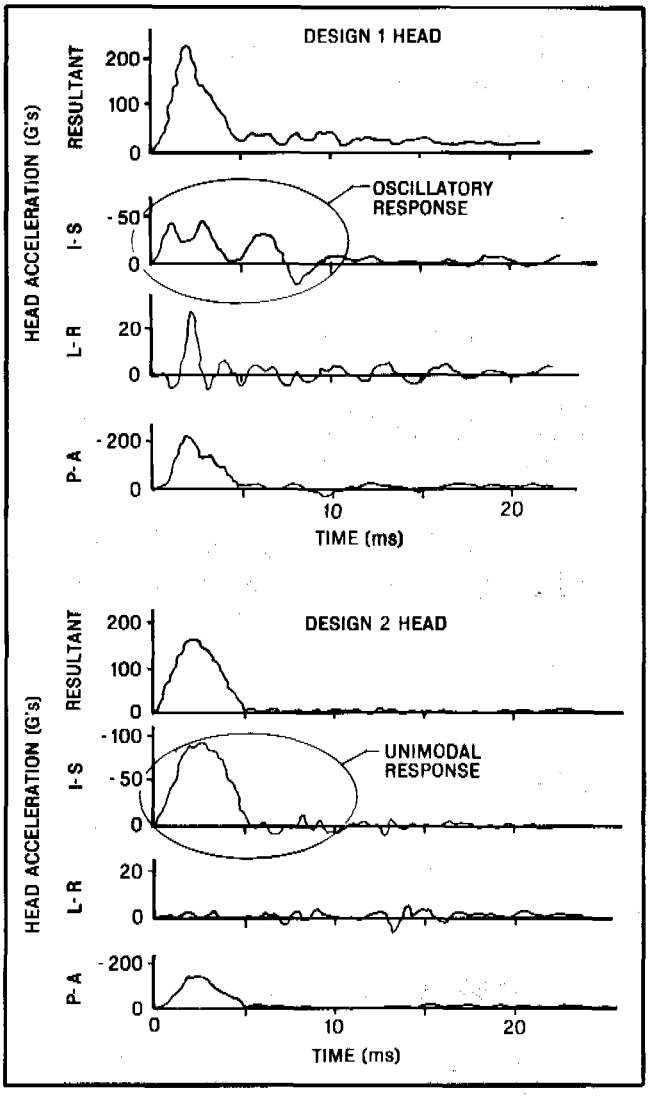

Figure 7. Typical head acceleration response curves for designs 1 and 2 from forehead impacts onto a rigid steel plate from a drop height of 376 mm.

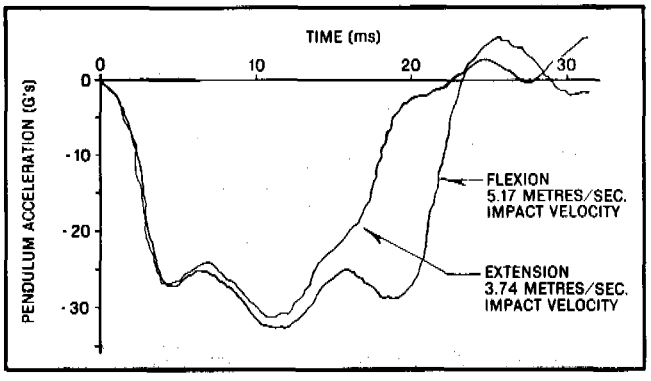

Figure 8. Deceleration pulses and initial velocities used to measure forward and rearward bending responses to designs 1 and 2 head-neck assemblies.

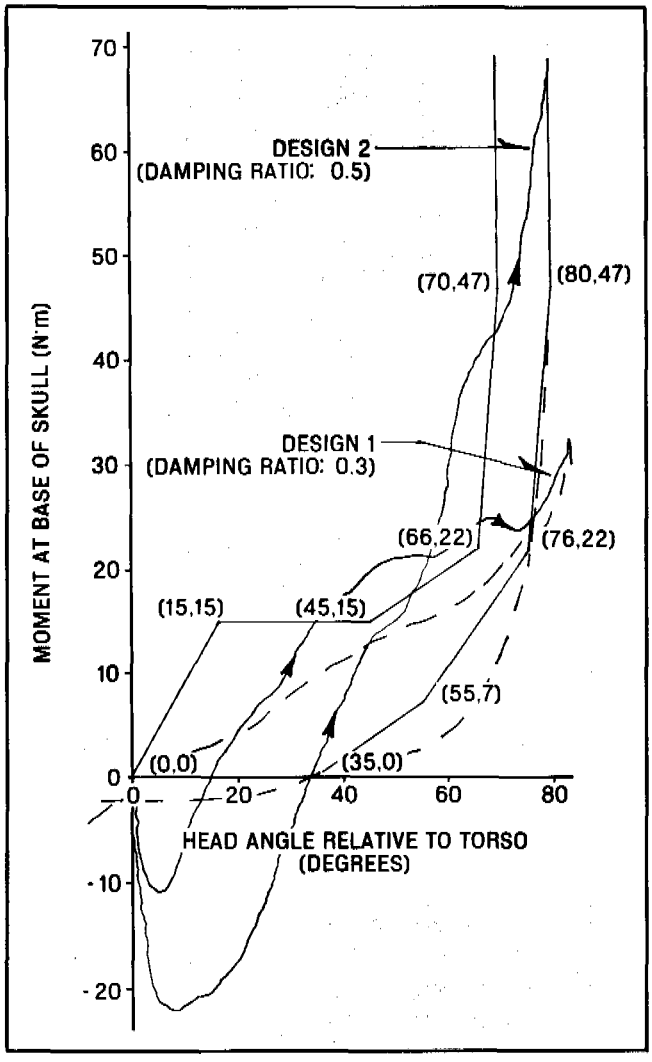

Figure 9. Forward bending responses of designs 1 and 2 head-neck assemblies compared to response envelope for a three-year-old child.

used to perform these tests. Typical deceleration pulses and velocities are shown in Figure 8. Response characteristics in forward flexion and rearward extension are shown in Figures 9 and 10, respectively. The ordinate of these curves is the moment measured with the neck transducer and the abscissa is the corresponding angular displacement of the head with respect to the pendulum arm.

The damping characteristic of the neck structure was determined from the head angular rotation-time curves. During a bending test, the head-neck system undergoes multiple flexion-extension cycles of progressively decreasing amplitude. A damping ratio was determined by dividing the difference in peak angles between the first and second cycles by the peak angle of the first cycle. These damping ratios are shown with their corresponding moment-angle response curves on Figures 9 and 10.

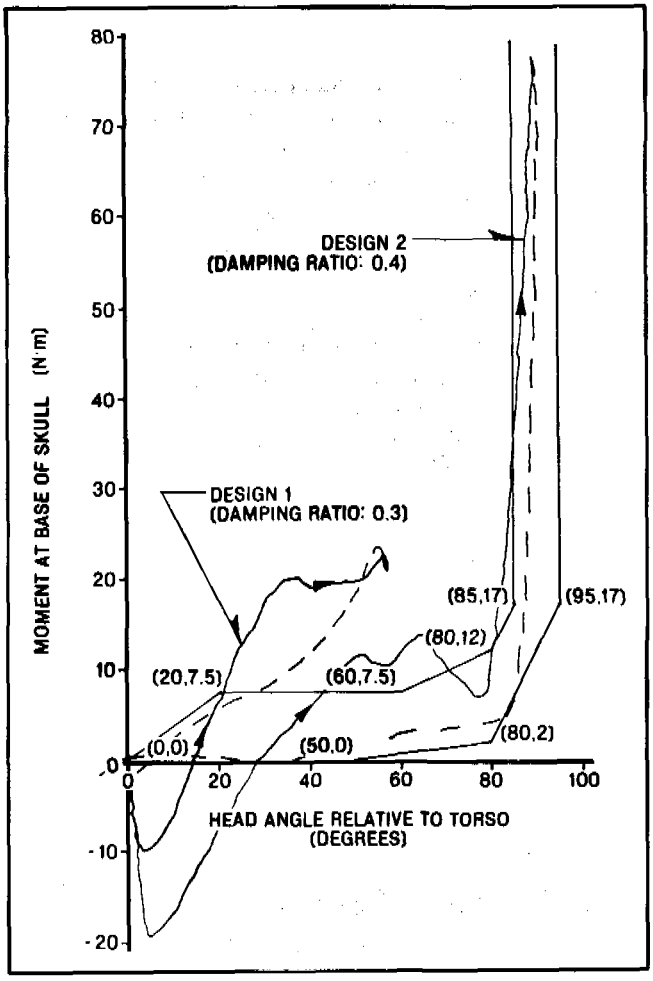

Figure 10. Rearward bending responses of designs 1 and 2 head-neck assemblies compared to response envelope for a three-year-old child.

Static Load—Deflection Test—The torso of the Design 1 dummy was subjected to a series of static load deflection tests over the course of the Inflatable Restraint (IR) development program. A 100 mm wide loading plate was centered over the middle instrumented front surface mass and a static load was applied sufficient to deflect the torso 25 mm. The resulting load-deflection curves for the various tests are shown in Figure 11. The curves demonstrate a wide range of static stiffnesses that is characteristic of closed foam materials. The results of these tests indicated that the static stiffness tended to increase with repeated stiffness testing; however, if the material was allowed to "relax" before retesting, the stiffness was close to its original value.

Use of Design 1 Dummy

The Design 1 dummy has been used in hundreds of inflatable restraint system development tests by General Motors and has proven to be a valuable test tool for assessing changes made to our various passenger inflatable restraint system concepts. These assessments were made in two ways. The first was a straightforward A to B comparison where the object was simply to reduce the magnitudes of the various dummy responses with a given IR design change. The second way was to predict the effect that an IR design change would have on an anesthetized animal's (a child surrogate) response. In order to do this latter type of an assessment, a correlation between the dummy's responses and observed animal injuries for similar exposure environments had to be established. Such a correlation study is the subject of a paper by Mertz and Weber (4) and is beyond the scope of this paper.

DESIGN 2 DUMMY

Design Considerations

As noted previously, the objective of the Design 2 dummy development program was to develop a dummy to eliminate any major deficiencies noted while using the Design 1 dummy.

Of major concern in using the Design 1 dummy was the lack of childlike bending response of the dummy's neck. Anesthetized animal tests (5) have shown that serious neck injuries could be produced by an inflating cushion, and child dummy tests (4) conducted under similar conditions resulted in high neck loads. However, both child surrogates, the anesthetized animals and the Design 1 dummy, had neck bending stiffnesses which were thought to be greater than that of a child. Further, it was hypothesized that a child with lower neck bending resistance would not experience high loads, and consequently, would not experience serious neck injuries in similar exposure environments. To determine the effect of neck stiffness on neck loads due to head/cushion interactions, it was proposed to develop a dummy neck structure whose bending resistance and range of motion would be more characteristic of a child's.

Two other modifications were considered for the Design 2 dummy. It was suggested that the chest should be replaced with a structure that had force-deflection response characterisics that simulate a child's and that a transducer to measure chest deflection should be added. Also, it was suggested that the rigid thoracic/lumbar spine should be replaced by a flexible structure. While these proposed modifications would certainly improve the biofidelity of the child dummy's responses, it did not appear that such modifications would greatly enhance the ability to interpret the significance of the cushion/torso interaction forces.

After review of these various suggested modifications, it was decided only to make the neck bending response more childlike in the Design 2 dummy. The following is a list of items which were considered important in order to improve the biofidelity of the neck bending response.

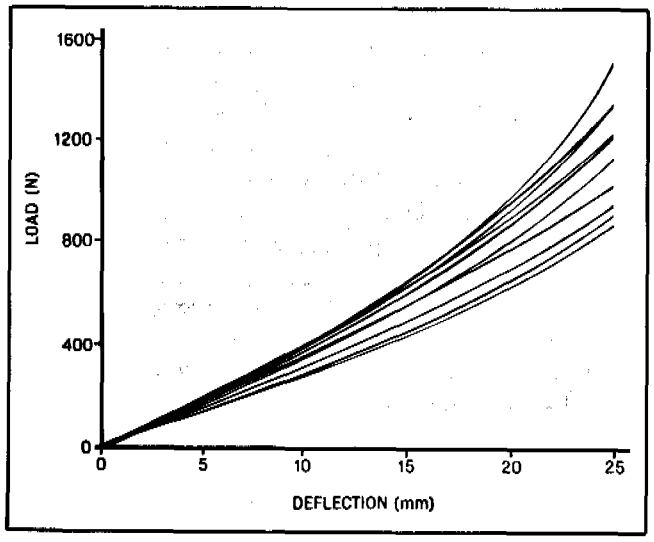

Figure 11. Static load-deflection responses for the chest structure used in designs 1 and 2.

i) The head geometric characteristics need to be childlike. The most important geometric characteristics are the locations of the center of mass and the head/neck interface relative to the exterior head surface. These dimensions control the magnitude of the moment arm of the forces applied to the head which bend the neck. Also, the head size and shape need to be childlike since these dimensions influence the magnitude of the cushion/head interaction forces.

ii) The inertial properties of the head need to be childlike with the head mass being most important because it controls the magnitude of the inertial force which bends the neck.

iii) The neck length needs to be childlike since it influences the trajectory that the head undergoes relative to the torso.

iv) The dummy's neck structure needs to simulate the fore/aft bending response of a child's neck.

It is apparent from this list that modifications to both the head and neck structures would be required in order to achieve a childlike neck bending response.

Head and Neck Geometric and Inertial Data

Table 1 and Figure 12 summarize the head and neck geometric and inertial data which were considered in the designs of the head and neck structures. The work of Snyder et al. (9) provided most of the child anthropometry data. Snyder gives data for various mean dimensions of children in the 2 to 3½ year old age bracket and 3½ to 4½ year old age bracket. A linear interpolation was done to calculate dimensions that would be representative of a 2½ to 3½ age range. The means of this age range were taken to represent a 3-year-old child and are the values given in Table 1.

For a number of the desired child dimensions, no anthropometry data were available. To obtain values for these dimensions, the adult anthropometry data listed in Table 1 were scaled using the following relationship:

$$\text{D child} = \frac{\text{C child}}{\text{C adult}} \times \text{D adult}$$

where

D child — Desired Child Dimension
D adult — Corresponding Adult Dimension
C child — Characteristic Length of Child
C adult — Corresponding Characteristic Length of Adult

The chin to front of neck dimension listed in the table was scaled from a measurement made on a 3-year-old child. The child head weight was calculated by multiplying the adult head weight by the cube of the ratio of characteristic lengths. This scaling relationship assumes that the densities of the adult and child head are equal.

The various characteristic lengths used for each calculation are given in Table 2.

Neck Bending Response Requirements

The adult fore/aft neck bending response envelopes described by Mertz et al. (11) were scaled to give the

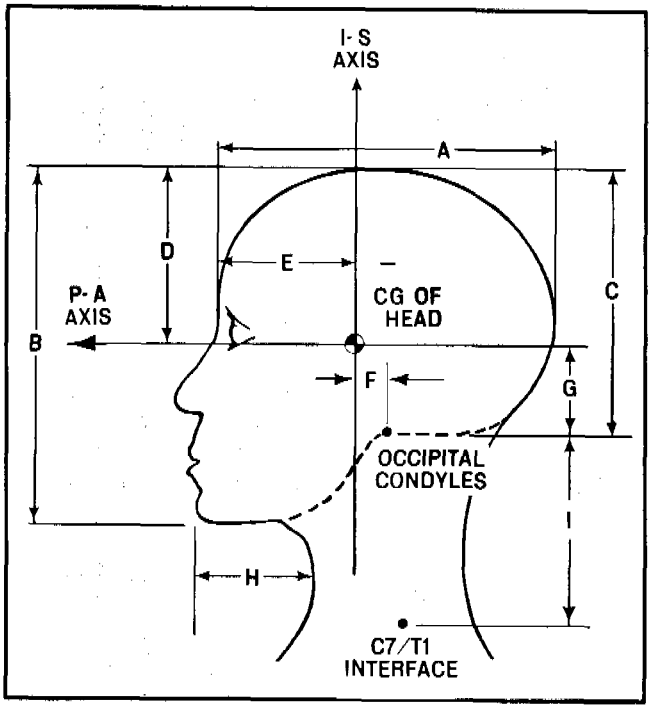

Figure 12. Definition of key head and neck dimensions.

Table 1. Head and neck anthropometric and inertial characteristics.

DESCRIPTION	SEE FIG. 12	50TH %ILE ADULT MALE VALUE	NO.	3 - YEAR OLD CHILD VALUE	NO.	DESIGN 1 DUMMY VALUE	% DIFF.	DESIGN 2 DUMMY VALUE	% DIFF.
HEAD CIRCUMFERENCE	-	572	6	496	9	479	-3	499	1
HEAD BREADTH	-	155	6	135	9	133	-1	139	3
HEAD LENGTH	A	196	6	176	9	163	-7	166	-6
HEAD HEIGHT	B	221	6	174	9	179	3	185	-5
HEAD VERTEX TO OCCIPITAL CONDYLES	C	152	6	120	SCALED	148	23	121	1
HEAD VERTEX TO HEAD C.G.	D	104	6	82	SCALED	81	-1	83	1
NASION TO HEAD C.G. (A-P)	E	84	6	75	SCALED	71.2	-5	66.1	-12
HEAD C.G. TO OCCIPITAL CONDYLES (A-P)	F	18	6	16	SCALED	-10	-163	16	0
HEAD C.G. TO OCCIPITAL CONDYLES (S-I)	G	48	6	38	SCALED	67	76	38	0
CHIN TO NECK	H	-	-	48	MEASURED	52	8	53	10
HEAD WEIGHT	-	4.5	6	2.9	SCALED	2.50	-14	2.95	2
NECK CIRCUMFERENCE	-	384	10	239	9	157	-34	220	-8
NECK BREADTH	-	-	-	72	9	51	-29	70	-3
NECK LENGTH	I	142	7	88	SCALED	82	-7	84	-5
NECK WEIGHT	-	1.4	7	0.34	SCALED	0.48	41	0.56	65
STANDING HEIGHT	-	1748	8	980	9	980	3	982	3
TOTAL WEIGHT	-	74.5	7	14.5	9	14.9	3	15.4	6

NOTES 1: DIMENSIONS ARE IN mm AND WEIGHTS ARE IN kg
2: NO. REFERS TO PAPER NUMBER GIVEN IN LIST OF REFERENCES.

neck bending response requirements for the 3-year old child dummy. The adult neck bending response is characterized by the neck resisting moment taken with respect to the head/neck interface (occipital condyles) as a function of the relative angle between the head and torso (Figures 13 and 14). In order to develop a neck bending response for the child, scale factors for the moment and angle needed to be determined.

Moment Scaling—The constant moment plateaus of the adult response envelopes were based on the static bending strength of the neck in resisting flexion and extension. These moments represent the levels at which the neck muscles are no longer capable of preventing the head from moving forwards or backwards in response to a static load applied to the head. Note that the magnitude of the static strength moment in resisting forward flexion is two times greater than the extension moment. This difference in magnitude is consistent with the anatomical observation that the majority of the neck muscle masses are located in the back of the neck and resist forward neck

Table 2. Characteristic lengths used in scaling dimensions.

SCALED DIMENSION	CHARACTERISTIC LENGTH
HEAD VERTEX TO OCCIPITAL CONDYLES (C)	HEAD HEIGHT (B)
HEAD VERTEX TO HEAD C.G. (D)	HEAD HEIGHT (B)
NASION TO HEAD C.G. (E)	HEAD LENGTH (A)
HEAD C.G. TO OCCIPITAL CONDYLES, A-P (F)	HEAD LENGTH (A)
HEAD C.G. TO OCCIPITAL CONDYLES, S-I (G)	HEAD HEIGHT (B)
NECK LENGTH (I)	NECK CIRCUMFERENCE
HEAD WEIGHT	HEAD CIRCUMFERENCE
NECK WEIGHT	NECK CIRCUMFERENCE

NOTE: LETTERS IN BRACKETS CORRESPOND TO DIMENSIONS GIVEN ON FIGURE 12.

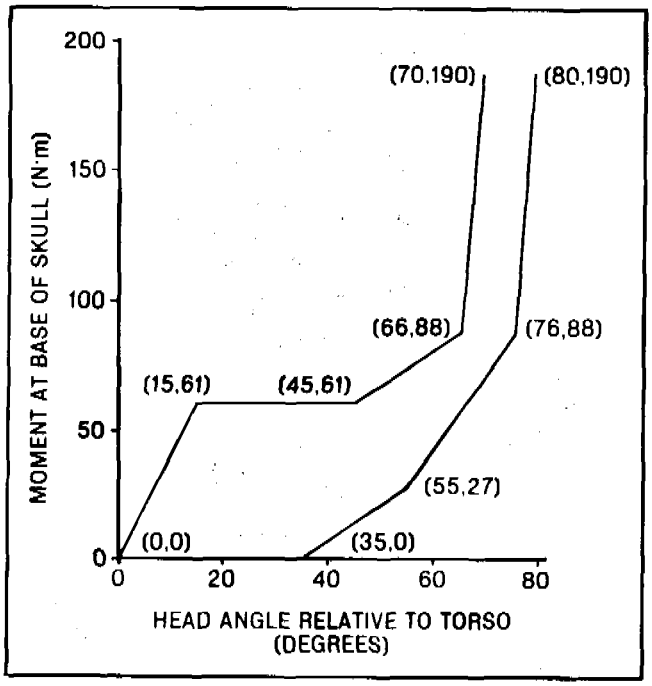

Figure 13. Forward neck bending response envelope for the 50th percentile adult male.

flexion. Similar distributions of muscle masses exist in children, but the total cross-sectional areas of their neck muscles are smaller than those of adults resulting in lower static neck strength moments. A relationship between the static neck strength moments for children and adults can be obtained by the following analysis.

From static equilibrium considerations, the magnitude of the static strength moment, M, is equal to the resultant of the neck muscle forces, F, multiplied by the effective moment arm, D, of this force.

$$M = F \times D \qquad (1)$$

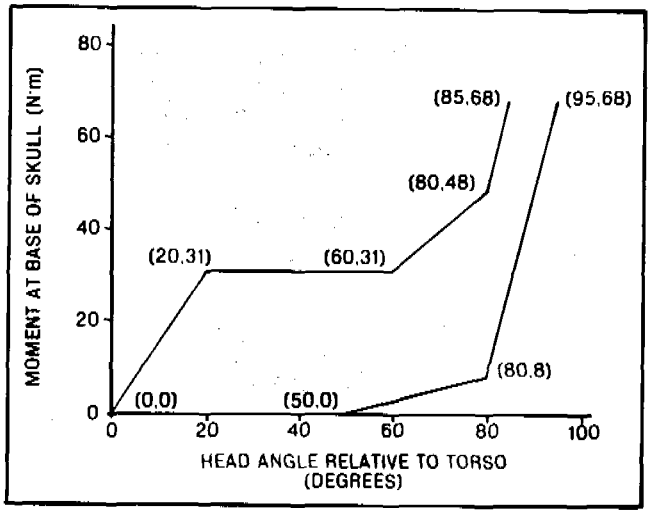

Figure 14. Rearward neck bending response envelope for the 50th percentile adult male.

The resultant neck muscle force is equal to the average stress level, S, in the muscles when the head begins to move multiplied by the cross-sectional area, A, of the muscles resisting the motion.

$$F = S \times A \tag{2}$$

Combining this equation with Equation (1) gives,

$$M = S \times A \times D \tag{3}$$

If we assume that the average stress level at which the head begins to move in response to a statically applied head load is the same for the adult as it is for the child, then the magnitudes of a child's static strength moments for flexion and extension can be calculated from the formula,

$$M \text{ child} = \frac{(A \times D) \text{ child}}{(A \times D) \text{ adult}} \times M \text{ adult} \tag{4}$$

The characteristic dimensions used to calculate the static strength moments for flexion and extension for a 3-year-old child are given in Table 2. The ordinate of the adult neck bending response envelope was scaled by the ratio,

$$\frac{M \text{ child}}{M \text{ adult}} \tag{5}$$

Angle Scaling—Table 3 summarizes the range of motion data which was considered for scaling the abscissa of the adult neck bending envelope to the child. Shown in the table are measurements taken on a 27-month-old female and a 7-year-old male, as well as data for adults (12, 13, 14). The range of motion for the 27-month-old female was slightly less than that of the 7-year-old male whose range was quite comparable to the various adult ranges. Based on these data, it was decided that no scaling of the adult head to torso angulation was required.

Child Neck Bending Response Corridors—The resulting 3-year-old neck bending response envelopes for flexion and extension are shown in Figures 9 and 10, respectively. The moment coordinates of the envelopes were obtained by applying Equation (5) to the corresponding adult moment coordinates. The angle coordinates were taken as their corresponding adult angle coordinates.

Note that this technique can be used to obtain neck bending response envelopes for any size person.

Table 3. Range of motion data for the head due to forward and rearward neck bending.

	MEASURED CHILD RANGES OF MOTION - DEG.		REFERENCED ADULT MALE RANGES OF MOTION - DEG.		
	27 MONTH FEMALE	7 YR-OLD MALE	REF. 12	REF. 13	REF. 14
FORWARD BENDING	45	60	50	60	67
REARWARD BENDING	50	60	50	61	77

Head Modifications

The Design 1 head characteristics are compared to those chosen to represent a 3-year-old child in Table 1. Generally, the comparisons indicate that the Design 1 head is smaller than the 3-year-old child. Major differences occur between the weights of the heads and between the locations of the head/neck interfaces relative to the head mass centers.

Since making a new head mold to the exact dimensions of the 3-year-old child given in Table 1 was not practical, the possibility of fabricating a new head mold to the size and shape of the ARL VIP-3C skin mold was investigated. When ARL indicated that such a mold could be easily and quickly fabricated, the decision was made to fabricate the Design 2 head to the ARL VIP-3C exterior head dimensions.

Figure 15 shows an exploded view of the Design 2 head and neck. With this design, an aluminum structure embedded in a compliant urethane head casting is used to attach the head to the neck structure and locate the head so that the head/neck interface is positioned consistent with child anthropometry. This structure also served as the mounting platform for the various head accelerometers. The desired head mass and its location

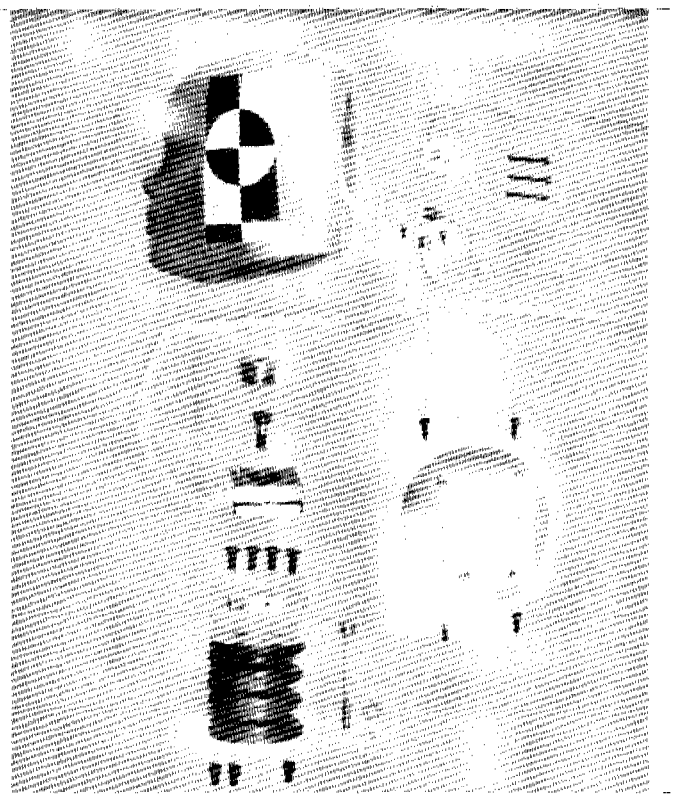

Figure 15. Exploded view of the instrumented design 2 head and neck which features modifications to improve geometry, mass and neck bending response.

were obtained by using ballast. A 2 mm diameter hole was drilled in each side of the head to identify the mass center location.

Head instrumentation was the same as Design 1, and consisted of an orthogonal cluster of three uniaxial accelerometers located at the head's center of gravity and two uniaxial accelerometers mounted with their sensitive axes parallel to measure sagittal plane angular acceleration. Figure 16 shows the locations of these accelerometers.

The various geometric and inertial characteristics of the Design 2 head are compared to those of the 3-year-old child in Table 1. Note the excellent agreement that was obtained for the head weight and the location of the head/neck interface (occipital condyles) relative to the head's center of mass.

Neck Modifications

Inspection of both the flexion and extension moment-angle response envelopes (Figures 9 and 10) indicates that the desired neck stiffness should be low up to a threshold angle at which stiffness becomes relatively high. This desired response can be thought of as a low resistance neck which suddenly bottoms out after a specified range of motion. Further inspection reveals that neck extension stiffness, prior to bottoming out, should be lower than the corresponding flexion stiffness. Thus a nonlinear rate neck with different flexion and extension responses is required.

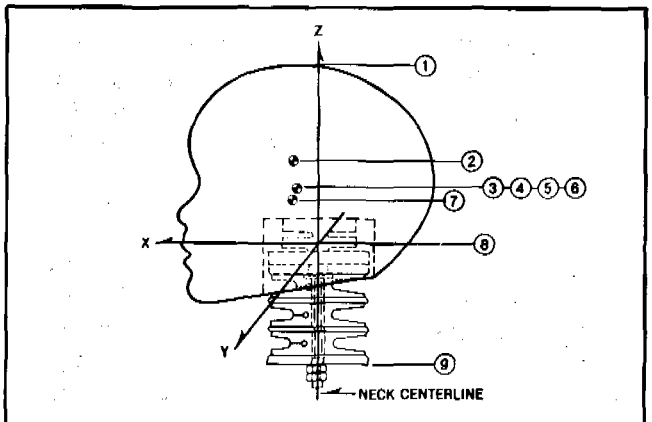

REF. PT.	DESCRIPTION	X	Y	Z
1	TOP OF HEAD	0.0	0.0	121.1
2	SUPERIOR HEAD ANGULAR ACCELEROMETER	23.1	21.3	60.4
3	HEAD CENTER OF GRAVITY	16.0	0.0	38.0
4	LATERAL HEAD ACCELEROMETER	16.0	-7.4	38.0
5	VERTICAL HEAD ACCELEROMETER	16.0	0.0	38.0
6	LONGITUDINAL HEAD ACCELEROMETER	20.1	0.0	38.1
7	INFERIOR HEAD ANGULAR ACCELEROMETER	23.1	19.4	30.9
8	NECK TRANSDUCER GAGE PLANE	0.0	0.0	0.0
9	BASE OF NECK	0.0	0.0	-84.0

ALL DIMENSIONS GIVEN IN mm

Figure 16. Sensitive element locations for the instrumentation used in the design 2 head and neck.

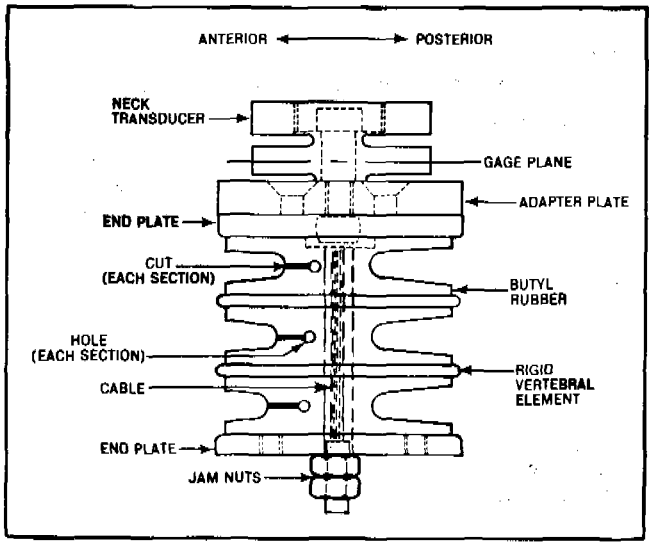

Figure 17. Schematic of the design 2 neck structure.

To achieve these desired characteristics, the concept shown schematically in Figure 17 was used in Design 2. This concept is based on the technique used in the development of the Hybrid III neck structure (15). Key components of the design are the bonded butyl rubber elements, vertebral discs, steel cable, and aluminum end plates.

Neck stiffness, prior to bottoming, is controlled by the design of the rubber sections. Each rubber element is cut from the front surface to the hole shown in Figure 17. Thus, only compression forces can be transmitted by the front portions of the rubber elements. When the neck is flexed forward, the total cross section of the rubber elements resists the bending action. However, when the neck is flexed rearward, only part of the cross section of the rubber elements resists the bending since the front portion cannot transmit tensile forces.

For both flexion and extension modes, the neck tends to bottom out at deflection angles which are designed into the physical geometry. This bottoming characteristic occurs when the rubber covered vertebral elements contact each other and significantly increase the neck's resistance to further deflection. A steel cable is contained within the neck at its axial centerline to help carry the additional tension loads which result when the neck bottoms out.

Neck length and diameter were chosen to better approximate human geometry. In the dummy, neck length is defined as the dimension from the gage plane of the neck transducer (representing the occipital condyles) to the base of the neck.

Threaded aluminum endplates provide convenient attachment of the neck to the head and torso. A neck mounting bracket was designed to interface the neck with

the torso and provide the desired standing height for the dummy.

Neck load measurements are made with the same instrumentation used in Design 1. However, the transducer's location relative to the mass center of the head and base of the neck is significantly different. Figures 3 and 16 provide a comparison of the geometric differences between the head/neck structures of Design 1 and 2. An inspection of Table 1 clearly demonstrates that the geometric and inertial characteristics of the head and neck structure of Design 2 are closer to those of the 3-year-old child than were those of Design 1.

Component Response Documentation

Head Drop Test—The head drop test conducted to document the forehead impact response of Design 1 head was repeated using the Design 2 head. A typical acceleration response curve is shown in Figure 7. Note the unimodal response curve and the absence of the undesirable resonance noted for the response of Design 1. By mounting the accelerometers to the rigid, aluminum structure in the head, the undesirable resonance was eliminated. While a desirable unimodal response was achieved, there is no assurance that the resulting acceleration level is typical of child's response. No child acceleration response data are available to make such a comparison.

Neck Bending Test—Dynamic neck bending tests were conducted to compare the response characteristics to the child neck bending response envelopes. The pendulum test fixture used in documenting the Design 1 neck response was used to produce forward flexion and rearward extension of the head/neck structure of Design 2. The rubber neck elements were tuned to give the desired neck response. Figures 9 and 10 show the neck response characteristics of Design 2 relative to the child neck bending performance envelopes for flexion and extension, respectively. Also shown are the responses of the Design 1 head/neck structure. Clearly, Design 2 responses more closely approximate the desired response envelopes.

Use of Design 2 Dummy

No inflatable restraint system development tests were conducted with the Design 2 dummy. Prior to completing the Phase 2 development program, the development work on the GM inflatable restraint was terminated. However, the Design 2 dummy was subjected to a limited test series using inflatable restraint hardware and dummy positions which had produced a range of neck injuries in anesthetized animals. In addition, Design 1 neck response data were available for each test condition selected. The results of these tests are discussed in the paper by Mertz and Weber (4).

SUMMARY

A description of the 3-year-old child dummy (Design 1) that was used extensively by General Motors Corporation in its second generation, passenger system inflatable restraint development program is given. The dummy used was a modified version of the ARL VIP-3C dummy and was instrumented to measure loads and accelerations that were thought to be associated with injuries observed or inferred from previous animal test programs of passenger inflatable restraint systems. These measurements were triaxial accelerations of the center of gravity of the head and the upper and lower ends of the one piece, rigid backbone; the angular acceleration of the head about a lateral axis; fore and aft linear accelerations at three mid-sagittal points located on the upper, mid and lower front surface of the torso; and mid-sagittal plane neck loads consisting of the fore-aft shear force, axial force and bending moment measured at the head-neck interface. No attempt was made to improve the biofidelity of the child dummy's response characteristics since such a development program would not have been compatible with the time constraint of the passenger inflatable restraint development program.

While the Design 1 dummy provided good insights into the significance of the cushion/dummy interaction forces, concern was expressed that the lack of biofidelity of the neck's bending response might lead to misinterpretation of the test results. Anesthetized animal tests that were being conducted to assess the significance of the child dummy measurements had shown that serious neck injuries could be produced for some combinations of hardware and test conditions. Child dummy tests conducted under similar exposure conditions had resulted in high neck loads. However, both child surrogates had neck bending stiffnesses which were thought to be greater than that of a child. It was hypothesized that a child with lower neck bending resistance would not experience high neck loads in a similar exposure environment and consequently would not experience severe neck injury.

To determine the effect of neck stiffness on neck loads due to head/cushion inteaction, a program was initiated to develop a dummy neck structure with childlike bending resistance and range of motion. Neck bending response guidelines were developed to characterize the fore and aft bending responses of a child's neck. These characteristics were inferred from those specified for an adult's neck by using geometric scaling factors. A description of the modified neck structure that was developed to meet these response guidelines is given. Since the geometric and inertial properties of the head influence how the neck is loaded, a new head structure was developed and is described. The new head-neck structures were mounted to the torso of the Design 1 dummy and the resulting child dummy configuration was called Design 2. Prior to using the Design 2 dummy to evaluate the performance of pas-

senger system inflatable restraint concepts, the GM Inflatable Restraint Development Program was terminated.

The improvements made to the head-neck structures of the Design 2 dummy should be useful for evaluating belt restraint performance. However, additional modifications of the thorax, backbone, abdomen and shoulder areas would be desirable if the dummy is to be used for that type of testing.

LIST OF REFERENCES

1. Patrick, L. M. and Nyquist, G. W., "Airbag Effects on the Out-of-Position Child", SAE 720442, May 1972.
2. Aldman, B., Anderson, A., and Saxmark, O., "Possible Effects of Air Bag Inflation on a Standing Child", Proceedings of the International Meeting on Biomechanics of Trauma in Children, Lyon, France, September 17–19, 1974.
3. U.S. Department of Transportation, Part 572, "Anthropomorphic Test Dummy", 38FR20449, August, 1973.
4. Mertz, H. J. and Weber, D. A., "Interpretations of the Impact Responses of a 3-year-old Child Dummy Relative to Child Injury Potential", 9th International Conference on Experimental Safety Vehicles, Kyoto, Japan, Nov. 1–4, 1982.
5. Mertz, H. J., Driscoll, G. D., Lenox, J. B., Nyquist, G. W., and Weber, D. A., "Responses of Animals Exposed to Deployment of Various Passenger Inflatable Restraint System Concepts for a Variety of Collision Severities and Animal Positions", 9th International Conference on Experimental Safety Vehicles, Kyoto, Japan, Nov. 1–4, 1982.
6. Hubbard, R. P. and McLeod, D. G., "Definition and Development of a Crash Dummy Head", Eighteenth Stapp Car Crash Conference, SAE 741193, 1974.
7. "Anthropomorphic Test Dummy", Final Report No. DOT-HS-299-3-569, December, 1973.
8. Diffrient, N., Tilley, A. R., Bardagjy, J. C., *Human Scale 1/2/3*, The MIT Press, 1974.
9. Snyder, R. G., Schneider, L. W., Owings, C. L., Reynolds, H. M., Golomb, D. H., and Schork, M. A., *Anthropometry of Infants, Children, and Youths to Age 18 for Product Safety Design*, SP-450, Society of Automotive Engineers, 1977.
10. *Anthropomorphic Source Book*, NASA Ref. Pub. No. 1024, Vol. 1, "Anthropometry for Design", 1978.
11. Mertz, H. J., Neathery, R. F., and Culver, C. C., "Performance Requirements and Characteristics of Mechanical Necks", *Human Impact Response—Measurement and Simulation*, Plenum Press, N.Y., 1973.
12. Dreyfuss, H., "The Measurement of Man—Human Factors in Design", 1967.
13. Granville, A. D. and Kreezer, G., "The Maximum Amplitude and Velocity of Joint Movements in Normal Male Human Adults", Human Biology, Vol. 9, 1937.
14. Buck, C. A., Dameron, F. B., Dow, M. J., and Skowlund, H. V., "Study of Normal Range of Motion in the Neck Utilizing a Bubble Goniometer", Archives of Physical Medicine and Rehabilitation, Vol. 40, 1959.
15. Foster, J. K., Kortge, J. O., and Wolanin, M. J., "Hybrid III—A Biomechanically-Based Crash Test Dummy", Proceedings of the 21st Stapp Car Crash Conference, SAE 770938, 1977.

Lateral Dummy Comparison Testing

K.-P. GLAESER
Federal Highway Research Institute
Federal Republic of Germany

ABSTRACT

The Federal Highway Research Institute (BASt) was engaged in comparison tests of the side impact dummies designed by:

—Highway Safety Research Institute/Department of Transportation (HSRI(DOT))
—Motor Industry Research Association (MIRA)
—Organisme National de Sécurité Routière (ONSER)
—Association Peugeot/Renault (APR).

In full scale side impact tests under the same test conditions the overall dummy behavior, repeatability, handling and durability of the different dummies were studied and compared.

In the research project "Lateral Dummy Comparison Testing" the following tests were carried out:

12 impact tests by means of a rigid moving barrier (1100 kg) against a VW Golf at an impact angle of 90° with a collision speed of 45km/h.
Variations:—4 dummy types (APR, HSRI (DOT), ONSER, MIRA)
—3 repetitions per test.

The loads and kinematics of the different dummies were compared.

INTRODUCTION

The side impact of passenger cars is the second most frequent collision type besides the frontal impact. Because of the low stiffness of the car side structure there is a high risk of a car occupant being severely injured. Side impact dummies, developed by different institutions in recent years represent a basic means of evaluating the side impact protection performance of cars. Within the frame of the "EEC Research Program on Biomechanics of Impacts with Relation to Future Vehicle Safety Regulations" in Phase 4 the following institutes took part in comparing 4 different dummy prototypes described in detail later:

—Motor Industry Research Association (MIRA)
—Instituut voor Wegtransportmiddelen (TNO) (Coordination and final summary report)
—Organisme National de Sécurité Routière (ONSER)
—Association Peugeot/Renault (APR)
—Federal Highway Research Institute (BASt)

TEST METHOD

The side impact tests carried out with the moving rigid barrier against a stationary car at an impact angle of 90° largely insure realistic and reproducible conditions of a standard side impact test.

The parameters used for the impact test within this projects were partly different from the EEVC WG6-proposal [1]:

—The chosen test velocity of 45 km/h lies ~ 10% under the 50 km/h proposed by the EEVC.
—The moving barrier was equipped with a rigid face according to SAE J 972 a, the EEVC proposed deformable elements.
—The mass of the moving barrier was fixed at 1100 kg, the EEVC proposes a mass of 950 kg.
—The impact angle of 90° into stationary test car is also proposed by the EEVC.

The test dummies thus had to sustain a largely realistic side impact test procedure and had to show their behaviour. Three tests with each of the four dummies were carried out to compare the repeatability of the dummies. Because of measuring problems, which are described later, one test with the HSRI (DOT)-dummy and one test with the APR-dummy were carried out additionally.

Test Configuration

The car type was a Volkswagen Golf with two doors. The test cars weighed 840 ± 10 kg. The impact velocity of the barrier was settled to 45 (± 1) km/h, the corresponding ΔV values for the test car were calculated from about 23 to 28 km/h.

The case car was hit on the left side in the middle between the front and rear axles. To evaluate the intrusion, the positions of 12 target points on the left side of the impacted car were measured relative to a reference plane before and after test. The dummy was belted with an automatic 3-point belt, the arms were positioned forward in driving position, the hands were on the steering wheel in 1/4 to 3 o'clock position (exception: HSRI-tests, the HSRI-dummy has no arms). The distances between the dummies (shoulder and pelvis) and interior parts were held constant. The integrated head rests were adjusted at their maximum height and their most frontward inclination.

The impact tests were filmed by 4 high-speed cameras. Two cameras were attached to the test car to film the motion of the dummy, two further stationary cameras were used.

The car was equipped with two switches to flash a spotlight. One at the moment of impact and one at the moment of shoulder/door contact.

Instrumentation and Measuring Data in General

The test car acceleration was measured 3-axial on the top of the transmission tunnel and the acceleration of the rigid barrier was measured in longitudinal direction. The seat belt forces were measured at four places, two on the lap belt, two on the shoulder belt. The analog measuring data were digitized according to the principle of pulse code modulation (PCM) and recorded by a PCM-tape recorder. In general the filtering of the analog measuring data was carried out by active analog lowpass filters, which correspond to SAE Recommended Practice J 211b.

DUMMY DESIGN,—INSTRUMENTATION AND DATA PROCESSING OF THE DIFFERENT DUMMIES

The HSRI-dummy and its design was presented several times [2,3]. The thorax consists of 5 ribs with ballast plates (to compensate the arm weight), which can rotate together around the thoracic spine and which were supported from the impacted rib side to the spine by a shock absorber. The tested dummy was equipped with a Taylor-shock absorber, filled with silicon oil. (In later tests of the other mentioned institutes a new version of shock absorber was used.) Between the ribs and the armless jacket there were foam pieces.

Figure 1 shows the HSRI-dummy.

Head, chest and pelvis of the dummy were equipped with 3-axial accelerometers. A linear potentiometer was mounted parallel to the shock absorber to measure the chest deflection. Two rib accelerometers were mounted, one on the right and one on the left upper rib in lateral direction.

According to the computer programs from NHTSA,

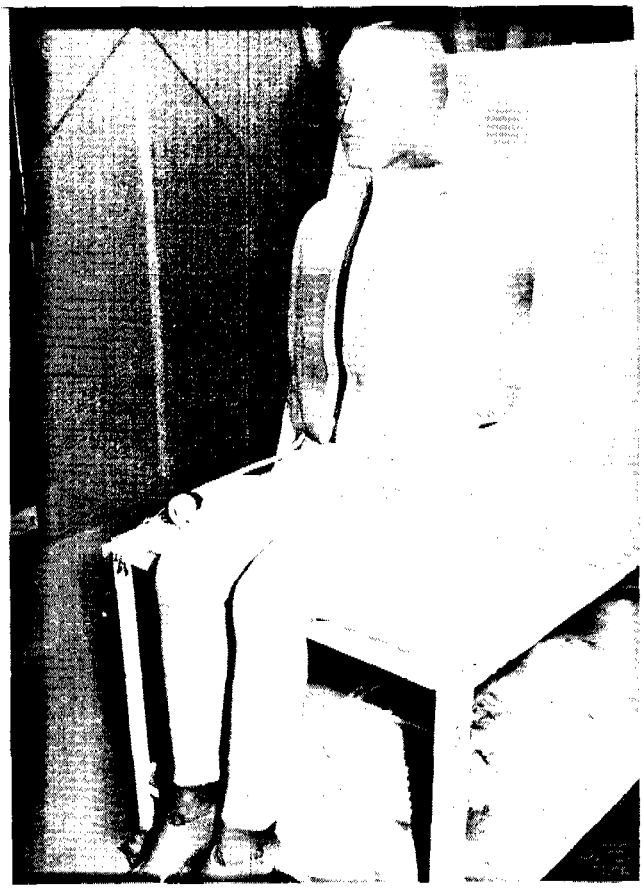

Figure 1. HSRI-dummy.

describing the data reduction procedures, the following data processing was carried out for the rib accelerometer signals:

—Data recording with a sampling rate of 8000 Hz
—Analog to digital conversion following the specification of channel class 1000 (SAE J 211b)
—Digital filtering of the data to class 180
—Subsampling data to a 1600 Hz sampling rate (reduction with factor 5)
—Digital filtering with Finit Impulse Response (FIR)-filter, passband frequency = 100 Hz for the rib accelerometer signals
—Calculation of injury predictor equations (B-factor of the left upper rib signal (BLUR)) and calculation of AIS and number of rib fractures (NRF) [4, 5] (see footnote in Table 1).

The head and neck, arms and lower leg assemblies of the *MIRA-dummy* are used from the standard Hybrid II-dummy, the thorax and shoulder, abdomen and pelvis were newly designed by MIRA. The dummy assembly was mounted as described in [6], (see Figure 2).

The thorax has six pairs of ribs, connected to the thoracic spine via 12 strain gauged plates which record the tensile and bending loads at the spine on each individual rib, (see Figure 2). These signals were recorded on both impacted and nonimpacted sides during tests. The resultant rib force on each rib was calculated by adding the mean values from the impacted and nonimpacted side. A deflection potentiometer was mounted on the 4th rib.

The pelvis was instrumented with a 3-axial load cell between the ilium and the spine, an uniaxial strain gauged force transduce at the acetabulum and one uniaxial strain gauged plate mounted across the pubic symphysis.

The accelerations of head, chest and pelvis were measured 3-axial.

The construction of the *ONSER-dummy* was different from the Hybrid II-dummy [7]. The thorax was developed for side impact testing by selecting a foam plastic for the thorax moulding to give a realistic load-deflection characteristic. The deflection of the thorax foam plastic was measured between the jacket and the thorax spine by means of a soft gear rack and a potentiometer, which is shown in Figure 3.

The shoulder consists of two spring supported pistons on each side which allow a shoulder instrusion and rotation.

Besides the above mentioned thorax deflection the ac-

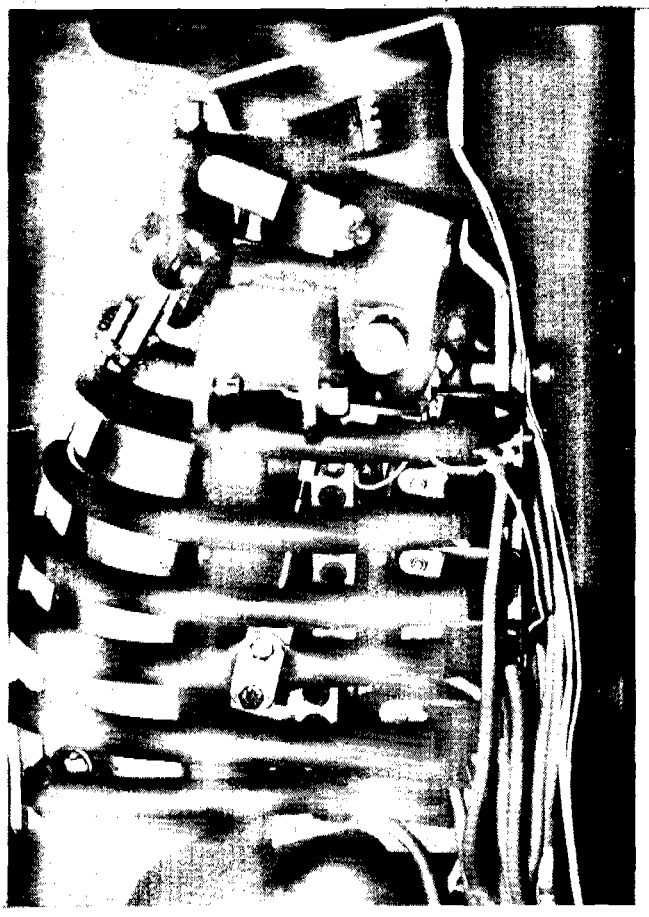

Figure 2. Thorax of the MIRA-dummy.

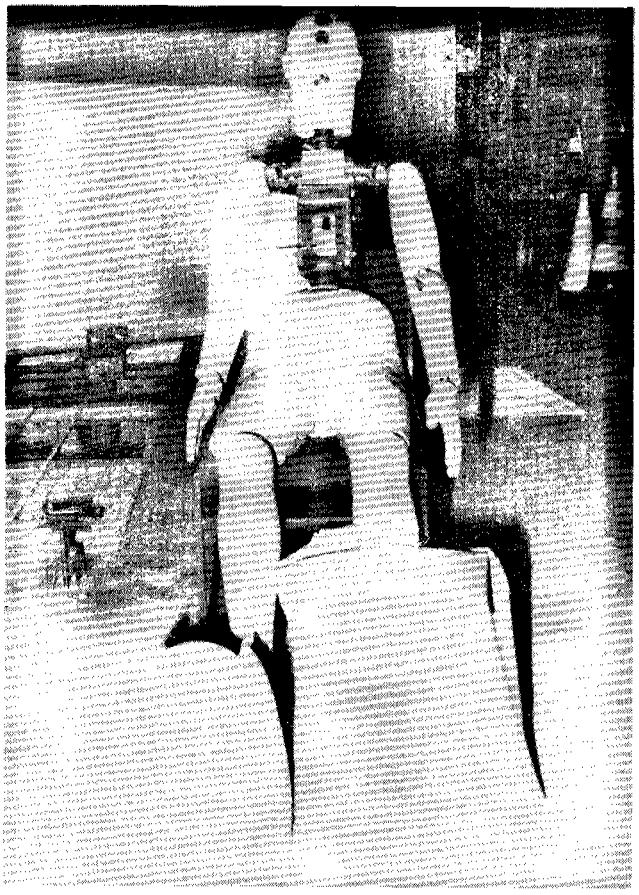

Figure 3. ONSER-dummy.

celeration of head, chest and pelvis was measured 3-axial at the provided locations.

The pelvis and lower extremities of the *APR-dummy* were taken from a Hybrid II-dummy, the head originates from the Hybrid III-dummy, the neck was an on top and on bottom with a ball joint modified Hybrid III neck version [8]. Thorax and upper extremities were designed by Peugeot/Renault and the used abdomen was developed by TNO [9]. The upper 3 and the lower 3 of the 6 ribs were connected on the impacted and nonimpacted side by a rubber spring loaded piston with the thoracic spine. The pistons on the impacted side are equipped with an optoelectronical deflection transducer. Figure 4 shows the APR-thorax and the inside of the TNO-abdomen.

The dummy was equipped with 3-axial accelerometers at the provided locations of the center of gravity of head, chest and pelvis. On the left and right upper rib an uniaxial accelerometer was mounted in lateral direction. The data processing was the same as for the HSRI-dummy, described above.

The TNO-abdomen was installed as described in [10] and the contact switch unit was adjusted to 4500 N, which means the critical penetration respectively force limit.

Table 1 shows the summarized measuring data of the different dummies in tabular form.

COMPARISON OF LOADS AND KINEMATICS

The impact speed of 45 km/h was achieved with deviations of ± 1 km/h. The maximum intrusion of the test car occurred on the car's waist line. At the dummy thorax level an intrusion of 300 ± 30 mm was measured. The ΔV-value for the B-post was calculated between 9 m/s and 11 m/s. This means a severe impact for the test car and for the tested dummies.

The comparison of the dummy test results was made under the aspect of dummy loads, kinematics, repeatability aspects particularly, durability and handling of the dummies. Table 2 shows the dummy loads in comparable form. The most interesting data of the dummy loads are also shown in Figure 5. The following data analysis was made using the mean values of each test series.

The head acceleration traces of the different dummies showed a different shape. The resultant accelerations ranged from 48 g for the MIRA-dummy to 98 g for the APR-dummy. The ONSER- and APR-dummy had besides the lateral component also a high acceleration component in vertical direction (> 60 g). The HIC was calculated between 115 (MIRA) and 835 (APR). The

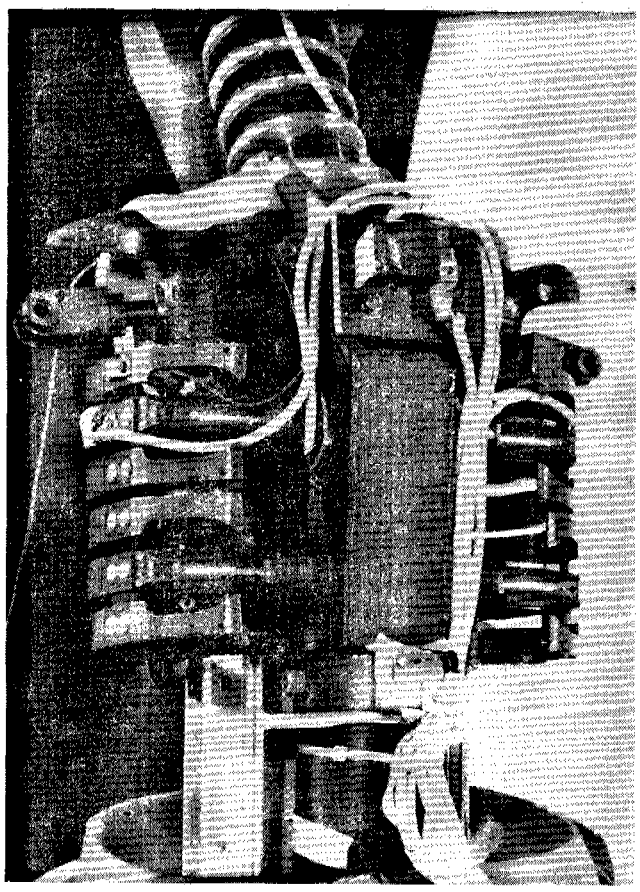

Figure 4. APR-thorax and TNO-abdomen.

Table 1. Measuring data on different dummies.

		HSRI (DOT)	MIRA	ONSER	APR*
Head	accel. x	x	x	x	x
	accel. y	x	x	x	x
	accel. z	x	x	x	x
	accel. res.	x	x	x	x
	HIC	x	x	x	x
Chest	accel. x	x	x	x	x
	accel. y	x	x	x	x
	accel. z	x	x	x	x
	accel. res.	x	x	x	x
	deflect.	x	x	x	x[1)]
	accel. LUR, RUR[2)]	x	—	—	x
	BLUR[3)]	x	—	—	x
	SI	x	x	x	x
	res. rib forces	—	x	—	—
Pelvis	accel. x	x	x	x	x
	accel. y	x	x	x	x
	accel. z	x	x	x	x
	accel. res.	x	x	x	x
	force hip y	—	x	—	—
	force pubis y	—	x	—	—
	force pelvis x	—	x	—	—
	force pelvis y	—	x	—	—
	force pelvis z	—	x	—	—

[1)] Two transducers
[2)] LUR = left upper rib, RUR = right upper rib
[3)] BLUR = B-factor of LUR-signal
* additionally abdomen force (TNO-abdomen)
AIS = 1,49 · BLUR-6,68
NRF = 10,73 · BLUR-64,1

Table 2. Main dummy data for comparison.

	Dummy Type		HSRI (DOT)		MIRA		ONSER		APR	
	Test Series		ESH 1-3		ESM 4-6		ESO 7-9		ESA 10-13	
	No. of Tests		4		3		3		4	
			Mean 3 ms	Stand. Dev. (±)	Mean 3 ms	Stand. Dev. (±)	Mean 3 ms	Stand. Dev. (±)	Mean 3 ms	Stand. Dev. (±)
Head	accel. y	[g]	78	5,5	43	4,8	40	8,1	76	13
	accel. z	[g]	12	7,6	26	5,8	62	12	67	11
	accel. res.	[g]	83	5,7	48	3,0	65	11	98	7,6
	HIC[1]	[—]	536	57	115	23	354	79	835	131
Chest	accel. y C.G.	[g]	39	5,7	94	34	120	12	136	13
	accel. res. C.G.	[g]	44	6,5	106	27	123	15	157	21
	accel. rib 1[2]	[g]	142	16	—	—	—	—	183**	33
	SI[1]	[—]	263	81	958	296	1259	388	1758	469
	BLUR[1]	[—]	7,41	0,C3	—	—	—	—	7,7**	0,42
	defl.[1]	[mm]	47,5**	3,5	58*	(—)	73	9	43,5[3]*	(—)
	res ribforce[1]	[kN]	—	—	6,82	2,3	—	—	—	—
Pelvis	accel. y	[g]	156	5,6	101	5,5	113	16	145	11,2
	accel. res	[g]	162	7,4	107	6,1	143	13	169***	12
	pelvis force	[kN]	—	—	4,4**	0,57	—	—	—	—
	pubis force	[kN]	—	—	5,6**	0,78	—	—	—	—
	hip force y	[kN]	—	—	1,2	0,15	—	—	—	—

[1]Due to max. value.
[2]Off 300 Hz filtered values.
[3]Mean of upper and lower transducer.
*Of one test.
**Of two tests.
***Of three tests.

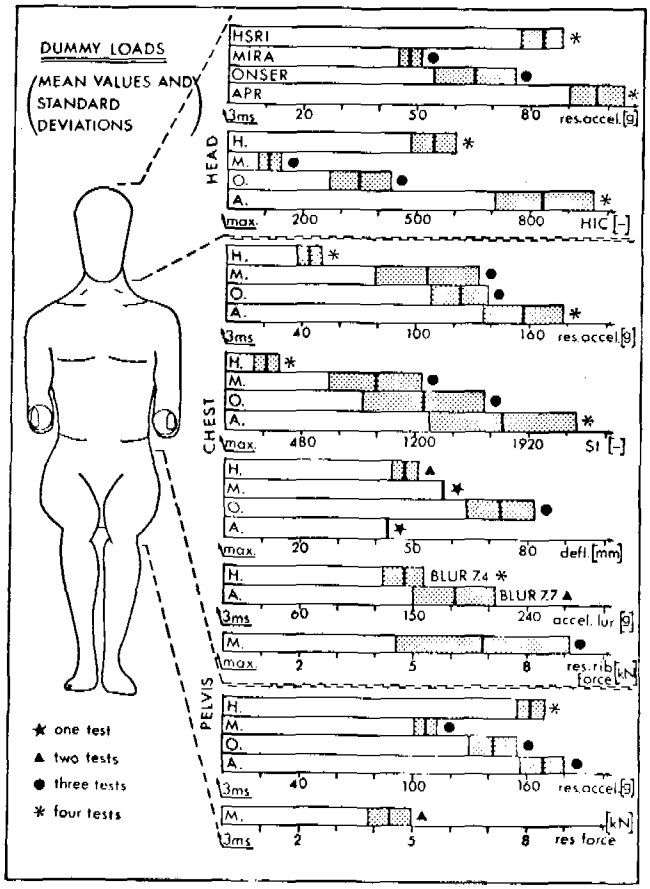

Figure 5. Dummy loads.

coefficients of variation for the resultant accelerations for all dummies were lower than 10%, except for the ONSER-dummy 17%. The variations for the HIC were much higher, for the MIRA- and ONSER-dummy about 20%, for the HSRI-dummy 11% and for the APR-dummy 16%.

The head bending of the different dummies in side window direction were similar for the ONSER- and MIRA-dummy and similar for the APR-and HSRI-dummy. No head impact against the side window occurred. Only the HSRI-dummy reached the side window level but the window was destroyed before that. The maximum head bending angles due to the vertical plane for the ONSER- and MIRA-dummy were 55–70° for the APR- and HSRI-dummy 80–105°.

The *thorax* responses of the different dummies also differed greatly. The resultant acceleration, mainly caused by the lateral component, was measured between 44 g for the HSRI- and 157 g for the APR-dummy, meaning a SI between 263 respectively 1758. For the MIRA- and ONSER-dummy a SI of about 1000 was calculated.

The coefficient of variation for the SI was, with about 30% for all dummies, very high. The acceleration of the left upper rib was measured for the HSRI-dummy to 142 g and for the APR-dummy to 183 g. Because of the low sensitivity of the BLUR and of the injury predicting parameters a BLUR of 7,4 for the HSRI- and of 7,7 for the APR-dummy was calculated, which means an AIS of 4,35 respectively 4,75 and a NRF of 15 respectively 18. The resultant rib forces of the MIRA-dummy had a mean value of 6,8 kN. The rib forces for single ribs showed very well the load distribution over the thorax, but with a partly poor repeatability.

The interpretation of the chest deflection had to be made very carefully because of the low number of successful measurements. The maximum internal chest deflections varied from ~ 43–73 mm for the different dummies. Film analyses of the external chest deflections were also not successful and are therefore not mentioned.

The thorax kinematics for the HSRI-dummy and the APR-dummy were similar. The bending angle of the thorax in door direction relative to the vertical plane varied for the HSRI-dummy 20 to 25° and for the APR-dummy between 15 and 20°. Both other dummies only reached 5–10°.

The *pelvis* accelerations of the MIRA-dummy with 107 g were the lowest, the ONSER-dummy had a resultant pelvis acceleration of 143 g and the dummies equipped with a Hybrid II pelvis (APR and HSRI) had similar values of about 165 g. The variations of the pelvis accelerations were very low (5–10%). The force measurements on the MIRA-dummy pelvis considering two transducer defects were successful and the repeatability with a coefficient of variation of less than 14% was sufficient.

COMPARISON OF DUMMY HANDLING AND DURABILITY

A comparison of the different dummy *handling* can only be made in comparison with the conventional Hybrid II-dummy. The ONSER-dummy and the APR-dummy were as easy to handle as the Hybrid II dummy, the HSRI- dummy had problems with the air-venting of the shock absorber and the MIRA-dummy with the magnitude of data channels. The magnitude of data channels must be also considered under the aspect that proposals exist to use more than one dummy in a side impact test. All the deflection transducers mounted by ourself or mounted by the dummy manufacturer were not sufficient during short impacts.

Except the HSRI-dummy all dummies had problems in respect to *durability*. The dummies with rib constructions had no damages to the ribs but the APR-dummy had problems with the easy outward motion of the rib supporting pistons and the ONSER- and MIRA-dummy with the shoulder construction. The neck of the APR-dummy at the level of the lower ball joint failed several times, because the rubber pieces left their original position. These damages must be seen also under the aspect of a possibly higher test speed in a standardized side impact test.

DISCUSSION OF TEST RESULTS AND CONCLUSIONS

The aim of this study was to compare 4 different dummies under the same test conditions in a full scale side impact test.

The test input parameters for the dummies: velocity of the rigid moving barrier, door intrusion etc., showed a good reproducibility but the dummy response of the different dummies varied much. In this project the differences in dummy response were discussed, the repeatability of dummy response of the same dummy in several identical tests was analyzed and dummy handling and durability studied.

On all dummies different techniques to measure the violence of impacts were used. For the thorax three different measuring methods are in use:

—chest deflection (internal, external)
—rib force
—rib acceleration, calculation of BLUR, AIS, NRF.

In addition, a problem that still needs to be discussed and settled is the comparison between identical measuring methods and their application on different dummies which originally had been developed for only one special measuring method.

Due to the comparable dummy loads it can be stated that the head response is completely different for the different dummies, as well accelerations and HIC. These differences can partly be explained by an additional z-component in the head acceleration normally occurring in lateral direction (ONSER, APR). The variation of head accelerations in single test series is lower than the variation of HIC. The head/neck-kinematics are influenced by the thorax behaviour.

In the thorax response the HSRI-dummy shows much lower accelerations (and SI) than all other dummies. The SI varies much for all dummies. The accelerations of the upper ribs, measured only on two dummies (HSRI and APR), are sufficiently reproducible signals and give therefore (and because of the low sensitivity) a low variation of the corresponding injury predicting parameters. The rib force measurement (MIRA-dummy) shows the force concentration onto single ribs quite well, but partly with a poor reproducibility. Because of several transducer defects not much can be said about the reproducibility of the chest deflection. Different thorax accelerations and single different chest deflection values of the different dummies lead to the assumption of different thorax stiffnesses.

The pelvis response shows the highest reproducibility and the dummies with the Hybrid II-pelvis show similar acceleration values, the others (ONSER-, MIRA-dummy) have lower values. The pelvis force measurement of the MIRA-dummy was sufficient and sufficiently reproducible.

Due to the kinematics of the dummies, they can be separated into two groups, first: dummies with a great head and thorax bending (HSRI(DOT),APR), second: dummies with a lower head and thorax bending (ONSER,MIRA). A conclusion due to the realism of the kinematic behaviour can not be drawn, because no cadaver data under the same test conditions exist.

From the described dummy handling and -durability problems the following suggestions for dummy improvement can be made. Because of several defects of the chest deflection transducers, these should be part of the dummy, should sustain impacts of short duration and record the chest deflection without vibration and interruption. This represents a suggestion applying to all dummies. For each dummy special improvements should be attempted:

—HSRI (DOT)-dummy:
  —mounting and air-venting of the "Taylor" shock absorber
—MIRA-dummy:
  —reinforcement of the shoulder construction
  —adding and averaging the A and B rib strain guage signals on each rib side by hardwarde, meaning a reduction of rib force channels to the half of their
—ONSER-dummy:
  —easy motion possibility of the shoulder pistons also during short (oblique) impacts
—APR-dummy:
  —easy motion possibility of the chest deflection pistons also during short (oblique) impacts
  —construction of the neck at the lower ball joint level.

In the critical examination the main emphasis should be placed on the aspect of biofidelity of the dummies. This was not a task of this project. An overall assessment of dummy behavior, especially under the aspect of biofidelity, will be made under inclusion of the results of the other contracting institutes. This will be done by TNO till the end of this year.

REFERENCES

1. EEVC: Working Group "Structures", Improved Side Impact Protection in Europe, 9th ESV-Conference 1982.
2. Melvin, J. W., et al.: Experimental Application of Advanced Thoracic Instrumentation Techniques to Anthropomorphic Test Devices, 7th ESV-Conference 1979.
3. Robbins, D. H. et al.: Assembly Procedures for HSRI-Side Impact Dummy Thorax, NHTSA DOT-HS-4-00321, 1980.
4. Eppinger, R. H. et al.: Development of a Promising Universal Thoracic Trauma Prediction Methodology, 22nd Stapp Car Crash Conference 1978.
5. Robbins, D. H., Lehmann, R. J.: Prediction of Thoracic Injuries as a Function of Occupant Kinematics, 7th ESV Conference, 1979.

6. MIRA Side Impact Dummy—Brief Specification for EEC Biomechanic Programme, Phase IV, MIRA 1982.
7. Cotte, J. P.: The ONSER 50 Dummy—A Research Tool for Safety, 8th ESV-Conference, 1980.
8. Fayon, et al.: Development and Performance of the APR-Dummy (APROD), 8th ESV-Conference, 1980.
9. Maltha, J., Stalnaker, R. L.: Development of a Dummy Abdomen Capable of Injury Detection in Side Impacts, 25th Stapp Car Crash Conference, 1981.

Side Impact: A Comparison Between HSRI-, APROD-, and HYBRID II Dummies and Cadavers

G. KLAUS
Volkswagenwerk AG, Wolfsburg, Chairman of FAT Working Group 5, "Biomechanics"
D. KALLIERIS
Institute for Forensic Medicine, University of Heidelberg

ABSTRACT

The effectiveness of vehicle engineering measures to increase passive safety will be examined by means of experimental simulation utilizing dummies. Suitable dummies, which can be used to simulate loadings on vehicle occupants during real accidents, must be available in order to be able to transform these results into real world accident scenarios.

Within its Working Group 5 "Biomechanics", the German Research Association for Automobile Technology (Forschungsvereinigung Automobiltechnik e.V., abbreviated "FAT"), an association of German automobile manufacturers (Verband der Automobilindustrie e.V., abbreviated "VDA") has set for itself the task to determine whether the HSRI dummy or the APROD dummy, which were newly developed especially for the side impact, will best correlate with the cadavers behavior. This is a further step within the extensive field of biomechanics to evaluate the relationships between protection criteria and occupant protection during a side impact. Along with the HSRI- and APROD dummies, the Hybrid II dummy was also examined since this dummy has been employed for some time in experimental simulation of side impacts.

This report describes, and presents the initial results of, "FAT" activities in the indicated research project.

INTRODUCTION

The work by the Forschungsvereinigung Automobiltechnik e.V., FAT, in the field of biomechanics, that is described in this report, is part of the FAT Research Project "Loading Limits and Injury Mechanics of Vehicle Occupants Wearing Seatbelts During Side Impact Collisions", a successor project to that of the same name for frontal impacts.

The study will be completed by the FAT Working Group 5, "Biomechanics". It is supported by the Arbeitsgemeinschaft Industrieller Forschungsvereinigungen e.V. (Industrial Research Associations Working Group, abbreviated "AIF"). The Institute for Forensic Medicine, University of Heidelberg, Professor Georg Schmidt, is the Contractor.

The objective of the project is to measure accelerations and forces on various dummies and cadavers by means of experimental simulation of a 90° vehicle-to-vehicle side impact, and to determine kinematics. Cadaver injuries are to be analysed and correlated to mechanical loadings. The tests have been initiated with the goal of being able to develop a statement regarding the suitability of the dummies for experimental simulation through comparison of the loadings and kinematics of the dummies examined with those of cadavers.

The Committee of Common Market Automobile Constructors (CCMC) has expressed its willingness to make available the Deformation Element of the Deformable Barrier that it developed for the simulation of 90° side impacts. The deformation behavior of the front structure of the striking vehicle, which corresponds to a mid-size European vehicle, will be simulated during a side impact at 50 km/h with this element.

The report describes the status of the project. Initial results are given.

STATEMENT OF WORK

The contractor shall complete the following tests:

—Cadaver Tests	:	15
—HSRI Dummy Tests	:	5
—APROD Dummy Tests	:	5
—Hybrid II Dummy Tests:		5

Kinematics and loading of dummies and cadavers are to be cross-compared and assessed. Additionally, cadaver injuries are to be determined according to AIS. The reproducibility of the tests under the same test parameters is to be examined.

TESTS AND TEST PARAMETERS

Striking and Struck Vehicles

Experimental simulation of a 90° vehicle-to-vehicle side impact will be accomplished with pre-defined test rigs (Figures 1 and 2). Figure 3 shows the test rigs before and after the test.

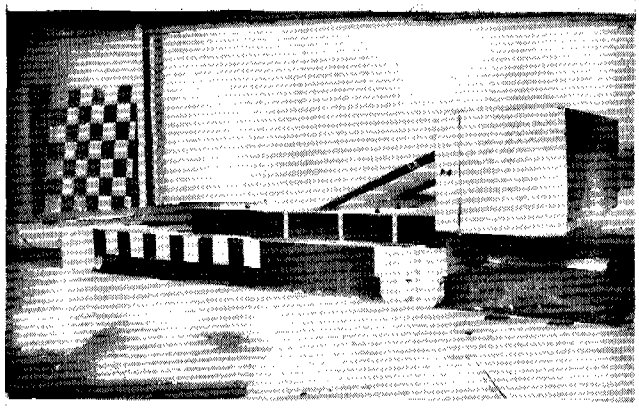

Figure 1. Side view of the sled with the CCMC deformation element used to simulate the striking vehicle.

—Striking Vehicle

The sled already available at the institute was used as the striking vehicle. This was fitted with one part of the CCMC barrier frame and the CCMC Deformation Element was mounted on the front of the frame (CCMC Report 1981). The weight of the striking vehicle, consisting of the sled, CCMC barrier frame, Deformation Element, and supplemental weights, amounted to 950 kg (Figure 1).

—Struck Vehicle

An Opel Kadett body mounted on a movable platform (dolly), was used as the struck vehicle (Figure 2). The weight of the struck vehicle, consisting of the dolly (Figure 4), car body, seat, test subject and supplemental weights, also amounted to 950 kg. The vehicle was impacted under an angle of 90° at a collision speed of 50 km/h.

Significant details of the test setup are defined as follows:

—Mass relationship of the vehicle with mounted superstructure:
$\mu = 1: m_1 = m_2 = 950$ kg
—Speed of the:
striking vehicle: 50 km/h
struck vehicle: 0 km/h
—Impact angle: 90°
—*Impact point:* SR
—Vehicles:
striking vehicle—sled with CCMC Deformation Element
struck vehicle—dolly with a mounted Opel Kadett two-door carbody
—Occupants: HSRI-, APROD-, Hybrid II Dummies, or Cadavers
—Seat position: on the impacted side, middle seat position
—Restraint system: 3-Point Automatic Belt
—Side windows and steering wheel removed.

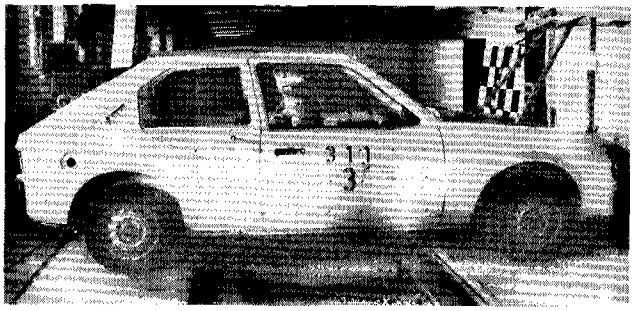

Figure 2. Side view of struck vehicle with Opel Kadett carbody.

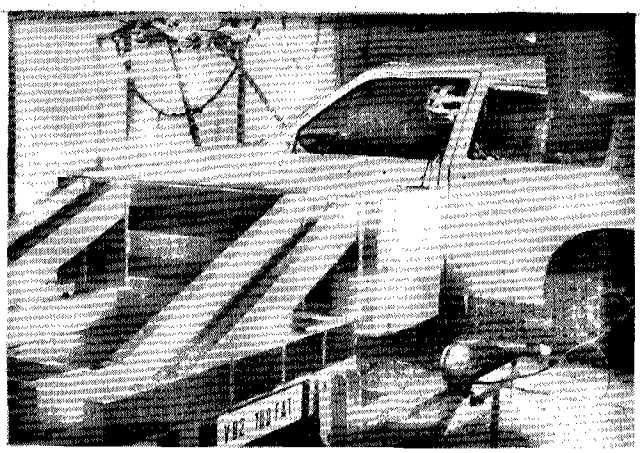

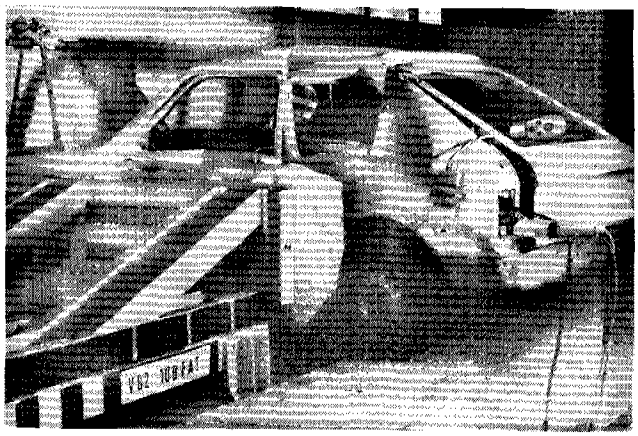

Figure 3. Deformable barrier and the Opel Kadett carbody on the dolly, before and after the crash.

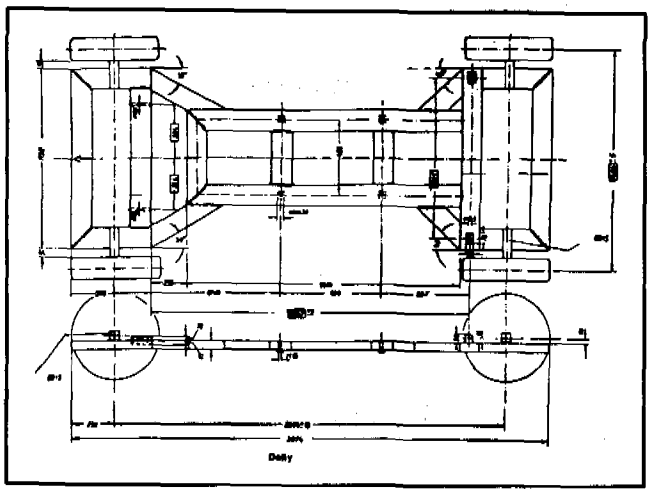

Figure 4. Design drawing of the movable platform (dolly).

Test Subjects

Dummy

Dummies under study are: the Side Impact Dummy developed by the Highway Traffic Safety Research Institute (HSRI), the omnidirectional Side Impact Dummy developed by the Association Peugeot-Renault (APROD), and the Hybrid II Dummy.

The HSRI Dummy was made available by NHTSA, the APROD Dummy by APR, and the Hybrid II Dummy by Opel AG.

Cadavers

Age, height and weight of cadavers for this project should be within the following areas:

—Age: 25–65 years
—Height: 165–180 cm
—Weight: 650–800 N

Measuring System

Two FM telemetry systems were employed for recording measurement data; four sets of 10 measurement channels to one multiplex system (direct channels) in each case. Multiplex signals were transmitted via cable and stored direct on an analog magnetic tape recorder. FM channels were used to register intrusion measurement with an inductive motion sensor.

Measurement Points

Striking Vehicle

Deceleration along the X-axis.

Struck Vehicle

Acceleration at the dolly along the Y-axis; acceleration at the inner side of the struck door along the Y-axis, and intrusion was measured at the inner side of the door and in the vicinity of the B-Pillar with an inductive motion sensor (Figure 5). As a cross-check, intrusion was optically determined with a marked telescoping rod (Figure 5).

The physical portion of deformation in the struck area was measured at the outside and the inside at 24 fixed points (Figure 6).

Test Objects

—Dummy

Head: acceleration at the head center of gravity, 3 axes, right and left in the Y and Z directions (Schmidt et al., 1978).

Figure 5. Inductive motion sensor (WA) and marked telescoping rod (TS).

Thorax: accelerometers as per the method recommended by NHTSA (Robbins et al., 1976, Figure 7).

Sternum, upper:	X-axis
Sternum, lower:	X-axis
4th Rib, left:	Y-axis
8th Rib, left:	Y-axis (X-axis)
4th Rib, right:	Y-axis
8th Rib, right:	Y-axis
Thorax vertebra 1 (T1):	3 axes

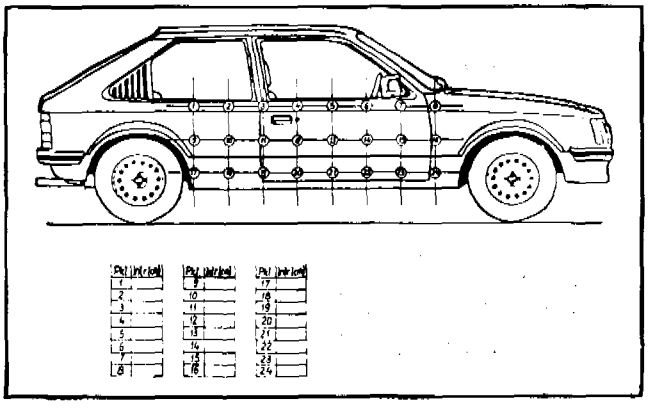

Figure 6. Deformation measurement points in the struck area at the outside and the inside ar 24 fixed points.

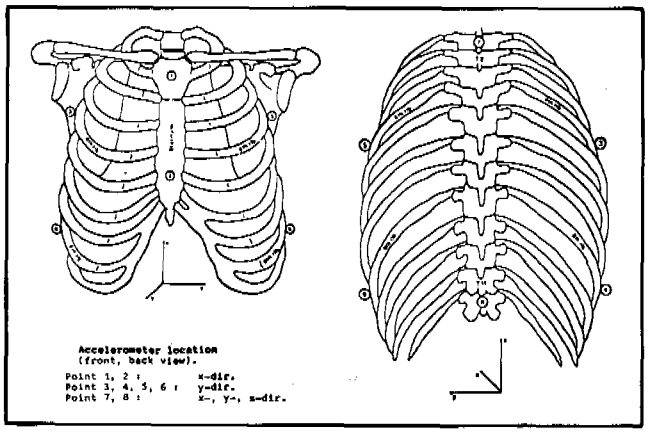

Figure 7. Locations of the thorax accelerometer of the 12 components method.

Thorax vertebra 12 (T12): 3 axes
Pelvis:
At the sacrum: 3 axes
At the center of gravity: 2 axes (X-Axis, Y-Axis)

—Cadaver

Head: acceleration right and left in the Y and Z axes

Thorax: 12 acceleration component measurement in keeping with NHTSA (as with the Dummy)
pressure on the lungs

Pelvis: At the sacrum, 3 axes

Measurement Evaluation

Measurement evaluation was accomplished at VW-AG. Head signals were filtered pursuant to SAE J 211a according to channel class 1000; chest and pelvis signals according to channel class 180, and the vehicle acceleration signals and seatbelt force signals according to channel class 60.

Photographic Documentation

The collision phase was documented with three high-speed cameras (stationary and onboard) at 500, 600 and 1000 frames per second.

FIRST TEST RESULTS

Partial results from 5 HSRI-, 4 APROD-, and 4 Hybrid II Dummy Tests and 8 Cadaver Tests are given in the following figures.

Figures 8-27 cross-compare the accelerations of the 4th rib on the impacted side, the 1st thoracic vertebra (T1), and the sacrum, as well as the head deflection angle, of the individual test subjects as a function of time.

For each test subject group the figures show the mean acceleration/time curve and the outer boundary of the

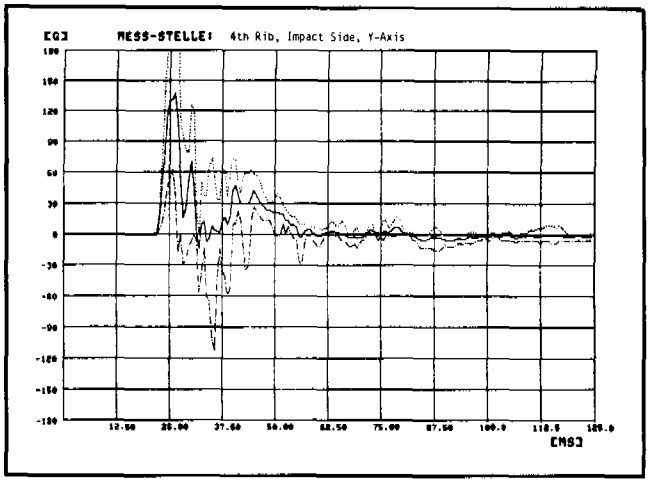

Figure 8. Lateral accelerations of the 4th APROD rib highest, mean and lowest values of 4 tests.

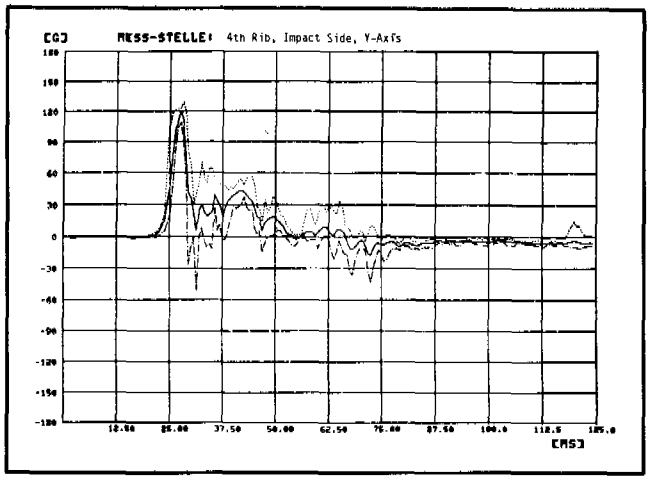

Figure 9. Lateral accelerations of the 4th HSRI rib highest, mean and lowest values of 5 tests.

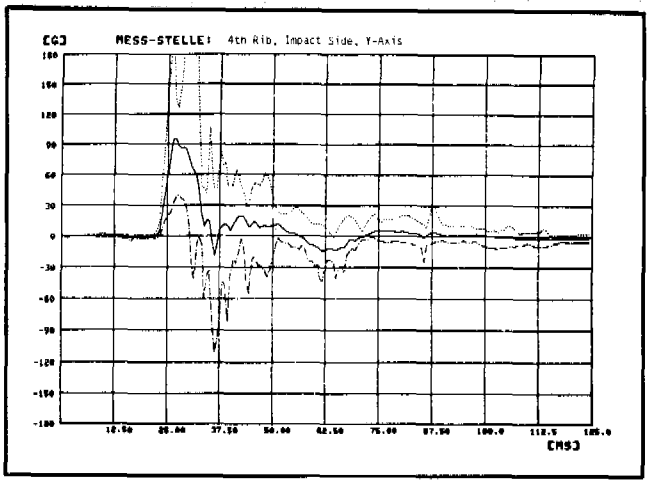

Figure 10. Lateral accelerations of the 4th cadaver rib highest, mean and lowest values of 8 tests.

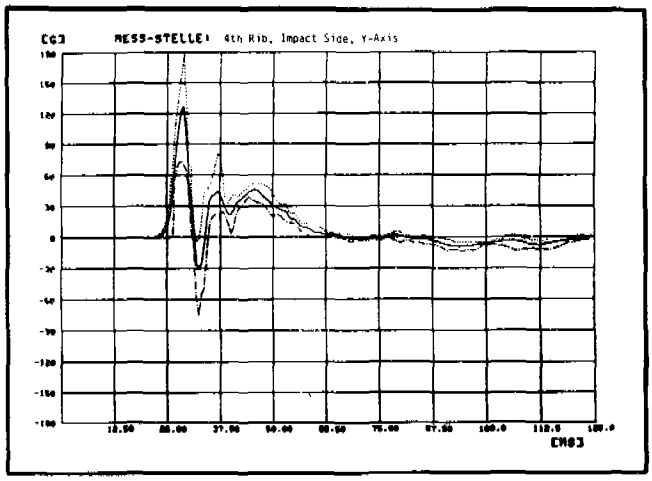

Figure 11. Lateral accelerations of the 4th Hybrid II rib highest, mean and lowest values of 4 tests.

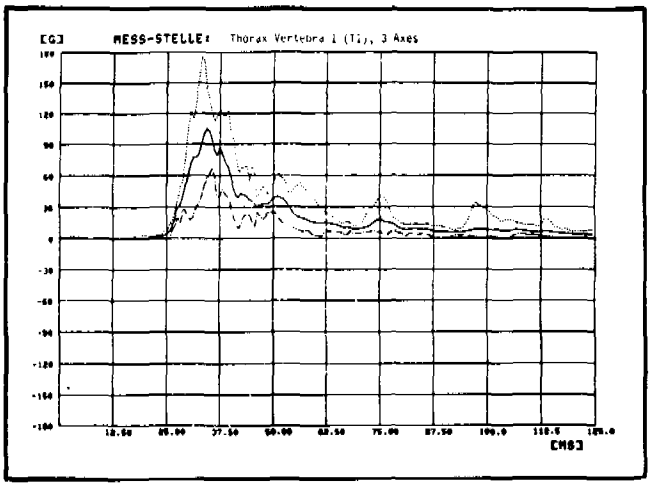

Figure 14. Resultant cadaver upper thorax accelerations highest, mean and lowest values of 8 tests.

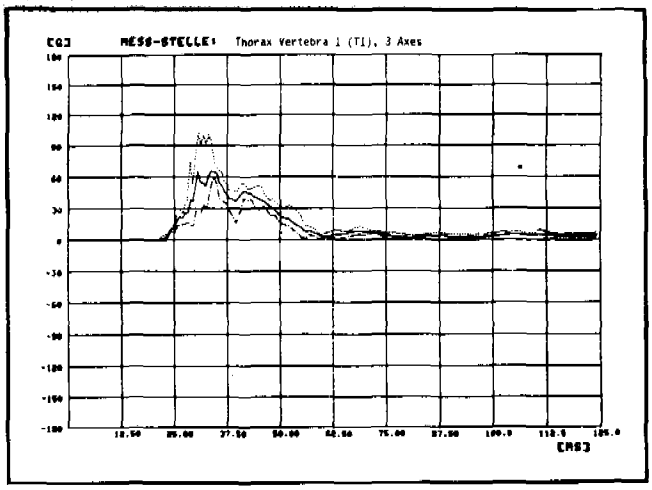

Figure 12. Resultant APROD upper thorax accelerations highest, mean and lowest values of 4 tests.

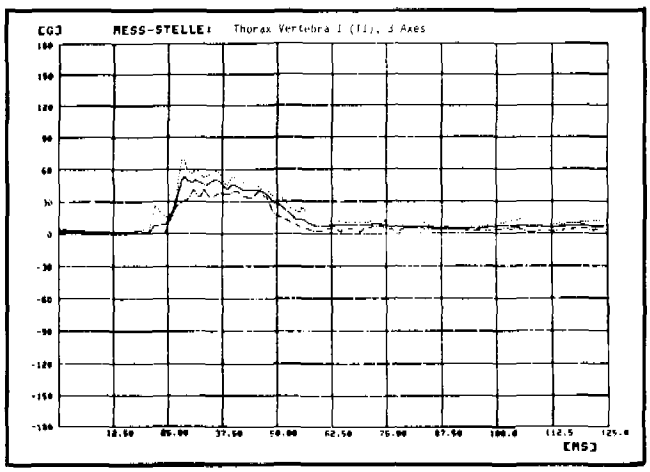

Figure 15. Resultant Hybrid II upper thorax accelerations highest, mean and lowest values of 4 tests.

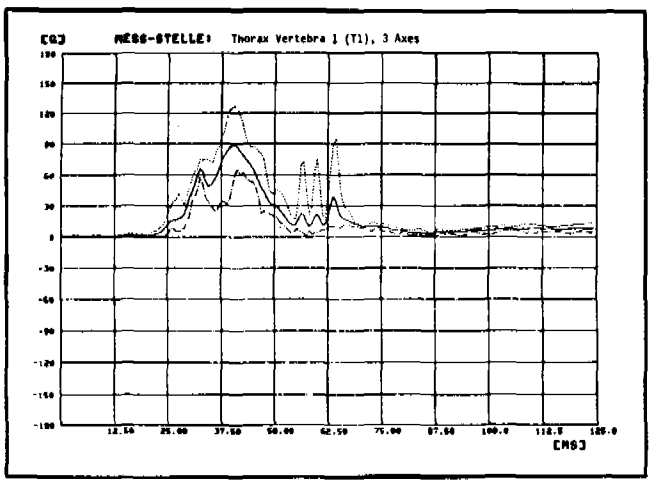

Figure 13. Resultant HSRI upper thorax accelerations highest, mean and lowest values of 5 tests.

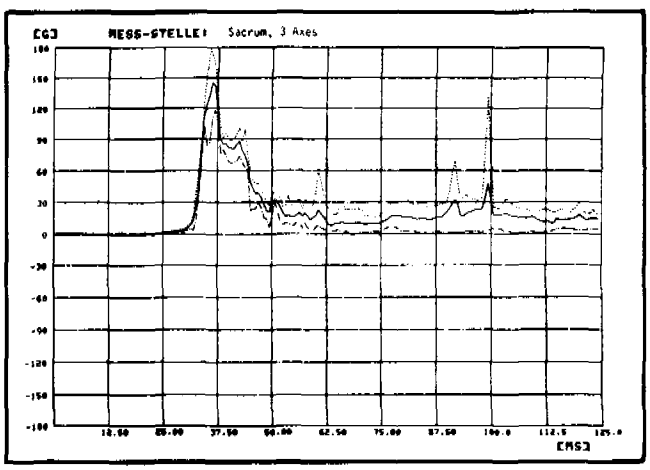

Figure 16. Resultant APROD sacrum accelerations highest, mean and lowest values of 4 tests.

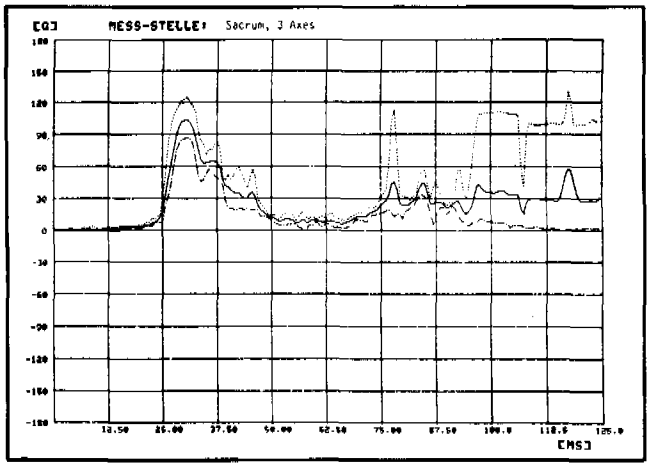

Figure 17. Resultant HSRI sacrum accelerations highest, mean and lowest values of 5 tests.

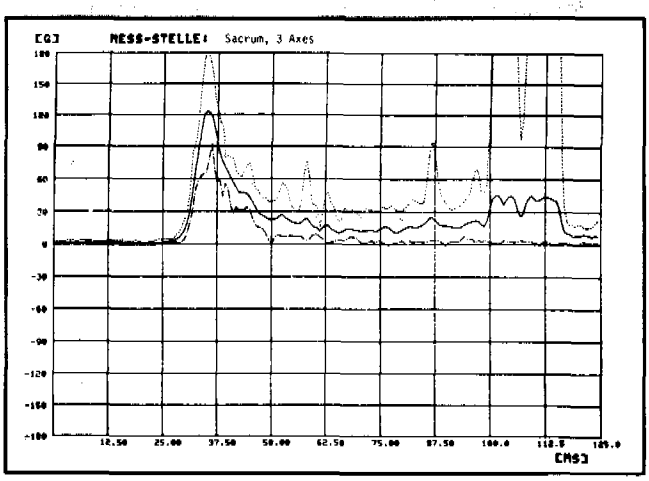

Figure 18. Resultant cadaver sacrum accelerations highest, mean and lowest values of 8 tests.

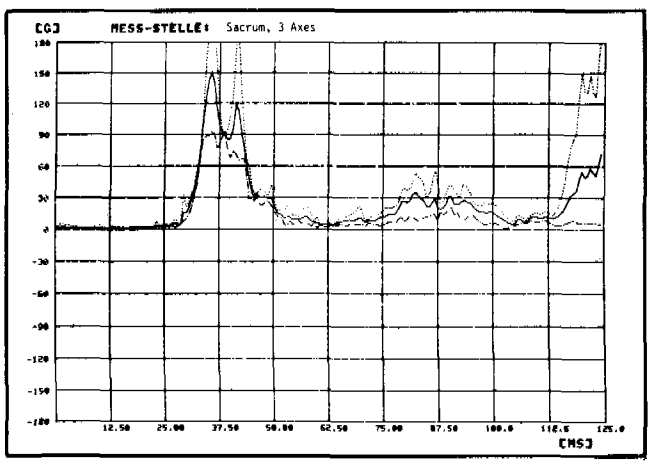

Figure 19. Resultant Hybrid II sacrum accelerations highest, mean and lowest values of 4 tests.

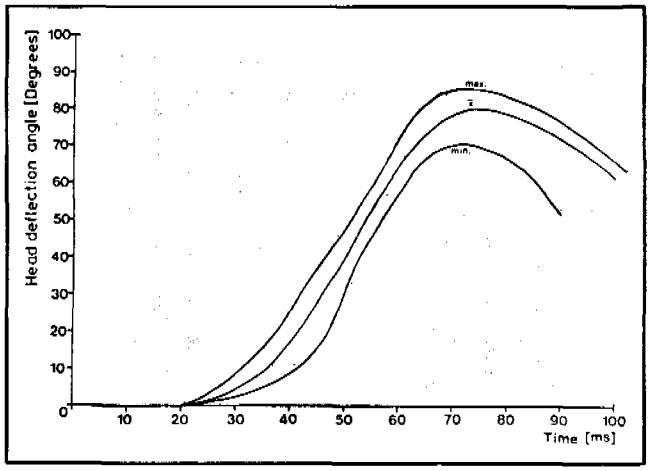

Figure 20. APROD head deflection angles highest, mean and lowest values of 4 tests.

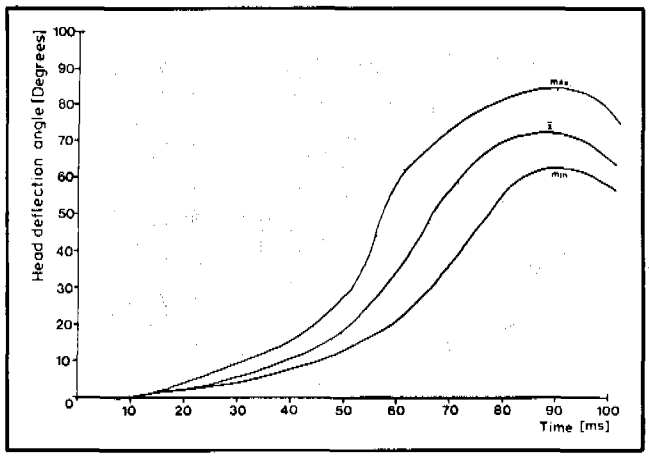

Figure 21. HSRI head deflection angles highest, mean and lowest values of 5 tests.

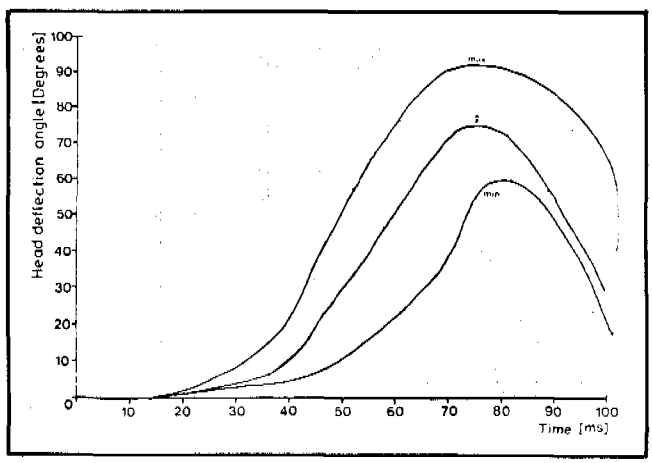

Figure 22. Cadaver head deflection angles highest, mean and lowest values of 6 tests.

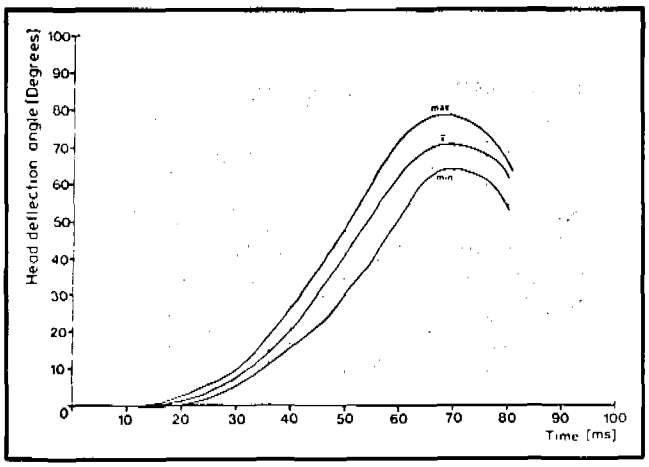

Figure 23. Hybrid II head deflection angles highest, mean and lowest values of 4 tests.

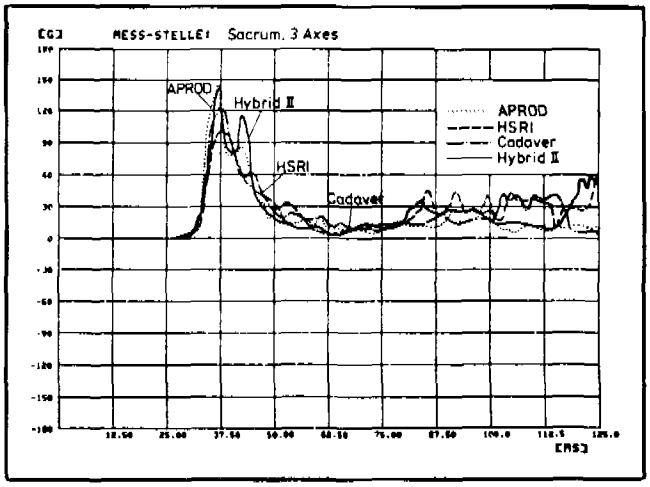

Figure 26. Mean resultant sacrum accelerations of APROD-, HSRI- and Hybrid II dummies and cadavers.

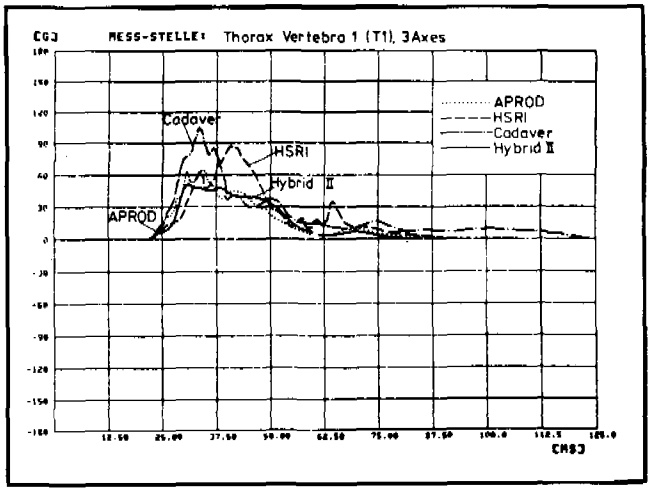

Figure 24. Mean resultant upper thorax accelerations of APROD-, HSRI- and Hybrid II dummies and cadavers.

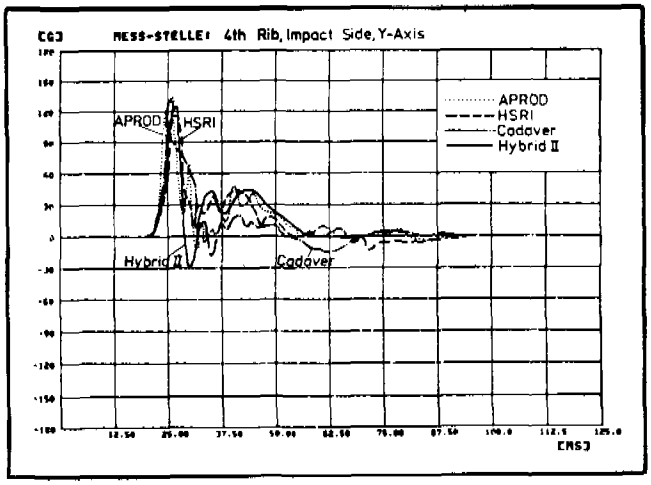

Figure 25. Mean resultant 4th rib accelerations of APROD-, HSRI- and Hybrid II dummies and cadavers.

acceleration/time field. It was necessary to adjust a few curves in time so that the start of acceleration at the applicable measurement point is the same within the text subject group. Placement in time of accelerations of individual measurement points with each other is thus not always assured. This will be documented for the individual tests in the final report.

Comparison of the mean acceleration/time curves shows the great variances between the dummies and the cadavers, particularly to Thoracic Vertebra 1 (Figure 24). The behavior here of the Hybrid II and the APROD dummies is similar. The curves in the first phase of the dummies are nearly the same in the area of the 4th rib (Figure 25). These differ in amplitude and time from those of cadavers.

The mean acceleration/time pattern for dummies and cadavers deviated less in the sacrum area (Figure 26). Figure 27 shows the mean curves of the head deflection angle as a function of time. Angular velocity is approx-

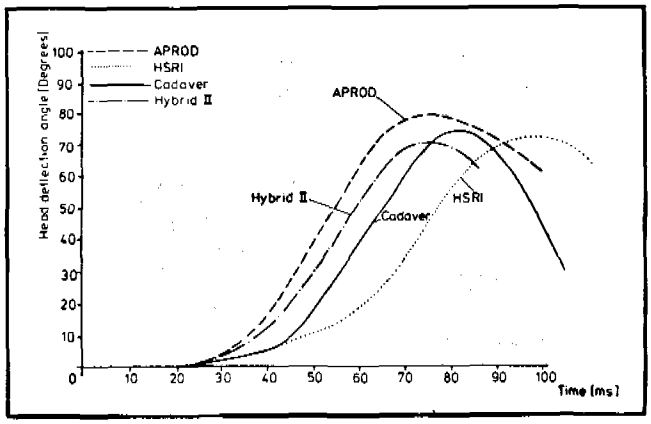

Figure 27. Mean head deflection angles of APROD-, HSRI- and Hybrid II dummies and cadavers.

imately the same at the beginning for the APROD and Hybrid II dummies and higher than that of cadavers and of the HSRI dummy. The mean maximum deflection angle is approximately the same for the cadavers and for the Hybrid II and HSRI dummies but smaller than that of the APROD dummy.

CONCLUSIONS

The initial results discussed in this status report of the ongoing project do not yet allow generally applicable statements to be made regarding the compatibility of the dummies examined but it can be said that all of the dummies examined must still be refined and are not yet ready for experimental simulation.

The test series has still not been completed and, additionally, loads were only determined at one collision speed and for one specific test configuration. The initial comparison, that has still not been accomplished with statistical procedures, of the mean acceleration/time and head deflection angle/time patterns in this report indicates that the development of the dummies examined, which were especially designed for the side impact, is still not complete. This finding is also confirmed by the fact that some of the dummies had unexpected structural failures.

Analysis of the results of this project could supply a contribution toward a more accurate simulation of side impact dummy behavior to the behavior of cadavers. It would be logical to correlate dummy loadings with cadaver injuries, and to derive protection criteria or loading limits respectively for belted occupants during a side impact, only after the loadings and the kinematics of dummies and cadavers are similar.

The final results will be made available towards the middle of the next year.

These results will show to what extent under these test conditions the behavior of the dummies is in conformity with that of the cadavers, thus enabling the necessary conclusions to be drawn with regard to the dummy modification and protection criteria.

Injury Criteria in Lateral Collisions, When an APROD Dummy is Used _

B. HUE, C. TARRIÈRE, Y. C. LEUNG, and A. FAYON
Laboratory of Physiology and Biomechanics, Peugeot S.A./Renault

C. GOT, A. PATEL
I.R.O.-I.R.B.A., R. Poincaré Hospital, Garches, France

ABSTRACT

Modifications brought to APROD dummy since the 8th ESV Conference in Wolfsburg are presented and explained. They result in new features of biofidelity and of dynamic response as regards the main body segments. Simultaneously, the injury criteria to be associated to the use of APROD in lateral collisions are discussed. They include in particular the case of the abdomen. Besides, the new head and neck assembly is matched to HIC 1500 and the thorax to a relative deflection criterion which is commented upon.

SINCE THE EIGHTH ESV CONFERENCE, numerous studies concerning biomechanics and future dummies have been performed. In particular, many researches were carried out in the framework of contracts with the E.E.C. They resulted in more precise requirements to be met by dummies; besides, their dynamic response was investigated. The APROD dummy underwent consequently several modifications; the purpose of this paper is related to this development and its consequences on the possible injury criteria when using the APROD.

TECHNICAL EVOLUTION—Three main grounds triggered the changes brought to APROD; they concern biofidelity, accidentological data and mechanics, respectively.

New biomechanical data are available which define the human head response to direct lateral impact, and which define the head kinematics, due to the neck response, when the body is pushed sidewards. To a certain extent, the APROD head and neck assemblies were modified accordingly.

Accidentological data showed the weight of abdominal injuries in lateral collisions (7). The abdominal section built by TNO (12) from APR data (7) is able to detect the likelihood of injuries and was incorporated with APROD body.

Dynamic testing showed some shortcomings of the previous APROD thorax. A mechanical analysis of the thorax response was performed which resulted in structural modifications.

These sundry improvements will be detailed below for each body segment.

Neck—For reasons of mechanical resistance and consistency of accelerometric measurements at the level of the head, the Part 572 dummy neck (which equipped

previously the APROD dummy) is essentially constituted with a hard rubber, cylinder. The inferior face of this rubber block stays integral with the thorax and the superior face with the head base. It arises from that a low magnitude of the head/neck relative displacement. Furthermore, the curvature radius of the head trajectory is too short (Fig. 1).

The analysis of car-to-car reconstructions and sled tests carried out with cadavers shows a very different response of the human subject head if the thorax is struck sideways. One can discern a translation phase which delays the tilt of the head and is due to its inertia when forces and torques transmitted by the neck are too low. Then comes an important rotation phase, if no impact occurs.

If these kinematics are analyzed, two rotation centers appear, each one being situated near the interfaces head/neck or neck/thorax, respectively.

Figure 1 shows other noticeable features of the human head and neck kinematics under the Ewing's test conditions (8) with 22 kph and 7 g.

In particular, the maximum angles reached by the head and the neck, and the maximum head sidewards displacements relatively to the thorax are mentioned.

In order to achieve an improved simulation of the human head bending motion during side impact, researches were devoted to modifications to be brought to the Hybrid III neck (the middle part of which is more flexible), in the areas of the head/neck and neck/thorax interfaces. One half-sphere was arranged at each neck extremity; both half-spheres were connected by a tensioned cable. The inclination of the head depended upon the neck rigidity and also upon the frictions between the half-spheres and their sockets, according to Figure 2.

The braces of rubbers that were placed between the head or the thorax respectively and the extremity of the neck play an important role in head-neck kinematics.

As for other modified body segments, the results obtained will be presented in the next section of the paper.

Head—As the modified neck is longer than the one which equips the Part 572 dummy, a Hybrid III head was chosen. This one allows to keep the same erect sitting

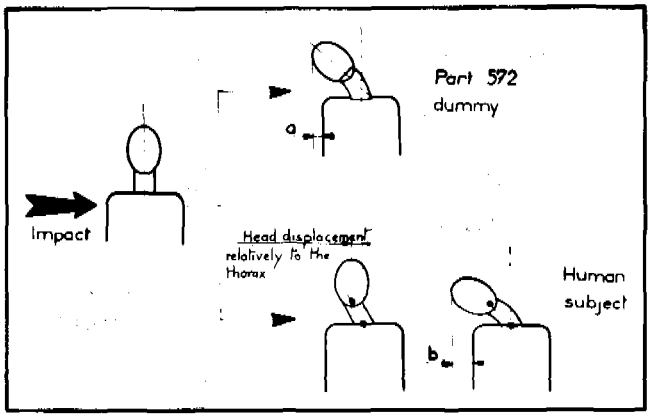

Figure 1. Neck motions in lateral impact.

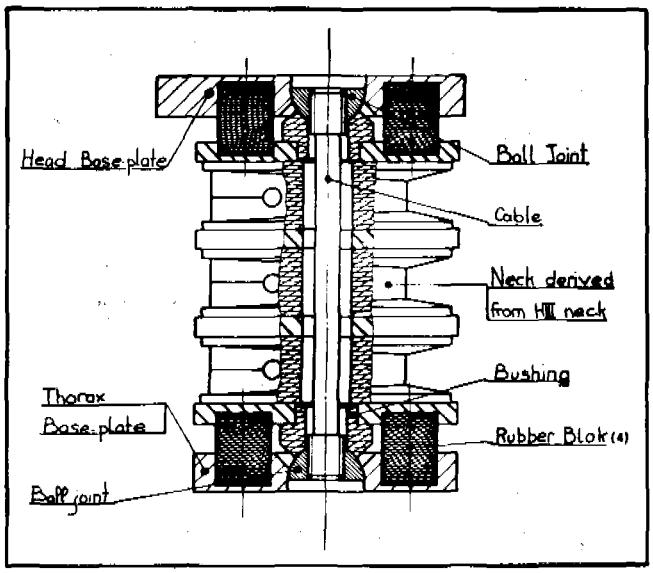

Figure 2. Sketch of APROD 82 neck.

height; besides, more humanlike impact responses are expected. These impact responses were not defined in the available literature. In the frame of an EEC research programme, cadaver drop falls were carried out onto paddings, the impact occurring on the parietal area of the head. Although the results of these tests are not yet complete (by the way, they are to be published by spring 1983), the duplication of these tests with the APROD dummy equipped with a Hybrid III head seems to indicate that the use of a Hybrid III head confers a more humanlike impact response. Particularly, the HIC levels are very close to those obtained during some cadaver tests.

Shoulder-clavical-arm—No modifications to note since the versions presented at the last ESV Conference. As a reminder, since 1980, APROD is equipped with clavicles in molded compact polyurethane with steel inserts, and such a clavicle was tested at speeds of up to 40 kph in rigid impacts.

Thorax—Three points have to be recalled concerning the requirements to be met by a lateral dummy thorax.

1) Only a proper stiffness of the thorax allows to get an accurate deformation of the side wall of the vehicle (Fig. 3), which may be equipped with paddings.

2) It is essential to duplicate the thorax deformation because the measurement of this deformation (called thoracic deflection) is a good injury predictor as previously presented (5).

3) A humanlike deformation of the thorax and the shoulder area is needed to enable a correct simulation of a possible head impact.

Lateral impacts with cadavers already published (1)(2) enabled to define the curve of force versus deflection of the impacted half-thorax (Fig. 4). Therefore, an important capacity of deformation had to be brought to the dummy thorax.

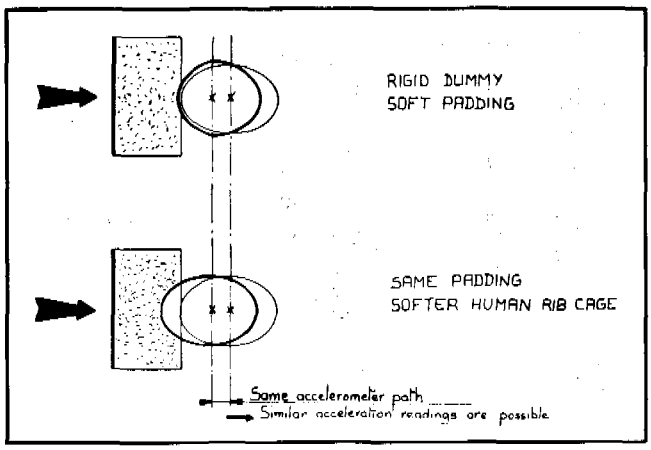

Figure 3. Stiffness of dummy rib cage must be human like and matched in padding stiffness.

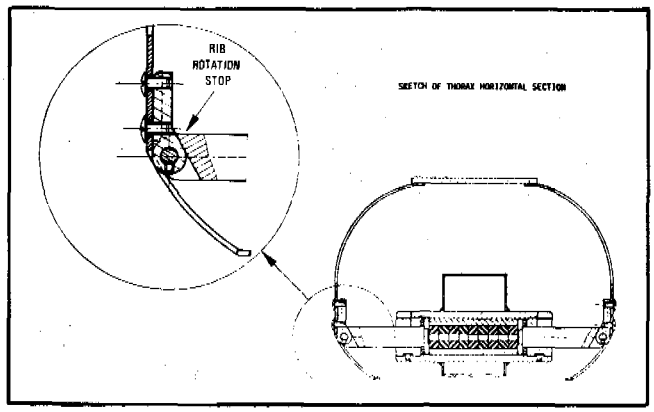

Figure 5. APROD 80.

APROD 80—In 1980, the horizontal section of the dummy's thorax was as presented on Figure 5.

A horizontal cylinder can be seen; two such cylinders are superimposed and each one of them corresponds to 3 pairs of ribs. The square crosssection of the pistons was designed to prevent the rib cage from collapsing diagonally when compressed in antero-posterior direction.

To get the previously shown force-deflection characteristics of the thorax, the main adjustment parameters were compression disks located inside the horizontal cylinders and the rib thickness.

APROD 81—Because a jamming of the pistons was noted, the APROD design was reviewed to get rid of this undesirable phenomenon.

If one looks to a simplified horizontal crosssection of the thorax, it appears that offset or oblique impact forces develop reaction forces on piston bearings, and therefore they increase friction.

It was noted that a modification of the joints between ribs and pistons could drastically diminish the reaction forces. The corresponding principle is shown on Figure 6. The limitation of the ribs outwards rotation, relatively to the pistons, is provided on the opposite side to impact, contrary to 1980 version.

Figure 7 shows the horizontal crosssection of APROD 81: the square section of the deflection tubes disappears.

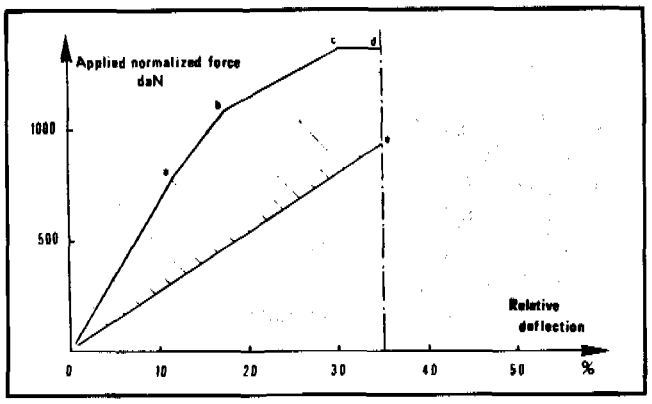

Figure 4. Corridor for force/deflection characteristic of the dummy.

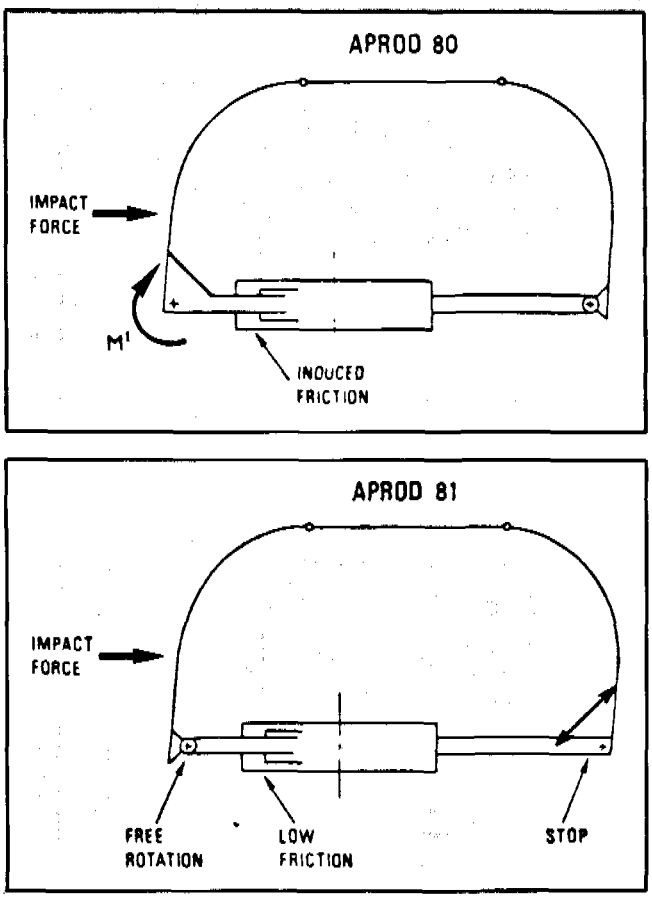

Figure 6. Principle sketch of the 80 and 81 rib cage kinematics.

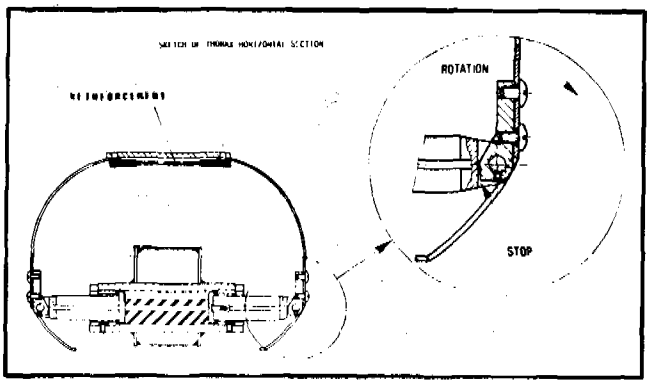

Figure 7. APROD 81.

Although this solution was satisfactory in its principle, it remained opened to criticism; in fact, the producing of such parts and of their guide-system was a delicate matter, and they were likely to produce excessive frictions, as soon as parallelism was not perfect. The pistons were hence redesigned; they got a circular cottered section, with the cotter acting as a stopping device in rotation motion during frontal impact. [In the beginning, the guide-system included self-lubricating rings. The fragility of these parts in frontal impacts led us to discard them in favour of a metal-on-metal guide-system, the gliding of which might be improved when necessary.]

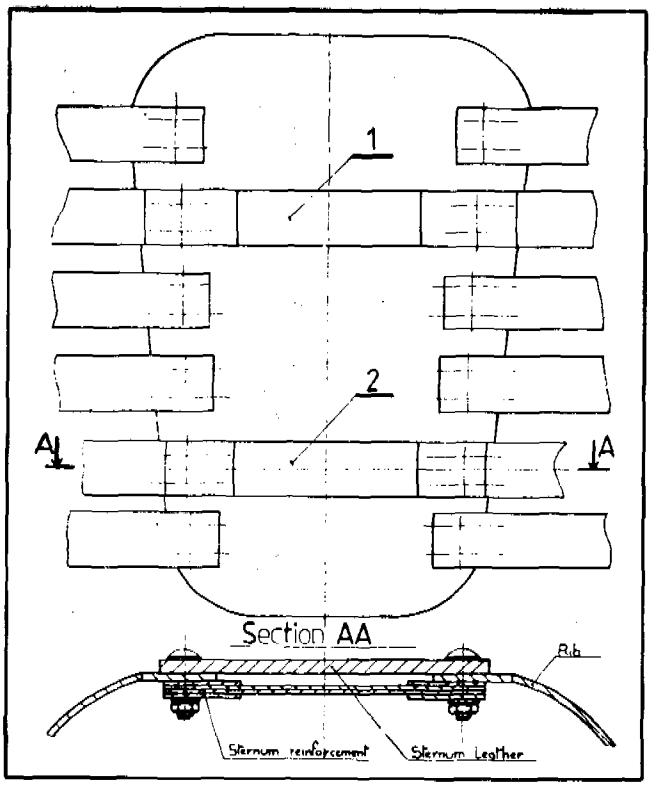

Figure 8. Sternum reinforcement locations

Inside the deflection tubes, rubber washers controlled the dummy's internal dynamic rigidity. During the occurrence of impact, the pile made by those washers underwent axial force and they often buckled. This instability had two consequences, i.e., unrepeatability of tests and the need to disassemble the dummy after every test in order to replace the washers. Thus, these washers were replaced by a triangular-shaped single piece, the hardness of which is 50-shore.

To prevent excessive rib cage deformations ensuing from oblique impact, it was decided to equip the APROD 81 with a reinforced breast plate (Fig. 8).

Abdomen—In lateral collision, the abdomen of presently existing dummies does not make it possible to evaluate the risk of occurrence of abdominal injuries. However, accidentological studies show that the statistical weight of the abdominal lesions, evaluated by means of a combination of their frequencies and their cubed AIS, is of the same magnitude as that of the head and thorax lesions, for which side impact protection criteria have already been contemplated.

In order to palliate this insufficiency, G. Walfisch et al. (7) defined, by means of tests with cadavers, the tolerance of the human abdomen area in terms of a couple force-penetration. Simultaneously, the dynamic data enabled a definition of an abdomen model to be integrated in a dummy. A first attempt for a protection criterion associated with measurement devices fitted into this abdomen is also made.

According to this work, the TNO developed a new instrumented abdomen section. A continuous force and penetration reading is not needed in order to check whether the tolerance limit is exceeded or not. Thus switches are placed inside the abdomen near the penetration limit; if those switches are designed to operate at a force limit, obtained from a pressure limit, then injury predictors at any point inside the abdomen at the required penetration level are installed according to the response of the switches. More details are already published (12). Six switches are located on the periphery of a drum shown on Fig. 9.

RESULTS OF TESTING

Neck results—Several sled tests were carried out for evaluating the improved neck. The procedure was similar to Dr. Ewing's tests with volunteers, with the greatest violence used (22 kph, 7 g). These tests confirmed that the achieved modifications confer to the neck a more satisfactory response according to the cadaver and volunteer data. However, the maximum angle reached by the head from the vertical axis remains too small, yet (Cf. here-under table).

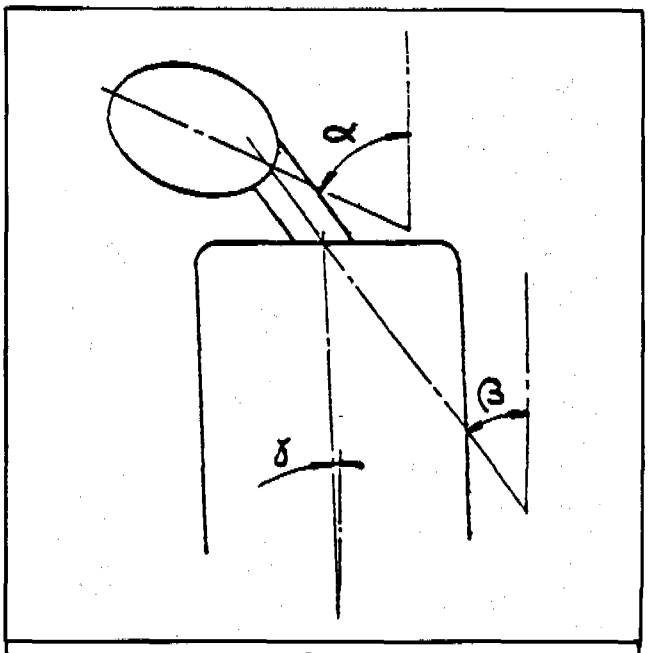

	α	β	γ	α − γ
APROD 82**	61	48	9	52
Cadaver	72	108*		
Volunteer	68	103*		

*Due to the head rotation around its z-axis, that displaces the targets, these values exceed the real ones.
**When new neck and TNO abdomen are fitted simultaneously on APROD 81, is referenced as APROD 82.

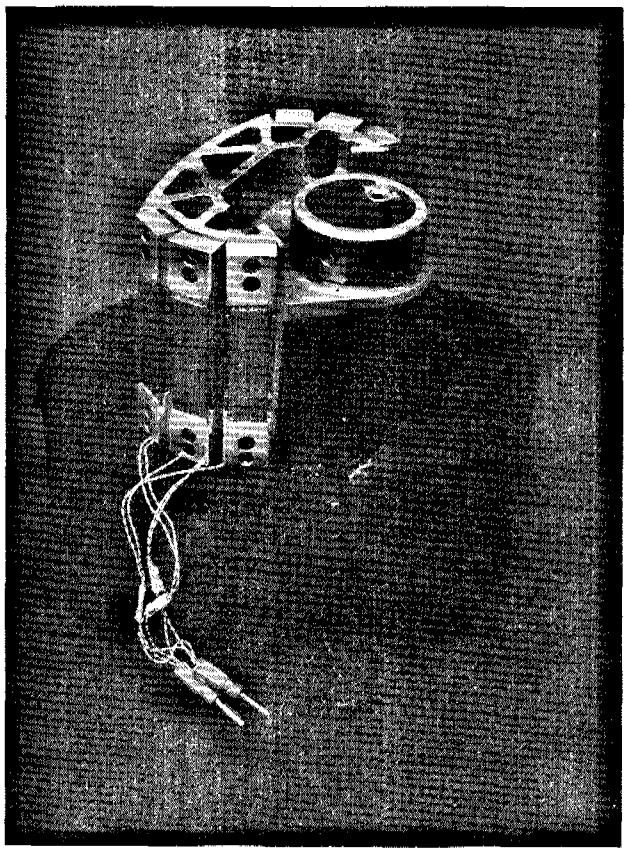

Figure 9. T.N.O. abdomen.

But, if tests under severe dynamic conditions are carried out, important technical problems will appear as regard the neck mechanical resistance. From the size and the geometry of ball-joints, excessive friction forces can be generated, inducing an insufficient rotation of the two half-spheres. It results in shearing forces which induce an important risk of neck cable rupture.

In order to increase the surface of the spherical bearings and diminish, too, the friction forces, we have been led to modify the size of the two half-spheres and the location of their centers. Although no more failure was recorded, we think that the present design is still not fully satisfactory (too much friction in the joints; neck elongation observed on volunteers and cadavers not properly duplicated). Thus, complementary studies were undertaken, which take into account the phenomena brought to light during the first evaluation.

Thorax results—drop tests: To evaluate the above presented improvements, thoracic drop falls were carried out. Test conditions are identical to those used to define the load-deflection corridor of the cadavers. The drop height was either 1 m onto rigid surfaces with the arm involved, or 2 m onto APR padding material with the arm out of the way.

The results are gathered in the here-under table and compared with the results obtained with the APROD 80 version, already presented at the 8th ESV Conference.

A difference appears between the half-thoracic deflection related to exterior dimensions and which is evaluated from film analyses and the intrusion of lower piston. But the deformation of the skin and the light amount of rib rotation and deformation (which are not measured by the transducer) are to be taken into account. Their cumulated values can be estimated at about 12,5 mm for these tests.

Drop Type	Impact Force (daN)		Translation of Lower Piston (mm)		Half-Thorax Deflection (mm)	
	80	82	80	82	80	82
1 m—rigid	900	920	1	6	~24	19.5
arm involved		1250		11	1	24
2 m—padding	630	570	23	36	48	~47
arm out of way		660		36		~47

For APROD 80, there was an almost constant deviation of 23 mm between the external deflection (recorded on film) and the internal deflection (measured by the transducer). This more important further deflection is due to the difference in kinematics of the 80 and 82 rib cages, when they are struck sideways.

Full scale tests—For evaluating the APROD 82 in such tests, two experimental collisions were carried out, in which APROD 82 was seated in the struck car on the struck side. As a matter of fact, these two tests are two supplementary reconstructions of a real accident involving two Peugeot 504, the precise description of which was presented at the 8th ESV Conference (4).

At this same conference, results of such reconstructions with an APROD 80 dummy occupying the struck car were also presented. Therefore, it enables, today, comparing the results obtained with an APROD 80, on the one hand, and with an APROD 82 on the other hand, under the same conditions.

The trajectories of the APROD head, linked to the displacement of the neck base are very close to that of the cadavers of already mentioned reconstructions (4). In particular for both human surrogates constituted by human subjects and APROD 82 dummies, the sidewards displacements of their heads were of the same order of magnitude. It is reminded that, due to the technology of the new neck of APROD 82, it is possible to duplicate more easily the translation of the head inside the passenger compartment which occurs before the head rotation phase, as previously recalled in this paper.

As regards the thorax, kinematics is satisfactory. Nevertheless, the thoracic deflection results for APROD 82 are rather low in comparison with the results for APROD 80. The differences in kinematics of 80 and 82 rib cages could be an explanation.

Regarding the abdomen, the switches have not been actuated, that cannot be correlated with the AIS = 4 abdominal lesion of the real victim. It seems that the distribution of the six switches at the periphery of the drum, where they are separated by 15° intervals, may be responsible for this failure. As a matter of fact, the direction of the forces applied to the abdomen may have exceeded the angular limits corresponding to the proper work of the switches.

PROTECTION CRITERIA TO BE MET WHEN USING THE APROD 82 DUMMY

1. Head—The results of the tests carried out with cadavers and APROD 82 dummies, since they display similarities in kinematics and in head impact response, show that it is possible to choose a protection criterion level close to the human tolerance, that is a HIC equal to 1500 according to a paper released during this ESV Conference (11) and other previous publications (8)(10).

2. Thorax—Previous studies (3,9) have shown that 35% of the half-thoracic relative deflection can be associated with 7 to 8 rib fractures for the middle class, as regards the overall resistance of the population at risk; this deflection figure can be used as a thoracic human tolerance, as far as force-deflection characteristics of APROD and human being are similar; so, a relative deflection equal to 35% could constitute for the APROD dummy a protection criterion. These 35% correspond at about 40 mm for the driving-in of the one piston, for which the deflection is the greater. This point will be precised by complementary tests under other conditions.

3. Abdomen—Even if it is necessary to redefine the force which triggers the switches, or the locations of these switches, it seems that the TNO abdomen can be kept inside of this dummy to develop a satisfactory abdominal protection criterion.

4. Pelvis—Previous studies have shown that it is possible to take the value of 100 g/3ms measured in the median sagittal plane of the dummy's pelvis as protection criterion for this body area.

DISCUSSION

At the 8th ESV Conference, it had been noted that some mechanical jammings appeared at the level of the thoracic pistons. It seems that the mechanical jammings have today disappeared as regards metallic parts, due to

		HIC	γ max. thorax	γ 3ms thorax	Half thoracic deflection	γ max. pelvis	γ 3ms pelvis	Abdomen switch
Part 572	1st test	309	75	60	—	110	100	
	2nd test	1017	72	60	—	—	—	
	3rd test	811	—	—	—	—	120	
APROD 80	1st test	737	62	60	42	190	125	
	2nd test	1130	42	38	36	188	140	
APROD 82	1st test	653	73	65	39	110	100	no
	2nd test	338	56	45	24	121	120	no
cadaver	1st test	440	121	95	43	107	90	
	2nd test	837	93	75	37	147	118	
	3rd test	110	104	70	—	128	105	

the improved paths of loadings and kinematics obtained from the modifications brought to the thorax (free rotation on side impact and stop on the opposite side—sternum reinforcements). However, for some drop fall tests onto rigid surface, it was observed an interruption of piston motion during impact. An in-depth analysis of these tests brought to light the existence of two main paths of loadings, through the piston and through the plastron respectively. The reinforcements of the plastron makes the corresponding transmitted forces no more negligible. As regards forces passing through pistons, it seems that an excessive friction of the rubbers, when compressed, can be responsible for a stopping of the piston displacement.

This point will be investigated and the rubber shape will be modified accordingly.

CONCLUSIONS

Improvements developed for the APROD dummy provided benefits as regards its biofidelity and its dynamic response. Some technical problems remain concerning the neck, for which a new study will be undertaken. It seems that the mechanical jamming, observed on the previous version have today disappeared as regards metallic parts.

Protection criteria for the main body areas have been proposed. APROD 82 can be used for improving side impact protection since it makes it possible to evaluate the degree of safety afforded.

ACKNOWLEDGEMENTS

This presentation has been made possible thanks to results obtained within the frame of the Joint Biomechanical Research Project KOB, and to results obtained from the E.E.C. research contracts which supported the development of this dummy and its testing, simultaneously with other types of dummies.

This paper reflects the author's opinion and commits the organizations quoted in no way.

REFERENCES

1. A. Fayon Y. C. Leung, R. L. Stalnaker, G. Walfisch, M. Balthazard, C. Tarrière, "Presentation of a frontal impact and side impact dummy, defined from human data and realized from a "Part 572" basis." Proceedings of the 7th International Technical Conference on E.S.V., Paris, June 1979.
2. R. L. Stalnaker, C. Tarrière, A. Fayon, G. Walfisch, M. Balthazard, J. Masset, C. Got and A. Patel, "Modification of Part 572 dummy for lateral impact according to biomechanical data". Proceedings of the 23rd Stapp Car Crash Conference, San Diego, October 1979.
3. A. Fayon, C. Tarrière, G. Walfisch, M. Duprey, M. Balthazard, "Development and performances of the APR dummy (APROD)," proceedings of the 8th International Conference on E.S.V., Wolfsburg, October 1980.
4. C. Tarrière, B. Hue, A. Fayon, G. Walfisch, "Reconstruction of side collisions", proceedings of the 8th International E.S.V. Conference, Wolfsburg, October 1980.
5. J. Sacreste, F. Brun-Cassan, A. Fayon, C. Tarrière, C. Got, A. Patel, "Proposal for a thorax tolerance level in side impacts based on tests performed with cadavers having known bone conditions", 26th Stapp Car Crash Conference, October 20-22, 1982, Ann Arbor, Michigan.
6. D. H. Robbins, J. W. Melvin, R. L. Stalnaker, "The prediction of thoracic impact injuries", proceedings of the 20th Stapp Car Crash Conference, Dearborn, October 1976.
7. G. Walfisch, A. Fayon, C. Tarrière, J. P. Rosey, F. Guillon, C. Got, A. Patel, "Designing of a dummy's abdomen for detecting injuries in side impact collisions", in proceedings of the 5th International IRCOBI Conference on the Biomechanics of Impacts, 9-10-11 September 1980, Birmingham, Great Britain, ONSER Secretariat, 109 Ave. Salvador Allende, 69500 Bron, France.
8. C. Tarrière, G. Walfisch, A. Fayon, C. Got, F. Guillon, A. Patel, "Acceleration, jerk and neck flection angle: their respective influences on the occurrence of brain injury", AGARD Conference, 1982, Köln, Germany.
9. G. Walfisch, F. Chamouard, D. Lestrelin, A. Fayon, C. Tarrière, C. Got, F. Guillon, A. Patel, J. Hureau, "Tolerance limits and mechanical characteristics of the human thorax and transposition of these characteristics into protection criteria", proceedings of the 7th International IRCOBI Conference on the Biomechanics of Impacts, September 1982, Köln, Germany.
10. C. Got et al., "Results of experimental model for closed head impact injury", proceedings of 20th Stapp Car Crash Conference, Dearborn, October 1976, SAE paper 760 825.
11. D. Lestrelin, C. Tarrière, G. Walfisch, A. Fayon, "Proper use of the HIC under different typical collision environments", proceedings of the 9th International Technical Conference on E.S.V., Kyoto, November 1982.
12. J. Maltha and R. L. Stalnaker, "Development of a Dummy Abdomen Capable of Injury Detection in Side Impacts", Proceedings of the 25th Stapp Car Crash Conference, San Francisco, Calif., Sept. 1981, SAE.

Proper Use of HIC Under Different Typical Collision Environments

D. LESTRELIN, C. TARRIÈRE,
G. WALFISCH, A. FAYON
Laboratory of Physiology and Biomechanics
Peugeot S.A./Renault

C. GOT, A. PATEL
I.R.O.-I.R.B.A., R. Poincaré Hospital,
Garches, France

J. HUREAU
Laboratory of Anatomy-Biomedical U.E.R.,
Saints-Pères, Paris V University

ABSTRACT

Authors present a synthesis of data concerning the relationship between HIC values and head injury levels, obtained from various methods and under several particular test conditions. Then, frontal collisions are discussed. Two cases are separately considered; when head impacts occur, and without head or neck impacts. Accidentological data allow one to conclude that no criterion is presently needed when no head impact is recorded. On the contrary, when head impacts are undergone, biomechanical data and analyses of kinematics are in favour of HIC 1500 as far as 3-point belt is used.

The other classical types of accidents are mostly relevant to the case of direct head impacts; HIC 1500 criterion may apply provided that a sufficient pressure distribution exists—besides, the protection of the face is a particular problem.

THE HEAD INJURY CRITERION (HIC) is an already old concept which was often criticized for both its mathematical formula and its relationships with any injury level. However, in 1982, no alternative candidate criterion appears which was sufficiently known and directly available from measurements on present dummies.

This paper aims in particular to determine if meeting the requirements of a HIC value in a dummy test can provide a better safety to real accident victims, by protecting them from rather severe injuries when they undergo similar impact conditions. Various accident circumstances will be examined.

FRONTAL COLLISIONS—RESTRAINED SUBJECTS AND DIRECT HEAD IMPACTS

First of all, some old data will be recalled because they have been used in the beginning in order to situate the tolerance levels.

Everybody knows the Wayne State University tolerance curve and the Eiband data (4) based on acceleration/time diagrams. They allowed C. W. Gadd to write (1):

> —In view of the scatter of the data, it is suggested that a straight line approximation on a log-log plot is sufficient at this time for head injury likely to result from front to rear head acceleration over a range of between approximately one and fifty ms. This brackets the pulse time duration encountered by vehicle interior head impacts.

This resulted in the 2.5 exponent.

However, on WSU curve, the data points located on the left side of the curve correspond to rigid head impacts when data points located on the right side are related to whole body exposures which do not involve a direct blow to the head (4). No obvious reason exists which gave the same tolerance level for these 2 very different types of assaults.

As regards whole body exposures, a sketch of Eiband data, from a J. Versace paper (2) is shown on Figure 1. Versace noted that "the military data summarized by Eiband are expressed in terms of the deceleration of the seat (it results in) almost certain amplification of acceleration at the subject's head".

When Versace's paper was presented, the mathematical formula which computes the HIC value according to standard 208 was not used. Today, one can observe that the line $1000 = TA^{2,5}$ drawn on Figure 1 corresponds, *at seat level,* to a higher 208-HIC value than 1000, due to the very definitions of the magnitude and duration of the acceleration which were used; only a value inferior to present 208-HIC, as this later uses the whole deceleration pulse, can be obtained. So, harnessed volunteers

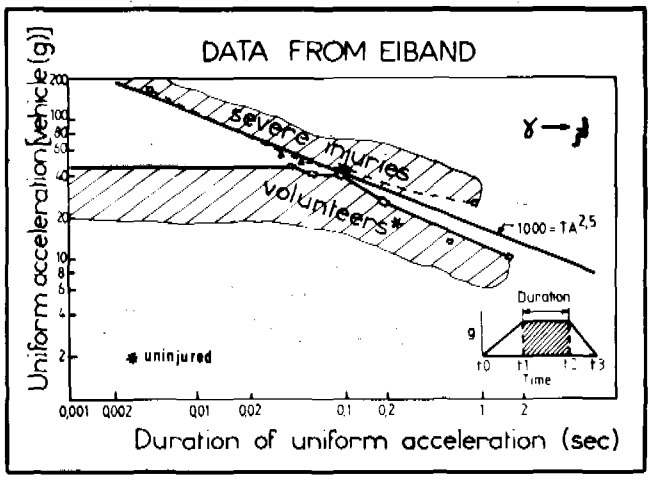

Figure 1. Data from Eiband, (J. Versace, in 15th Stapp car crash conference).

Table 1. Head injuries with and without head impacts. Belt wearers in frontal collisions—front places.

ΔV (kph) AIS	0	1	2	3	4	5	6	Totals
			Head AIS Versus ΔV—No Contact—					
≤20	271	0	0	0	0	0	0	271
21-30	221	0	0	0	0	0	0	221
31-40	142	0	0	0	0	0	0	142
41-50	56	0	0	0	0	0	0	56
51-60	14	0	0	0	0	0	0	14
61-70	4	0	0	0	0	0	0	4
>70	0	0	0	0	0	0	0	0
	708	0	0	0	0	0	0	708
			Head AIS Versus ΔV—With Contact—					
ΔV (kph)	0	1	2	3	4	5	6	Totals
≤20	1	34	3	0	0	0	0	38
21-30	2	29	8	1	0	0	0	40
31-40	1	62	19	2	0	0	0	84
41-50	1	53	33	7	0	1	0	95
51-60	0	22	15	3	1	5	0	46
61-70	0	2	11	2	0	4	0	19
>70	0	0	1	0	0	0	0	1
	5	202	90	15	1	10	0	323
			Head AIS Versus—Contact Questionable—					
ΔV (kph)	0	1	2	3	4	5	6	Totals
0-max	0	8	1	0	0	0	0	9
			Head AIS Versus Mean γ—No Contact—					
Mean γ	0	1	2	3	4	5	6	Totals
≤4	208	0	0	0	0	0	0	208
5-6	269	0	0	0	0	0	0	269
7-8	134	0	0	0	0	0	0	134
9-10	53	0	0	0	0	0	0	53
11-12	26	0	0	0	0	0	0	26
13-14	13	0	0	0	0	0	0	13
15-16	2	0	0	0	0	0	0	2
17-18	2	0	0	0	0	0	0	0
19-20	0	0	0	0	0	0	0	0
21-22	1	0	0	0	0	0	0	0
>22	0	0	0	0	0	0	0	0
	708	0	0	0	0	0	0	708
			Head AIS Versus Mean γ—With Contact—					
Mean γ	0	1	2	3	4	5	6	Totals
≤4	0	18	2	0	0	0	0	20
5-6	4	57	9	0	0	0	0	70
7-8	1	56	12	2	0	0	0	71
9-10	0	31	28	2	0	3	0	64
11-12	0	21	20	4	0	0	0	45
13-14	0	16	10	4	1	1	0	32
15-16	0	2	5	2	0	1	0	10
17-18	0	1	2	0	0	5	0	8
19-20	0	0	1	1	0	0	0	2
21-22	0	0	1	0	0	0	0	1
>22	0	0	0	0	0	0	0	0
	5	202	90	15	1	10	0	323
			Head AIS Versus Mean γ—Contact Questionable—					
Mean γ	0	1	2	3	4	5	6	Totals
0-max	0	8	1	0	0	0	0	9

probably sustained HIC values superior to 1000 without head or neck lesions.

This constitutes an earlier indication that, when no direct head impact occurs, the isolated Standard 208-HIC requirement brings no supplementary protection to the occupant. As a matter of fact, such runs with restrained volunteers exist which exhibit high S.I. or HIC value without head or neck injuries. According to Gadd (5), S.I. about 1500 were sustained by volunteers; therefore, one has to look at available accidentological data to check, if injuries are reported among restrained occupants in frontal collisions, without head impact, but under severe deceleration pulses.

Finally, the severities of head injuries, with and without head impact, were investigated by means of the data obtained from the IRO/PEUGEOT S,A/RENAULT multidisciplinary accident analysis.

The sample involves 1040 front seat occupants wearing a 3-point seat belt and who sustained a frontal collision.

For each subject sample, the following parameters are known:

—collision severity in terms of speed variation (ΔV) and car average deceleration (mean γ),
—localisation and severity, in terms of AIS of head injuries,
—injury causation; a head impact is assumed taking into account the recorded interior deformations (steering wheel, dashboard . . .) and the very nature of the observed lesions.

Table 1 makes a summary of available results.

Head injuries are distributed according to the collision severity in terms of ΔV on one hand, and mean γ on the other hand. They concern 708 occupants without head impact and 323 which sustained a head impact. In 9 cases, the occurrence or not of a contact could not be established.

In the analyzed sample, in frontal collisions without head impact, seat belt wearers never reached the head AIS value 2, i.e., a short loss of consciousness, at any collision severity.

On the contrary, among seat belt wearers which were submitted to a skull trauma, AIS $\geq$ 2 cases correspond to more than one third of the cases.

When a ΔV equal to 50 kph is exceeded, no head injury is found without head impact for 18 cases recorded; with head impact, 15 occupants out of 66 sustained an AIS $\geq$ 3.

Same results are observed when mean γ exceeds 12g.

In conclusion, head injuries are negligible without head impact in a sample which includes the most severe head-on collisions, since 1040 occupants were taken into account without selection.

As a complement, the severities of neck injuries were also examined when a head/neck impact occurs or not.

The sample and the methodology are the same as previously.

The cases for which direct neck impacts occur were added to the cases of head impacts, in order to keep separated the cases of pure posterior-anterior neck bending.

Table 2 shows a summary of the results.

In the analysis, neck injuries are distributed according to the severity of the frontal collision in ΔV on one hand, and in mean γ on the other hand.

—656 occupants without head or neck impact are involved
—339 with a head or neck impact are involved
— 45 cases could not be classified.

Beyond 50 kph, no neck AIS $\geq$ 2 is observed among 18 cases without head or neck impact. With such impacts, 4 AIS $\geq$ 2 are recorded out of 66 cases.

So, when no direct head or neck impact occurs, the risk of considerable neck injury is very little, and head injuries are negligible.

Furthermore, in some cases of the sample, the thoracic restraint is likely to have exceeded in terms of equivalent decelerations on dummies the classical limits. In addition to accidentological results, thinking of the existence of a prescribed limit for the thorax in any set of injury criterion, one concludes that no criterion is needed when no head or neck contact occurs in frontal collisions.

TOLERANCE TO DIRECT BLOWS TO THE HEAD

Only the cases where blows to the head are sustained have to be taken now into account. Blows without whole body exposure will be considered firstly.

Coming back to the WSU curve and to another already mentioned reference (4), 2 assessments can be made:

—As regards head impacts, it is very likely that American football players sustained HIC near 1500 in some cases since "football helmets were designed to attenuate head impacts to an S.I. of less than 1500 in a simulation of severe football head impacts" (30).
—Conversely, data points on the left side of the WSU curve, which corresponds to a lower S.I., are related to fractures and short duration impacts. Thus, a distinction appears necessary between padded impacts and the rigid ones which commonly produce fractures.

The head tolerance to skull fracture will be examined below.

RIGID IMPACTS AND SKULL FRACTURES

In 1971, the results of a research about human tolerance to skull fracture were published by Hodgson and Thomas

Table 2. Neck injuries with and without head and/or neck impact. Belt wearers in frontal collisions—front places.

				Neck AIS Versus ΔV—No Contact—				
ΔV (kph) AIS	0	1	2	3	4	5	6	Totals
≤20	250	9	0	0	0	0	0	259
21-30	200	4	0	0	0	0	0	204
31-40	121	4	0	0	0	0	0	125
41-50	48	2	0	0	0	0	0	50
51-60	13	1	0	0	0	0	0	14
61-70	4	0	0	0	0	0	0	4
>70	0	0	0	0	0	0	0	0
	636	20	0	0	0	0	0	656
				Neck AIS Versus ΔV—With Contact—				
ΔV (kph)	0	1	2	3	4	5	6	Totals
≤20	35	6	0	2	0	0	0	43
21-30	37	6	0	0	0	0	0	43
31-40	76	12	1	1	1	0	0	91
41-50	84	10	1	1	0	0	0	96
51-60	38	5	2	1	0	0	0	46
61-70	15	3	0	0	0	1	0	19
>70	1	0	0	0	0	0	0	1
	286	42	4	5	1	1	0	339
				Neck AIS Versus ΔV—Contact Questionable—				
ΔV (kph)	0	1	2	3	4	5	6	Totals
0-max	8	34	1	1	0	1	0	45
				Neck AIS Versus Mean γ—No Contact—				
Mean γ (g)	0	1	2	3	4	5	6	Totals
≤4	193	7	0	0	0	0	0	200
5-6	245	4	0	0	0	0	0	249
7-8	117	4	0	0	0	0	0	121
9-10	46	2	0	0	0	0	0	48
11-12	21	2	0	0	0	0	0	23
13-14	10	1	0	0	0	0	0	11
15-16	1	0	0	0	0	0	0	1
17-18	2	0	0	0	0	0	0	2
19-20	0	0	0	0	0	0	0	0
21-22	1	0	0	0	0	0	0	1
>22	0	0	0	0	0	0	0	0
	636	20	0	0	0	0	0	656
				Neck AIS Versus Mean γ—With Contact—				
Mean γ (g)	0	1	2	3	4	5	6	Totals
≤4	18	3	0	2	0	0	0	23
5-6	63	12	1	1	0	0	0	77
7-8	67	5	1	0	0	0	0	73
9-10	60	4	1	0	1	0	0	66
11-12	37	7	0	1	0	0	0	45
13-14	26	6	0	0	0	1	0	33
15-16	6	3	1	1	0	0	0	11
17-18	6	2	0	0	0	0	0	8
19-20	2	0	0	0	0	0	0	2
21-22	1	0	0	0	0	0	0	1
>22	0	0	0	0	0	0	0	0
	286	42	4	5	1	1	0	339
				Neck AIS Versus Mean γ—Contact Questionable—				
Mean γ (g)	0	1	2	3	4	5	6	Totals
0-max	8	34	1	1	0	1	0	45

Table 3. Results of head impacts at fracture level, published by: V. R. Hodgson and L. M. Thomas at the 15th Stapp Conference, SAE.

Cad No.	Drop ht., in	Vel., ft/sec	Peak Force, lb	Peak A_{CG} Result, G	Mean A_{CG}, G	Pulse Time, s	Peak A_{a-p}, G	(SI) (A_{CG})	(SI) (A_{a-p})	EDI (A_{CG}) Resp, in	EDI (A_{a-p}) Resp, in
Front—Flat Plate											
1747	10	7.3	1600	230	75	0.0076	195	794	400	0.14	0.11
1701	10	7.3	1450	370	123	0.0045	345	2020	1800	0.18	0.12
1699	10	7.3	1700	270	87	0.0076	230	1280	792	0.17	0.13
1805	10	7.3	1450	190	63	0.0076	150	565	390	0.13	0.11
1873	25	11.5	2100	240	85	0.0061	195	1020	724	0.16	0.13
1857	30	12.7	2000	220	83	0.0076	220	1250	561	0.19	0.11
Average	14	8.9	1720	250	86	0.0068	220	1150	780	0.16	0.12
Front—8 in Radius Hemisphere											
Average	21	10.3	1400	—	—	0.0068	220	—	565	—	0.12
Front—3 in Radius Hemisphere											
Average	15	9.7	1030	—	—	0.0064	190	—	550	0.13	—
Front—1 in Radius Cylinder—Sagittal Plane											
Average	16	8.5	1960	—	—	0.0048	280	—	910	—	0.12

Table 3 bis. Comparison of Alderson 50th percentile dummy to cadaver response at fracture level front-flat plate; published by: V. R. Hodgson and L. M. Thomas at the 15th Stapp Conference, SAE

	Subject	Drop ht., in	Peak Force, lb	Pulse Time (Force), s	Peak Accelerate, G: res	Peak Accelerate, G: a-p	Pulse Time (accelerate), s	Severity Index: A_{res}*	Severity Index: A_{a-p}	EDI (A_{a-p}) Resp, in.
(Cadavers)	Average	14	1720	0.0051	250	220	0.0068	1150	780	0.12
	Dummy	10	2350	0.0034	305	270	0.0072	1680	890	0.10
		15	3070	0.0034	325	290	0.0072	2040	1150	0.12
		20	4000	0.0028	425	384	0.0061	3270	2020	0.14

*A_{res} = Resultant of A_{a-p} and $A_{transverse}$ measurements of dummy.
A_{res} = Resultant CG Acceleration (A_{CG}) for cadavers.

(6). Hereunder is a duplication of a part of the conclusions of this study. Besides, Table 3 gives numerical results. Embalmed moist human cadavers were used.

"These test results confirm that frontal bone fracture occurs in the human cadaver at the same level of acceleration as predicted by the Wayne State University Tolerance Curve.

Average values of SI and EDI (*) computed for six impacts which produced linear skull fractures due to frontal rigid flat plate impact are in close agreement with critical values predicted by authors of these two methods.

For the drop height range which produced linear fracture in the cadaver due to frontal impact against a rigid flat plate, the SI for the Alderson 50th percentile dummy head acceleration response was much higher than for the cadaver".

These conclusions can be commented as follows.

Pulse durations (Table 3) remained inferior to 8 ms: the impacted areas were rigid, unyielding surfaces.

When resultant accelerations at the center of gravity are available, HIC 1000 appears here a reasonable estimate of skull fracture tolerance (by interpretating the published S.I. values). Here, accelerations give a good estimate of the loading imposed to the head, because the whole path of loading concerns skull bones with a single impact in frontal area. However, the tolerance level suggested by these experiments has not to be kept as far as head-on car collisions are concerned, because of the very nature of impacted area, because of the differences in the paths of loadings, and because of the different dummy head responses.

As regards the impacted areas, presently no unyielding surface of infinite mass exists in a car, under the conditions of the contemplated dummy tests.

The surfaces in contact with the head yield more or less; Figure 2 shows the much longer impact durations and HIC computation intervals which commonly appear

(*) EDI: see (29)

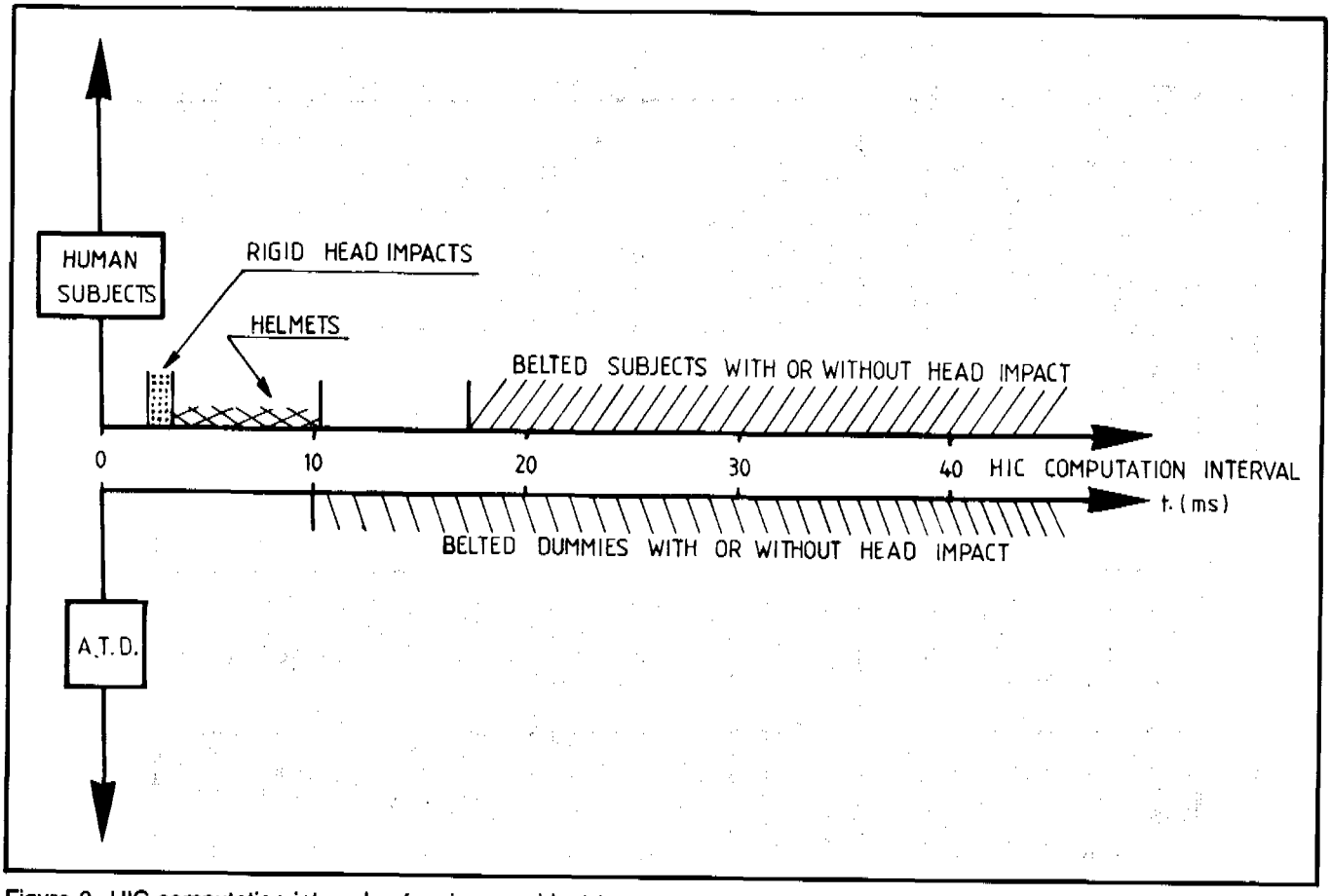

Figure 2. HIC computation intervals of various accident types.

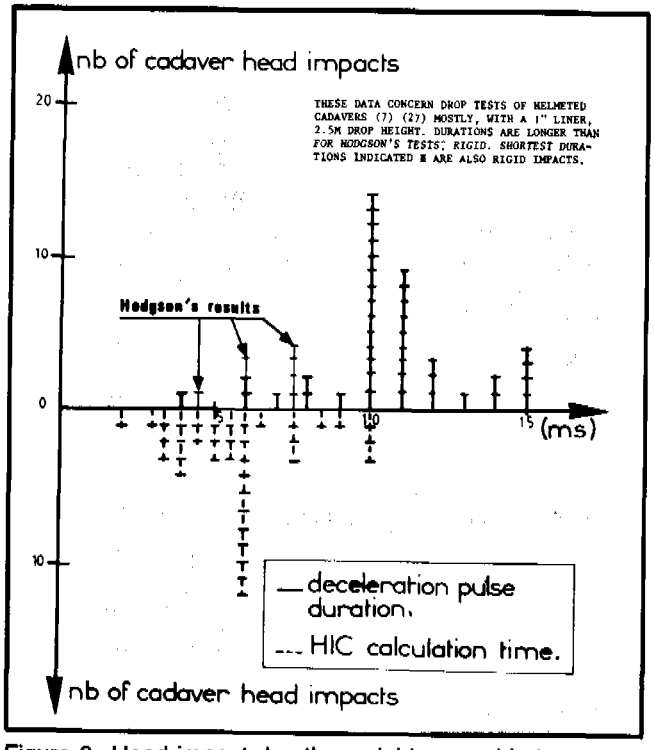

Figure 3. Head impact durations, rigid vs. padded.

in automobile collisions; Figure 3 illustrates the increase in head impact durations which occurs as soon as some padding is provided. The difference in impacted areas justifies thus the research of the tolerance level to head-impact which better fits the conditions of frontal collisions.

As regards the paths of loadings the head of a restrained occupant can be decelerated essentially by two ways: impact forces and neck forces, these latter being sufficient when no impact occurs. HIC computation cumulates these two phenomena without isolating the part of each one. This point will be also detailed later on. (Fig. 4).

As regards the dummy head response, the lowest lines of Table 3 show a much higher acceleration of VIP 50 head: S.I. on the average was 1150 for a 14 in. drop height of cavavers; VIP 50 head reaches 1680 for 10 in. drop height and 2040 for 15 in.

Finally, authors of (6) intended to use some fit between tolerance to skull fracture and tolerance to mild concussion. The previous remarks concerning the double path of loading of the head in frontal collisions and the pulse duration apply. The order of magnitude of HIC computation interval in (6) might be 3 ms.

At last, it may be concluded that HIC 1000 concerns

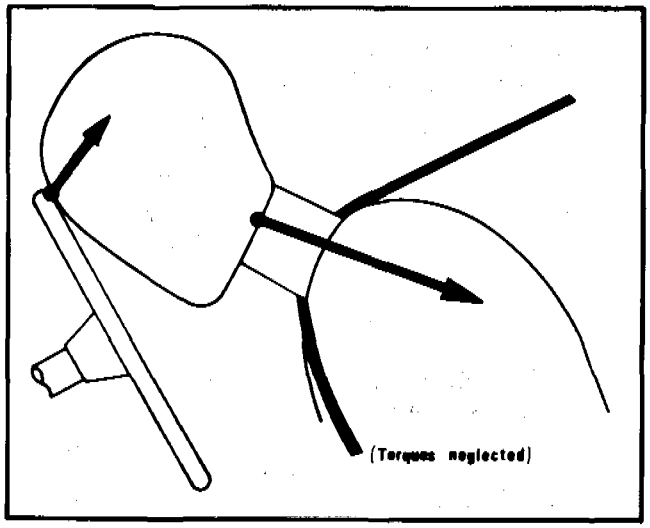

Figure 4. Impact force is only a part of forces stopping the head.

rigid impacts of short duration which relate to skull fracture but does not apply to the requirements of restrained occupants *in a car environment*.

BETTER ESTIMATE OF HEAD TOLERANCE TO DIRECT IMPACT

"Better estimate" means: with longer impact durations than the previous ones, against rigid unyielding surfaces. When fresh unembalmed cadavers are used, for investigating the closed brain injury risk, a vascular injection method was developed by Got et al. (7) which allows the detection of capillary ruptures due to impact. Series of drop tests were performed, head striking more or less padded surfaces, or wearing a helmet; Figure 3 recalls the durations.

Table 4. Brain injuries distribution among 133 scannerised patients.*

Contusion Alone:	42	(31%)
Contusion Alone or Associated:	72	(55%)
Oedema Alone:	28	(21%)
Oedema Alone or Associated with Sub-Arachnoidal Blood:	38	(28%)
Oedema Alone or Associated with All Types of Brain Injuries:	53	(40%)
Brain-Stem:	12 or 13	(10%)
Extra-Dural Hematoma Alone:	5	(4%)
Extra-Dural Hematoma Alone or Associated:	15	(11%)
Sub-Dural Hematoma Alone:	5	(4%)
Sub-Dural Hematoma Alone or Associated:	13	(10%)

*Mostly traffic victims.
This chart could be obtained in the framework of a research contract with the European Economic Community.

Simultaneously, a method for computing the linear and angular accelerations at the center of gravity of the head, by means of 9 accelerometers, was implemented. When the injection method is already described (7) and used by other teams, it was not the case as regards the computation of acceleration. Therefore, some details are presented here.

A complete set of acceleration measurements is achieved on the skull periphery in order to obtain by computerization the following data:

—Every kinematic feature of the head movement and, particularly, angular velocities and accelerations in terms of time.
—The resultant linear acceleration at the head center of gravity and the usual parameters calculated by means of this function (γ max, γ 3 ms, S.I., HIC).

A method using accelerometers is implemented with a so-called 3-3-3 configuration, as described by Alem (28). For improving its accuracy, the distance between transducers has to be as large as possible. Tests were performed in order to evaluate the robustness of the whole procedure. Some parameters appeared of secondary importance; they are:

—Using a computation process with simple or double precision,
—Filtering of analog data, as far as HIC is concerned, with 600-1000 Hz range.

On the contrary, the choice of the integration method, the precision on the locations and the orientations of the transducers, the number of channels appeared of primary importance. These findings lead us to improve the methodology; as examples:

—A RUNGE-KUTTA integration method with a constant integration step was tested and eliminated;
—A photographic method for measuring the angles of the accelerometers in the anatomic reference frame was implemented (rigid metallic rods replace the transducers just before the test, when photographs are made).
—Due to the number of channels available, the computation of the accelerations can be made according to several ways. So, one can check that results yielded are similar. Besides, a graphic display of the computed head kinematics is obtained; therefore, a comparison with the films is possible.

This method could not be systematically used in (7) but it was the case of (27), a more recent paper of the same team. This explains the slightly different values which can be found for some same subjects, when comparing (7) and (27), this latter paper displays more data points.

HIC computation interval was usually between 3 and 7 ms, i.e., closer to automotive needs.

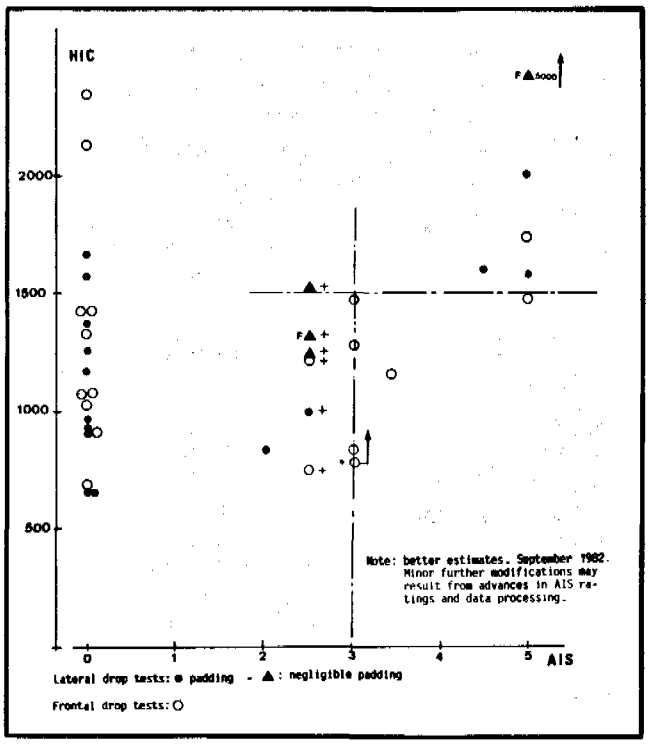

Figure 5. Relationship between HIC/AIS (the whole HIC value due to impact). Drop tests, mainly from (7) and (27), including reviews.

(★) HIC questionable. 8 accelerations only. Probably higher (1200 ?)
(+) AIS 2.5, mean AIS 2 or 3. Better estimate impossible.
(F) Skull fracture

So, authors in (7) were enabled to claim for a *threshold* of HIC 1500 for the appearance of AIS > 3 level brain injuries when skull is impacted and they wrote: "with regard to pure frontal impact without fractures, it would seem that an acceleration pulse linked to an HIC exceeding 1500 could be supported by the head of a living person (. . .) without severe injury in the majority of cases."

Figure 5 displays a summary of the experimental results which support this conclusion. Figure 6 is an attempt to present them in terms of probability of occurrence of injuries, the severities of which reach a given level. Figures 5 and 6 take into account the human subjects of (27).

In (7), the discussion of these results was fairly deep: some of the points commented upon were:

—the detection of injuries:
When oedema type injuries cannot be detected, one may observe that the frequency of oedema *alone* is low among brain injuries (21%—Table 4).
—the compatibility with results of the other teams using vascular injection (8) (11), which was checked,
—the comparison with dummy tests, that gives different results according to the test conditions,
—the comparison of the "cadaver tolerance" to that of a living person (28),
—the scatter of individual tolerances,
—the difference between the threshold at which injury appear and a "tolerance level", which is necessarily higher according to the authors; as a matter of fact, authors assumed like L. M. Patrick (12) that the tolerance level corresponds to 50% of the population considered undergoing an AIS $\geq$ 3, when this population is submitted to the assaults corresponding to the tolerance level.

Besides, it was noted that facial impacts occurred with lower acceleration levels under conditions of impact for which simulation by the rigid Part 572 head is unsatisfactory. This problem remains unsolved; however, the more the impact force is distributed on a larger area, the closer to the skull tolerance is the facial tolerance (1), in terms of applied force.

Discussions and Conclusions of (27) in addition mentioned that, among the considered parameters for analysing the results of the sample of cadaver drop tests, i.e., γ max, γ 3ms, the maxima of angular acceleration and velocities, HIC gave the best explanation of the results in terms of injuries.

Discussion about the most validated criterion and the most sound tolerance level are not terminated today in the cases of pure skull impacts. However, even if HIC 1500 were not yet evident, the case of the restrained occupant has to be considered now in order to examine the differences between a direct head impact and a frontal collision, when both deliver a HIC 1500 value.

CASE OF RESTRAINED OCCUPANT

Let us consider a car driver and a front passenger, submitted to the same frontal collision. Figure 7 shows the corresponding head resultant accelerations in a typical case, when two Part 572 dummies are used.

Of course, if human beings were considered, instead of dummies, the rationale would be identical. The head of the driver underwent two impacts, one against the rim and the second against the hub of the steering-wheel. From the beginning of the collision to the head impact, γ R for driver and passenger are similar. The increase of the driver head severity index with the time, by a continuous computation of $\int \gamma^{2.5} dt$, is also drawn on the Figure 7.

The first impact is accompanied with a small increase of the S.I.; the second one by a noticeable one, which lies around 1000 S.I. units (Δ_2(SI) on Fig. 7). This increase is not entirely due to the impact, as explained below. What is the corresponding severity of such an impact? During the head contact, two sets of forces are acting simultaneously, i.e., impact forces and neck restraint forces. (Fig. 4).

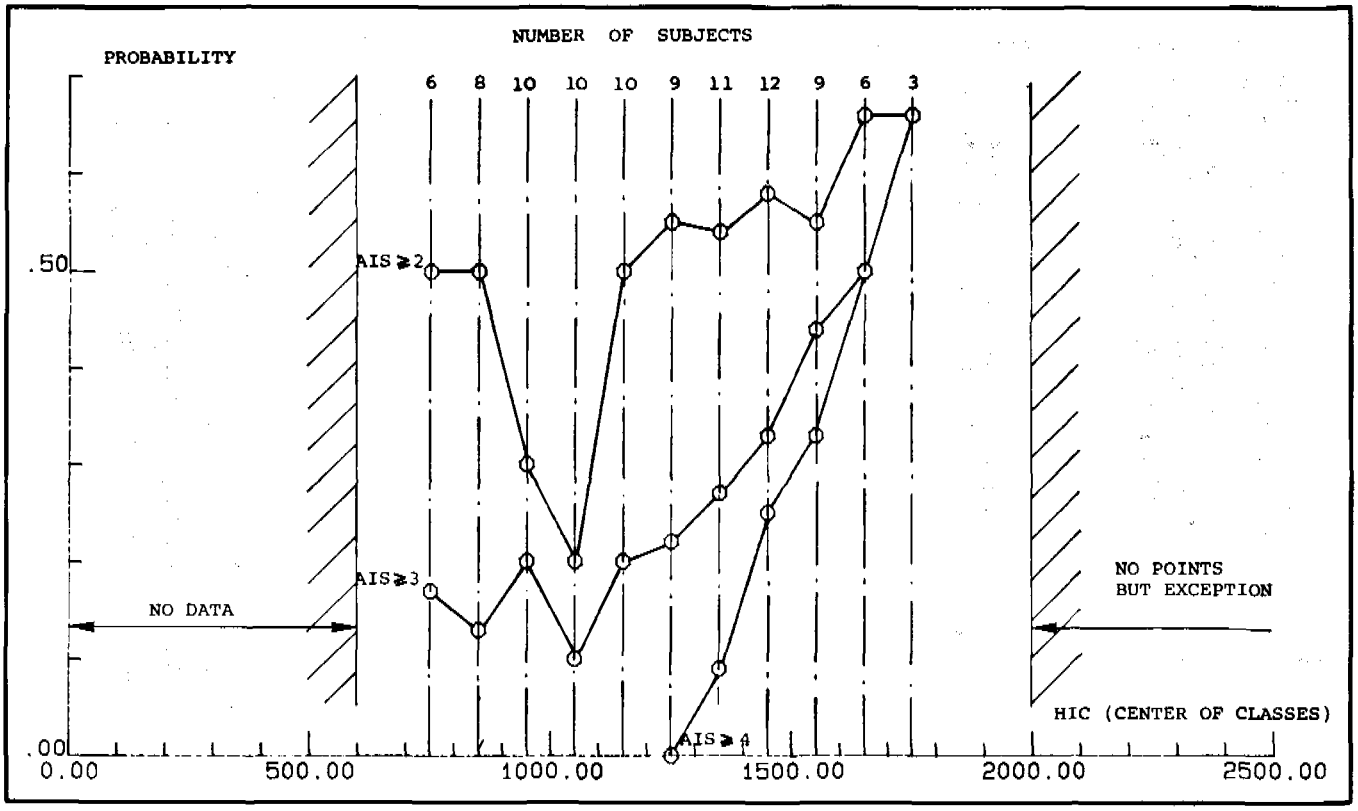

Figure 6. Direct head impacts · probability of exceeding a given A.I.S. level versus HIC value ·
Note: Each plotted point at HIC = X represents the tests with HIC included between (X−150) and (X +)

Without impact, the head would have sustained here more than 60 g's, according to the passenger resultant on the Figure 7.

With impact, a peak up to 170 g is reached, but only a part of this deceleration is due to the impact. A geometrical addition of the forces is necessary at each instant. The severity index (Gadd, 1) associated to the impact alone, is:

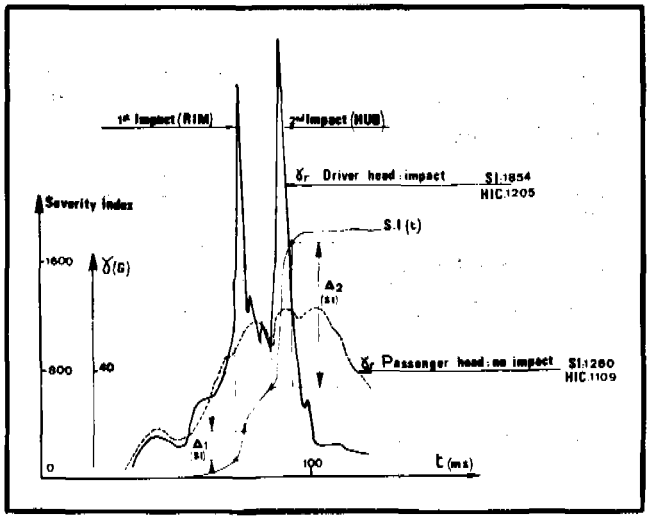

Figure 7. Typical head resultant acceleration: frontal collision—restrained dummy.

$$\int \left\| \vec{\gamma}_R - \vec{\gamma}_F \right\|^{2,5} dt$$

Returning to the example on Figure 3, during the duration of the impact, the increase of S.I. due to the neck forces only is about 220; the S.I. due to impact forces might be 650, e.g.; this latter value was estimated with the following assumptions: impact forces perpendicular to neck forces, triangular shape of impact forces pulse.

For illustrating the correctness of this argument and for confirming the order of magnitude of much evaluations, a mathematical model was used. It is a 2 D and 10 degrees of liberty model, called PRAKIMOD. It was already described at the 8th E.S.V. Conference (34).

Here head on collisions were simulated. The occupant aimed at is a P572 dummy wearing an automatic 3-point seat belt, with a gliding buckle. The characteristics for the restraint are fairly good. All the data are as realistic as possible, according to available data from real cars. However, the speed variation of the simulated vehicle reached 65 kph, in order to get high HIC values; that differs from full-scale testing. It seems that mathematical modeling generally yields lower HIC than dummies. Besides the shortages of the mathematical simulation, such as a long and constant radius for the head trajectory, this may be due to the lack of a 3rd dimension and to the absence of any technological shortcomings which give acceleration discontinuities in dummy testing.

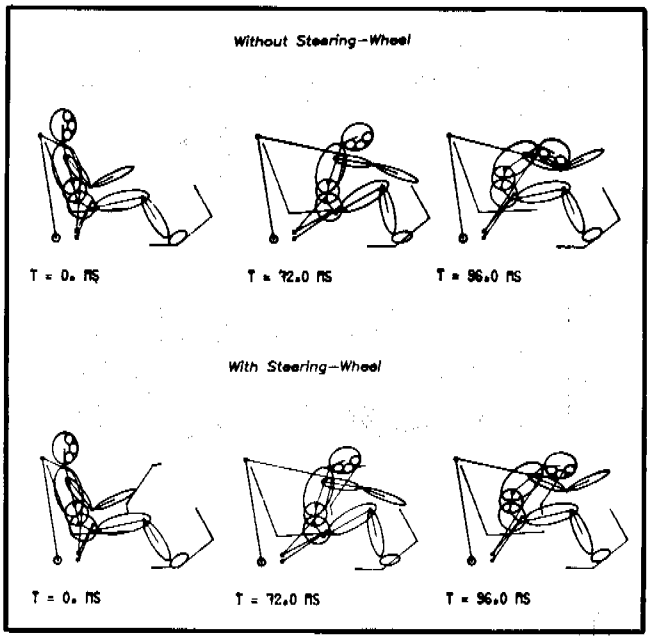

Figure 8. Compared kinematics for the two simulations.

tical, except a steering wheel which is simulated in only 1 out of these 2 cases. (Figure 8). Head accelerations,

As a reminder, mathematicals models are good tools for the study of isolated parameters, or for a dynamical analysis, i.e., forces and energies managements. However, one cannot rely upon the values yielded for any parameter without an in-depth validation. One of the greatest interests of mathematical modeling is enabling one to get values for parameters which cannot be measured in dummies; the present use enters this category.

The purpose here is not to find HIC values which were obtained with dummies, the goal is to get an order of magnitude for the phenomenon roughly evaluated above, related to the respective influences of the head impact and of the head restraint by the neck forces. Thus, 2 simulated runs were performed. Their conditions are iden-

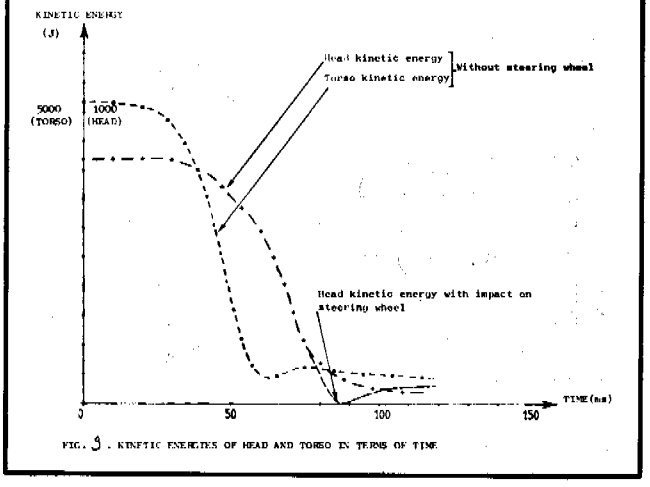

Figure 9. Kinetic engeries of head and torso in terms of time.

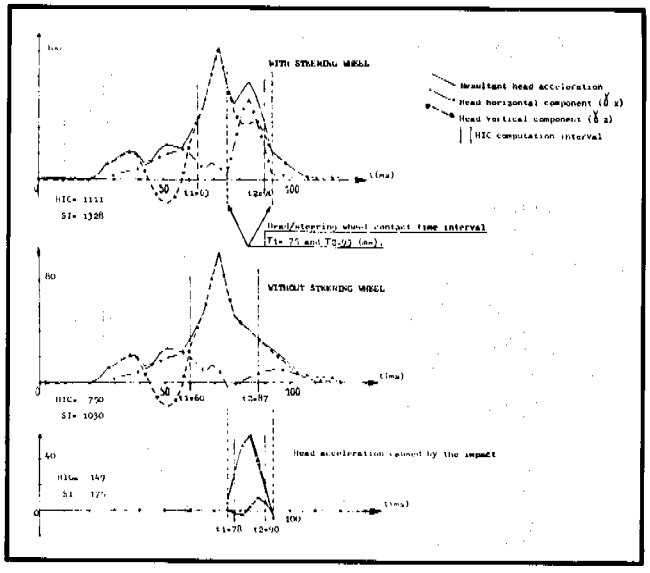

Figure 10. Mathematical Modeling: Comparison between the head accelerations of restrained occupants with and without the head impact. This figure brings in light the accelerations caused by the only head impact.

without steering wheel, are shown on Figure 10. The maximum acceleration reaches 104 g (t = 72 ms), a short time before the head impact; the acceleration level exceeded during 3 ms is 91. The components, when maximum occurs, are 9.9 g for γ x and 103.7 g for γ z, in an anatomical frame. This illustrates the role of the neck in the increase of the S.I.: the thoracic restraint induces a head restraint; corresponding forces have a direction roughly along the neck axis. Kinetic energy of the head decreases slowly (Figure 9); the centripetal acceleration, simultaneously, produces a strong increase of S.I. and HIC. According to this first mathematical run, S.I. is 1328 and HIC 1111; in the 2nd run, without steering wheel, the maximum head acceleration reaches 103 g (γ_x = 8.9 g; γ_z = 102.2 g) at the same time as previously (72 ms). The absence of hands-steering wheel contact forces explains the little differences of values. The important point is the decrease of S.I. and HIC values; S.I. falls from 1328 to 1030 and HIC from 1111 to 750.

For obtaining the effect relevant to the impact alone, the forces transmitted by the neck were eliminated in another computation. S.I. consequently falls to 175 and HIC to 149. (Fig. 10).

A summary of the previous results is as follows:

—The head/steering wheel impact, which is the only possible head injury causation according to real accidents, corresponds to a S.I. equal to 175, an HIC equal to 150 in this simulation. These very low values may be associated to the absence of hazard.

—The head restraint forces due to the neck correspond to S.I. 1030, HIC 750, from the 2nd simulation.

—Then the steering wheel is added (1st simulation), and therefore when impact forces and neck forces

are cumulated, S.I. increases to 1328 and HIC to 1111 for the whole pulse duration.

Mathematical modeling confirms that the HIC, when computed for a restrained occupant with the occurrence of a mild head impact, can reach high values without any correspondence with the severity of the blow, in terms of injuries. By the way, mathematical modeling showed also, by means of other runs, that a less efficient restraint could significantly diminish the HIC values.

Coming back to full-scale testing with dummies, the resultant head deceleration curve shown on Figure 3 is an example where 208-HIC value exceeds 1000 without exceeding 1500, and where recorded impacts are tolerable, even if the most severe head impact protection criteria are used. As far as the thorax restraints are used, high values of HIC can be recorded and can simultaneously correspond to mild impacts.

One may object that human tolerance under these particular loading conditions (i.e., impact occurring during a severe head movement) are not identical to the tolerance to isolated impacts. That is a challenge for research. However, today, experiments with cadavers, in particular, can be referred to.

EXPERIMENTS WITH RESTRAINED CADAVERS

From the 18th Stapp, many experiments were reported which deal with the *whole body restraint* (WBR) of fresh unembalmed cadavers: Schmidt (13)(18), Cromack (14), Patrick (15), Cesari (16)(22), Fayon (17), Walsh (19), Alem (21), Schimkat (24).

Tests where simultaneously a head injury detection was feasible on the cadaver by means of a vascular injection method, and where HIC computation was achieved have to be considered here. Besides, among these data, tests of belted occupants who sustained head impacts will be selected.

—Walsh (19) reports the case of the so-called subject CALMAN 2, who hits a steering-wheel. No face, brain and skull damage were found. HIC value 736 on a lateral triaxial accelerometer. He reported also in (20) other cases with head AIS 0, but low HIC values.

—Data from Alem, (21), as published in the proceedings of the 22nd Stapp Car Crash Conference, are not complete (although they exist in other reports.)

—Cesari did not publish HIC values associated to the injury data related to cadavers, except in particular cases. One HIC 2412 case associated to AIS 0 for the head for a driver is mentioned. His rationale was rather to relate measurements to the injuries of the real victims of the accidents that he reconstructed. The same author, from another series of reconstructions (23) reported one HIC 260 associated to a frontal scalp AIS 2, due to a steering-wheel radius, one HIC 634 associated to a nose fracture due to the steering-wheel spider.

This rises two head important problems:

—Let one consider 2 cases of AIS 3 of restrained occupants, due to impacts against two different surfaces; for example, a poorly padded hub and a fairly collapsible dashboard. The severity AIS 3 will be reached, e.g., at 40 kph in the first case and at 60 kph in the second one. The head accelerations induced by the restraint forces will be much higher in the second case, and eventually the HIC value will be higher too. Such phenomena may explain, up to a certain extent, some of the discrepancies between the results of different teams. Besides, using less padded cars in simulations or reconstructions may lead to lower HIC values at the same injury level. This points out the interest in the test conditions which use as much as possible the environmental conditions of actual cars, even if tolerances only are considered.

—The protection of the face is a particular and intricate problem for which neither the skull and brain protection criteria, nor the Part 572 rigid dummy faces are adapted. The use of a deformable face as described by Tarrière et al. (25) allows someone to estimate the risk of facial injury; a complementary criterion concerning the face would so be added to the HIC which is related to closed brain injuries.

The cooperation between the Institute of Orthopaedic Researches in Garches (France) and Peugeot/Renault Association made it possible to gather numerous related results; the corresponding runs were carried out in the framework of sundry researches and were mostly unpublished up to now. Among this data base, results were selected according to the following criteria:

—simulated frontal collision with a 3-point belt restraint

—head impact

—HIC value $\geq$ 1000. It was previously checked that in the sample, HIC $<$ 1000 did not contain noticeable head AIS values (superior to 2).

At present time, these piled up tests are not fully processed as regards computerization. The number of recorded acceleration channels is indicated in the Table 5 which summarizes the results, Figures 11 and 12 complete this Table; 3 HIC values are often given which are obtained from the accelerometers on right and left temples and on occipital bone respectively. It results in a better estimate of the HIC value at the center of gravity, that everyone can appreciate in a fourth column.

These high values of HIC are mainly due to the high severities of these collisions.

As a conclusion, in reported experiments, under the

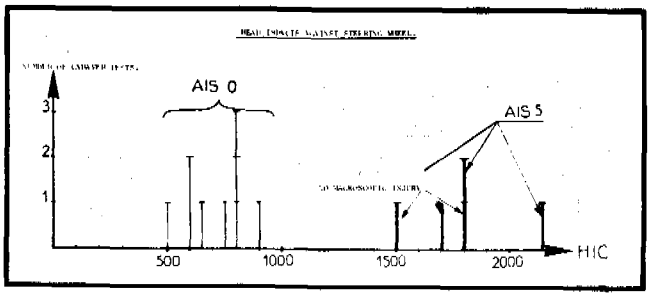

Figure 11. Frontal Collisions: Cadavers restrained by a 3-point belt 50 kph impact speed 65 kph drivers.

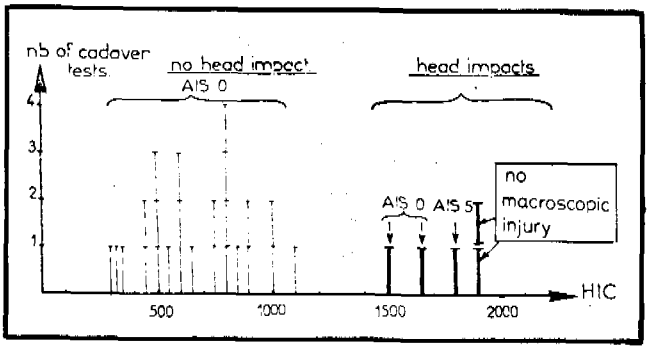

Figure 12. Frontal Collisions: Cadavers restrained by a 3-point belt 50 kph impact speed 65 kph—right front passengers.

conditions of a 3-point belt restraint in frontal impact, HIC values up to 1500 (and slightly more) are recorded when a head impact occurs, without occurrence of any AIS > 2 head and neck injuries.

EXPERIMENTS WITH RESTRAINED DUMMIES

These experiments are useful as far as an accurate injury reference is available, which can be associated to the results of measurements performed on the dummy. This only condition is not sufficient. The remark related to padded and unpadded head impacts inside a car has also to be kept in mind. Some data are related to series of reconstructions, some others are related to individual accident cases. In this later case, particularly, one has to check the similarities between the impacts sustained by the dummies and by the cadavers or the real victims. Otherwise the conclusions are doubtful. However, the dummy can mitigate the impact severity, relatively to human beings, in some cases. This rule is not an absolute one.

Patrick (12) released the results of a combined program of accident investigation staged collisions and simulated collisions involving 3-point harnessed occupants in frontal collisions.

With a Sierra 1050 dummy and velocities up to 40 mph, the equation for the HIC was:

$$HIC = 92.8\ BEV - 1789$$

(BEV = Barrier Equivalent Velocity)

giving 1000 at 30 mph and 3130 at 53 mph. But there were no AIS 3 head injuries in his sample: head injuries

Table 5. Frontal collisions with 3 pt belted cadavers—cases of head impacts.

Test #	Test Type	Impact speed kph	Stopping distance mm	Place	γ** Number	HIC left temple	HIC right temple	HIC occipital bone	HIC minimum estimated	Skull AIS	Brain AIS	Type impact observations
10	sled + car body	64	660	D	5	2011	3050	—	1800	0	NI	Forehead/hub
126/1	sled + car body	65	1000	D	9	6816	1791	5952	1800	0	4	Forehead/hub
2	sled + car body	50	480	D	5	> *1719	> *3314		1700	6	NI	hub + rim skull basis circ. fract.
115-1	car	50	900	D	6	—	1623	2365	1500	0	NI	forehead/hub + rim
13	sled + car body	62	540	P	6	2340	3490		2100	6	NI	skull basis circ. fracture
60-2	car/cart† oblique	60		P	9	2240	3460	2160	1900	2	NI	forehead/rim
8	sled + car body	65	660	P	5	2100	2310	—	1900	0	NI	top of head/ dashboard
117-4	sled + car body	50	505	rear	9	1945	1830	2640	1800	0	5	forehead/top of front seat; neck influence
124-2	sled + car body	66.5	1020	P	9	1790	1990	2765	1650	0	0	
126-2	sled + car body	65	1000	P	8	—	1585	2525	1500	0	0	

No Injuries Recorded Below 1500

Abbreviations and Notes
N.I. = No vascular injection, but no gross macroscopic injury in the mentioned cases.
* = 2 components only.
† = Each vehicle.
**i.e. = Number of correct acceleration measurements, after the test.

were separated from facial injuries; for these latter, there was a fractured mandible rated AIS 3.

"It should be stressed that 3130 is a tolerable value", was his conclusion, since he locates the tolerance at AIS 3 level.

Of the already mentioned Cesari's paper in 23rd Stapp Car Crash Conference (22) which deals with accident reconstructions, the following table, where the AIS 0 cases were suppressed, can be excepted.

Each line corresponds to one reconstruction.

Head AIS real victim	Height real victim	H.I.C. dummy
2	1.57	293
3	1.85	450
2	1.63	2777
1	1.65	316

Only the case AIS 3 will be discussed here, because of the interest of this level of severity. The vehicle deformations "appeared slightly less important than those of the actual accident"; some differences in the heights of the victim and of the dummy can be also noted. These facts are not a criticism; they emphasize the paramount importance of every detail to achieve an accurate reproduction. Belt slack, driver's position, steering wheel orientation and so on. Consequently, comparisons of *similar samples* of real accidents and of simulations may be useful to get some ascertainty. This case needed to be confirmed (by the way, the cadaver HIC in a similar reconstruction previously noted was 2412, associated to AIS 0).

KOB reconstructions (23), as regards frontal collisions, display the results of 2 accidents which were reconstructed three times with dummy and with cadavers. Unfortunately, the severities of the real accidents are rather low and no head AIS > 1 can be claimed.

Reported experiments with restrained dummies do not display sufficient data to suggest a modification of HIC 1500 statement.

OTHER TYPES OF SEVERE HEAD ACCELERATIONS IN TRAFFIC ACCIDENTS

They are mainly due to lateral collisions and to accidents involving pedestrians. In lateral collisions, one can distinguish 2 types of circumstances. On one hand, when the head strikes a part of the side wall and is mainly decelerated by this impact; on the other hand, when the head undergoes no impact, what gives the whole loading to the neck.

In case of impact, and with a sufficient pressure distribution, the tolerance level previously applies and an HIC 1500 is reasonable; the use of a correct lateral impact dummy prevents from any transposition problem. When no impact occurs, a neck tolerance problem may arise. Further research, related to this topic, is needed; it will involve firstly accident data before any other development of transducers and dummies.

As regards pedestrians, they are for the most part, hit on their side, when crossing a road. Their head strikes generally a part of the vehicle, which can be the bonnet, or the windscreen surroundings. The head impact is a lateral one, where no problem with the neck arises, as it was told previously for a class of lateral impacts; the situations of pedestrians and of side collisions victims are comparable. As regards pedestrians, the violence of their head impacts are conditioned by the technology of the dummy; with a suitable dummy, like a modified lateral impact dummy, the tolerance level previously defined applies, and therefore like for lateral impacts, the value of 1500 not to be exceeded for HIC is reasonable.

DISCUSSION

1. HIC was often criticized as regards its correlation with injuries. One of the most comprehensive study was made by Newman (3). He found the absence of correlation between numerous HIC values and corresponding AIS levels.

   However, the reported cases encompassed a lot of different surrogates and many types of accidents; one can find simultaneously tests using obsolete dummies, cadavers and mathematical modeling. Correspondences may exist, if they do, between one type of surrogate which undergoes one given type of accident, and the associated AIS value, given by one method.

   Here a HIC/AIS correlation was never claimed; only a threshold in the cases of a very large majority of impacts was proposed.
2. In frontal collisions, some prefer HIC 1000 to HIC 1500 because their opinion is that HIC 1000 offers a better protection. If the limits concerning body loadings could be managed independently, it could be right. As a matter of fact, the results of measurements made on the sundry body segments of a dummy are not independent; therefore, the *overall* protection offered by all the criteria gathered has to be considered firstly.

   Without considering the dummy, many possibilities exist which decrease the HIC value in one given test while lowering the overall safety level in the majority of collision circumstances: concentrating the restraint forces on the upper part of the thorax, making these forces as high as tolerated or, on the contrary, defining a very weak restraint which prevents the head rotation; one can also increase the trend to submarine and the severity of knee impacts. It emphasizes the interest of a complete and homogeneous set of injury criteria.

   Besides, the 2 above mentioned kinds of methods for diminishing the HIC work properly, except as regards safety. More, if a failure of the restraint occurs,

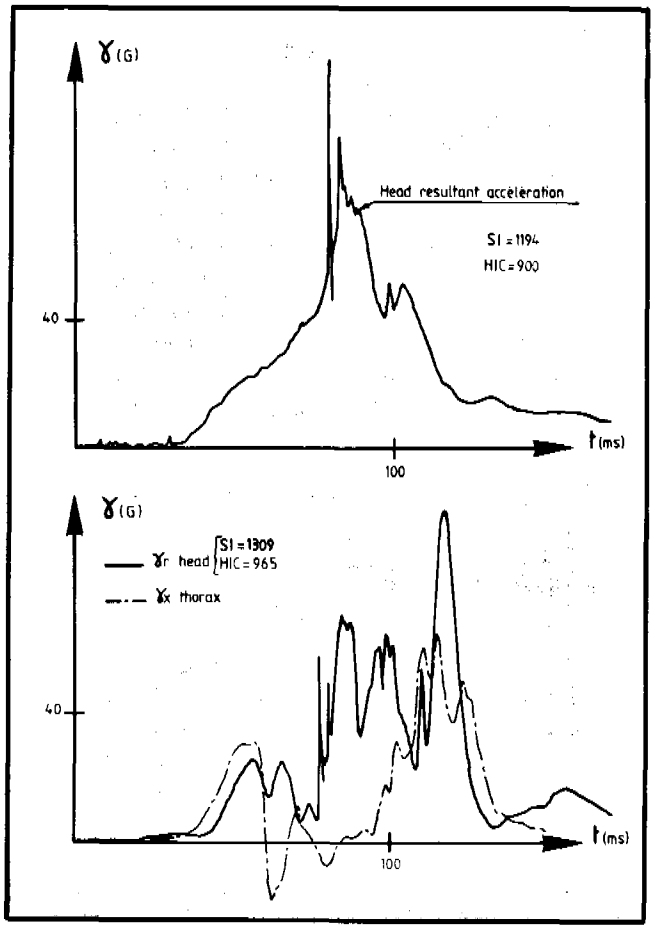

Figure 13. Example of low HIC with incorrect restraints—See text.

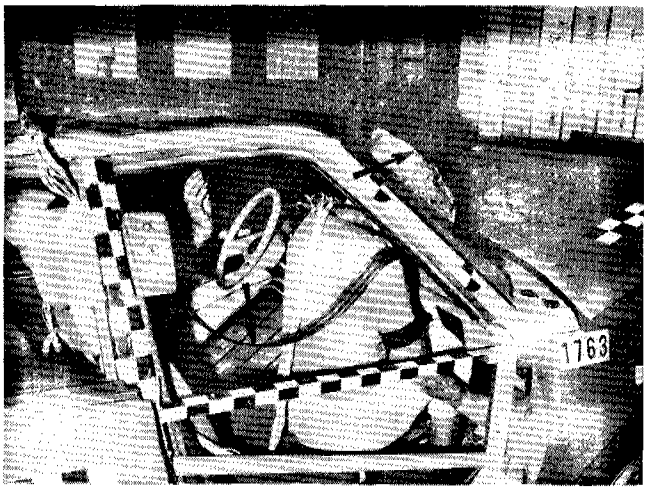

Figure 13 bis. Low HICd with failure of the experimental prototype belt. (Corresponds to Figure 13, above).

such as a webbing breakage, HIC can remain below 1000. Figure 13 shows the results of 2 tests under the same conditions as in Figure 7. Above, the restraint was concentrated in the upper part of the thorax by raising the B-pillar anchorage point and allowing more pelvis forward displacement. It resulted in a sufficiently low HIC; however, the webbing acted on the neck during the collision. Below is another case: webbing broke during the collision; due to the lack of head rotation, HIC remained at a low level.

3. A protection criterion that matches the tolerance level of the weaker population does not afford the maximum overall protection benefit for the whole population at risk. Further work is needed in that field; for example, J.A. Searle (26) proposed mathematically an optimum between 50% and 80% of the median tolerance, for another similar problem.
4. In all that precedes, the HIC computation which was considered, as a matter of fact, was like in US Standard 208. This point is emphasized because several ways for computing HIC exist. However, the arguments of this paper show that only the impact phase of the deceleration pulse is likely to produce injuries. Therefore, an HIC computation limited to the contact phase between the head and a part of the vehicle interior is sound. It raises some technical problems which are in process of solution.
5. Recent papers (31)(32) claimed for a correspondence between HIC 1000 and AIS 3. Their rationale is the following: accident analyses (33) allow characteristics recorded in a given type of frontal collisions to be related to AIS values.

   In parallel, the characteristics associated with the same particular type of accident (AC) can be translated in terms of "dummy loadings" and hence give a basis for injury criteria. These DL (dummy loadings) are deduced from the characteristics of accidents by a simple two-dimensional mathematical model (10 degrees of freedom), which is claimed to have been validated by full size dummy tests. The reliability of the results with regard to HIC may be contested.

   In accident data, there were 318 restraint occupant of all sizes with 178 having an AIS between 1 and 6 for the head, of which 115 were AIS 1. There remains 6 AIS 3, 9 AIS 4, 3 AIS 5 in relation to the "AC" or "EAC" (equivalent accident characteristics) which are used to define the dummy criteria.

   Even if all the characteristics of accidents having an influence were accurately recorded, the statistical basis is insufficient.

   Even if the mathematical model is valid for a given accident or several accidents, the HIC is a function of a resultant acceleration which can only be poorly simulated. In effect:

   —the model is two-dimensional;
   —the mathematical simulation of the neck is not sufficiently accurate in models (number or articulations, reaction torque of the joints at the limit of the range of motions, etc. . . .).
   —the simulation of impacts can only be made with a perfect knowledge of the dynamic laws of load-de-

flection of impacted surfaces, and this in the direction of movement.

—effects due to intrusion, and steering wheel displacements are not properly simulated.

By the way, it was noted here previously that mathematical modeling seemed to yield lower HIC values than full-scale testing.

These inexactitudes lead to errors even in supposing that, at the top of the thorax, the impact of acceleration is perfectly simulated. It will be remembered furthermore that a variation of 17.6% of acceleration figure modifies by 50% the HIC for the same time period.

This recent study, therefore, does not justify the HIC of 1000.

CONCLUSIONS

—When no head impact occurs in present frontal collisions, there is no need of a particular head protection criterion.

—HIC 1000 is matched to rigid impacts of short duration onto the head with an unrestrained body, and it is not matched to car environment.

—HIC 1500 is a sufficient estimate of head tolerance to direct impact in frontal and lateral directions.

—In frontal collisions, when occupants are restrained, HIC 1500 corresponds to a less severe head impact + injury risk when compared to an unrestrained occupant who receives the same HIC value.

—Full-scale experiments with cadavers and dummies support the HIC 1500 statement.

—A different approach is suggested for facial protection.

—Computation of HIC during head contact period is desirable.

ACKNOWLEDGEMENTS

Accidentological section of this paper could be issued thanks to the work of C. Thomas and G. Faverjon.

This study uses results obtained by carrying out research contracts with the French Administration (A.T.P.) and, more recently, with E.E.C. This text commits them in no way.

REFERENCES

1. C. W. Gadd, "Use of a Weighted Impulse Criterion for Estimating Injury Hazard", in 10th Stapp Car Crash Conference, 1966, SAE.
2. J. Versace, "A Review of the Severity Index", in 15th Stapp Car Crash Conference, 1971, SAE.
3. J. A. Newman, "Head Injury Criteria in Automotive Crash Testing", in 24th Stapp Car Crash Conference, 1980, SAE.
4. A. Eiband, "Human Tolerance to Rapidly Applied Accelerations: a Summary of the Literature", NASA Memorandum 5-19-59 E, June 1959.
5. C. W. Gadd, "Tolerable Severity Index in Whole-Head, non-Mechanical Impact", in 15th Stapp Car Crash Conference, 1971, SAE.
6. V. R. Hodgson, L. M. Thomas, "Comparison of Head Acceleration Injury Indices in Cadaver Skull Fractures", in 15th Stapp Car Crash Conference, 1981, SAE.
7. C. Got et al., "Results of Experimental Head Impacts on Cadavers", in 22nd Stapp Car Crash Conference, 1978, SAE.
8. A. M. Nahum, R. W. Smith, "An Experimental Model for Closed Head Impact Injury", Proceedings of 20th Stapp Car Crash Conference, SAE paper 760 825, 1976, SAE.
9. A. M. Nahum, R. W. Smith, C. C. Ward, "Intracranial Pressure Dynamics During Head Impact", Proceedings of 21st Stapp Car Crash Conference, SAE, 1977.
10. R. L. Stalnaker, J. W. Melvin, G. S. Nusholtz, N. M. Alem, J. B. Benson, "Head Impact Response", Proceedings of 21st Stapp Car Crash Conference, SAE, 1977.
11. L. M. Patrick, N. Bohlin, A. Andersson, "Three-Point Harness Accident and Laboratory Data Comparison", S.A.E. paper 741 181, 18th Stapp Car Crash Conference, SAE, 1974.
12. G. Schmidt, D. Kallieris, J. Barz, R. Mattern, "Results of 49 Cadaver Tests Simulating Frontal Collision of Front Seat Passengers", 18th Stapp Car Crash Conference, SAE, 1974.
13. J. R. Cromack, H. H. Ziperman, "Three-Point-Belt Induced Injuries: A Comparison Between Laboratory Surrogates and Real World Accident Victims", 19th Stapp Car Crash Conference, SAE, 1975.
14. L. M. Patrick, R. S. Levine, "Injury to Unembalmed Belted Cadavers in Simulated Collisions", 19th Stapp Car Crash Conference, SAE, 1975.
15. D. Cesari, M. Ramet, "Comparison Between In-the-Field Accidents and Reconstructed Accidents with Dummies and with Cadavers", 19th Stapp Car Crash Conference, SAE, 1975.
16. A. Fayon, C. Tarrière, G. Walfisch, C. Got, A. Patel, "Thorax of 3-Pt Belt Wearers During a Crash (Experiments with Cadavers), 19th Stapp Car Crash Conference, SAE, 1975.
17. G. Schmidt, D. Kallieris, J. Barz, R. Mattern, J. Klaiber, "Neck and Thorax Tolerance Levels of Belt-Protected Occupants in Head-on Collisions", 19th Stapp Car Crash Conference, SAE, 1975.
18. M. J. Walsh, D. J. Romeo, "Results of Cadaver and Anthropomorphic Dummy Tests in Identical Crash

Situations", 20th Stapp Car Crash Conference, SAE, 1976.
19. M. J. Walsh, B. J. Kelleher, "Evaluation of Air Cushion and Belt Restraint Systems in Identical Crash Situations Using Dummies and Cadavers", 22nd Stapp Car Crash Conference, SAE, 1978.
20. N. M. Alem, B. M. Bowman, J. W. Melvin, J. B. Benson, "Whole-Body Human Surrogate Response to Three-Point Harness Restraint", 22nd Stapp Car Crash Conference, SAE, 1978.
21. D. Cesari, M. Ramet, "Evaluation of Human Tolerance in Frontal Impacts", 23rd Stapp Car Crash Conference, SAE, 1979.
22. D. Cesari, in a"Unfall und Sicherheitsforschung Strassenverkehr", Heft 34, 1982, p. 24, edited by "Bundesanstalt für Strassenwesen", Bereich Unfallforschung, Köln.
23. H. Schmikat, R. Weissner, G. Schmidt, "A Comparison Between Volkswagen Automatic Restraint and 3-pt Automatic Belt on the Basis of Dummy and Cadaver Tests", 18th Stapp Car Crash Conference, 1974, SAE.
24. C. Tarrière, Y. C. Leung, A. Fayon, C. Got, A. Patel, P. Banzet, "Field Facial Injuries and Study of their Simulation With Dummy", 25th Stapp Car Crash Conference, 1981, SAE.
25. J. A. Searle, J. Bethell, G. Baggaley, "The Variation of Human Tolerance to Impact and Its Effect on the Design and Testing of Automotive Impact Performance," 22nd Stapp Car Crash Conference, 1978, SAE.
26. C. Tarrière, G. Walfisch, A. Fayon, C. Got, F. Guillon, A. Patel, J. Hureau, "Acceleration Jerk and Neck-Flection Angle: Their Respective Influences on the Occjurrence of Brain Injury", Agard Conference, Köln, 1982.
27. N. M. Alem et al., "Whole body response research program", Final report HSRI, Apr. 1978—Report N° UM-HSRI, 77-39.
28. J. Brinn, S. E. Staffeld, "Evaluation of Impact Test Accelerations;" A Damage Index For the Head and Torso", 14th Stapp Car Crash Conference, SAE paper 700902.
29. SAE J 885, Apr. 1980.
30. K. Langwieder et al., "Comparison of Passenger Injuries on Frontal Car Collisions with Dummy Ratings in Equivalent Simulations," 23rd Stapp Car Crash Conference.
31. F. Kramer, H. Appel et al., "Evaluation of Protection Criteria by Combining Results of Computer and Experimental Simulations with Results of Accident Investigation", 5th Conference IRCOBI, 1980, Secrétariat IRCOBI, 109 Av, S, Allende, 69500—Bron, France.
32. HUK Data.
33. D. Lestrelin et al., "PRAKIMOD": Mathematical Simulation, 8th International Technical Conference on E.S.V., Wolfsburg, 1980.

Possible Positions and Postures of Unrestrained Front-Seat Children at Instant of Collision

F. MONTALVO, R. W. BRYANT and H. J. MERTZ
General Motors Corporation

3680

ABSTRACT

The development of any front-seat passenger inflatable restraint system should consider the added deployment forces applied to occupants who may be close to the instrument panel at the time of deployment. A major factor influencing occupant position and posture is the effect of preimpact braking which often occurs prior to the collision. Most susceptible to preimpact braking are small, unrestrained children who can move off the front edge of the seat during hard braking and be near or against the instrument panel in a variety of different positions and postures at the instant of collision. Based on an analysis of hard-braking tests conducted with anesthetized baboons and child dummies, 13 positions are identified as being representative of the expected child positions. An estimate is given that, of the 149 small children (infants through four years old) expected to be unrestrained front-seat occupants in collisions of sufficient severity to deploy an inflatable restraint system per million car-years of exposure, 51 of them will be in one of these 13 positions near the instrument panel at the instant of collision.

INTRODUCTION

Animal studies (1, 2, and 3) have shown that there is a potential for serious head, neck, thorax, and abdomen injuries when animals are placed close to the instrument panel and a passenger inflatable restraint cushion is deployed. In order to assess the performance of various inflatable restraint system concepts relative to these potential injury modes, knowledge of expected child positions and postures near the instrument panel at the instant of collision is needed. This paper describes how estimates

of reasonable child positions and postures were determined, as well as a procedure that was used to estimate the number of children who would be expected to be in each of these positions at the time of deployment of an inflatable restraint system per million car-years of exposure.

CHILD POSITIONS AND POSTURES NEAR INSTRUMENT PANEL

Child positions and postures near the instrument panel at the instant of a collision are dependent on the riding positions and postures of children and the degree of preimpact braking that occurs prior to the collision event. Estimates of child riding positions and postures were obtained from a report prepared by Opinion Research Corporation (ORC) under a contract with the National Highway Traffic Safety Administration (NHTSA) (4). The report summarizes the observations that were made of child occupants during a survey of cars stopped for traffic lights in 19 metropolitan areas from July to December 1979. The data collected for each child occupant included: age, sex, seated position, posture (sitting, standing, etc.), occupant location (on seat or floor), orientation of the occupant's knees (facing forward, biased left or right), and usage of restraints. Table 1 summarizes the results of the survey for unrestrained, front-seat children estimated to be one to four years old. Described in the table are the child's posture; whether the child was on the seat or on the lap of another front-seat occupant; the orientation of the child's knees; and support of the child's back. The positions of the child's arms were assumed. The number of children observed in each position is given. The table is ordered by frequency of observed child position with the more-frequent position listed first. Each child position is assigned a line number for ease of reference. Table 2 is a similar summary for unrestrained, front-seat children estimated to be less than one year old. A total of 1604 unrestrained, front-seat children, ranging in age from infant to four years old, were observed. Thirteen hundred were one to four years old and 304 were less than one year old. Fifty-one different positions were observed for the older children, and 31 positions were noted for the younger children.

To aid in determining the possible positions and postures that children in these various riding positions could be forced to assume as a result of preimpact braking, a series of hard-braking tests was conducted using anesthetized baboons and a child dummy that were representative in stature and weight of a three-year-old child.

Table 1. Front-seat ride positions of one to four-year-old children based on ORC survey (4)

Line	ORC Cases	Posture	Child is on	Location of Child on Seat/Floor	Knee Direction O'Clock	Back is to	Arm Position
1	331	Sitting	Seat	Rearward	12:00	Seat	Down
2	109	Sitting	Seat	Forward	12:00	Nothing	Up, hands on sill
3	106	Standing	Seat	Forward	12:00	Nothing	Up, hands on I/P
4	95	Standing	Seat	Rearward	12:00	Seat	Down
5	89	Sitting	Seat	Forward	1:30	Nothing	Up, hands on I/P
6	87	Sitting	Lap	Rearward	12:00	Person	Down
7	80	Standing	Seat	Mid	3:00	Nothing	Up, hands on sill
8	55	Sitting	Lap	Rearward	10:00	Seat	Down
9	51	Kneeling	Seat	Mid	3:00	Nothing	Up, hands on sill
10	30	Standing	Seat	Rearward	10:30	Seat	Down
11	27	Sitting	Seat	Rearward	10:30	Seat	Down
12	27	Sitting	Lap	Forward	12:00	Nothing	Up, hands on I/P
13	27	Sitting	Lap	Forward	1:30	Nothing	Up, hands on sill
14	24	Sitting	Seat	Mid	9:00	Door	Down
15	17	Standing	Floor	Rearward	12:00	Nothing	Up, hands on sill
16	16	Standing	Lap	Mid	6:00	Nothing	Down
17	14	Kneeling	Lap	Mid	3:00	Nothing	Up, hands on sill
18	12	Kneeling	Seat	Forward	12:00	Nothing	Up, hands on I/P
19	11	Standing	Lap	Rearward	1:30	Person	Down
20	10	Lying	Seat	Rearward	Down	Nothing	Up
21	9	Lying	Lap	Mid	Up	Person	Down
22	8	Kneeling	Lap	Mid	1:30	Person	Up, hands on sill
23	7	Standing	Floor	Rearward	3:00	Nothing	Up, hands on sill
24	6	Kneeling	Seat	Rearward	12:00	Seat	Down
25	5	Sitting	Floor	Rearward	3:00	Nothing	Down
26	5	Lying	Seat	Rearward	12:00	Seat	Down
27	4	Lying	Lap	Mid	Down	Nothing	Down
28	3	Sitting	Lap	Mid	9:00	Door	Down
29	3	Standing	Floor	Rearward	12:00	Seat	Down
30	3	Standing	Lap	Forward	12:00	Nothing	Down
31	3	Kneeling	Seat	Mid	9:00	Door	Down
32	3	Lying	Seat	Rearward	Up	Seat	Down
33	2	Sitting (Between adult's legs)	Seat	Mid	12:00	Person	Down
34	2	Sitting	Seat	Mid	10:30	Person	Down
35	2	Standing (Torso twisted toward driver)	Seat	Rearward	12:00	Door	Down
36	2	Standing	Seat	Rearward	9:00	Door	Down
37	1	Sitting (Torso twisted toward driver)	Seat	Rearward	12:00	Door	Down
38	1	Sitting	Floor	Rearward	12:00	Seat	Down
39	1	Sitting	Floor	Forward	12:00	Nothing	Down
40	1	Sitting	Floor	Mid	9:00	Door	Down
41	1	Sitting (Between adult's legs)	Floor	Rearward	10:30	Person	Down
42	1	Sitting (Adult sideways on seat facing outside window, legs folded)	Lap	Mid	12:00	Seat	Down
43	1	Standing (Between adult's legs)	Seat	Mid	12:00	Person	Down
44	1	Standing	Seat	Rearward	10:30	Person	Down
45	1	Standing	Lap	Rearward	12:00	Person	Down
46	1	Kneeling	Seat	Rearward	1:30	Seat	Down
47	1	Kneeling	Seat	Mid	10:30	Person	Down
48	1	Kneeling	Floor	Rearward	3:00	Nothing	Down
49	1	Kneeling (Adult sideways on seat facing side window, legs folded)	Lap	Mid	12:00	Seat	Down
50	1	Kneeling	Lap	Forward	12:00	Nothing	Up, hands on I/P
51	1	Lying (Or torso is twisted)	Seat	Forward	12:00	Nothing	Up

Table 2. Front-seat ride positions of children less than one yeare old based on ORC survey (4)

Line	ORC Cases	Posture	Child is on	Location of Child on Seat/Floor	Knee Direction O'Clock	Back is to	Arm Position
1	59	Sitting	Lap	Rearward	10:30	Person	Down
2	56	Lying	Lap	Rearward	Up	Person	Down
3	52	Sitting	Lap	Rearward	12:00	Person	Down
4	17	Sitting	Lap	Rearward	6:00	Nothing	Down
5	17	Sitting	Seat	Rearward	12:00	Seat	Down
6	14	Standing	Lap	Rearward	6:00	Nothing	Down
7	13	Sitting	Lap	Forward	12:00	Nothing	Up on I/P
8	12	Standing	Lap	Rearward	10:30	Person	Down
9	8	Lying	Seat	Rearward	Up	Seat	Down
10	8	Lying	Lap	Rearward	Down	Nothing	Up
11	7	Kneeling	Lap	Rearward	6:00	Nothing	Down
12	6	Sitting	Seat	Rearward	9:00	Nothing	Down
13	4	Sitting (Between adult's legs)	Seat	Mid	12:00	Person	Down
14	4	Sitting	Seat	Rearward	9:00	Person	Down
15	4	Standing	Seat	Mid	6:00	Nothing	Down
16	3	Sitting (Legs over edge of seat with adult's hands around waist)	Seat	Forward	12:00	Nothing	Down
17	3	Lying	Seat	Mid	Down	Nothing	Up
18	2	Sitting	Floor	Rearward	1:30	Person	Down
19	2	Standing	Lap	Rearward	12:00	Person	Down
20	2	Kneeling	Lap	Rearward	10:30	Person	Down
21	1	Sitting	Seat	Rearward	1:30	Seat	Down
22	1	Sitting (Adult sideways on seat with legs folded, facing two o'clock)	Lap	Mid	12:00	Seat	Down
23	1	Sitting	Lap	Rearward	9:00	Door	Down
24	1	Standing	Seat	Rearward	12:00	Seat	Down
25	1	Standing (Between adult's legs)	Seat	Mid	10:30	Person	Down
26	1	Standing (Adult holding infant's balance)	Lap	Mid	12:00	Nothing	Down
27	1	Kneeling	Seat	Rearward	3:00	Nothing	Down
28	1	Kneeling (Adult sideways on seat with legs folded, facing two o'clock)	Lap	Mid	12:00	Seat	Down
29	1	Lying	Seat	Rearward	12:00	Seat	Down
30	1	Lying (Lying on left side with knees on chest--folded upward)	Floor	Rearward	10:30	Seat	Down
31	1	Lying (On right side)	Lap	Rearward	12:00	Person	Down

The results of these tests are described in a paper by Stalnaker, et al. (5). The various child surrogates were placed in the high-frequency riding positions noted in Table 1, and their trajectories in response to hard braking were determined by analyzing high-speed movies of the braking event. Based on these analyses, 13 child positions were identified as being representative of reasonable child positions near the instrument panel. Characterizations of these positions are shown in Figure 1 and are denoted as the "Z-Positions".

NUMBER OF CHILDREN IN THE VARIOUS Z-POSITIONS

In order to determine the number of children that may be in any one of the 13 Z-positions at the instant of collision, per million car-years of exposure, estimates for the following parameters are needed.

1. N = Number of unrestrained, front-seat children that can be expected to be in collisions of sufficient severity to deploy an inflatable restraint system, per million car-years of exposure.
2. $(F)_{RPJ}$ = The relative frequency of each ride positions identified in Tables 1 and 2 for infant through four-year-old children.
3. $(PZI)_{RPJ}$ = The probabilities that a child will be in various Z-positions at the instant of collision for each ride position.

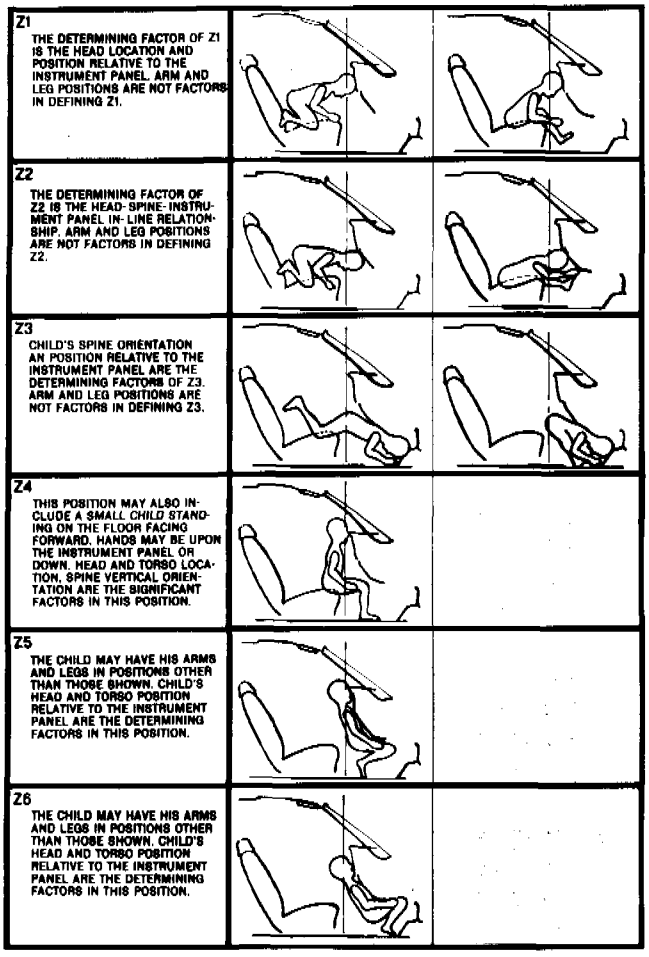

Figure 1. Thirteen child positions (Z-positions) identified as reasonable positions for children near the instrument panel at the instant of collision.

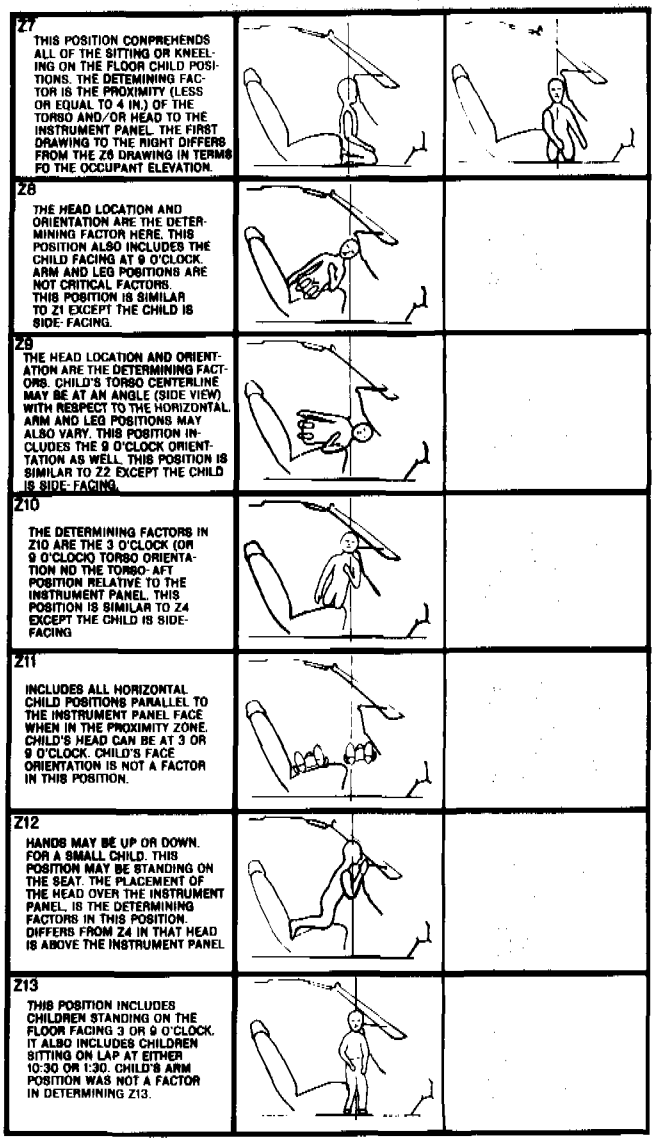

Figure 1. (Continued). Thirteen child positions (Z-positions) identified as reasonable positions for children near the instrument panel at the instant of collision.

With these estimates, the number of children expected to be in a given Z-position can be calculated by,

$$N_{ZI} = \Sigma_{RPJ} (F)_{RPJ} \cdot N \cdot (PZI)_{RPJ}$$

Estimate for N

An estimate for N can be obtained by multiplying the number of collisions that would be of sufficient severity to deploy an inflatable restraint system per million car-years of exposure, N_D, by the probability of a child (infant to four years old), P_C, being in such an accident.

$$N = N_D \cdot P_C$$

Accident data from the GM Motors Insurance Corporation (MIC) file were used to estimate N_D and P_C. Photographs of car damage were used to estimate the number of collisions (M_{DC}) that might have resulted in a deployment of an inflatable restraint system if such a system had been installed in the cars. A deployment-type collision was defined as an accident where the primary direction of impact was between ten and two o'clock with an estimated equivalent barrier speed of 12 miles per hour or greater. For these types of collisions, the number of front-seat children (M_C), infant to four years old, were counted. N was estimated by projecting M_{DC} to a million car-year exposure based on an estimate of the frequency of occurrence of injury accidents per million car-years. This calculation gave an estimate for N_D of 3732 deployments per million car-year exposure. P_C was taken as the ratio of M_C divided by M_{DC}, or 0.040. Using these values for N_D and P_C in the above equation, N was estimated to be 149 unrestrained, front-seat children (infant to four years old) involved in collisions of sufficient severity to deploy an inflatable restraint system, per million car-years of exposure.

Estimate for $(F)_{RPJ}$

The relative frequency of each ride position was calculated by dividing the number of children observed in a given position (see Tables 1 and 2) by 1604, the total number of children observed.

Estimate for $(PZI)_{RPJ}$

To determine the probabilities that a child would be in various Z-positions at the instant of collision for each ride position, estimates of the frequency and duration of preimpact braking and the times that the child would enter and leave the appropriate Z-positions during the braking event for each ride position had to be obtained.

The Cornell Aeronautical Laboratory (CAL II-A, CAL II-B), Highway Safety Research Institute (HSRI), and Oakland County, Michigan (OAKLAND) Multi-Disciplinary Accident Investigation-level (MDAI) data files were used to estimate the relative frequency of preimpact braking (FPIB) in deployment-type accidents. These accident data files contain information on preaccident traveling speed, as well as vehicle speed at impact. The difference between these two speeds was assumed to be the vehicle slow-down speed as a result of preimpact braking. A search of these data files produced 1633 accident case cars where information concerning any accident-avoidance maneuver was given, as well as traveling and impact speeds. Of these 1633 case cars, a total of 1061 (65 percent) had "brake" or "brake and steer" coded as an accident-avoidance maneuver.

The velocity changes noted for the various accidents were used to estimate the corresponding braking times by assuming that the average deceleration level was a constant 0.75 g's. A curve, estimating the probability that an accident, which is severe enough to deploy an inflatable restraint, would have various levels of preimpact braking, was generated and is shown in Figure 2. Note that this curve reflects the previous observation that 65 percent of these accidents will have some level of preimpact braking.

Estimates of the times that a child enters and leaves a given Z-position, after the start of braking for each ride position, were based on analysis of the kinematics of anesthetized animal tests by Stalnaker, et al. (5), which were used to identify the various Z-positions. The animal tests showed that the fore-aft seat position had a major influence on the resulting Z-positions and the times that the animals entered and left a given Z-position. Since the Opinion Research Corporation report (4) did not specify the seat position for the various ride positions, it was assumed that their observations were equally divided between seat full forward and full rearward. Once estimates were obtained for the times a child would enter and leave the various Z-positions for each ride position, the corresponding probabilities that an accident would occur during these times were obtained from Figure 2.

Estimate of N_{ZI}

The data used to calculate N_{ZI} can be visualized as a matrix of 13 columns and 164 rows as shown in Table 3. Each column represents one of the 13 Z-positions. Each

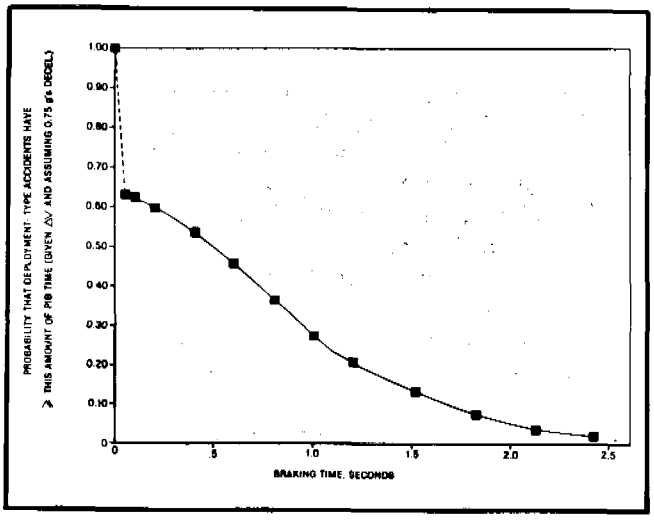

Figure 2. Probabilities that deployment-type accidents have various amounts of preimpact braking.

Table 3. Format used to calculate the number of children expected to be in each Z-position at the instant of collision for deployment-type accidents per million car-years exposure.

Line	ORC Children/ Total Children	Estimated Number of Children 10^6 C-Y	Factor for Seat Position	Possible Child Positions Near Instrument Panel, N_{ZI} Z1	Z2	Z3	Z4	Z5	Z6	Z7	Z8	Z9	Z10	Z11	Z12	Z13	Not in Proximity
1	331/1604	149	0.5	0.0414/0.636	0.0575/0.884	0.1475/2.268											0.7536/11.586
2	109/1604	149	0.5				0.0290/0.147	0.0683/0.346	0.0417/0.211	0.4570/2.314							0.4040/2.045
3	106/1604														0.5176/2.548		0.4824/2.375
4	95/1604	149	0.5	0.0380/0.168	0.0684/0.302	0.1154/0.509											0.7782/3.434
5	89/1604	149	0.5				0.0686/0.284	0.1803/0.745	0.2700/1.116	0.0487/0.201							0.4324/1.787
⋮																	
164	1/1604	149	0.5														1.000/0.046
Totals (N_{ZI} and Not in Proximity)				9.539	1.443	3.445	9.506	2.541	1.586	5.435	1.841	0.213	3.269	0.176	8.557	3.158	98.389

row represents one of the possible 164 ride positions (82 ride positions for seat full forward and 82 ride positions for seat full rearward).

To illustrate how Table 3 was developed, consider Line 4. According to Line 4 of Table 1, 95 of the 1604 children were observed in this position. And in Table 3 the "149 children per million car-years" is the value of N discussed previously. The factor, "0.5", accounts for the assumption that half of the 95 children were sitting on seats that were full rearward. (There will be a separate line for the calculations assuming the seat was full rearward.) The top line numbers for Line 4 under the various Z-positions represent the probabilities that the child will be in each of the various Z-positions at the time of collision. For this ride position, it was estimated that the probabilities of a child being in the Z1, Z2, or Z3 position at the time of collision are 0.038, 0.0684, and 0.1154, respectively. The probability of a child being in any of the other Z-positions is zero. The last column of the table gives the probability that the child will not be in any of the Z-positions (not in the proximity of the instrument panel) at the time of collision and is 0.7782 for Line 4. The numbers under the probabilities for Line 4 are estimates of the number of children (infant through four years old) that can be expected per million car-years of exposure. These numbers were calculated by multiplying the various probabilities by the frequency of the ride position (95/1605 $\times$ 0.50) and the number of children (149 infants through four-year-olds) expected to be in accidents of sufficient severity to deploy an inflatable restraint system per million car-years of exposure. Thus, for Line 4, the number of children per million car-years exposure expected to be in Z1, Z2, and Z3 positions are 0.168, 0.302, and 0.509, respectively. These types of calculations were carried out for each of the 164 lines.

An estimate for the total number of children expected to be in a given Z-position was obtained by adding the number of children in the corresponding Z column. The results of these summations are tabulated at the bottom of each Z column. For example, it is estimated that there will be 9.539 children (infants through four-year-olds) in the Z1 position at the instant of collision per million car-years of exposure.

The results of these calculations for each Z-position are summarized in Figure 3. Note that the most-frequent Z-positions are Z1, Z4, and Z12. The least-frequent are Z9 and Z11. Also, note that of the 149 unrestrained, front-seat children (infant through four years old) who are expected to be in accidents that would be of sufficient severity to deploy an inflatable restraint system per million car-years exposure, a total of 51 of them are expected to be in the proximity of the instrument panel at the time of collision.

DISCUSSION

Several difficulties were encountered in identifying possible positions and postures close to the instrument panel of unrestrained, front-seat children at the instant of collision and estimating the number of children expected to be in each position per million car-years of exposure. The accident data files used to estimate preimpact braking times gave only estimates of velocity changes. Any error trend in these estimates will affect the shape of the curve of Figure 2 and, consequently, the probabilities used for

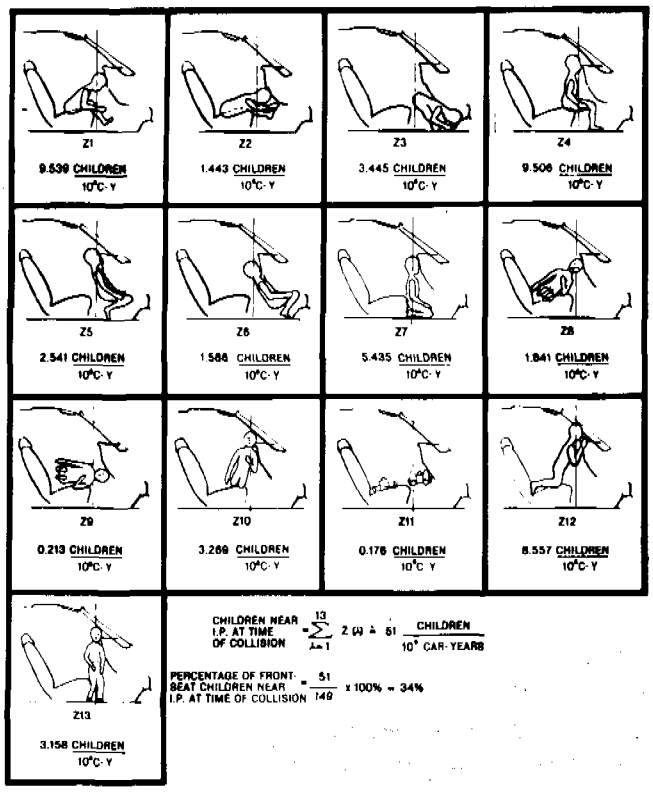

Figure 3. Number of children expected to be in the various Z-positions at the instant of collision per million car-years exposure.

determining the number of children expected to be in each Z-position.

Animal kinematic data were used to estimate the times children would enter and leave various Z-positions for a given ride position. Stalnaker, et al. (5), noted that the animals' kinematics were characteristic of relaxed or sleeping children and that different kinematics would be expected of children who tense their muscles in anticipation of the collision event. Consequently, the estimates given for the number of children in the various Z-positions are biased toward relaxed and sleeping children.

SUMMARY

Based on a million car-years of exposure, it was estimated that there would be 3732 cars involved in collisions of sufficient severity to deploy an inflatable restraint system, if the cars were so equipped. In these accidents there would be 149 unrestrained, front-seat children ranging in ages from infant to four years old. Of these children, 51 of them would be close to the instrument panel at the time of collision, either due to their initial ride position or due to preimpact braking. Thirteen positions and postures were identified as being characteristic of reasonable child positions close to the instrument panel at the instant of collision. Estimates of the number of children expected to be in each position, per million car-years of exposure, are given. This information should be useful in assessing the performance of various passenger inflatable restraint concepts relative to the question of the potential of injuries to children who may be close to the instrument panel in a collision where an inflatable restraint is deployed.

LIST OF REFERENCES

1. Patrick, L. M., and Nyquist, G. W., "Airbag Effects on the Out-of-Position Child", Society of Automotive Engineers, United States, Publication SAE 720442, May 1972.
2. Aldman, B.; Anderson, A.; and Saxmark, O., "Possible Effects on Air Bag Inflation on a Standing Child", Proceedings of the International Meeting on Biomechanics of Trauma in Children, Lyon, France, September 17-19, 1974.
3. Mertz, H. J.; Driscoll, G. D.; Lenox, J. B.; Nyquist, G. W.; and Weber, D. A., "Responses of Animals Exposed to Deployment of Various Passenger Inflatable Restraint System Concepts for a Variety of Collision Severities and Animal Positions", Proceedings of the Ninth Technical Conference on Experimental Safety Vehicles, Kyoto, Japan, November 1-4, 1982.
4. "Child Restraint and Occupant Position Data—Survey of Cars in the Traffic Population, July-December 1979", Opinion Research Corporation Report prepared for the United States National Highway Traffic Safety Administration, March 1980.
5. Stalnaker, R. L.; Klusmeyer, L. F.; Peel, H. H.; White, C. D.; Smith, G. R.; and Mertz, H. J., "Unrestrained, Front Seat, Child Surrogate Trajectories Produced by Hard Braking", Proceedings of the 26th Stapp Car Crash Conference, Publication SAE 821165, October 1982.

Frontal Impact Component Test Evaluation of Current Anthropomorphic Test Device Technology

ROGER A. SAUL
National Highway Traffic Safety Administration
Vehicle Research and Test Center
East Liberty, Ohio

ABSTRACT

This paper presents the component test results of a program designed to evaluate frontal impact anthropometric test device hardware and instrumentation advancements which have been made since the development of the Part 572 dummy. In addition to the Part 572, the GM Hybrid III and Association of Peugeot-Renault dummies are included in the evaluation. The component test results presented in this paper describe the temperature sensitivity, biofidelity, repeatability, durability, and symmetry characteristics of the dummies in frontal impacts.

INTRODUCTION

The Part 572 dummy was standardized as an automotive test device in the early 1970's. It is specified as the occupant for Federal Motor Vehicle Safety Standard 208 frontal rigid barrier crash testing; and has also been used in frontal research, development, and evaluation programs. This dummy represents the "state-of-the-art" in hardware development, instrumentation, and associated injury criteria at the time FMVSS 208 was issued. Anthropomorphic test device (ATD) technology has advanced in several areas since that time due to the effort and resources invested by private industry, the National Highway Traffic Safety Administration, and foreign governments. The purposes of this program are:

i) to evaluate current dummy hardware and instrumentation technology, and
ii) to select a dummy for use in Agency research, development, and assessment programs.

Two dummies, the GM Hybrid III (1) and the APR'81 (2) (Association of Peugeot-Renault), have had the most significant advancements. These two and the Part 572 are included in this evaluation program. The project is comprised of two evaluation phases: component and system level. The approach being taken is as follows:

1. Initial Dummy Calibration—Each dummy was thoroughly tested prior to evaluation testing to ensure that it had been manufactured according to its specifications.
2. Component Level Evaluation—As described below, a series of tests were conducted on the various dummy body components.
3. Dummy Calibration Checks—The dummy calibrations were checked following the component level testing.
4. Systems Level Evaluation—A series of HYGE sled tests are being conducted in 3-point belt restraint and distributed loading systems. The dummies are also being tested in an unrestrained environment.

This paper discusses only the component level evaluation results.

TEST MATRIX DEVELOPMENT

Biofidelity, repeatability, and reproducibility are, of course, the primary factors of consideration for dummy evaluation. It has also been shown that the dummy responses may be sensitive to temperature (3), impact orientation (4), and age of the ATD materials (3). Reproducibility (comparative response of multiple ATDs) and material aging were not included as factors in establishing the test matrix for this study.

The component test matrix to evaluate dummy biofidelity was constructed to assess the dummy frontal performance through a series of tests which, although relatively simple, could be directly compared to the biomechanics data. A review of the literature published since standardization of the Part 572 was made to establish these biomechanics performance criteria. Those shown in Table 1 were selected as being the most appropriate for component test comparisons, but it should be noted that these are largely based on cadaver testing. While the similitude of the cadaver to the living human has not been established, the cadaver data have generally been accepted as the best available data for biofidelity. A recent paper by Patrick (5), however, would indicate that there are differences between cadaver thorax response and human response. It should be recognized, therefore, that the component test evaluations of the dummies for biofidelity will actually be a determination of fidelity to cadaver based data.

The sensitivity of dummies to temperature variations was investigated by Seiffert and Leyer (3) through a series of component calibration and full system sled tests with the Part 572 dummy in 1975 over a temperature range of 68-140°F. Significant dependencies of the calibration test results were observed over this wide temperature range, and the dummy motion was found to be different in the system tests. One of the conclusions made by Seif-

Table 1. Summary of Biomechanic Performance Criteria Sources.

Body Region	Source	Data Collection Methodology	Subject Response Measurements
Head	Hodgson et. al. (6,7,8)	Whole cadaver pallet drop tests; head impacts to load cell	Resultant Head Acceleration
Neck	Mertz et. al. (9,10)	Whole cadaver and volunteer sled tests in flexion and extension	Moment about Occipital Condyle vs. Head Rotation
Thorax	Neathery (11)	Whole cadaver rigid pendulum impact	Impact Force vs. Sternal Deflection
Femur	Horsch et. al. (12)	Rigidly mounted cadaver femur and lower legs	Peak Impact Force

fert and Leyer was that a temperature range should be specified for restraint system crash tests. Most of the crash tests conducted by the NHTSA specify that the temperature of the dummy be stabilized at a level between 66 and 78°F (13,14). Consequently, dummy response variations due to temperature within this range were of primary concern in the present study. Temperature sensitivity tests were conducted on the dummy head and thorax sections at three temperatures; those being 72°F as the median, and 65 and 80°F taken for the extremes.

The effect of impacting the Part 572 dummy head, thorax, and knees at various angles to determine response differences was reported by Daniel, et al.(4). They found that the dummy responses in these body regions could vary significantly depending upon the impact orientation. Of particular interest in the present study was the indication that the dummy response was not necessarily symmetrical (i.e., the response resulting from an impact at a certain angle was not duplicated when the dummy was impacted from the same angle on the opposite side). Although the dummy response resulting from one angle should not be expected to match the response from another, it is not unreasonable to expect the dummy to perform symmetrically. Evaluations of the dummy symmetrical properties were made by conducting impacts to the head, thorax, and knees at an angle of 15° orientation from both the left and right side of the dummies.

Repeatability was evaluated by repeating each test for biofidelity, temperature sensitivity, and symmetry three times for each of the dummies. Although it has been suggested that a relatively large number of repeat tests may be required to provide a statistically adequate sampling (15), the component test environment is relatively simple and not as susceptible to test set-up variations as more sophisticated testing might be.

Specific component tests to evaluate the durability of the dummy components were not included as a part of the test matrix design. Damaged parts were noted during the course of testing, however, and this became a factor in evaluating the dummy performance.

To summarize, the component test matrix was designed to evaluate the Part 572, APR '81, and Hybrid III dummies for biofidelity, temperature sensitivity, symmetry, repeatability, and durability. Tests were conducted on the head, neck, thorax, and knees (femurs) to evaluate these factors. Since the APR '81 dummy differs from the Part 572 in the thorax only; the APR '81 head, neck, and femur responses on the component level were assumed to be identical to the Part 572 responses. The component test matrix is summarized in Table 2, showing the dummies used and the evaluation factors considered by each test series.

TEST PROCEDURES

Prior to conducting the component test series, the Part 572 and Hybrid III dummies were calibrated. Post-test calibrations were conducted upon completion of the component tests. The APR dummy was subjected to 14 and 22 fps thorax impact tests before and after the component tests. Since calibration specifications are not available for the APR device, it was assumed to be in "calibration". The dummies were soaked at the test temperature for a minimum of four hours prior to testing. The temperature gradient in the dummy was monitored with thermocou-

Table 2. Component Test Matrix.

Test Series	Evaluation Factor				Dummies Tested		
	Repeatability	Biofidelity	Temp. Sensitivity	Symmetry	Part 572	APROD '81	Hybrid III
Head Drop 8.4 fps	X	X			X		X
Head Drop 6.3 fps	X	X			X		X
Neck Extension Mini-sled 24 fps	X	X			X		X
Neck Flexion Mini-sled 32 fps	X	X			X		X
Thorax Impact 14 fps, 72°F	X	X	X		X	X	X
Thorax Impact 20 fps, 72°F	X	X			X	X	X
Thorax Impact 22 fps, 72°F	X	X			X	X	X
Knee Impact 11#, 6.9 fps	X	X			X		X
Knee Impact 51-1/2#, 6.9 fps	X				X		X
Head Impacts 7.8 fps, 65°F	X		X		X		X
Head Impacts 7.8 fps, 72°F	X		X		X		X
Head Impacts 7.8 fps, 80°F	X		X		X		X
Thorax Impacts 14 fps, 65°F	X		X		X	X	X
Thorax Impacts 14 fps, 80°F	X		X		X	X	X
Head Impact 7.8 fps, ± 15°	X			X	X		X
Thorax Impact 14 fps, ± 15°	X			X	X	X	X
Knee Impact 11#, ± 15°	X			X	X		X

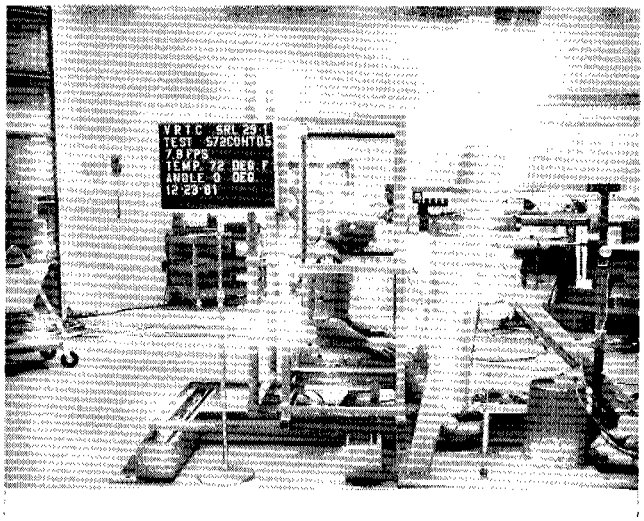

Figure 1a. Fully alligned head impact set up.

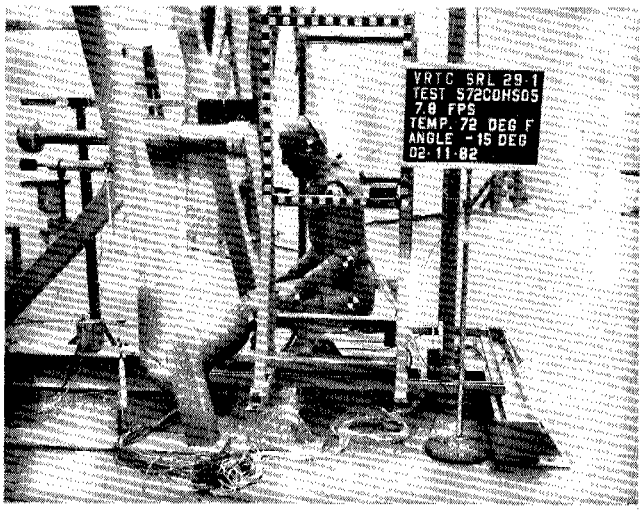

Figure 1b. Symmetry test hard impact set up.

ples placed in the dummy head and thorax for the temperature sensitivity tests to ensure stabilization at the test temperature. Except as noted below, all data were analog filtered at SAE J211 Class 1000 and digitized at 8000 Hz. The data were then digitally filtered to the appropriate SAE channel class. Specific details of the various test series are described below.

The head drop tests to assess the dummy head biofidelity were conducted using a Part 572 head calibration fixture. The procedure was identical to the calibration procedure except for the drop height. The 8.4 fps impacts were dropped from a height (measured between the rigid surface and the dummy forehead) of 13.15 inches. The 6.3 fps impacts were dropped from a 7.4 inch height.

A linear transfer pendulum was used to impact the dummy heads for temperature sensitivity and symmetry evaluation. The impacting velocity of the 51.5 lb ram was nominally 7.8 fps and measured by a light trap just prior to impact with the dummy. The ram impacting surface was 6 inches in diameter. The dummies were positioned such that the orientation of the head relative to the impacting surface was identical to the calibration specifications (i.e., the forehead was the impact location and the dummy nose was ½ inch posterior). The test set up is shown for a Part 572 in Figure 1a. The dummy positioning for the head symmetry tests was the same as described above, except that the seat was rotated ±15° and then translated to allow the contact point of the dummy to occur on the piston centerline (see Figure 1b).

The linear transfer pendulum was also used to conduct the thoracic impact tests. The temperature sensitivity, biofidelity (72°F temperature baseline), and symmetry tests were conducted at nominally 14 fps impact velocity. Biofidelity tests were also conducted at 20 and 22 fps impact speeds. The dummy thoraxes were positioned as specified in their respective calibration procedures. The set ups are shown in Figures 2a and b for the Part 572

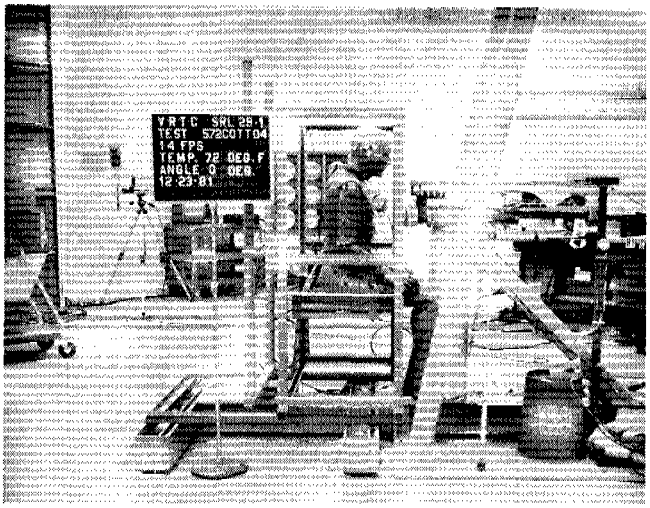

Figure 2a. Thorax temperature sensitivity and biofidelity test set up.

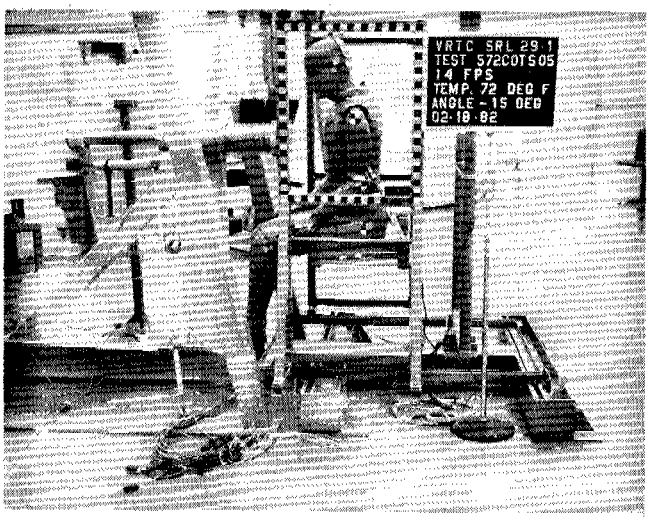

Figure 2b. Thorax symmetry test set up.

Table 3. Mini-Sled Head/Neck Deceleration Pulse Criteria.

Test Configuration	Test Velocity (fps)	Average Test Deceleration (g's)	Stopping distance (in)
Flexion	32	17	10
Extension	24	6	17

dummy. The symmetry tests were conducted using the same dummy positioning; seat rotation and translation were similar to the head symmetry procedure.

A mini-sled was used to test neck flexion and extension properties. The sled's fluid impact accelerator (16) (Figure 3) was used as a velocity generator to propel the mini-sled platform (Figure 4) along the rails until engagement with a roller tape mechanism (Figure 5). The tapes were designed to control the sled deceleration with an essentially square wave pulse as described in Table 3. The angular motion of the heads were determined through photographic film digitization.

The 11 pound knee impact tests were conducted identically to the Hybrid III knee calibration test. The knee was rigidly mounted onto the test fixture (see Figure 6) and impacted at 6.9 fps by the 11 pound pendulum supported by four wires. The pendulum impacting acceleration (and force) were filtered to SAE J211A Channel Class 600 to be consistent with the calibration procedure. It should be noted that the cadaver data (12) were filtered at Class 1000. The 52 pound knee impact tests were conducted with the linear transfer pendulum per Part 572 calibration procedures. The test set up is illustrated in Figure 7.

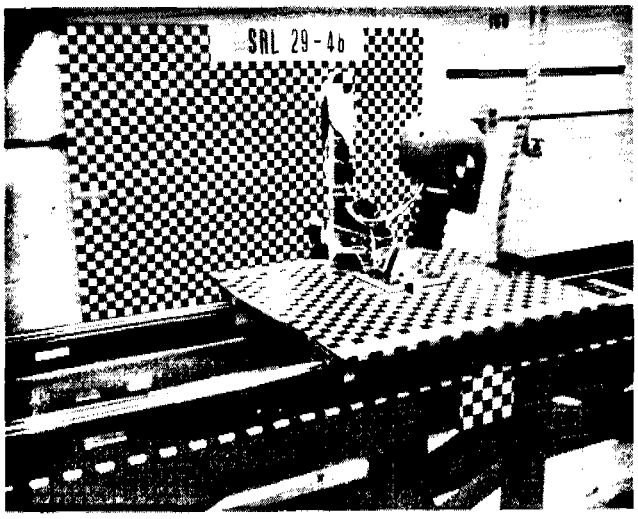

Figure 4. Mini-sled platform.

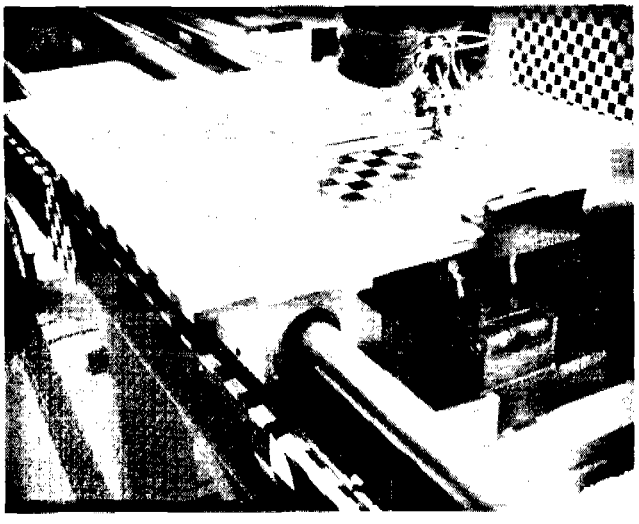

Figure 5a. Roller tape mechanism at platform engagement.

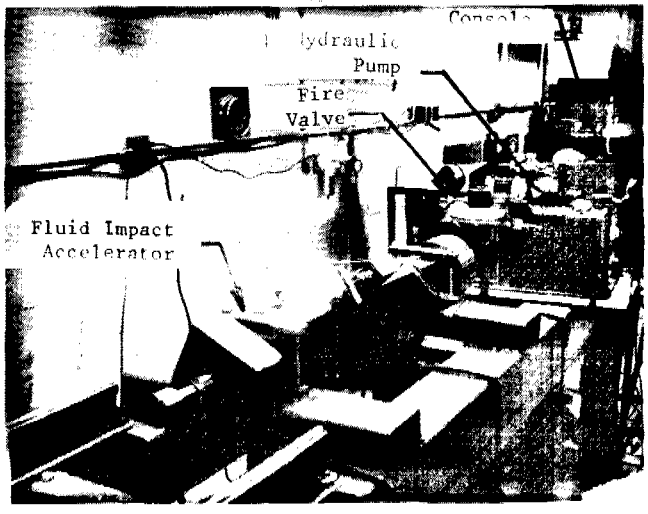

Figure 3. Mini-sled fluid impact accelerator.

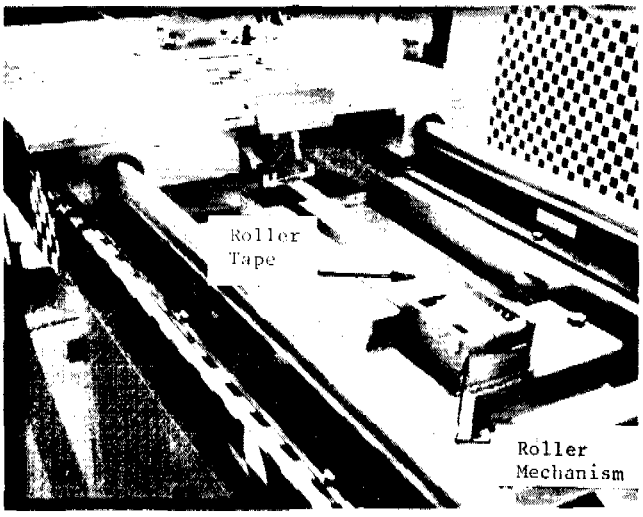

Figure 5b. Roller tape mechanism after energy absorption.

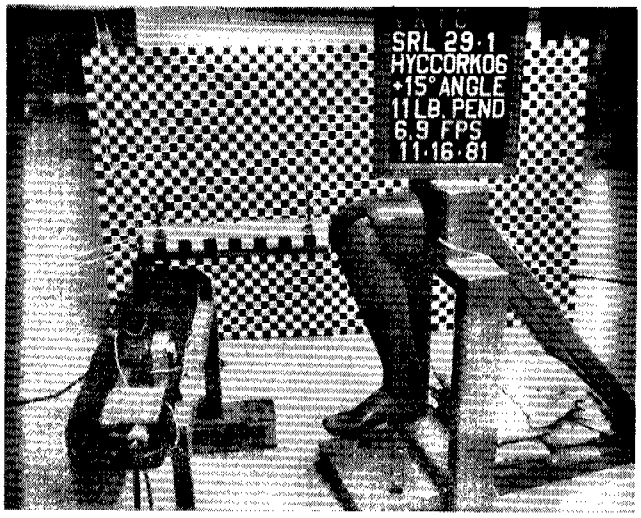

Figure 6. 11 pound knee impact test set up.

Table 4. Head drop biofidelity results.

Test Series	Test Number	Test Date	Drop Velocity (fps)	Peak Resultant Acc. (G's)	Peak Lateral Acc. (G's)	HIC	Cadaver Peak Acc. Response (G's)
Part 572 13.15 in	572COHD01	7-14-82	8.4	302.23	1.73	1033.35	230
	572COHD02	7-15-82	8.4	291.65	4.56	945.02	
	572COHD03	7-19-82	8.4	291.31	2.31	945.39	
Hybrid III 13.15 in	HYCCOHD01	7-21-82	8.4	229.15	5.47	626.43	230
	HYCCOHD02	7-21-82	8.4	240.13	5.73	694.29	
	HYCCOHD03	7-22-82	8.4	245.41	1.69	717.45	
Part 572 7.4 in	572COHD04	7-19-82	6.3	182.52	0.93	357.87	115
	572COHD05	7-19-82	6.3	184.91	1.76	365.26	
	572COHD06	7-20-82	6.3	179.96	0.77	348.71	
Hybrid III 7.4 in	HYCCOHD04	7-22-82	6.3	144.81	3.49	251.44	115
	HYCCOHD05	7-22-82	6.3	146.29	3.51	260.79	
	HYCCOHD06	7-22-82	6.3	139.83	3.39	230.54	

RESULTS AND DISCUSSION

Biofidelity

The head impact biofidelity data are summarized in Table 4. On the basis of peak head acceleration response, it is apparent that the Hybrid III head more closely simulates the cadaver response at both 6.3 and 8.4 fps impact velocities than the Part 572 (APR) headform. As might be expected from the peak accelerations, the HIC values for the Hybrid III are lower than the Part 572. While a HIC value of approximately 1000 is obtained for the Part 572 dummy under test conditions simulating cadaveric skull fracture threshold levels, the Hybrid III produces a HIC of approximately 700. Although the Hybrid III dummy head produces a more cadaveric response than the Part 572, a performance criterion of HIC equal to 1000 does not appear appropriate for the Hybrid III if skull fractures are to be limited.

The Hybrid III is the only dummy which currently has neck instrumentation capable of measuring performance according to the criteria established by Mertz. (Although a neck transducer has been manufactured for a Part 572 dummy, the necessary modifications to the neck molding have not yet been proven adequate in NHTSA tests.) The Hybrid III flexion and extension performance is shown, respectively, in Figures 8 and 9, and show generally good agreement with the results published by Foster et al. (1). The flexion loading corridor includes the effects of chin contact to the torso. The tests on the mini-sled did not have chin contact, explaining the lack of neck torque above 60 ft lb. The comparison of the Part 572 and Hybrid III head rotation in Figures 10 and 11 indicates good agreement in flexion, but the Part 572 neck is considerably stiffer than the Hybrid III in extension.

The response of the three dummies to thoracic impact at 14 fps are demonstrated in Figures 12-14. The APR and Hybrid III dummies have the greatest amount of

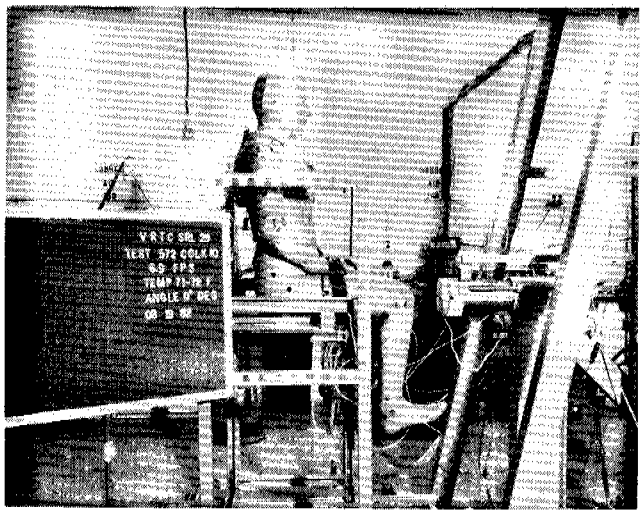

Figure 7. 52 pound knee impact test set up.

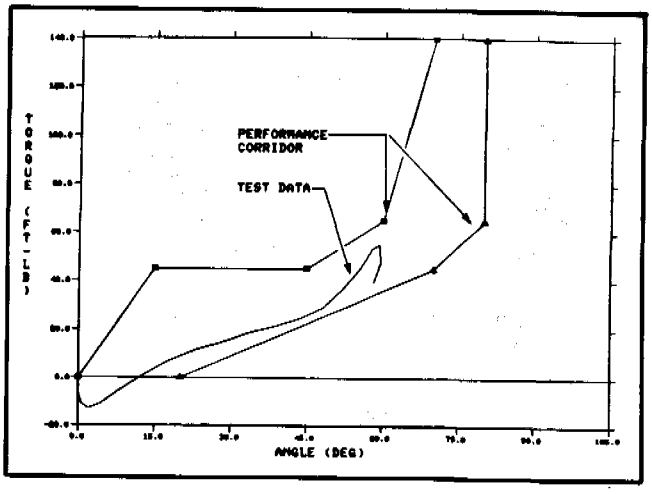

Figure 8. Hybrid III neck flexion response.

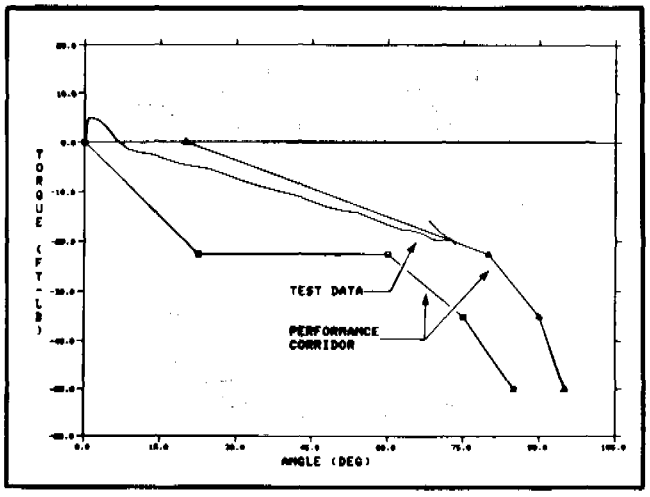

Figure 9. Hybrid III neck extension response.

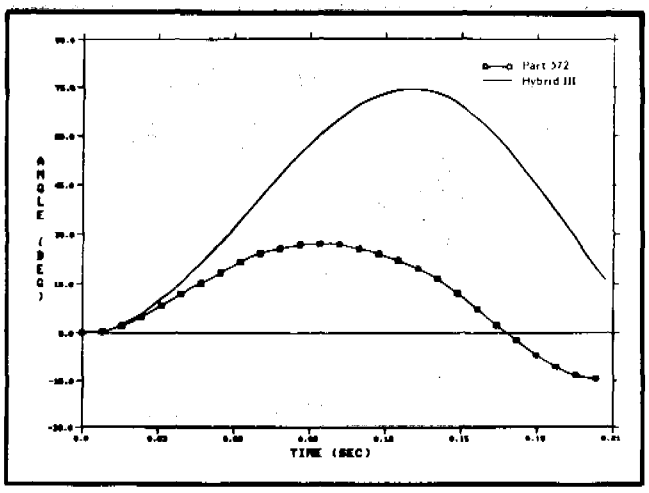

Figure 11. Part 572 versus Hybrid III extenison response.

deflection (approximately 1.25 inches), but require approximately an additional 0.6 inch deflection to meet the minimum deflection criterion specified by the corridor. The Hybrid III peak force level, however, is in better agreement with the corridor. The Hybrid III response under 22 fps thoracic impacts is almost entirely within the corridor, whereas the Part 572 and APR both have force levels considerably higher and sternal deflections lower than the performance corridor (Figures 15-17). From Figures 12-17, it is apparent that the Hybrid III dummy most closely simulates the response corridor derived from the cadaver data.

The 11 lb fully aligned knee impact biofidelity test results are summarized in Table 5. Since the Hybrid III knee calibrations are based on these cadaver data, it is not surprising that the Hybrid III agreement with the cadaver data is better than the Part 572 knee impact results. The lower Hybrid III peak pendulum impact forces are also observed for the 52 lb impacts (Table 6) with data filtered at 1000 Hz cutoff frequency. When

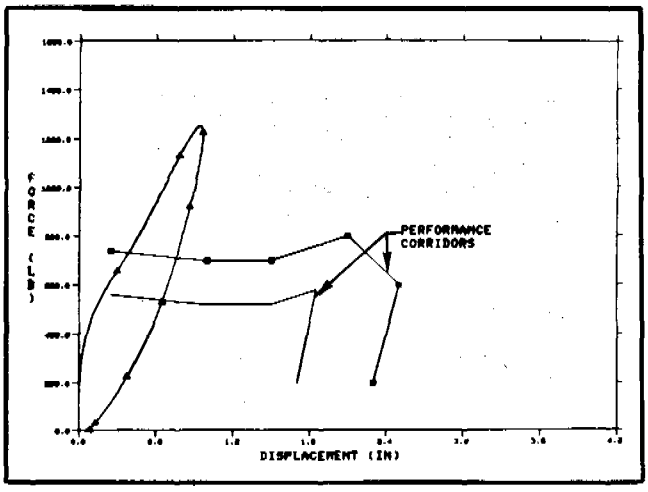

Figure 12. Part 572 thorax biofidelity, 14 FPS.

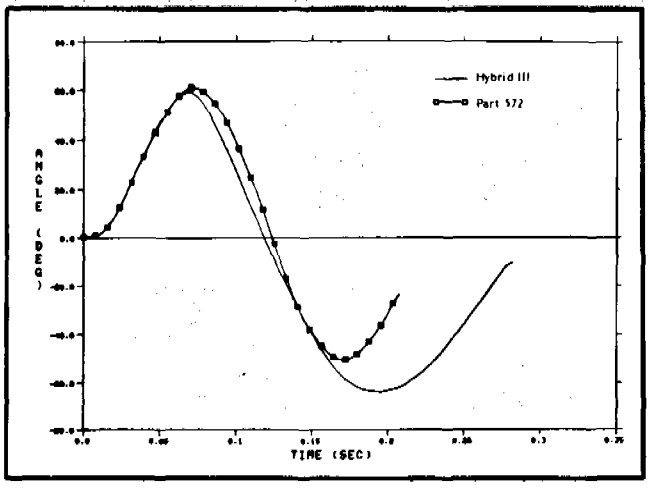

Figure 10. Part 572 versus Hybrid III flexion response.

Table 5. Aligned 11 lb. knee impact test results.

Test Series	Test Number	Test Series Peak Pendulum Force (lbs.)	Mean Peak Pendulum Force Mean (lbs.)	Cadaver Response (lbs.)
Hybrid III	HYCCALK08	1331.5		
Left Knee	HYCCALK09	1359.9	1356.2	1282.
0° Impact	HYCCALK10	1377.3		
Hybrid III	HYCCARK07	1327.6		
Right Knee	HYCCARK08	1358.4	1353.7	1282.
0° Impact	HYCCARK09	1375.2		
Part 572	572COLK07	2516.9		
Left Knee	572COLK08	2475.9	2465.20	1282.
o° Impact	572COLK09	2402.8		
Part 572	572CORK07	2217.7		
Right Knee	572CORK08	2151.4	2180.60	1282.
o° Impact	572CORK09	2172.7		

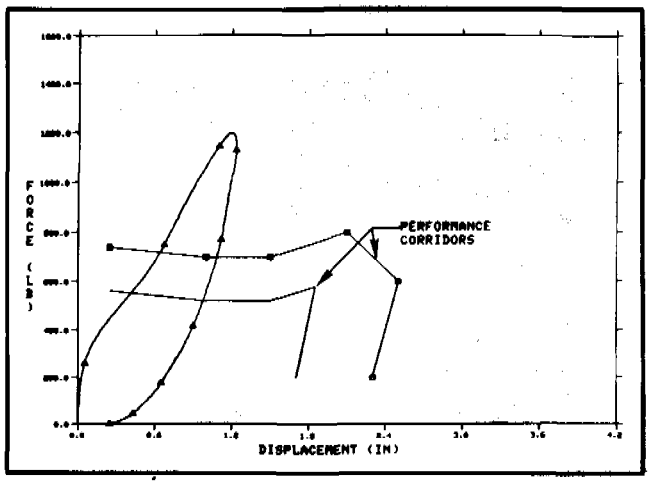

Figure 13. APR thorax biofidelity, 14 FPS.

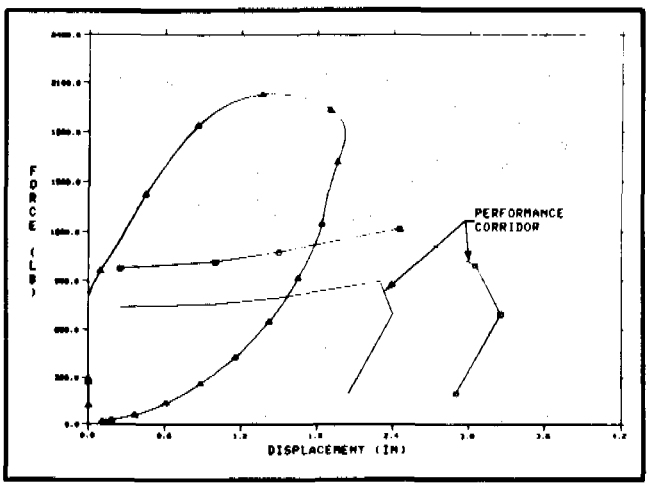

Figure 16. APR thorax biofidelity, 22 FPS.

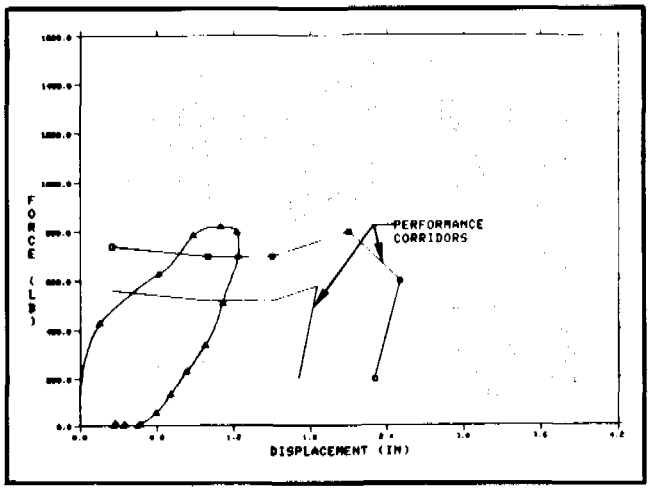

Figure 14. Hybrid III thorax biofiedlity, 14 FPS.

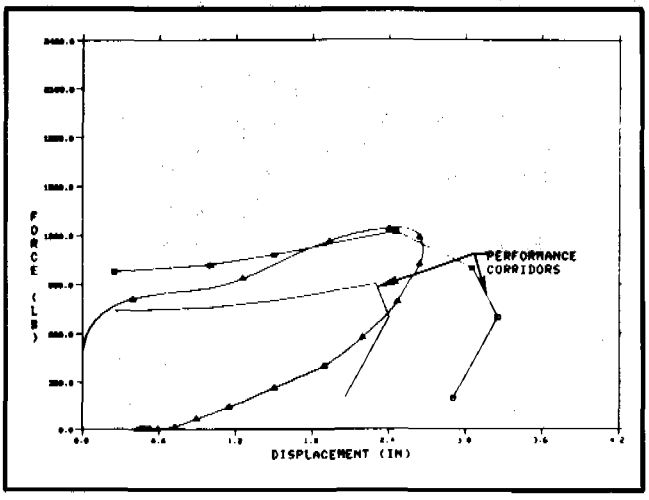

Figure 17. Hybrid III thorax biofidelity, 22 FPS.

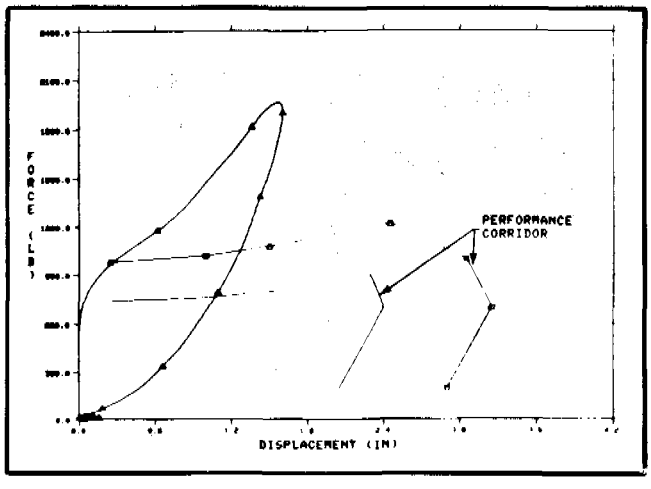

Figure 15. Part 572 thorax biofidelity, 22 FPS.

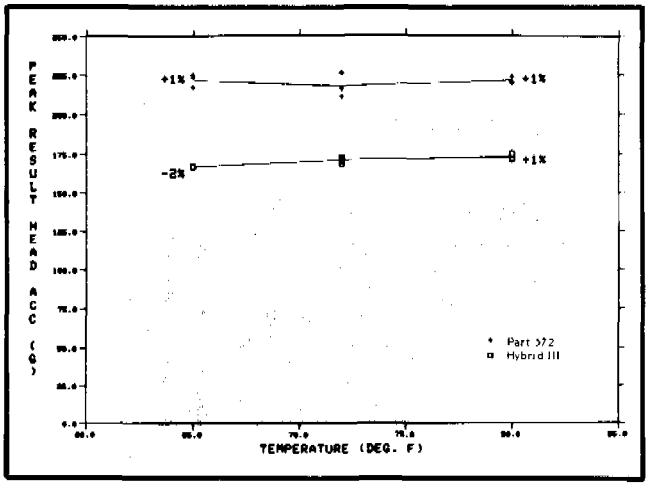

Figure 18. Head impact temperature sensitivity.

Table 6. Transfer pendulum knee impact results.

Test Series	Test Number	Test Date	Velocity (fps)	Peak Femur Load (lbs) (1000 Hz filtered)	Peak Femur Load (lbs) (100 Hz filtered)	Peak Pendulum Force (lbs) (100 Hz filtered)
Part	572COLK10	8-19-82	6.86	2457	788	965
572	572COLK11	8-19-82	6.90	2865	846	1051
Left Knee	572COLK12	8-19-82	6.90	2876	846	1055
Part	572CORK10	8-20-82	6.89	2149	805	962
572	572CORK11	8-20-82	6.92	2571	851	1025
Right Knee	572CORK11	8-20-82	6.89	2539	850	1038
Hybrid	HYCCOLK07	8-19-82	6.89	1523	863	1022
III	HYCCOLK08	8-19-82	6.93	1651	868	1046
Left Knee	HYCCOLK09	8-19-82	6.92	1649	868	1015
Hybrid	HYCCORK07	8-18-82	6.88	1503	866	983
III	HYCCORK08	8-18-82	6.89	1461	865	1012
Right Knee	HYCCORK09	8-18-82	6.88	1464	848	1009

filtered at 100 Hz, the peak pendulum force is nearly identical for the two dummies indicating that the lower responses for the Hybrid III are due to knee padding rather than structural differences.

Temperature Sensitivity

Results of the head impact temperature sensitivity tests are shown in Figure 18. The test data indicate that neither the Part 572 nor Hybrid III headforms have responses which are sensitive to temperature variations over the standard range of testing. The Part 572 peak resultant head acceleration response at 80°F and 65°F was 1% higher than at 72°F, and the Hybrid III head acceleration response ranged only from 2% lower at 65°F to 1% higher at 80°F. These percentage deviations from the 72°F response are also shown on Figure 18.

The thorax response variations due to temperature changes were much more significant (Figures 19 and 20). The chest acceleration response for all three dummies was consistent in a trend of reduced peak acceleration at 80°F, and increased acceleration at 65°F. The total acceleration response variation range for the Part 572 was 14% compared to 24% and 35% for the APR and Hybrid III, respectively. Somewhat more pronounced response variation occurred for the three dummies for sternal deflection. Consistent with the acceleration response, the trend for all three dummies was one of increased deflection for increasing temperature. The total sternal deflection response variation range for the Part 572 was only 9%; while the APR range was 19%, and the Hybrid III ex-

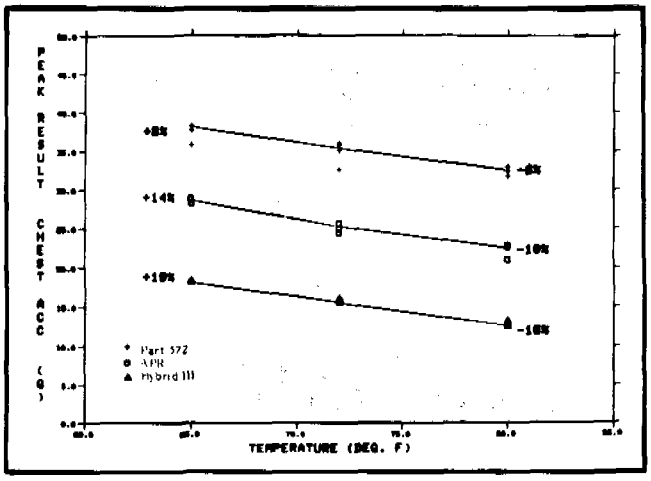

Figure 19. Thorax impact chest acceleration temperature sensiitivity.

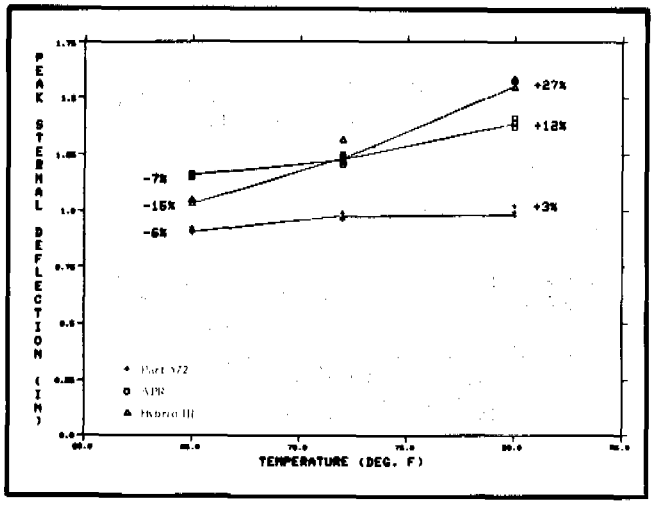

Figure 20. Thorax impact sternal deflection temperature sensitivity.

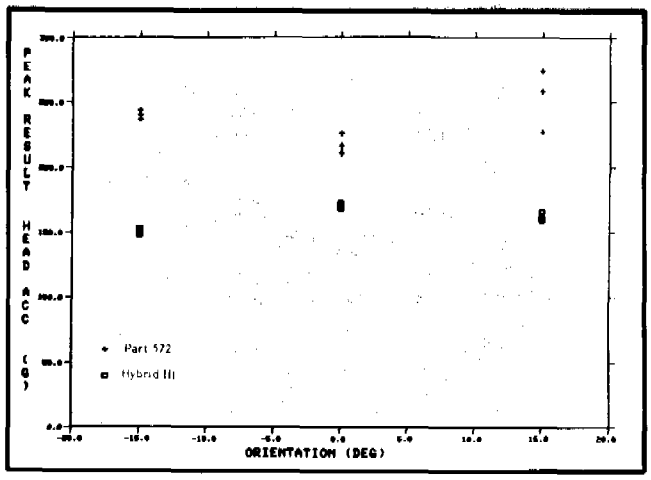

Figure 21. Head symmetry—acceleration response.

perienced a 42% change in sternal deflection between 65 and 80°F. The acceleration and sternal deflection variations from 72°F are shown in Figures 19 and 20.

The sensitivity of the dummy thorax deflection to temperature appears to be related to the damping material/steel thickness ratio of the rib designs. The steel thickness for the Part 572 dummy is 0.125 inch compared to 0.058 and 0.078 inch thicknesses for the APR and Hybrid III, respectively. The damping material thickness ranges from 1/4 inch for the Part 572 to approximately 0.4 inch for the Hybrid III. The damping material/steel thickness ratio is nearly two and one-half times greater than the Part 572 for the Hybrid III. The ratio for the APR dummy is comparable to the Hybrid III; but is not as sensitive to temperature, possibly due to a different rib attachment design.

These response variations for both the APR and the Hybrid III dummies over this temperature range are clearly unacceptable for normal engineering practice. To be useful as automotive test devices, both the APR and Hybrid III require either design changes to the thorax to reduce the temperature sensitivity, or temperature conditions controlled to a range of approximately 5°F (reducing variability to 15% or less). A third alternative would be to monitor the dummy thoracic temperature and make adjustments to the response accordingly. However, the assumption for this alternative is that each batch of rib damping material has the same sensitivity to temperature.

Symmetry

The symmetry features of the three dummies did not prove to be significantly different for impacts at ± 15° from fully aligned. The head symmetry tests (Figure 21) resulted in approximately a 5% difference between the + 15° and − 15° acceleration response on the Part 572 compared to a 7% difference on the Hybrid III. It was also noted that the Part 572 aligned impact response was slightly lower than the off-center response, whereas the Hybrid III aligned response was slightly higher.

The thorax symmetry test results are presented in Figures 22 and 23. The Part 572 chest acceleration had the greatest amount of difference between the + 15° and − 15° impacts. It had an 11% difference compared to less than 2% for the APR and Hybrid III dummies. Sternal deflection was not measured in either the APR or Part 572 dummy symmetry tests since their measurement devices were not designed for such impact configurations. The Hybrid III sternal deflection was measured, but exhibited only a 3% response difference from a +15° and − 15° impact location. As was the case for the head symmetry tests, the aligned thorax responses were only slightly different from the off-centered impacts. The impact responses for both the Part 572 and the Hybrid III dummies was slightly higher for the aligned impacts, and the APR was slightly lower.

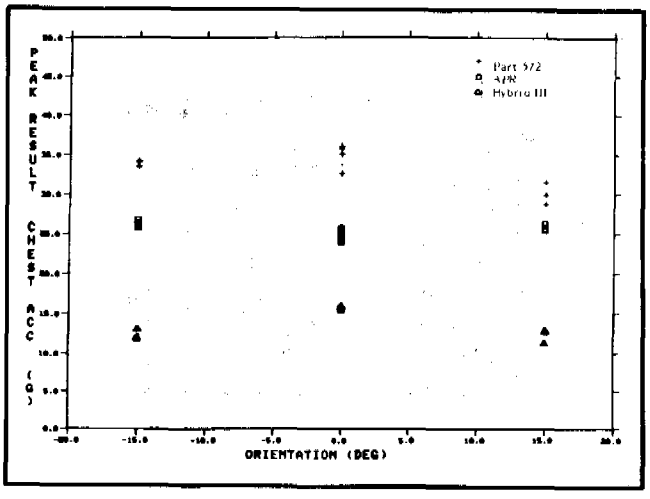

Figure 22. Thorax symmetry—chest acceleration response.

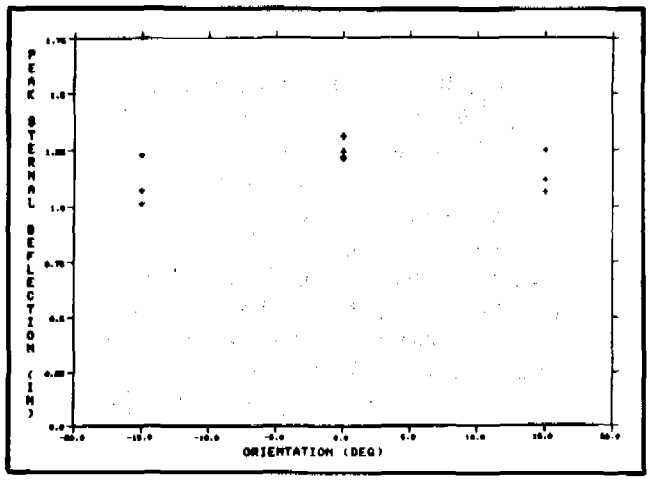

Figure 23. Thorax symmeltry—Hybrid III chesst deflection.

The knee symmetry test results are shown in Figure 24. The Hybrid III had smaller differences in the + 15° and − 15° femur load responses than did the Part 572.

REPEATABILITY AND DURABILITY

Each character on Figures 18-24 represents a particular test, and the scatter is an indication of the dummy repeatability under the various test conditions. Review of these figures indicates that the repeatability of all three dummies is good, and not a major concern in the overall evaluation.

Durability of the Part 572 dummy is superior to the Hybrid III and APR dummies based on a comparison of the pre- and post-test dummy calibrations. The Part 572 dummy maintained its calibration throughout the component testing; whereas the APR dummy changed by approximately 15%, and the Hybrid III dummy thorax displacement increased by 30% (at 14 fps pendulum impact velocity). The increased Hybrid III thorax displacement was most likely caused by cracks which had begun to form in the rib damping material during the component tests.

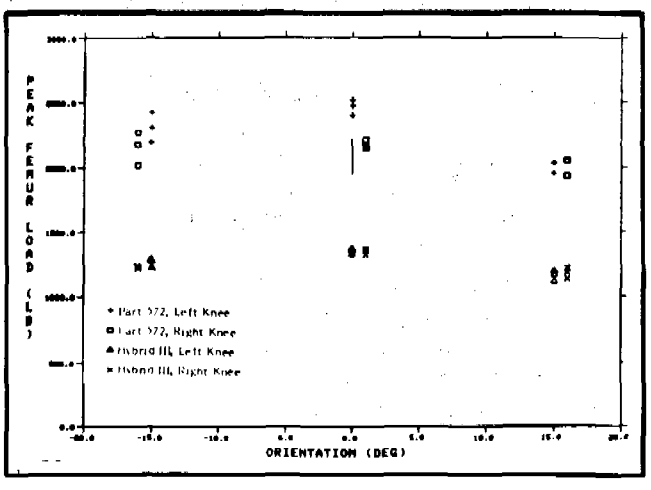

Figure 24. 11 pound knee symmetry test results.

CONCLUSIONS

Based on the component tests which were conducted on the Part 572, APR '81, and Hybrid III dummies, the following conclusions are made:

—The Hybrid III dummy exhibits the best fidelity to cadaver based data. It is noted, however, that the similitude of cadaver based data to living humans remains to be established.

—The APR dummy thorax experiences deflections which are more cadaver-like than the Part 572, but the peak force levels are much higher than cadaver data.

—The Hybrid III and APR dummy thorax responses have greater sensitivity to temperature than the Part 572, and either design modification or a tightly controlled temperature environment is necessary to make them suitable as automotive test devices.

ACKNOWLEDGEMENTS

The discussion and conclusions in the paper represent the opinions of the author and not necessarily those of the NHTSA. Many people have made significant contributions to the project including Tom MacLaughlin, Rolf Eppinger, and Mark Haffner. The author would also like to acknowledge Ed McGhee, Gerda England, and Susan Weiser for their efforts in the project and manuscript preparation.

REFERENCES

1. Foster, J. K., Kortge, J. O., Wolanin, M. J., "Hybrid III—A Biomechanically-Based Crash Test Dummy," Twenty-First Stapp Car Crash Conference, SAE Paper No. 770938, 1977.
2. Fayon, A., Leung, Y. C., Stalnaker, R. L., Walfisch, G., Balthazard, M., Tarrière, C., "Presentation of a Frontal Impact and Side Impact Dummy, Defined From Human Data and Realized From a "Part 572" Basis," Seventh ESV Conference, June 5-8, 1979.
3. Seiffert, U. W. and Leyer, H. E., "Dynamic Dummy Behavior Under Different Temperature Influence," Twentieth Stapp Car Crash Conference, SAE Paper No. 760804, 1976.
4. Daniel, R. P., Trosien, K. R., Young, B. O.,"The Impact Behavior of the Hybrid II Dummy," Nineteenth Stapp Car Crash Conference, SAE Paper No. 751145, 1975.

5. Patrick, L. M., "Impact Force Deflection of the Human Thorax," Twenty-Fifth Stapp Car Crash Conference, SAE Paper No. 811014, 1981.
6. Hodgson, V. R. and Thomas, L. M., "Breaking Strength of the Human Skull versus Impact Surface Curvature," Report No. HS-801-002, Final Report, November 1973.
7. Hodgson, V. R. and Thomas, L. M., "Comparison of Head Acceleration Injury Indices in Cadaver Skull Fracture," Fifteenth Stapp Car Crash Conference, 1971, SAE Paper No. 710854.
8. Hodgson, V. R. and Thomas, L. M., "Head Impact Response," SAE Vehicle Research Institute Report, VRI 7.2, 1975.
9. Mertz, H. J. and Patrick, L. M., "Strength and Response of the Human Neck," Fifteenth Stapp Car Crash Conference, SAE Paper No. 710855, 1971.
10. Mertz, H. J., Neathery, R. F., and Culver, C. C., "Performance Requirements and Characteristics of Mechanical Necks," Human Impact Response, October 2-3, 1977, Plenum Press.
11. Neathery, R. F., "Analysis of Chest Impact Response Data and Scaled Performance Recommendations," Eighteenth Stapp Car Crash Conference, SAE Paper No. 741188, 1974.
12. Horsch, J. D. and Patrick, L. M., "Cadaver and Dummy Knee Impact Response," Automobile Engineering Meeting, SAE Paper No. 760799, October 18-22, 1976.
13. Laboratory Procedure for FMVSS 208, "Occupant Crash Protection" TP-208-05, July 10, 1981.
14. Laboratory Procedure for Vehicle Assessment, FMVSS 212, 219, and 301-75, IP-212-02, April 29, 1980.
15. McAdams, H. T., "The Repeatability of Dummy Performance," Human Impact Response, October 2-3, 1972, Plenum Press.
16. Monk, M. W. and Sullivan, L. K., "Side Impact Sled and Padding Development," Report No. DOT-HS-805-889, Appendix I, February 1981.

Responses of Animals Exposed to Deployment of Various Passenger Inflatable Restraint System Concepts for a Variety of Collision Severities and Animal Positions

H.J. MERTZ
General Motors Corporation

G. D. DRISCOLL and J. B. LENOX
Southwest Research Institute

G. W. NYQUIST and D. A. WEBER
General Motors Corporation

3681

ABSTRACT

This paper summarizes the results of tests conducted with anesthetized animals that were exposed to a wide range of passenger inflatable restraint cushion forces for a variety of impact sled—simulated accident conditions. The test configurations and inflatable restraint system concepts were selected to produce a broad spectrum of injury types and severities to the major organs of the head, neck and torso of the animals. These data were needed to interpret the significance of the responses of an instrumented child dummy that was being used to evaluate child injury potential of the passenger inflatable restraint system being developed by General Motors Corporation. Injuries ranging from no injury to fatal were observed for the head, neck and abdomen regions. Thoracic injuries ranged from no injury to critical, survival uncertain. Graphs are presented that show associations between the severity of the animal injuries by body region and selected measured animal responses and restraint system-accident characteristics. Caution must be used in interpreting the significance of these injuries relative to the expected performance of passenger inflatable restraint systems since aggressive restraint system concepts and accident conditions were selected for some tests in order to produce severe injuries.

INTRODUCTION

An important consideration in the development of a passenger inflatable restraint system is to assess the significance of the interactions that may occur between deploying cushions and children who may be close to the instrument panel at the time of deployment (1-8). Analyses by Takeda and Kobayashi (8), Stalnaker et al. (9) and Montalvo et al. (10) have demonstrated that children may be close to the instrument panel in a variety of positions and postures at the instant of a collision either due to their precrash "seated" position or due to the effects of preimpact braking. Tests sponsored by General Motors at Wayne State University (1) and by Volvo at Chalmers University (7) have shown that it is possible to produce significant brain, heart, liver and spleen injuries in anesthetized animals exposed to the impacts of deploying cushions of several concepts of passenger inflatable restraint systems. In the GM program, anesthetized

baboons and chimpanzees were used as child surrogates. The Volvo program used anesthetized pigs. Unfortunately, no attempt was made in either program to develop a test device (instrumented child dummy) to aid in understanding the relationships between the observed animal injuries and the cushion-collision interaction forces. However, these programs did demonstrate the need to consider such interactions in the development of passenger inflatable restraint systems (2,3).

When General Motors started its development of a second-generation passenger inflatable restraint system, the interaction between the deploying cushion and the "out-of-position" child was again identified as a topic requiring further study. Concurrent with their inflatable restraint development program, GM initiated a program to develop a test device (an instrumented, 3-year-old child dummy) that could provide measures of the various cushion interaction forces thought to be associated with the type of injuries observed in the previous animal test programs. Such an instrumented child dummy was developed by GM (11) and was used extensively in their second-generation, passenger inflatable restraint development program. While the child dummy provided measurements to make relative comparisons between different passenger inflatable restraint concepts, no biomechanical data existed that would allow intepretations of the dummy responses relative to the severities of injuries that a child might experience in similar exposure environments. An animal test program was needed to provide such a basis. This paper presents the results of the test program that was conducted to obtain the animal injury data. Correlations between the observed animal injuries and corresponding child dummy response measurements are not discussed in this paper. That analysis is the subject of a separate paper by Mertz and Weber (12).

PROGRAM SCOPE

The program conceived was to subject anesthetized animals to a broad range of passenger cushion deployment-simulated collision exposure environments. The specific animal exposure environments were to be selected from child dummy tests that produced a wide range of dummy responses. It was anticipated that test conditions selected by this process would produce a wide range of animal injury types and severities that could be associated with the measured dummy responses.

Southwest Research Institute (SwRI) was contracted by GM to carry out the animal testing portion of the animal injury-child dummy response correlation study. The specific test conditions, test hardware, and animal positions were prescribed by GM based on their child dummy test results. SwRI was responsible for conducting the animal tests and documenting the types and severities of the injuries experienced by the animals.

Physiological measurements such as electrocardiogram (ECG), aortic blood pressure, evoked response, pinch withdrawal and palpebral reflex were made. Blood samples were drawn for gas analysis to aid in assessing the significance of pulmonary injuries. Since past experience had shown that serious internal organ trauma in animals may not be clinically diagnosed (1), all surviving animals were sacrificed usually 24 hours posttest, and gross necropsies were performed. Histopathology was done on the brain, spinal cord, heart and lungs.

A team of medical specialists was formed by SwRI to assess the significance of the observed animal injuries. The team consisted of a neurophysiologist, a neuropathologist, a cardiac pathologist, a cardiologist, a pulmonary specialist and a SwRI Senior Research Physician who served as the medical team leader. The medical specialists were directed to assess the severity of the animal injuries as if the injuries had occurred to a three-year-old child. In addition, each specialist was asked to develop a "dictionary" for his specialty that would describe the types of lesions observed and the injury severity ratings ascribed to the injuries. These dictionaries were to be "living" documents; that is, the specialists were encouraged to revise them based on the results of control tests that were conducted during the program. The medical team leader was responsible for the final injury severity ratings assigned to each test animal.

Each animal injury was assigned two injury severity values. One described the short-term consequences of the injury in terms of threat-to-life (TL value) and the other described the long-term consequences in terms of the potential for permanent impairment (PI value). General descriptions of the TL and PI severity classifications are given in Table 1. The TL descriptors were taken from "The Abbreviated Injury Scale—1980 Revision" (13). However, the injury descriptions contained in the dictionaries developed by the medical specialists are more detailed than those given by The Abbreviated Injury Scale, since each animal was necropsied and much more detailed injury information was available than would be available for a similar human injury. On the other hand, very little data were available on the long-term consequences of the animal injuries, since the animals were usually sacrificed 24 hours postimpact. For the most part, the PI ratings were based on the medical specialist's judgment of the most probable long-term consequences of the various injuries. While the PI ratings are quite subjective, they do serve an important need to rank the severities of brain, cervical spine and heart injuries relative to the potential for permanent impairment of major body functions.

To provide mechanical indicators of the severity of the various exposure environments, accelerometers were attached to the heads and torsos of the animals. The placement and procedure used to mount the accelerometers were chosen so as to not induce injury during the impact

Table 1. General descriptions of threat-to-life (TL) and permanent impairment (PI) injury severity classifications.

TL VALUE	DESCRIPTION OF THREAT-TO-LIFE CATEGORIES
0	NO INJURY
1	MINOR (NOT LIFE-THREATENING)
2	MODERATE (NOT LIFE-THREATENING)
3	SERIOUS (NOT LIFE-THREATENING)
4	SEVERE (LIFE-THREATENING, SURVIVAL PROBABLE)
5	CRITICAL (LIFE-THREATENING, SURVIVAL UNCERTAIN)
6	MAXIMUM (NOT SURVIVABLE)

PI VALUE	DESCRIPTION OF PERMANENT IMPAIRMENT CATEGORIES
0	NO INJURY
1	MINOR (POTENTIAL FOR SOME IMPAIRMENT OF MINOR BODY FUNCTION)
2	MODERATE (SOME IMPAIRMENT OF MINOR BODY FUNCTION)
3	MAJOR (POTENTIAL FOR IMPAIRMENT OF MAJOR BODY FUNCTION, IF UNTREATED)
4	SUBSTANTIAL (PARAPLEGIA)
5	EXTENSIVE (QUADRIPLEGIA)
6	TOTAL (IRREVERSIBLE COMA/DEATH)

or compromise the animal's ability to withstand the impact.

CARE AND USE OF ANIMALS

Southwest Research Institute (SwRI) Animal Medicine Program and Facilities are approved by the American Association for Accreditation of Laboratory Animal Care and the United States Department of Agriculture. Approval by these organizations is based on guidelines of the Animal Welfare Act of 1970 and the Guide for Care and Use of Laboratory Animals. In addition, all protocols involving animal care and testing are subjected to a review by the SwRI Animal Care Committee. This program was reviewed and approved by the SwRI committee as well as the General Motors Corporation Animal Use Committee.

TEST PROTOCOL

Preimpact

Two to three days prior to a test, two pigs whose weights were within the desired range of 15 ± 1 kg were selected as test candidates from the pig herd maintained at SwRI for the test program. These animals were sedated, weighed, depilated and given a physical examination by the veterinarian. Radiographs were taken of each animal and were examined for possible skeletal fractures and abnormal bone growth. On the day of the test, one of the pigs was selected as the test pig, the other serving as the backup. The test pig was sedated and an extensive set of anthropometric measurements was made. Then the animal was anesthetized and incisions were made to expose both femoral arteries. A blood pressure catheter was inserted into one femoral artery and was advanced towards the heart to the level of the xiphoid process. A 16-gauge catheter was placed in the other femoral artery for the purpose of drawing blood samples for gas analyses.

Just prior to transporting the animal to the sled facility, an accelerometer mounting bracket was applied to the animal's nose using two screws located in the midsagittal plane and a wire wrapped around the plate through the animal's mouth. A polyurethane foam solution was injected between the plate and the snout, and when cured, provided a stable accelerometer mounting bracket.

At the test facility the animal was connected to the physiological monitoring equipment and monitored at 15-minute intervals for one hour prior to the placement of the animal on the impact sled. At each interval the following parameters were recorded: blood pressure, 6-lead ECG, heart rate, respiration, rectal temperature, reflex responses to toe and ear pinch, palpebral reflex, pupil size and reactivity to light, and muscle tonus. Drugs were administered in sufficient dosages to produce an animal that was immobile and had adequate pain suppression while retaining good neurological response levels for the physiological testing.

During this hour monitoring period, the accelerometers and the tethering harness were attached to the animal. Four uniaxial accelerometers were mounted to the nose bracket. Three of these accelerometers were positioned with their sensitive axes orthogonal with two of the axes lying in the midsagittal plane of the animal's head. The fourth accelerometer was mounted with its sensitive axis lying in the midsagittal plane, oriented parallel to the sensitive axis of the ventro-dorsal accelerometer and positioned 38 mm closer to the tip of the animal's snout. Two configurations of accelerometers were used for the torso. For the first configuration, a triaxial accelerometer package was attached to the animal's spine at the level of the sixth thoracic spinous process using a nylon strap that encircled the animal's chest. After several tests, it became apparent that this configuration had the potential to injure the thoracic spinous process during rebound into the seat for some of the animal positions. To alleviate this condition, a second configuration consisting of four uniaxial accelerometers was developed. Three of the accelerometers were mounted to the sternum, one each at the presternal protuberance, mid sternum, and xiphoid process. Their sensitive axes were oriented ventral-dorsally, normal to the sternum. The fourth accelerometer was mounted to the thoracic spine at the level of the sixth spinous process. Its axis was oriented ventral-dorsally, normal to the spine. All four accelerometers were encased in individual, thin rubber disks that were held in place

by tape that encircled the animal's thorax. This configuration produced no indications of inducing any injury to the animal.

After the one-hour monitoring period was completed, blood was drawn for gas analysis and a complete set of visual and somatosensory evoked responses were taken. The animal was then taken to the sled and placed in the desired position. The animal was held vertically by a tether that was released just prior to cushion deployment. Its buttocks were supported by the seat, floor or foam blocks depending on the choice of animal position. Longitudinal and lateral position of the animal was maintained by paper tape that prevented the animal from translating rearward during the time the sled was being accelerated to the desired velocity, yet let the animal translate forward freely during the collision simulation. The tape was easily torn by the deploying cushion or by the rebound of the animal and had no effect on the animal's kinematics in response to the deploying cushion.

Once the animal was positioned it usually took ten minutes to balance and calibrate the instrumentation and go through the sled firing procedure. During this time the animal's position and physiological responses were continually monitored. Drugs were administered as required to assure a motionless animal with acceptable physiological response levels.

Postimpact

After the impact, the sled was moved under an exhaust fan to change and filter the interior air of the body buck, a safety procedure used when a number of tests are contemplated using sodium azide inflators. When visible emissions had abated, the body buck was opened and a preliminary examination of the animal was done by the attending medical doctor or veterinarian, who wore a respirator. Photographs were taken of the animal's position. The animal was then removed from the buck, sponged off and carried to the medical observation table where the physiological monitoring equipment was reconnected. The one-hour monitoring procedure described under preimpact was repeated. Two full sets of evoked responses were obtained during this period for comparison with the pretest data.

At the end of the one-hour postimpact monitoring period, blood was drawn for gas analysis. The blood pressure catheter was removed and the incision closed. The animal was transported to the SwRI X-ray facility where a full set of postimpact radiographs were taken. From the X-ray facility, the animal was returned to its holding cage for observation. At the end of the observation period (usually 24 hours), the animal was sedated and blood was drawn for gas analysis. Then, the animal was transported to the Necropsy laboratory where it was sacrificed and the gross necropsy was performed by the veterinary pathologist.

TEST CONDITIONS

The test conditions were selected by GM based on their analysis of child dummy tests that they had conducted at GM. For each animal test conducted at SwRI, a similar child dummy test was conducted at GM. This procedure was used to allow associations to be drawn between the observed animal injuries and corresponding measured child dummy responses. A summary of the test conditions is given in Table 2.

Simulated Crash Pulses—Three different sled deceleration pulse shapes were used during the test program. The severity of these simulated collisions can be described by their mean sled decelerations and velocity changes. Two constant-deceleration pulse shapes were used. The most severe pulse had a 14.5 g deceleration level with a change in velocity of 56 km/h. The other had a constant deceleration level of 8.4 g with a velocity change of 33.6 km/h. The third pulse shape was more trapezoidal and represented a car-to-car impact of longer duration. It had a mean deceleration level of 4.3 g and a velocity change of 28.5 km/h, and this was the mildest collision pulse used. The sled pulse used for each animal test is listed in Table 2.

Animal Positions—Seven basic animal positions, each representing a possible child position (9, 10), were used in the deployment tests. Examples of each position are shown in Figures 1 through 7. Table 3 provides descriptions of each position, distances between landmarks on the animal and the interior that were used in positioning the animals, and rationales for selecting each position for testing. Figure 8 shows the locations of the animal positioning landmarks relative to car interior landmarks. Deviations from these nominal dimensions were made during the course of the program in an effort to maximize the severity of the cushion/animal interaction. The nominal position and deviation for each animal test are given in Table 2.

Positions 1, 6 and 7 were used in preliminary tests that were conducted to select the animal species to be used as the principal surrogate for the test program. In the actual test program only Positions 1-5 were used. Position 6 was not used because the preliminary tests showed that the interaction between the animal and cushion was unpredictable for this position. In one test, the cushion deployed over the top of the animal's head. In a second test of the same position, the cushion deployed under the animal's chin. Position 5 was used instead of Position 6 in the test program in order to eliminate this inconsistency of cushion-animal interaction. Position 7, a side-facing position of the animal, was not used in the test program because the preliminary tests showed that the injury types and severities for this position were comparable to those of Position 1, the front-facing equivalent of Position 7.

Inflatable Restraint Systems—A summary of the inflatable restraint system concepts used for the various

Table 2. Summary of test conditions.

ANIMAL NUMBER	SLED KINEMATICS VEL. (km/h)	SLED KINEMATICS ACC. (G)	INFLATABLE RESTRAINT SYSTEM INFLATOR TYPE	INFLATOR ACTUATE (ms)	CUSHION TYPE	FOLD TYPE	COVER TYPE	ANIMAL POSITION NOMINAL	DEVIATIONS FORE-AFT (mm)	DEVIATIONS UP-DOWN (mm)	SEAT TYPE	SEAT POSITION
PIG 8	50.8	13.2	2	22	2	3	NONE	1	0	0	MODIFIED	FORWARD
PIG 9	54.9	14.3	2	20	2	1	NONE	1	0	6U	MODIFIED	FORWARD
PIG 10	56.8	14.8	2	20	2	2	NONE	1	0	0	MODIFIED	FORWARD
PIG 12	56.5	14.8	2	20	2	3	NONE	1	0	0	MODIFIED	FORWARD
PIG 13	56.8	14.8	2	20	2	1	NONE	2	19A	13U	MODIFIED	REAR
PIG 14	57.0	14.9	2	21	2	1	NONE	2	0	0	MODIFIED	REAR
PIG 15	57.0	14.8	2	20	2	3	NONE	1	16F	25U	MODIFIED	FORWARD
PIG 16	56.6	14.7	2	21	2	3	2	3	0	0	STD.	REAR
PIG 17	55.9	14.6	2	21	2	1	2	3	0	0	STD.	REAR
PIG 18	54.5	14.0	3	20	1	1	1	2	0	0	MODIFIED	REAR
PIG 19	33.3	8.4	4	28	1	1	1	2	44F	25D	MODIFIED	REAR
PIG 21	33.6	8.5	3	28	1	1	1	3	44F	13D	STD.	REAR
PIG 22	33.8	8.5	3	28	1	1	1	2	44F	25D	MODIFIED	REAR
PIG 23	33.8	8.4	3	18	1	1	1	2	0	0	MODIFIED	REAR
PIG 24	55.7	14.2	5	20	3	3	3	1	0	0	MODIFIED	FORWARD
PIG 25	34.0	8.6	5	28	3	3	3	1	0	0	MODIFIED	FORWARD
PIG 26	33.6	8.5	5	28	3	3	3	3	13F	0	STD.	REAR
PIG 29	33.6	8.5	6	29	4	1	3	2	0	0	MODIFIED	REAR
PIG 35	34.2	8.6	5	26	4	1	3	2	0	0	MODIFIED	REAR
PIG 38	33.7	8.6	5	28	4	1	3	2	0	0	MODIFIED	REAR
PIG 41	32.9	8.3	5	36	4	1	3	2*	13A	25U	MODIFIED	FORWARD
PIG 44	33.5	8.5	5	28	4	1	3	2*	0	25U	NONE	PADDING
PIG 46	32.9	8.3	3	0	1	1	1	3	44F	13D	STD.	REAR
PIG 47	33.4	8.3	3	29	1	1	1	3	44F	13D	STD.	REAR
PIG 51	33.6	8.3	7	27	5	4	3	1	6F	0	MODIFIED	FORWARD
PIG 52	33.8	7.8	7	28	5	4	3	3	6F	0	STD.	REAR
PIG 67	34.6	8.8	9	28	5	4	3	3	3F	3U	STD.	REAR
PIG 68	32.6	8.2	8	28	6	4	3	4	0	0	STD.	MID
PIG 69	34.2	8.6	8	27	6	4	3	3	6F	0	STD.	REAR
PIG 70	33.2	8.4	9	29	5	4	3	2	6F	0	MODIFIED	REAR
PIG 72	33.4	8.5	9	28	5	4	3	2	3F	25U	MODIFIED	REAR
PIG 80	28.3	4.2	10	25	7	5	3	3	30F	0	STD.	REAR
PIG 81	28.5	4.3	10	25	7	5	3	1	51F	3U	MODIFIED	REAR
PIG 83	28.8	4.3	10	25	7	5	3	3	41F	51D	STD.	REAR
PIG 84	28.8	4.3	10	25	7	5	3	2	51F	0	MODIFIED	REAR
PIG 85	28.9	4.3	10	25	7	5	3	4	0	0	STD.	MID
PIG 87	28.4	4.2	10	25	7	5	3	3	57F	51D	STD.	REAR
PIG 88	28.6	4.4	10	25	8	5	3	3	60F	51D	STD.	MID
PIG 89	28.4	4.2	10	25	8	5	3	2	51F	0	STD.	REAR
PIG 91	28.7	4.3	10	25	8	5	3	1	32F	38U	STD.	REAR
PIG 93	28.4	4.2	10	25	8	5	3	4**	-	-	STD.	MID
PIG 94	28.1	4.3	10	25	8	5	3	4	0	0	STD.	MID
PIG 151	28.6	4.2	10	25	8	5	3	5	0	0	STD.	MID
BAB 6	55.9	14.3	2	20	2	1	2	3	13F	6U	STD.	REAR
BAB 7	28.3	4.2	10	25	8	5	3	4	0	0	STD.	MID
BAB 8	28.6	4.2	10	25	8	5	3	5	0	0	STD.	MID

NOTES: * LOWER TORSO RESTRAINED BY STRAP
** TETHER SUPPORT RELEASED PRIOR TO SLED DECELERATION. PIG NOT IN POSITION 4 AT TIME OF CUSHION DEPLOYMENT.

animal tests is given in Table 2. Ten different types of inflators were used in combinations with eight types of cushions, four types of cushion folds, and three types of covers. Inflators 1, 3 and 4 were compressed gas inflators. The other inflators used sodium azide to generate the cushion inflation gases. All ten inflators had different gas flow characteristics. Cushions 1 through 4 were "circular cylinder designs" of diferent volumes and incorporated an internal knee restraint cushion (2). Cushions 5-8 were different concepts of "L-shaped" cushions (14). Fold 1 was an "accordion" fold that was symmetrically folded on top and bottom. This fold allowed the cushion to be deployed horizontally rearward. Folds 2-5 were different versions of a "top pleated" fold. These were asymmetrically folded with the bottom most part of the cushion being the layer nearest the cushion door. This type of fold restricted the initial rearward movement of the cushion and resulted in a more upward cushion trajectory. Cover 1 was a foam-filled construction. Covers 2 and 3 were injection moldings of different lengths and cross-sectional shapes.

Front Seat Description—Production type seats were used for the tests. In some instances, the seat cushion and frame had to be modified in order to place the animal in the desired position. For these tests, the front of the seat frame was removed and the thickness of the cushion padding was adjusted to give the desired seat height. Table 2 gives a summary of the seat positions and indicates whether or not the seat was modified for the various tests conducted.

ANIMAL SPECIES SELECTION

The primary consideration for the selection of an animal species to be used as the child surrogate for the test program was that its weight and size be comparable to a 3-year-old child, since that size child dummy was being used by GM in their passenger inflatable restraint system development program (11). Three animal species, the chimpanzee, the baboon and the pig, were considered as candidates for the animal model. Based on comparable

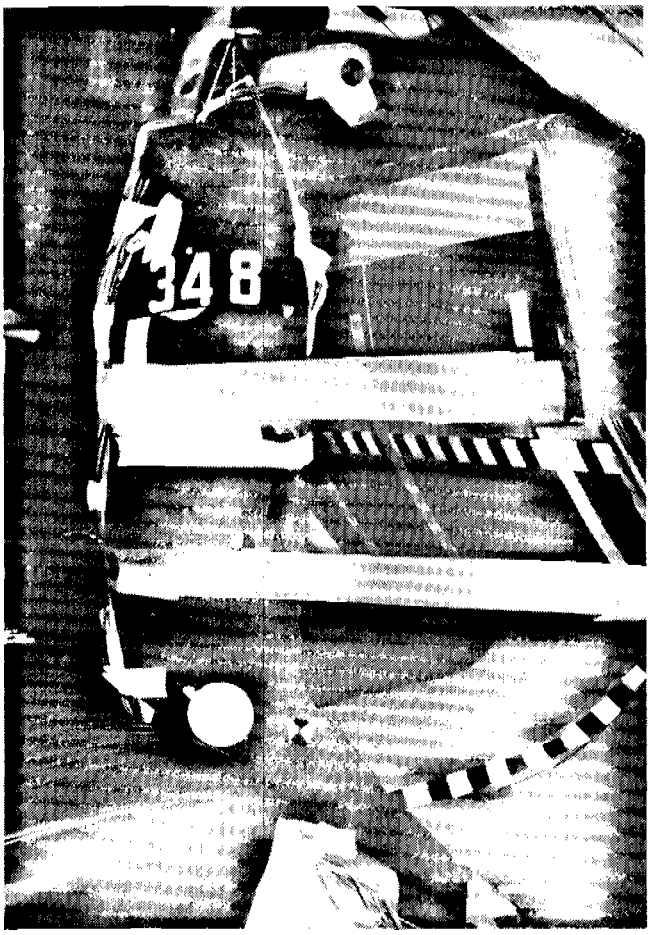

Figure 1. Animal position 1.

size and shape, the chimpanzee was the most logical choice. However, the test protocol required that each animal be impacted only once and necropsied for injury identification. This procedure required that a large quantity of animals be available for testing in order to meet the program objective of producing a broad spectrum of injury types and severities. A sufficient quantity of chimpanzees was not available to meet this program requirement. Consequently, only the baboon and pig were considered as possible animal models for this program.

The pig was selected as the animal model for the 3-year-old child for the following reasons:

i) it was available in large enough quantities to support the test program,
ii) it had more favorable anthropometric characteristics for its chest and abdomen than the baboon,
iii) its physical stage of development was similar to a 3-year-old child's, and
iv) it appeared to be more susceptible to injury than the baboon based on the results of a preliminary test program.

Limited testing was to be done with baboons for comparison purposes. The following is a detailed discussion of the reasons the pig was selected as the primary animal model for the test program.

Size and Shape Considerations—Table 4 gives typical size and shape measurements for the baboon, pig and a 3-year-old child of comparable weights. The pig was considered the preferred animal model over the baboon for investigating the potential for child thoracic and abdominal injuries since the breadths and circumferences of its chest and abdomen compare more favorably to the child's. Both the pig and the baboon have a major anthropometric deficiency as a child thoracic injury model in that their chest depth-to-width ratios are the inverse of the child's. Because of this geometric difference, both animals' fore-aft chest stiffnesses are much greater than the child's resulting in greater force levels required to produce compression type injuries to the thoracic organs.

For assessing the potential for child neck injuries, the pig has an advantage over the baboon since its head-neck length compares more favorably to the child's. However, both species have a number of major deficiencies as neck injury models. The pig has no chin protuberance for interacting with the deploying cushion since its neck attaches to the rear of its skull, resulting in its snout being somewhat aligned with its cervical spine. In contrast, the

Figure 2. Animal position 2.

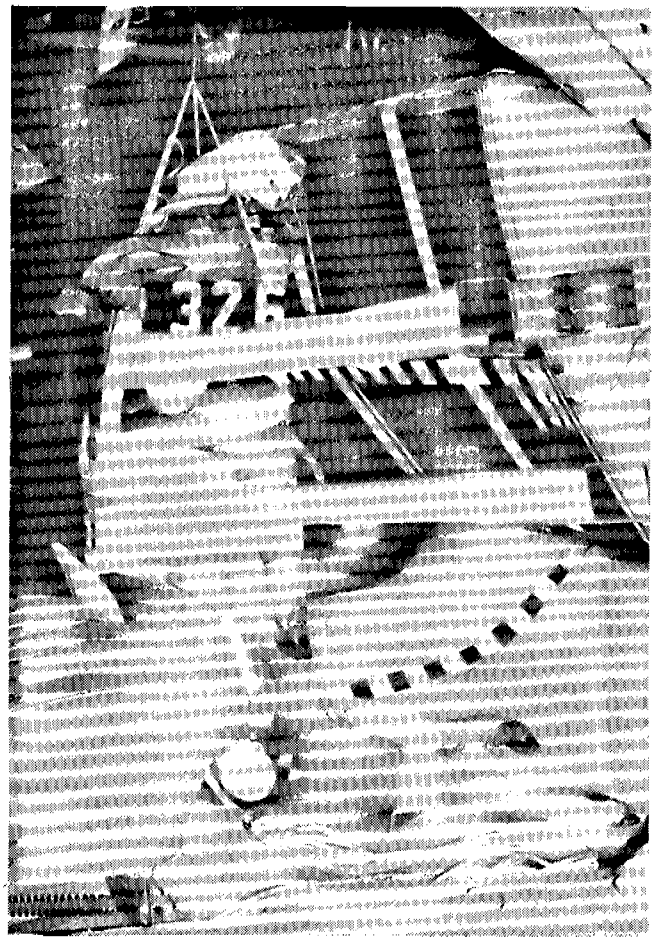

Figure 3. Animal position 3.

baboon's neck attaches to the base of the skull similar to the human. However, its long muzzle provides an accentuated, simulated chin protuberance. The fore-aft range of motion of the pig's head-neck structure is much less than the child's, resulting in a smaller degree of rearward motion required to produce a hyperextension neck injury. The baboon can undergo a greater degree of hyperextension than the child. The pig's neck circumference is twice as large as the child's due to its large dorsal neck muscles. However, these muscles have little influence on its head-neck kinematics since the animal is anesthetized. The cervical vertebrae of the pig and child are of similar size.

Neither animal species is considered a good model for assessing the potential for child brain injuries since their brains are much smaller in size than a child's.

Physical Development Consideration—The ages of a baboon and pig of comparable weight of a 3-year-old child are 4.3 years and 10 weeks (0.19 years), respectively (Table 4). To estimate an age of equivalent physical development for these animals, the animal's age was multiplied by the ratio of the ages that humans (15.5 years) and the animals (baboon—4.0 years and pig—0.7 years) begin to produce mature sperm. These calculations gave equivalent physical development ages of 16.6 and 4.2 years for the baboon and pig, respectively. Based on this analysis, the state of physical development of a pig and a 3-year-old child of similar weight are quite comparable. The baboon's physical development is much more advanced.

Injury Susceptibility Consideration—To determine if either species was more susceptible to injury than the other, a preliminary test series was conducted using 5 pigs and 5 baboons. Four pigs and four baboons were tested in Positions 1 and 7 with two of each species exposed in each of the two positions. A single test of each species was conducted in Position 6. Examples of these animal positions are shown in Figures 1, 6 and 7. The inflatable restraint system used for these preliminary tests consisted of Inflator 1, Cushion 1, Fold 1 and Cover 1. The sled pulses were characterized by a 13.6 g plateau and a 50 km/h velocity change. The cushion was actuated 21 ms after the beginning of the simulated collision event. A standard bench seat was used in the full forward position for these tests. The injury types and severities produced by these exposures are given in Table 5.

For Positions 1 and 7, the cushion-animal involvements were quite similar and produced similar types of injuries.

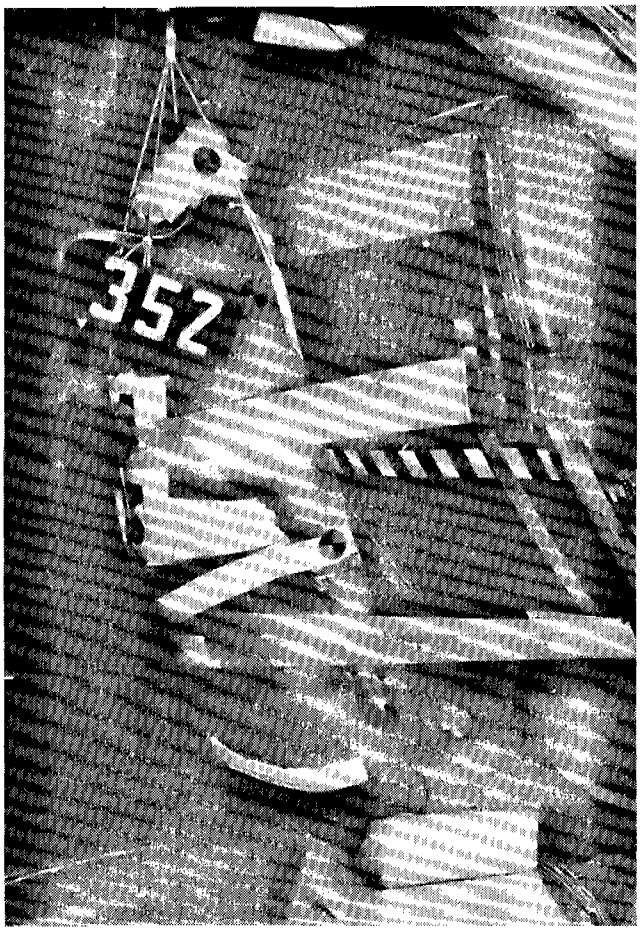

Figure 4. Animal position 4.

Table 3. Description of Animal Positions.

ANIMAL POSITION			ANIMAL TO INSTRUMENT PANEL REFERENCE		SELECTION RATIONALE
POS. NO.	FIG. NO.	DESCRIPTION	REFERENCE POINTS	DISTANCE (mm)	
1	1	SPINE VERTICAL, HEAD ABOVE I.P. BROW, XIPHOID 50 MM ABOVE CENTERLINE OF INFLATOR.	XIPHOID TO INFLATOR CENTERLINE	325 REAR 50 ABOVE	• EXPOSE ABDOMEN TO DEPLOYING CUSHION/COVER. • EXPOSE HEAD AND NECK TO UPWARD DEPLOYING L-CUSHION DESIGN.
2	2	SPINE VERTICAL, SNOUT ON I.P. BROW, XIPHIOD AT SAME LEVEL OF INFLATOR CENTERLINE.	XIPHIOD TO INFLATOR CENTERLINE	300 REAR 0 ABOVE	• EXPOSE THORAX TO DEPLOYING CUSHION/COVER.
3	3	SPINE VERTICAL, SNOUT AT I.P. BROW, PRESTERNAL PROTUBERANCE AT LEVEL OF TOP OF COVER.	PRESTERNAL PROTUBERANCE TO INFLATOR CENTERLINE	290 REAR 115 ABOVE	• EXPOSE HEAD/NECK TO DEPLOYING CUSHION/COVER.
4	4	SIMILAR SNOUT & PRESTERNAL PROTUBRANCE LOCATIONS AS POSITION 3, LOWER TORSO ROTATED FORWARD PARALLEL TO COVER.	PRESTERNAL PROTUBERANCE TO INFLATOR CENTERLINE	240 REAR 115 ABOVE	• EXPOSE HEAD/NECK AND TORSO TO DEPLOYING CUSHION/COVER.
5	5	SPINE 30° TO HORIZONTAL, SNOUT MIDWAY BETWEEN TOP OF COVER AND I.P. BROW.	TIP OF SNOUT AND I.P. PANEL	AGAINST I.P. PANEL	• EXPOSE HEAD/NECK TO UPWARD DEPLOYING L-CUSHION DESIGN.
6	6	SPINE HORIZONTAL, SNOUT JUST ABOVE TOP OF COVER.	TIP OF SNOUT & I.P. PANEL	AGAINST I.P. PANEL	• EXPOSE HEAD/NECK TO COMPRESSION LOADING OF DEPLOYING CUSHION/COVER.
7	7	SAME AS POSITION 1 EXCEPT ANIMAL IS FACING LEFT INSTEAD OF FORWARD, SHOULDER AGAINST I.P. BROW.	XIPHIOD TO INFLATOR CENTERLINE	325 REAR 100 ABOVE	• EXPOSE SIDE OF ABDOMEN TO DEPLOYING CUSHION/COVER • DETERMINE EFFECT OF ORIENTATION OF INJURY TYPE AND SEVERITY.

Table 4. Typical size, shape and mass measurements for 15 kg pigs, baboons, and children.

MEASUREMENT	AVERAGE OF 5 PIGS	AVERAGE OF 4 BABOONS	3-YEAR-OLD MALE CHILD	
			VALUE	REF.*
AGE (YEARS)	0.19	4.3	3	-
EQUIVALENT CHILD AGE (YEARS)**	4.2	16.3	3	-
MASS (kg)	14.9	15.2	14.9	15
SEATED HEIGHT (mm)	746	641	592	15
HEAD-NECK LENGTH (mm)	241	147	226	15
HEAD WIDTH (mm)	111	110	136	15
FORE-AFT HEAD MOTION (DEG)	45	110	105	12
NECK CIRCUMFERENCE (mm)	421	271	243	15
CHEST CIRCUMFERENCE (mm)	529	509	516	15
CHEST BREADTH (mm)	138	110	165	15
CHEST DEPTH TO BREADTH RATIO	1.33	1.44	0.67	15
ABDOMINAL CIRCUMFERENCE AT UMBILICUS (mm)	580	392	486	15
ABDOMINAL BREADTH AT UMBILICUS (mm)	147	125	165	15

NOTES:

* NUMBERS REFER TO PAPERS IN LIST OF REFERENCES.

** EQUIVALENT CHILD AGE = $\frac{\text{HUMAN PUBERTY AGE}}{\text{ANIMAL PUBERTY AGE}}$ x (ANIMAL TEST AGE)

The pig, however, appeared to experience more severe injuries. For Position 6, the animal-cushion interactions were quite different. The cushion deployed under the pig's snout driving the animal upwards and rearwards, hyperextending its neck. For the baboon, the cushion deployed

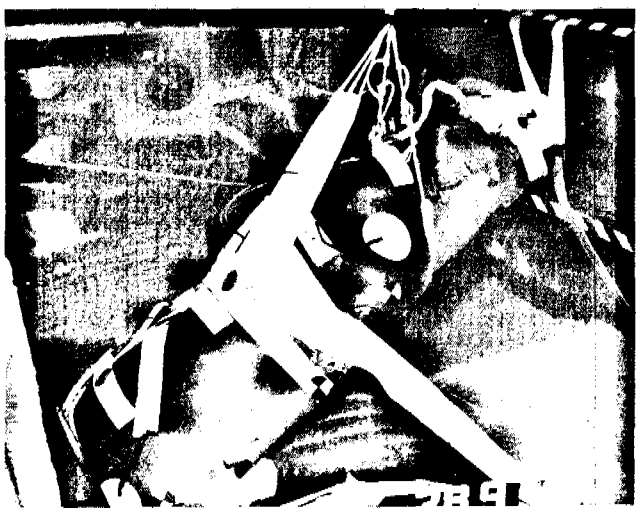

Figure 5. Animal position 5.

Table 5. Summary of animal injuries and severities for the preliminary test series.

BODY REGION INJURED ORGANS	ANIMAL POSITION 1				ANIMAL POSITION 7				ANIMAL POS. 6	
	PIG 1 (TL)	PIG 3 (TL)	BAB 1 (TL)	BAB 3 (TL)	PIG 2 (TL)	PIG 4 (TL)	BAB 2 (TL)	BAB 4 (TL)	PIG 5 (TL)	BAB 5 (TL)
HEAD										
BRAIN	6	2	3	3	2	3	3	2	6	3
NECK										
CERVICAL SPINE/CORD	4	0	0	3	0	3	0	0	4	2
TRACHEA	3	0	0	3	0	2	2	3	0	2
THORAX										
THORACIC SPINE	0	0	0	3	0	3	3	0	0	3
RIBS	0	2	0	0	0	0	0	0	2	0
HEART	3	0	0	0	0	3	0	0	0	0
LUNGS	3	2	1	0	1	1	3	1	3	0
ABDOMEN										
DIAPHRAGM	2	2	0	0	0	2	0	0	0	0
LIVER	4	2	2	3	3	3	3	1	2	0
GALL BLADDER	0	0	0	3	0	0	0	0	0	0
SPLEEN	0	3	3	3	0	4	0	0	1	0
INTESTINES	0	0	2	2	0	0	2	2	1	0
MESENTERY	1	2	1	1	0	1	0	0	1	0
KIDNEY	0	0	0	1	0	0	0	0	0	0
BLADDER	0	0	1	0	0	0	0	0	0	0

Figure 6. Animal position 6.

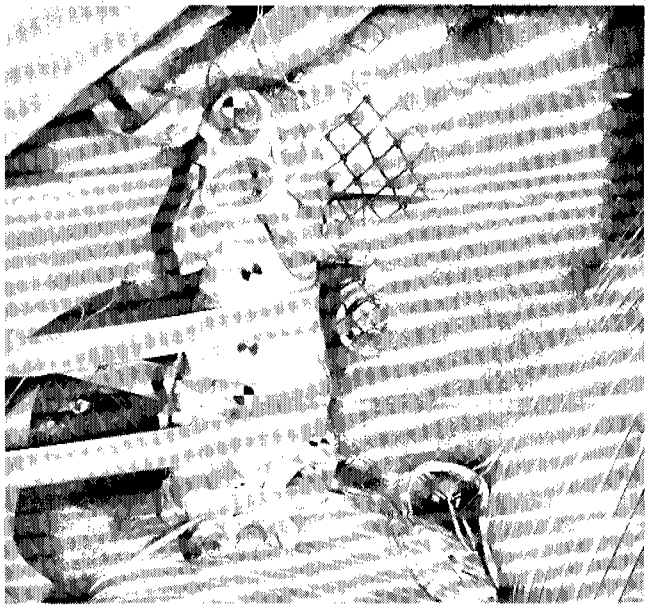

Figure 7. Animal position 7.

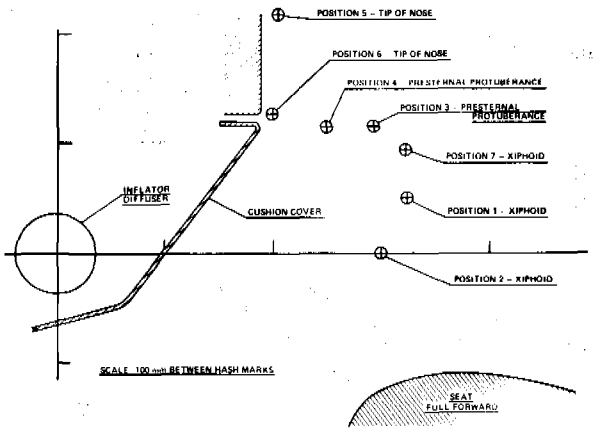

Figure 8. Locations of animal positioning landmarks relative to car interior landmarks.

over its head and there was minimum cushion-animal interaction. Based on these limited tests, the pig appeared more susceptible to injury than the baboon.

TEST RESULTS

Forty-three pigs and three baboons were subjected to the deploying cushion-collision interaction forces. The means and standard deviations of pertinent size, shape and mass measurements of these animals are given in Table 6. A summary of test results is given in Table 7 for each animal exposed to the deployment-collision forces for the test conditions given in Table 2. The peak internal inflator pressure is given in Table 7 for all the gas generating inflators. No pressures are listed for Inflators 3 and 4 which used compressed gas. Care should be exercised in interpreting the HIC and peak resultant head acceleration values since head acceleration was not measured at the center of gravity of the animal's head. Overall injury severity ratings in terms of threat-to-life (TL) and threat-of-permanent impairment (PI) are given for the body regions of the head, neck, thorax and abdomen.

For the pig tests, threat-to-life injuries ranging from 0 to 6 were observed for the head, neck and abdominal regions. Thoracic injuries ranged from TL equal to 0 to 5. The most significant pig injuries were subdural brain hemorrhages, partial transection of the cervical cord, rupture of the apical odontoid ligament, excessive straining of the membranes and ligaments surrounding the atlas-occipital region, cervical spine fractures, lung and heart contusions, persistent abnormal ECG readings, extensive rib fractures, liver tears, and lumbar spine fractures. Five of the animals (Pigs 8, 14, 15, 16 and 17) died as a result of their injuries. These test results indicate that the primary program objective of obtaining a wide spectrum of injury types and severities to the head, neck and torso regions was achieved.

The three baboon tests provided results similar to those observed in the preliminary test series. The baboon injury types were similar to the pigs, but the severities were somewhat less.

Caution must be used in interpreting the significance of these animal injuries relative to the expected performance of passenger inflatable restraint systems in general. It must be remembered that the objective of the study required using very aggressive passenger inflatable restraint system concepts for some of the tests in order to produce severe injuries to the animals. Because severe injuries were produced does not imply that all passenger inflatable restraint system concepts are aggressive. The fact is animals were exposed to several passenger inflatable restraint system concepts that were much less aggressive than the systems used to produce many of the severe animal injuries.

DISCUSSION OF RESULTS

Significant Animal Injuries

Head Injuries—Seven of the forty-six animals had significant (TL or PI ratings equal or greater than 3) head injuries. A summary of these injuries is given in Table 8. Four of these animals (Pigs 8, 15, 16 and 17) suffered fatal brain injuries. A photograph of the brain of Pig 8 is shown in Figure 9. Note the extensive subdural hemorrhage.

Table 6. Means and standard deviations of pertinent size, shape and mass measurements for the tested animals.

MEASUREMENT	PIGS			BABOONS		
	MEAN	STD. DEV.	COEFF. VAR.	MEAN	STD. DEV.	COEFF. VAR.
AGE (YEARS)	0.20	0.02	10%	5.2	0.8	15%
BODY MASS	15.7	1.0	6%	16.0	1.5	9%
BRAIN & SPINAL CORD	0.096	0.006	6%	0.183	0.005	3%
HEART	0.091	0.015	16%	0.068	0.007	10%
LIVER	0.490	0.078	16%	0.305	0.035	11%
SPLEEN	0.039	0.011	28%	0.028	0.019	68%
LEFT KIDNEY	0.044	0.006	14%	0.029	0.005	17%
RIGHT KIDNEY	0.042	0.006	14%	0.028	0.004	14%
SEATED HEIGHT	723	34	5%	661	13	2%
HEAD - NECK LENGTH	219	19	9%	125	6	5%
HEAD BREADTH	108	5	5%	110	6	5%
NECK CIRCUMFERENCE	448	28	6%	247	60	24%
STERNUM LENGTH	161	12	7%	159	12	8%
CHEST BREADTH	144	17	12%	112	17	15%
CHEST DEPTH	186	17	9%	146	7	5%
CHEST CIRCUMFERENCE	542	17	3%	499	54	11%
ABDOMINAL CIRCUM.	600	27	5%	463	11	2%
ABDOMINAL BREADTH	143	24	17%	143	16	11%

NOTES: BODY AND ORGAN MASSES GIVEN IN kg.
DIMENSIONS GIVEN IN mm.

Table 7. Summary of test results.

ANIMAL NUMBER	PEAK INFLATOR PRESSURE (Mpa)	HIC*	PK. HEAD RESULT. ACC.* (G)	PEAK V-D SPINE ACC. (G)	PEAK V-D STERNUM ACC.** (G)	PEAK BLOOD PRESSURE (mm Hg)	ANIMAL INJURY SEVERITY			
							HEAD (TL/PI)	NECK (TL/PI)	THORAX (TL/PI)	ABDOMEN (TL/PI)
PIG 8	19.0	--	--	--	--	375	6/6	6/6	5/3	0/0
PIG 9	14.4	--	--	114	--	570	2/1	0/0	3/1	3/2
PIG 10	17.0	19300	675	101	--	500	4/3	0/0	2/1	2/1
PIG 12	16.7	8570	350	120	--	310	2/0	4/4	3/2	2/1
PIG 13	18.4	1080	164	147	--	530	0/0	3/3	4/3	5/4
PIG 14	15.2	2470	143	152	--	600+	3/2	4/4	5/4	6/6
PIG 15	17.4	10300	494	132	--	490	6/6	6/6	4/2	4/4
PIG 16	16.1	22800	798	--	--	370	6/5	5/4	3/2	2/1
PIG 17	15.7	6270	264	--	--	600	5/4	5/4	4/3	4/2
PIG 18	--	7410	321	259	--	325	4/2	3/3	4/3	4/2
PIG 19	--	1760	146	--	--	390	0/0	2/1	1/0	1/0
PIG 21	--	5060	309	--	--	530	1/1	3/3	3/1	0/0
PIG 22	--	3790	240	--	--	610	2/1	4/4	2/1	3/1
PIG 23	--	--	--	--	--	280	0/0	3/1	3/1	2/1
PIG 24	6.0	--	--	93	--	190	2/2	3/4	2/1	2/1
PIG 25	6.8	1350	180	55	--	210	0/0	5/5	2/1	2/1
PIG 26	5.6	1120	133	48	--	210	2/1	4/4	2/1	0/0
PIG 29	7.1	1760	193	69	--	380	2/1	3/4	2/1	4/2
PIG 35	5.5	--	--	121	--	240	2/2	0/0	4/3	4/2
PIG 38	5.9	1980	136	104	--	390	2/2	0/0	3/2	0/0
PIG 41	4.7	433	94	79	--	230	2/1	0/0	1/0	0/0
PIG 44	4.6	102	53	--	--	210	0/0	0/0	1/0	0/0
PIG 46	--	897	194	--	--	360	2/2	0/0	1/0	2/1
PIG 47	--	1770	151	--	--	260	0/0	3/3	2/1	1/1
PIG 51	9.8	866	103	46	--	195	0/0	0/0	(3/2)	2/1
PIG 52	10.3	2140	175	61	--	235	1/0	3/4	2/1	2/1
PIG 67	11.0	1220	121	84	--	220	2/1	0/0	1/1	2/1
PIG 68	6.1	--	--	57	--	400	2/1	3/2	3/2	3/2
PIG 69	5.5	1270	137	60	--	200	0/0	0/0	1/0	0/0
PIG 70	11.1	1020	170	52	--	260	2/1	4/4	2/1	0/0
PIG 72	11.6	765	164	63	--	330	0/0	0/0	2/0	2/2
PIG 80	10.8	455	132	38	1040U	145	2/1	0/0	0/0	0/0
PIG 81	10.6	325	100	35	1260U	160	0/0	1/1	1/0	0/0
PIG 83	10.9	450	93	43	685U	178	1/1	0/0	1/0	0/0
PIG 84	11.3	765	190	97	1110U	110	0/0	3/3	1/0	0/0
PIG 85	9.7	2440	184	166	1400L	420	0/0	3/4	2/0	0/0
PIG 87	9.7	1400	252	78	1740M	205	0/0	2/1	1/0	0/0
PIG 88	8.9	620	168	62	1340L	255	1/0	0/0	1/0	1/1
PIG 89	9.4	345	107	63	1300L	220	0/0	0/0	2/1	0/0
PIG 91	9.2	335	76	27	1520M	220	1/0	0/0	1/0	0/0
PIG 93	9.7	1850	221	97	570U	480	0/0	3/4	2/1	1/1
PIG 94	9.3	3000	332	86	2220L	625	2/1	4/4	2/1	4/3
PIG 151	9.5	1015	128	23	103U	250	1/1	0/0	2/1	0/0
BAB 6	13.0	3480	167	--	--	400	1/1	0/0	2/1	2/1
BAB 7	9.7	4810	243	297	2340U	490	1/0	3/3	3/1	4/3
BAB 8	9.5	2650	215	30	1190L	270	0/0	2/1	2/0	3/2

NOTES:
* NOT MEASURED AT CENTER OF GRAVITY OF THE HEAD.
** ACCELEROMETER GIVING PEAK RESPONSE: U-UPPER, M-MID, L-LOWER.
( ) - THORACIC INJURY MAY HAVE OCCURRED PRETEST.

Neck Injuries—Twenty-four of the forty-six animals experienced significant neck injuries. Table 9 gives a summary of these injuries. Two of the animals (Pigs 8 and 15) suffered fatal neck injuries. Pig 8 had a subluxation of the atlanto-occipital joint with torn joint ligaments and extensive subdural and subarachnoid hemorrhages of the cervical cord. Pig 15 had a fracture of the dorsal arch of C5 including the articular process and a partial transection of the cervical cord at the level of C5.

The most frequent neck injury observed was hemorrhage within the atlas-occipital joint capsules and/or hemorrhage dorsal of the membrane covering the midsagittal-ventral aspect of the atlas-occipital junction. Such hemorrhages were observed in twenty of the twenty-four animals with significant neck injury and appeared to be a good indicator of the onset of damage to the apical odontoid ligament, the ligament extending from the tip of the odontoid process to the occiput. In a number of instances, hemorrhage of the apical odontoid ligament was observed and was rated as TL/PI = 3/4.

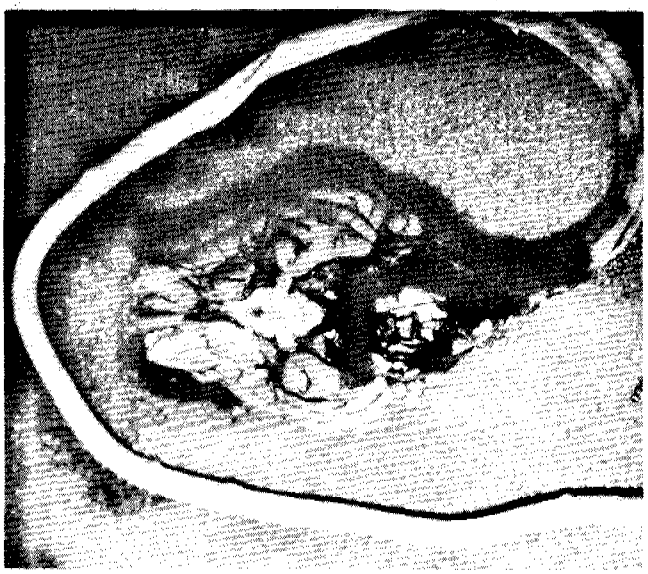

Figure 9. Brain of pig 8 showing extension subdural hemorrhage.

Table 8. Summary of animals with significant brain injuries.

ANIMAL NUMBER	HEAD INJURY SEVERITY (TL/PI)	INJURY DESCRIPTION	COMMENTS
8	6/6	DURAL SINUS LACERATION, EXTENSIVE SUBDURAL AND SUBARACHNOID HEMORRHAGE. NO PALPEBRAL REFLEX RESPONSE.	PIG DIED 12 MINUTES POSTIMPACT OF HEAD/NECK INJURIES.
15	6/6	SEVERE CONTUSION OF BRAIN STEM & CERVICAL CORD. NO PALPEBRAL REFLEX RESPONSE.	PIG DIED 2 1/4 MINUTES POSTIMPACT OF HEAD/NECK INJURIES.
16	6/5	SEVERE SUBDURAL & SUBARACHNOID HEMORRHAGE OF BRAIN STEM. ABSENT, DIMISHED, THEN ABSENT PALPEBRAL REFLEXES.	PIG DIED 39 MINUTES POSTIMPACT OF HEAD/NECK INJURIES.
17	5/4	DIFFUSE SUBARACHNOID HEMORRHAGE. ASYMMETRIC, THEN ABSENT PALPEBRAL REFLEXES. MARKED DEPRESSED RESPIRATION AND BLOOD PRESSURE.	PIG DIED 55 MINUTES POSTIMPACT OF APPARENT BRAIN STEM INJURY.
10	4/3	ACUTE BRAIN CONTUSION, ISCHEMIC, LEFT DORSAL TEMPORAL LOBE. ABSENT, THEN DEPRESSED PALPEBRAL REFLEXES.	
18	4/2	DIFFUSE BRAIN CONTUSION. PALPEBRAL REFLEXES DIMINISHED FOR 30 MINUTES POSTIMPACT.	RESPIRATION AND BLOOD PRESSURE DEPRESSED FOR 10 MINUTES POSTIMPACT.
14	3/2	PARENCHYMAL HEMORRHAGE. ASYMMETRIC, THEN ABSENT PALPEBRAL REFLEXES.	PIG DIED 24 MINUTES POSTIMPACT DUE TO BLOOD LOSS FROM SEVERELY LACERATED LIVER.

Fractures of the cervical spine were observed in three animals (Pigs 15, 17 and 68). Pig 15 had a fracture of the lateral arch of C5 including the articular process which resulted in partial transection of the cervical cord. This fracture was rated TL/PI = 5/4 because of the consequences of the fracture relative to severe damage to the cord. Pig 17 experienced a similar type fracture of C6 without involvement of the articular process or cord and was rated as TL/PI = 4/3. Both of these fractures were rated more severe than the rating given in the AIS-80 code (13) because of the potential for severe cord damage. Pig 68 experienced a simple fracture of the spinous process of C7 which was rated as TL/PI = 3/2.

Significant pathological changes in the cervical cord were found in only four of the twenty-four animals (Pigs 15, 25, 12 and 47) that had significant neck injuries. Pig 15 had the most severe cord trauma, a partial transection which was rated as TL/PI = 5/3. Pig 47 had cord damage rated as TL/PI = 3/3 without any evidence of cervical spine damage. It is difficult to understand how the cord could be damaged without attendant cervical spine damage. Perhaps the pathological observations of petechial hemorrhages is an artifact of the histology or necropsy protocol.

Thoracic Injuries—Sixteen of the forty-six animals had significant thoracic injuries. These injuries are summarized in Table 10. None of the animals experienced fatal thoracic lesions; however, Pigs 14 and 8 did suffer critical (TL/PI = 5/4 and 5/3, respectively) thoracic injuries. Pig 14 had extensive rib fractures, a first and second degree AV block followed by an incomplete right bundle branch block, and pathological damage to the heart and lungs. This animal died 24 minutes postimpact of blood loss from a severely lacerated liver. Pig 8 had a fracture of the body of T8, profound bradycardia and pathological damage to the heart and lungs. This animal died two minutes postimpact of fatal head and neck injuries.

Twelve of the sixteen animals had significant pathological damage to the heart. Six had significant lung damage. Significant changes in ECG occurred in five animals, including one baboon. Five animals had rib fractures with Pig 14 having the most extensive fractures. Three animals (Pigs 8, 18 and 68) had thoracic vertebral fractures. The heart lesion noted for Pig 51 may not have been related to the impact since histology indicated that it may have been an old injury.

In a number of cases, the overall thoracic injury rating is more severe than any of the individual ratings. These

Table 9. Summary of animals with significant neck injuries.

ANIMAL NUMBER	NECK INJURY SEVERITY (TL/PI)	CERVICAL SPINE			OTHER (TL/PI)
		SPINAL CORD (TL/PI)	ATLAS-OCCIPUT JOINT DAMAGE (TL/PI)	FRACTURE (TL/PI)	
PIG 8	6/6	2/2	6/6	0/0	
PIG 15	6/6	5/3	4/4	5/4	PARTIALLY SEVERED CERVICAL MUSCLE (3/3).
PIG 25	5/5	3/2	5/5	0/0	
PIG 16	5/4	2/1	4/4	0/0	
PIG 17	5/4	1/0	3/3	4/3	
PIG 26	4/4	2/1	4/4	0/0	
PIG 94	4/4	2/1	4/4	0/0	
PIG 70	4/4	0/0	3/4	0/0	HEMORRHAGE, ATLAS-AXIS JOINT (3/3).
PIG 22	4/4	0/0	4/4	0/0	
PIG 14	4/4	2/2	4/4	0/0	
PIG 12	4/4	3/2	4/4	0/0	HEMORRHAGEIC CERVICAL MUSCLE (3/2).
PIG 85	3/4	0/0	3/4	0/0	
PIG 52	3/4	0/0	3/4	0/0	
PIG 29	3/4	0/0	3/4	0/0	
PIG 24	3/4	0/0	3/4	0/0	
PIG 93	3/4	1/0	3/4	0/0	
BAB 7	3/3	0/0	3/3	0/0	
PIG 18	3/3	2/1	3/3	0/0	
PIG 13	3/3	0/0	3/3	0/0	
PIG 84	3/3	0/0	3/3	0/0	
PIG 21	3/3	0/0	0/0	0/0	HEMORRHAGE, ATLAS-AXIS JOINT (3/3).
PIG 47	3/3	3/3	0/0	0/0	
PIG 68	3/2	0/0	0/0	3/2	
PIG 23	3/1	0/0	0/0	0/0	CONTUSED MUCOSAL SURFACE, LARYNX (3/1).

Table 10. Summary of animals with significant thoracic injuries.

ANIMAL NUMBER	THORACIC INJURY SEVERITY (TL/PI)	THORACIC OBSERVATIONS				OTHER (TL/PI)
		LUNG DAMAGE (TL/PI)	HEART DAMAGE (TL/PI)	ECG (TL/PI)	RIB FRACTURE (TL/PI)	
PIG 14	5/4	3/1	3/2	4/4	3/2	
PIG 8	5/3	4/2	4/2	4/2	0/0	FRACTURE OF BODY OF T8 (3/3).
PIG 35	4/3	2/0	4/3	2/1	0/0	
PIG 18	4/3	2/1	3/2	3/2	2/1	FRACTURE OF SPINOUS PROCESSES OF T4-T7 (2/1).
PIG 17	4/3	3/1	3/2	3/3	2/1	
PIG 13	4/3	2/1	3/2	0/0	0/0	HEMORRHAGE, VENA CAVA (3/2).
PIG 15	4/2	4/2	3/1	0/0	0/0	
PIG 68	3/2	2/1	3/2	0/0	0/0	FRACTURE OF SPINOUS PROCESS OF T1 (2/1).
PIG 51	3/2	1/0	3/2	0/0	0/0	HEART LESION MAY NOT BE IMPACT RELATED.
PIG 38	3/2	2/1	3/2	0/0	0/0	
PIG 16	3/2	2/1	3/2	2/1	0/0	
PIG 12	3/2	0/0	3/2	0/0	1/0	
BAB 7	3/1	2/1	1/0	3/0	0/0	
PIG 23	3/1	2/1	2/1	0/0	0/0	BLOOD STAINED FORTH IN BRONCHI (3/1).
PIG 21	3/1	3/1	2/1	0/0	0/0	
PIG 9	3/1	3/1	1/0	0/0	0/0	

higher severity ratings reflect the possible synergistic effect of multiple significant thoracic injuries.

The most frequent gross cardiac pathology observations were subendocardial petechiae and/or eccyhmoses of the interventricular septum and/or papillary muscle of the left ventricle. Such hemorrhages were observed in both impacted animals and in non-impacted, control animals. Since it was not possible to separate the artifactually jinduced hemorrhages from impact-induced hemorrhages, all such hemorrhages were rated as impact induced. Changes in the animal handling and euthanasia techniques were instituted in an attempt to reduce the occurrence of artifactually induced hemorrhages.

Table 11. Summary of animals with significant abdominal injuries.

ANIMAL NUMBER	ABDOMINAL INJURY SEVERITY (TL/PI)	ABDOMINAL ORGANS						OTHER (TL/PI)
		LIVER (TL/PI)	DIAPHRAGM (TL/PI)	SPLEEN (TL/PI)	KIDNEY (TL/PI)	GALL BLADDER (TL PI)	INTESTINE (TL PI)	
PIG 14	6/6	6/6	3/1	0/0	0/0	0/0	0/0	
PIG 13	5/4	5/4	0/0	0/0	2/1	0/0	0/0	MESENTERY HEMORRHAGE (3/1).
PIG 15	4/4	4/4	3/1	0/0	0/0	0/0	0/0	
BAB 7	4/3	4/3	0/0	2/1	3/2	0/0	3/2	SEVERE HEMORRHAGE OF OMENTUM (3/2) & PORTAL VEIN (4/3).
PIG 94	4/3	4/3	2/1	0/0	0/0	0/0	0/0	
PIG 35	4/2	4/2	0/0	0/0	0/0	0/0	0/0	
PIG 29	4/2	4/2	0/0	0/0	0/0	2/1	0/0	
PIG 18	4/2	4/2	0/0	0/0	0/0	0/0	0/0	
PIG 17	4/2	4/2	0/0	0/0	0/0	0/0	0/0	
BAB 8	3/2	1/1	0/0	0/0	0/0	3/2	2/1	
PIG 68	3/2	3/2	0/0	0/0	2/1	0/0	0/0	
PIG 9	3/2	3/2	0/0	0/0	0/0	0/0	3/2	
PIG 22	3/1	3/1	0/0	0/0	0/0	0/0	0/0	

Abdominal Injuries—Thirteen of the forty-six animals, including two of the three baboons, had significant abdominal injuries (Table 11). The liver was the most frequently injured abdominal organ. Nine of the fourteen animals had lacerated lobes and/or junctional tears of the liver which were rated as TL equal to four or greater. Pig 14 died 24 minutes postimpact of blood loss from the severely lacerated liver shown in Figure 10. Pig 13 had a deep rent on the right lobe of the liver that resulted in ischemic necrosis of the parenchyma, peripheral to the tear, Figure 11.

Distribution of Various Mechanical Response Measurements Within Discrete Injury Classifications

For each animal, the mechanical response measurements listed in Table 7 were paired with threat-to-life (TL) injury severity ratings for selected body regions. HIC's were paired with the TL ratings for the head, peak

Figure 10. Severely lacerated liver of pig 14.

Figure 11. Ischemic necrosis of the liver of pig 13 peripheral to the laceration.

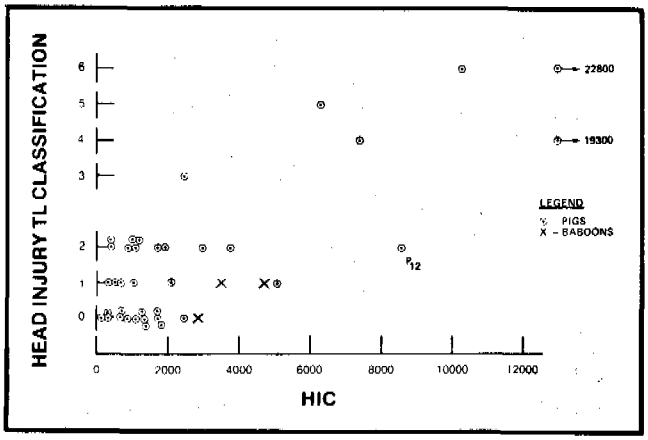

Figure 12. Distributions of head HIC values within the various head TL classifications.

resultant head accelerations with neck injury TL ratings, and peak ventro-dorsal thoracic spine accelerations with the thorax and the abdomen TL ratings. These pairings are displayed in Figures 12 through 15 for the body regions of the head, neck, thorax and abdomen, respectively. The thoracic injury rating for Pig 51 was not plotted since the injury could have occurred pretest. The thoracic and abdominal injury ratings for Baboon 8 were not plotted because the sensivity axis of the thoracic spine accelerometer was not aligned with the direction of the cushion-animal interaction force for the animal position that was used (see Figure 5). The TL ratings are shown as discrete classifications, ranked in terms of increasing injury severity. Linearity of severity should not be assumed between the integers assigned to the various classifications.

Note that for a given body region, many of the mechanical response ranges for the various discrete TL classifications overlap. Two possible reasons for these overlaps are: i) the animals have different levels of injury susceptibility, and ii) the measured response values chosen may not be the most appropriate indicators of the injury severity rating of the body region. It may be that a given injury type can be produced by a variety of mechanisms,

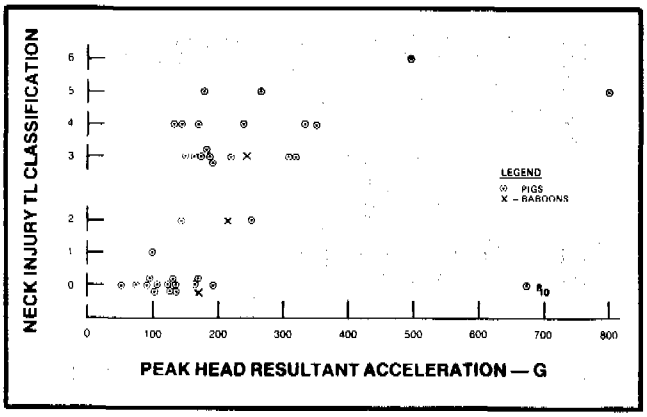

Figure 13. Distributions of head resultant acceleration values within the various neck TL classifications.

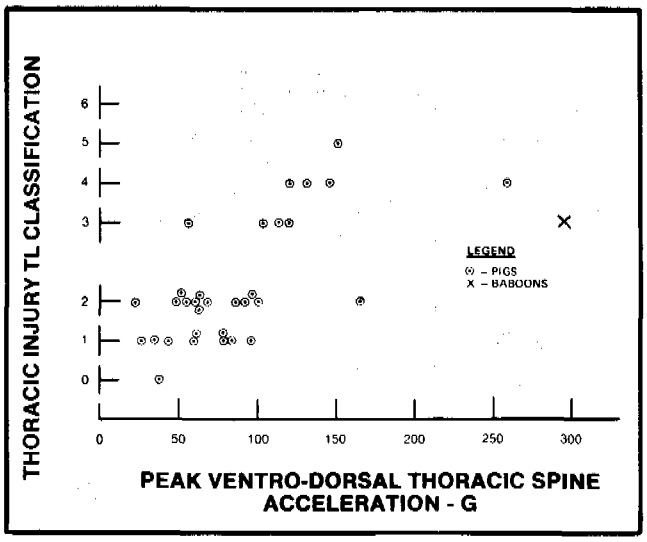

Figure 14. Distributions of peak ventro-dorsal thoracic spine acceleration values within the various thoracic TL classifications.

each related to a different physical parameter or combinations of parameters. The implication of these overlaps is that given a value of one of the measured responses, the injury severity classification for the corresponding body region is not uniquely defined. In such cases, one must speak of the probability for various levels of injury severity.

In several cases, an extreme of a mechanical response range for a given body region and injury severity classification appears to be an outlier. Such outliers could be due to a number of causes such as mechanical response measurement artifacts, undiagnosed injuries, or injuries that occur as the result of procedural techniques and not the test environment. For example, Pig 12 had a HIC of 8570, but only a moderate head injury (see Figure 12,

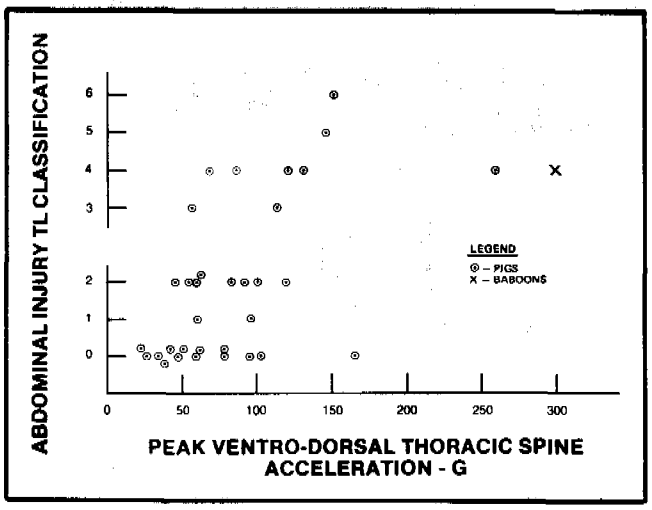

Figure 15. Distributions of peak ventro-dorsal thoracic spine acceleration values within the various abdominal TL classifications.

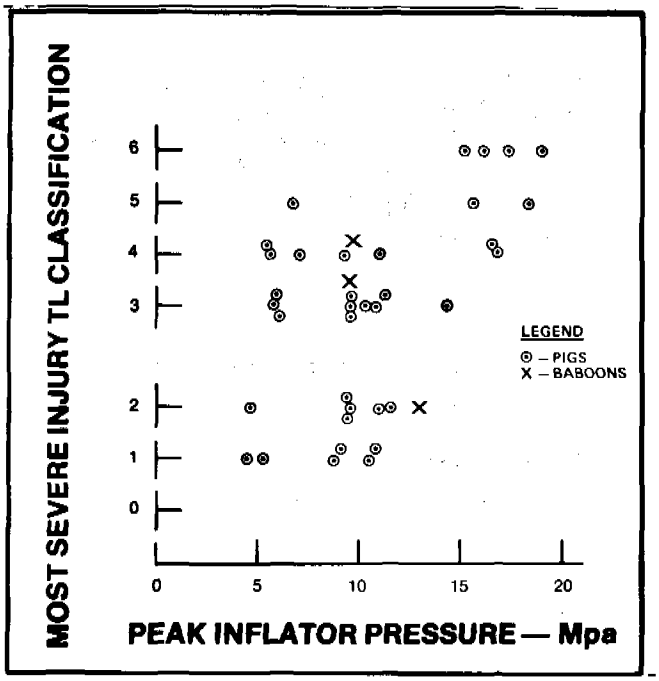

Figure 16. Association between peak inflator pressure and most severe injury.

TL = 2 Classification). The resultant head acceleration of Pig 12 had two distinct peaks and the HIC time interval contained both peaks. The HIC value for either peak, individually, would be lower and probably would be more representative of the severity of the head impact environment. As a second example of an outlier, Pig 10 had peak resultant head acceleration of 675 g's without any apparent neck injury (Figure 13, TL = 0 Classification). In this case, it is quite possible that Pig 10 had an undiagnosed neck injury since the dissection technique used to detect neck injuries was not developed until later in the program.

Peak inflator pressure was paired with the highest TL rating experienced by the animal. A plot of these pairings is given in Figure 16. Note the strong association between the more aggressive inflators (peak pressures of 15 Mpa or greater) and the more severe injuries (TL's of 5 and 6).

SUMMARY

Forty-six anesthetized animals (forty-three pigs and three baboons) were subjected to a variety of deploying cushion-collision interaction forces which produced a broad spectrum of injury types and severities to the major organs of the head, neck and torso of the animals. The severity of the animal injuries were rated as if the injuries were sustained by a 3-year-old child. For the pig tests, threat-to-life (TL) injuries ranging from no injuries (TL = 0) to non-survivable injuries (TL = 6) were identified for organs of the head, neck and abdomen. Thoracic organ injuries ranged from no injuries (TL = 0) to critical injuries (TL = 5). The more significant injuries were subdural brain hemorrhages, partial transection of the cervical cord, rupture of the apical odontoid ligament, excessive straining of the membranes and ligaments surrounding the atlas-occipital region with attendant hemorrhaging, cervical spine fractures, lung and heart contusions, persistent abnormal ECG readings, extensive rib fractures, liver tears and lumbar spine fractures. Five of the pigs died as a result of their injuries. Three baboons were used in the program and experienced similar, but less severe injuries than pigs that were exposed to similar test environments. The animal injury data were needed to interpret the significance of the responses of a specially instrumented child dummy (11) that was being used in GM's passenger inflatable restraint development program. That interpretation is the topic of a separate paper by Mertz and Weber (12).

ACKNOWLEDGEMENTS

The program described in this paper was a multi-disciplinary project requiring the efforts of many people. The authors would like to express their appreciation to the instrumentation, sled and animal care staffs of Southwest Research Institute for handling the many details of conducting the tests; to the medical specialists for their interpretation of the animal injuries and to the management and staffs of Passenger Inflatable Restraint group of Fisher Body and the Inflatable Restraint Project Center of Current Product Engineering of General Motors Corporation for their support of this project. A special note of thanks is given to Vernon Lancaster who handled the logistics of the test hardware and to Dr. K. D. Carey and Ned Zamora his assistant who conducted the animal necropsies.

LIST OF REFERENCES

1. Patrick, L. M. and Nyquist, G. W., "Airbag Effects on the Out-of-Position Child", 2nd International Conference on Passive Restraints, SAE 720442, 1972.
2. Campbell, D. D., "Air Cushion Restraint Systems Development and Vehicle Application", 2nd International Conference on Passive Restraints, SAE 720407, 1972.
3. Klove, E. H. and Olgesby, R. N., "Special Problems and Considerations in the Development of Air Cushion Restraint Systems", 2nd International Conference on Passive Restraints, SAE 720411, 1972.
4. Smith, G. R., Hurite, S. S., Yanik, A. J., and Greer, C. R., "Human Volunteer Testing of GM Air Cushions", 2nd International Conference on Passive Restraints, SAE 720443, 1972.
5. Wu, H., Tank, S. C., and Petrof, R. C., "Interaction Dynamics of an Inflating Air Bag and a Standing Child", SAE 730604, 1973.

6. Lundstrom, L. C., "Rating Air Cushion Performance to Human Factors and Tolerance Levels", Fifth International Technical Conference on Experimental Safety Vehicles, 1974.
7. Aldman, B., Anderson, A., and Saxmark, O., "Possible Effects of Airbag Inflation on a Standing Child", Proceedings of the International Meeting on Biomechanics of Trauma in Children, Lyon, France, 1974.
8. Takeda, H. and Kobayashi, S., "Injuries to Children From Airbag Deployment", 8th International Technical Conference on Experimental Safety Vehicles, 1980.
9. Stalnaker, R. L., Klusmeyer, L. F., Peel, H. H., White, C. D., Smith, G. R., and Mertz, H. J., "Unrestrained, Front Seat, Child Surrogate Trajectories Produced by Hard Braking", Proceedings of the Twenty-Sixth Stapp Car Crash Conference, October 20-22, 1982.
10. Montalvo, F., Bryant, R. W., Mertz, H. J., "Possible Positions and Postures of Unrestrained Front-Seat Children at the Instant of Collision", Proceedings of the Ninth International Technical Conference on Experimental Safety Vehicles, Nov. 1-4, 1982.
11. Wolanin, M. J., Mertz, H. J., Nyznyk, R. S., and Vincent, J. H., "Description and Basis of a Three-Year-Old Child Dummy for Evaluating Passenger Inflatable Restraint Concepts", Proceedings of the Ninth International Technical Conference on Experimental Safety Vehicles, Nov. 1-4, 1982.
12. Mertz, H. J., and Weber, D. A., "Interpretations of the Impact Responses of a 3-Year-Old Child Dummy Relative to Child Injury Potential", To Be Published.
13. The Abbreviated Injury Scale—1980 Revision, AAAM, Morton Grove, IL, 1980.
14. United States Patent 4290627, "L-Shaped Inflatable Restraint Cushion", Sept. 22, 1981.
15. Snyder, R. G., Schneider, L. W., Owings, C. L., Reynolds, H. M., Golomb, D. H., Schork, M. A., *Anthropometry of Infants, Children, and Youths to Age 18 For Product Safety Design*, SP450, SAE, Warrendale, PA, 1977.
16. Diffrient, N., Tilley, A. R., Bradagjy, J. C., "Design Requirements for Infants and Children", *Human Scale (TM) 1/2/3*, MIT Press, Cambridge, 1974.

Interpretations of the Impact Responses of a 3-Year-Old Child Dummy Relative to Child Injury Potential

H. J. MERTZ and D. A. WEBER
General Motors Corporation

3682

ABSTRACT

An analysis is presented that was used to interpret the significance of response measurements made with a specially instrumented, 3-year-old child dummy that was used to evaluate child injury potential of the second-generation, passenger inflatable restraint system that was being developed by General Motors Corporation. Anesthetized animals and a specially instrumented child dummy, both 3-year-old child surrogates, were exposed to similar inflating-cushion, simulated collision environments. The exposure environments were chosen to produce a wide spectrum of animal injury types and severities, and a corresponding broad range of child dummy responses. For a given exposure environment, the animal injury severity ratings for the head, neck, thorax and abdomen are paired with dummy response values corresponding to these body regions. These data are used to develop relationships that can be used to predict the probability of an animal experiencing significant injuries to these body regions based on the child dummy response measurements. A rationale is developed for interpreting the predicted animal injury severities relative to child injury severities.

INTRODUCTION

A specially instrumented, 3-year-old child dummy (1) was used to evaluate the performance of the second-generation, passenger inflatable restraint system being developed by General Motors Corporation. While it was possible to assess the performances of various inflatable restraint concepts based on the relative magnitudes of the child dummy response measurements, no basis existed to interpret these measurements relative to child injury potential. In previous studies by General Motors Corporation (2) and Volvo (3), anesthetized baboons, chimpanzees and pigs were used as child surrogates to estimate the child injury potential of various passenger inflatable restraint concepts. Unfortunately, no attempt was made in either program to develop a test device (instrumented child dummy) to aid in understanding the relationships between the observed animal injuries and the cushion-collision interaction forces.

To develop a basis for interpreting the responses of the child dummy relative to child injury potential, an animal test program was again needed. The program proposed was to expose anesthetized animals and the specially instrumented child dummy to similar deploying cushion-collision interaction environments. Exposure environments were chosen to produce a wide range of animal injury types and severities, and a corresponding broad

spectrum of child dummy responses. This scheme would allow association to be made between the animal injury severity ratings for the head, neck, thorax, and abdomen and the dummy response measurements for the corresponding body regions. A detailed description of the animal test program and observed animal injuries is given by Mertz et al. (4). The following describes the analyses that were done of that animal injury data and the corresponding child dummy response data to estimate child injury potential due to inflating cushion-collision interactions.

PAIRED ANIMAL INJURY AND CHILD DUMMY RESPONSE DATA

Animal Tests

Forty-three pigs and three baboons were subjected to a spectrum of deploying cushion-collision interaction forces, with each animal being subjected to a single exposure (4). Physiological measurements made pre- and postimpact were: blood pressure, 6-lead ECG, heart rate, respiration, rectal temperature, visual and somatosensory evoked responses, reflex responses to toe and ear pinch, palpebral reflex, pupil size and reactivity to light, muscle tonus, and blood gases. Drugs were administered in sufficient dosages to assure that the animal was immobile and had adequate pain suppression while retaining good neurological response levels for the physiological testing. If the animal survived the exposure, it was sacrificed usually 24 hours posttest. A detailed gross necropsy was performed on all animals. Selected sections of the brain, spinal cord, heart and lungs were examined microscopically.

The resulting physiological and pathological data were evaluated by a team of medical specialists that consisted of a neurophysiologist, a neuropathologist, a cardiac pathologist, a cardiologist, a pulmonary specialist and a biomechanics specialist/physician who was the team leader. The medical specialists were directed to assess the severity of the animal injuries as if the injuries had occurred to a 3-year-old child. When all the injuries for a given animal had been rated, injury severity ratings in terms of threat-to-life (TL) and permanent impairment (PI) were assigned to the body regions of the head, neck, thorax and abdomen. For the head, neck and abdomen, the overall body region TL ratings ranged from no injuries (TL = 0) to nonsurvivable injuries (TL = 6). Thoracic injury severity ratings ranged from no injuries (TL = 0) to critical injuries (TL = 5). In the following analysis, these TL ratings for the four body regions of each animal will be paired with corresponding child dummy response measurements. The PI ratings will not be used in this paper.

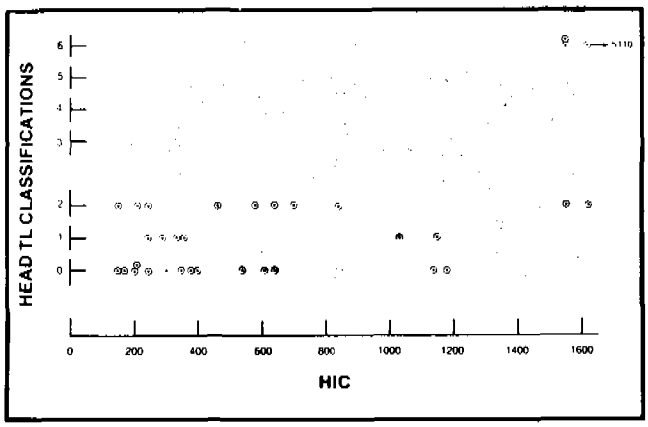

Figure 1. Paired child dummy HIC values and animal head TL values.

SELECTION OF CHILD DUMMY AND ANIMAL TEST DATA

For each animal exposed, a similar test was conducted using the instrumented child dummy. High-speed films of paired animal and dummy tests were reviewed to determine if the kinematics of the animal and dummy were similar. In a number of cases, gross differences in kinematics were noted. Data from those tests were excluded from the correlation analysis. A comparison of inflator characteristics was made between paired dummy and animal tests. In several cases, gross differences were noted in the performance of the inflators and the results of those tests were excluded from further analysis. The remaining paired animal and child dummy data were subjected to the following analysis.

ANALYSIS OF CHILD DUMMY AND ANIMAL TEST DATA

The head injury severity TL rating for each animal was paired with the child dummy HIC value that was measured in a similar exposure environment. These pairings are depicted in Figure 1. Similar pairings were done for the head TL ratings and peak child dummy neck tensions (Figure 2), the neck TL ratings and peak child dummy neck tensions (Figure 3), the thoracic TL ratings and peak child dummy upper-spine resultant accelerations (Figure 4) and maximum rate of chest compressions (Figure 5), and the abdominal TL ratings and peak child dummy lower-spine resultant accelerations (Figure 6) and maximum rate of abdominal compressions (Figure 7). Child dummy neck tensions were paired with head TL ratings (Figure 2) because the significant head injuries that were produced in the test program were subdural hemorrhages that appeared to be related to rapid rearward displacement of the animal's head relative to its torso. Neck tension along with HIC were thought to be good indicators of severity of this kinematic behavior. Conse-

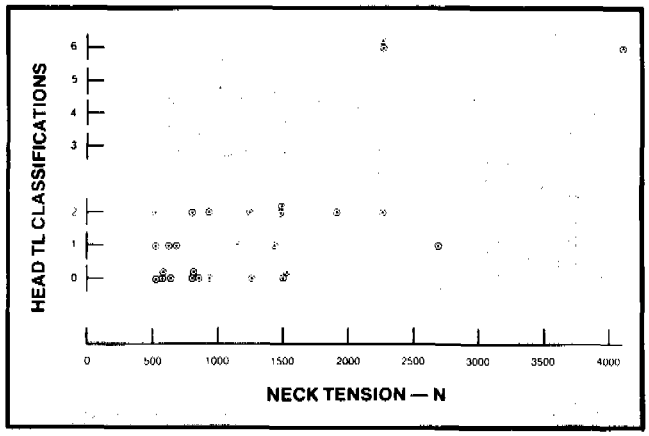

Figure 2. Paired child dummy neck tension values and animal head TL values.

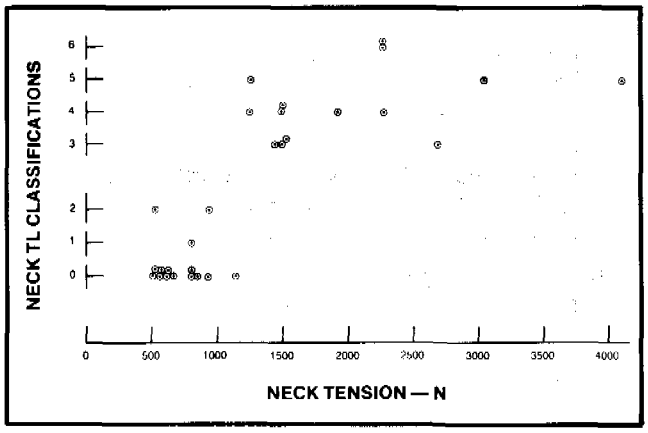

Figure 3. Paired child dummy neck tension values and animal neck TL values.

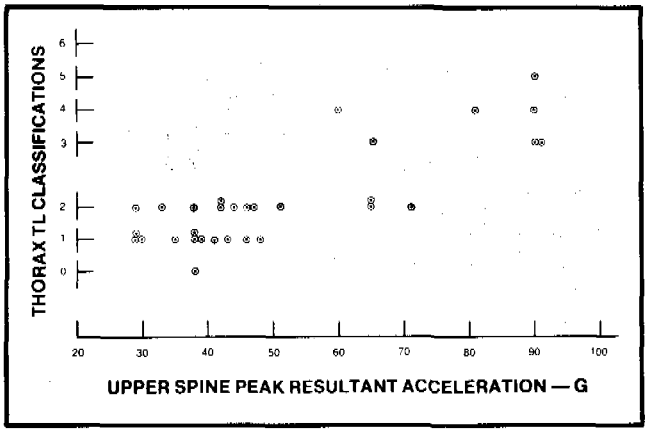

Figure 4. Paired child dummy peak upper-spine resultant acceleration values and animal thoracic TL values.

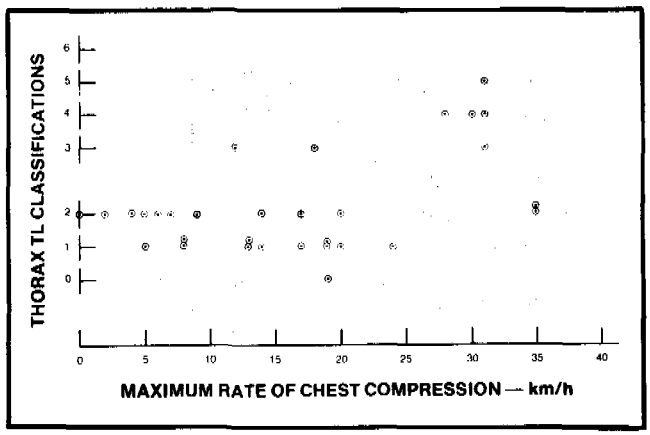

Figure 5. Paired child dummy maximum rate of chest compression values and thoracic TL values.

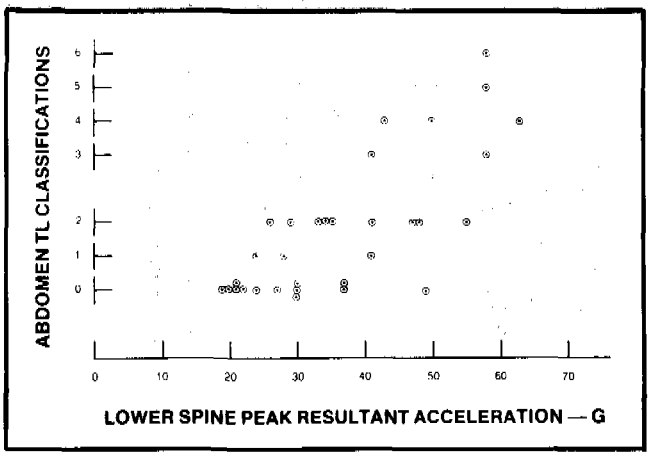

Figure 6. Paired child dummy peak lower-spine resultant acceleration values and animal abdominal TL values.

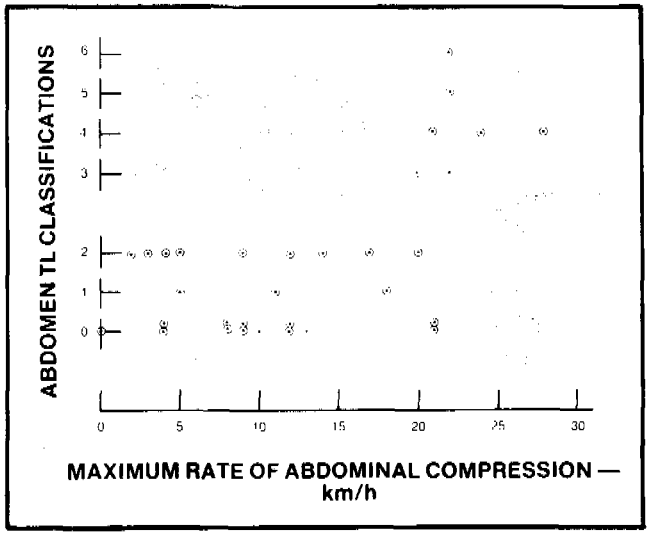

Figure 7. Paired child dummy maximum rate of abdominal compression and animal abdominal TL values.

quently, both child dummy responses were paired with the animal's head TL ratings.

To emphasize that linear relationships do not exist between the integer values assigned to the various injury severity classifications, adjacent TL classifications shown on Figures 1-7 are separated by a space. A larger space is used between the TL = 2 and TL = 3 classifications to distinguish between significant injuries (TL = 3, 4, 5 and 6) and nonsignificant injuries (TL = 0, 1 and 2).

DISCUSSION OF ANIMAL INJURY—CHILD DUMMY RESPONSE ASSOCIATIONS

Extremes of Injury Severity Classifications

The extremes of the range of the child dummy response data for a given body region and TL classification are bounds for the child dummy response value that is associated with 50 percent of the animals experiencing that level of injury severity for the prescribed body region. The lowest child dummy response value of the range is a conservative estimate of the 50 percent value, while the largest value is a nonconservative estimate. The actual 50 percent value will lie somewhere between the extremes and will not be, in general, the mean value of the child dummy response data associated with the given TL classification.

Distribution of Dummy Response Data for a Prescribed TL Classification and Body Region

There are two important features of the distribution of dummy response data for a prescribed TL classification and body region that need to be considered. First, the mean value of the child dummy response data for a given injury severity classification and body region is always greater than the child dummy, 50 percent response value. To understand why the mean value is a nonconservative estimate, the procedure used to select the test conditions must be examined. Test conditions were selected to obtain a broad range of child dummy response data for the body regions of the head, neck, thorax and abdomen. It was conjectured that the selection process would result in exposure environments that would produce a wide spectrum of animal injury types and severities, which it did. The test conditions were not selected to determine what levels of the child dummy response would correspond to the thresholds of the various injury severity classifications for the four body regions of the animal population that was tested. Such an approach would have required conducting multiple tests (6 or greater) for many, many levels of child dummy responses. Hundreds of animals and a similar number of inflatable restraint systems would be needed, both of which were clearly inconsistent with the program time frame and resources. With the approach that was used, it is unlikely that any animal was exposed to the exact test condition needed to produce the levels of injury severities that resulted. For this reason, the measured child dummy response values that were paired with the resulting injury severity ratings are greater than (very seldom equal to) the threshold values for the animal. Consequently, the mean value of the child dummy response data for a given injury severity classification and body region is greater than the 50 percent value.

A second important feature is that the distribution of the child response data within a given injury severity classification for a given body region can be highly dependent on the investigator's choice of test conditions. This feature can be illustrated by the following example.

Assume that all the animals have the same well-defined thresholds (child dummy HIC values of 600, 1000, 1500) for TL = 2, 3 and 4 head injuries. With this assumption, all child dummy HIC values between 600 and 999 will be paired with animal TL's of 2 and all HIC values between 1000 and 1499 would be paired with TL = 3 head injuries. The investigator selects his test matrix so that the child dummy HIC values range from 500 to 2000. If he chooses to conduct most of his tests for the TL = 3 range (1000 to 1499) close to the threshold of 1000, then the average for the TL = 3 classification will be close to 1000. However, if he chooses instead to conduct most of his test for this range close to 1499, then the average will be close to 1499. An even distribution of tests over the range will give an average close to 1250. All three of these mean HIC values are dependent on the investigator's choice of exposure environments and are nonconservative estimates of the child dummy 50 percent value for the threshold of TL = 3 injuries, which in this example is 1000.

Overlap of Ranges of Child Response Data of Adjacent Injury Severity Classifications

If in the preceding example the assumption was made that the animals had different thresholds of dummy HIC values for TL = 3 head injuries, then an overlap in HIC values would exist between the ranges of the TL = 2 and TL = 3 injury severity classifications. Let's assume further that the actual ranges of HIC values for the TL = 2 and 3 classifications are 600 to 1000 and 800 to 1500, respectively. Then, for HIC values within the overlap (800 to 1000), an uncertainty exists as to the injury severity level that a given animal might experience. For HIC values within the overlap, estimates of the percent of animals experiencing TL = 2 and TL = 3 head injuries are needed.

One approach to estimating these percentages is to assume that the thresholds of HIC values for TL = 3 injuries are normally distributed within the overlap. Implicit in this assumption is the requirement that the HIC value corresponding to the mid-point of the overlap is the child dummy 50 percent value. To estimate how the

percent of animals experiencing TL = 3 head injuries varies, all the HIC values within the overlap (both those associated with TL = 2 injuries and TL = 3 injuries) are ranked ordered. These HIC values are assigned median ranking values based on their order numbers (5). The lowest and highest median ranking values and their corresponding HIC values are plotted on normal probability paper. A line drawn through these two points provides estimates of the percent of animals expected to experience TL = 3 head injuries for various child dummy HIC values. The median ranking values of the other HIC values within the overlap are not plotted since their distribution can be biased by the investigator's choice of test conditions.

It is possible that the test conditions and/or animals are chosen so that there is no overlap of the HIC values paired with TL = 2 and TL = 3 head injuries. If such is the case, then the 50 percent HIC value is taken as the average of the highest HIC value corresponding to a TL = 2 head injury and the lowest HIC value corresponding to a TL = 3 head injury. The highest TL = 2 HIC value is assigned the median ranking value of 0.2063 and the lowest TL = 3 HIC value is assigned a value of 0.7937. These are the median ranking values for the first and third order numbers for a sample size of three (5).

Both of these approaches have two shortcomings. The lowest HIC value within the overlap will usually be greater than the threshold HIC value for that animal and the highest HIC value will be less than the threshold HIC value for its corresponding animal. Thus, the median ranking value assigned to the lowest HIC value will be somewhat less than the true median ranking value for that HIC value. The reverse is true for the median ranking value assigned to the highest HIC value. The implications of these shortcomings are that the percent of the animals experiencing TL = 3 head injuries is underestimated for HIC values below the 50 percent value and overestimated for HIC values greater than the 50 percent HIC value. For the case where there is no overlap, the reverse of this implication is true, since the roles of the lowest TL = 3 HIC value and the highest TL = 2 HIC value are interchanged in defining the median ranking values. In both cases, the error in estimating the child dummy 50 percent value depends on how close the median rankings assigned to the extreme HIC values are to their true values.

APPLICATION OF MEDIAN RANKING TECHNIQUE TO ANIMAL INJURY—CHILD DUMMY RESPONSE ASSOCIATIONS

A review of the data shown on Figures 1-7 indicates that in most cases there is considerable overlap between the ranges of child dummy responses for the various injury severity classifications for a given body region. Within these overlaps, one must speak of the percent of animals expected to experience various levels of injury severity for a given value of child dummy response. The median ranking technique discussed previously can be applied to these data if the seven classifications of injury severity can be reduced to two. This can be accomplished by defining two groups: significant injuries (TL = 3, 4, 5 and 6) and nonsignificant injuries (TL = 0, 1 and 2). The results of applying the median ranking technique to the data shown on Figures 1-7 grouped in this manner are given in Figures 8-14, respectively. The percent of animals expected to have nonsignificant injuries for a given body region is 100 percent minus the percent estimated to have significant injuries. The curves of Figures 8-14 should not be construed as showing causative relationships, since the analysis is based on associations made of measured child dummy responses and observed animal injuries. These curves can be used to define a set of child dummy response values corresponding to any prescribed percent of significant animal injuries for the body regions of the head, neck, thorax and abdomen.

RELATIONSHIP BETWEEN OBSERVED ANIMAL INJURIES AND POSSIBLE CHILD INJURIES

The curves shown in Figures 8-14 provide estimates of the probable occurrence of significant animal injuries for various levels of measured child dummy responses. What

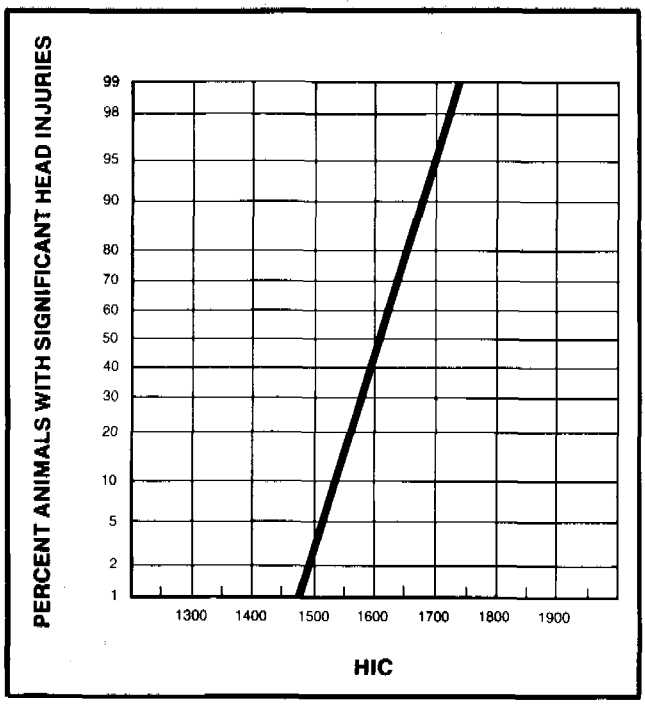

Figure 8. Percent of animals experiencing a significant head injury (TL greater than 2) as a function of child dummy HIC.

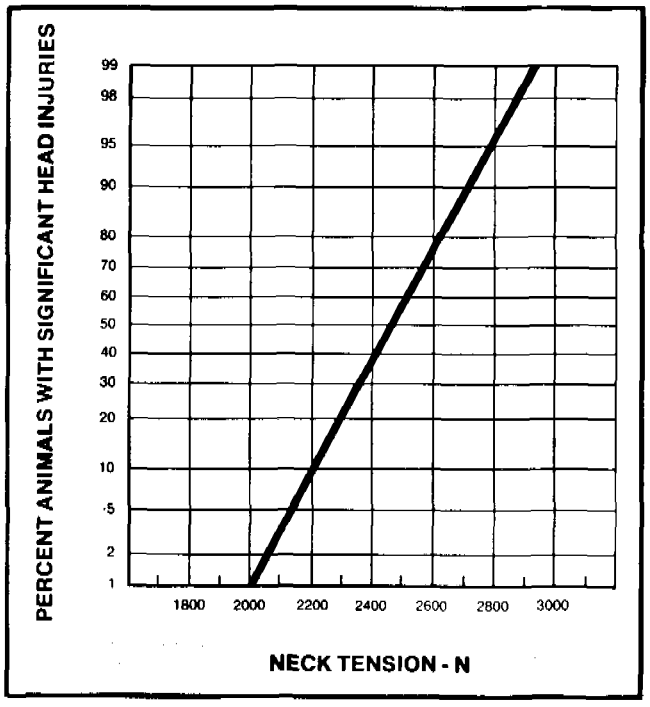

Figure 9. Percent of animals experiencing a significant head injury (TL greater than 2) as a function of child dummy neck tension.

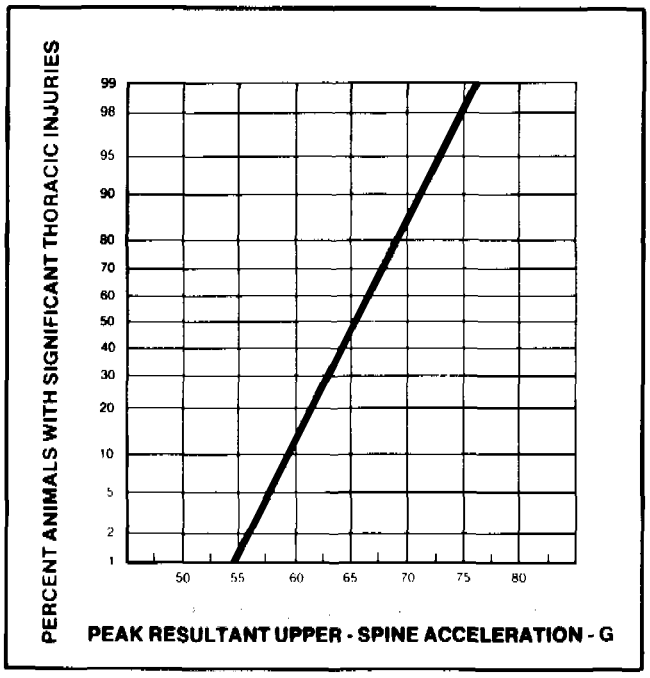

Figure 11. Percent of animals experiencing a significant thoracic injury (TL greater than 2) as a function of child dummy peak upper-spine resultant acceleration.

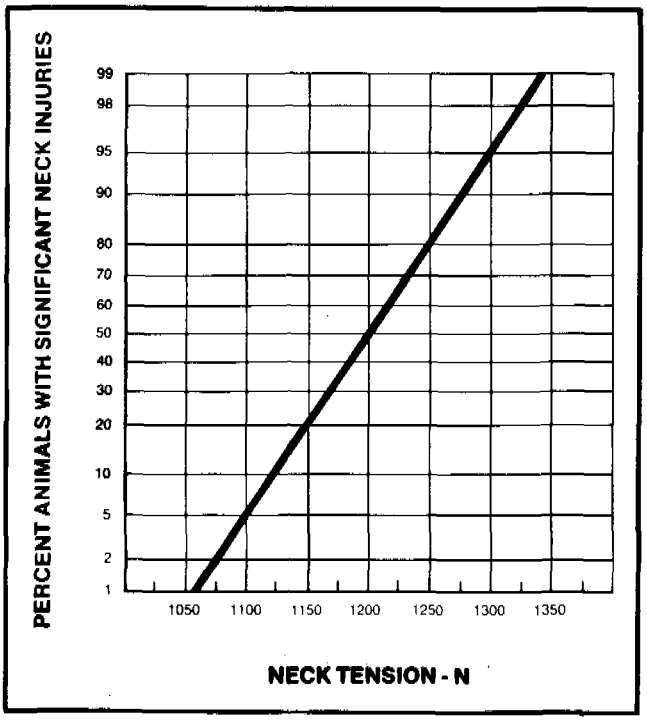

Figure 10. Percent of animals experiencing a significant neck injury (TL greater than 2) as a function of child dummy neck tension.

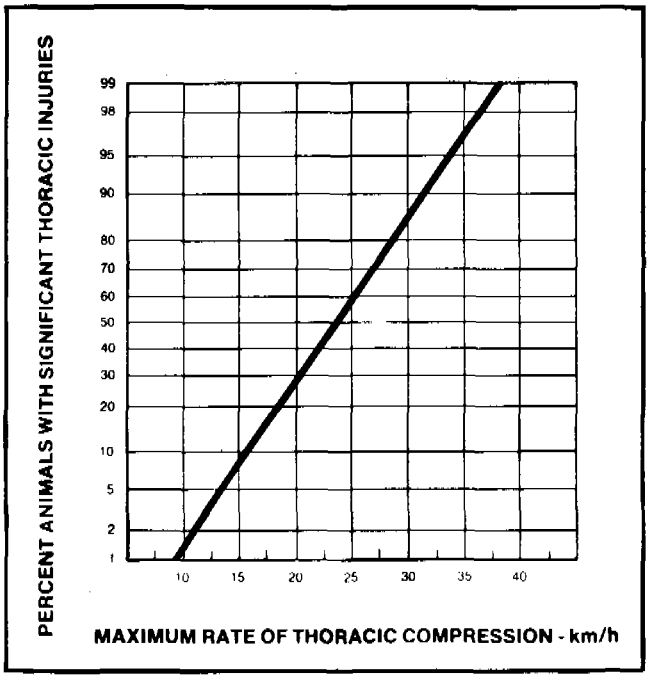

Figure 12. Percent of animals experiencing a significant thoracic injury (TL greater than 2) as a function of child dummy maximum rate of chest compression.

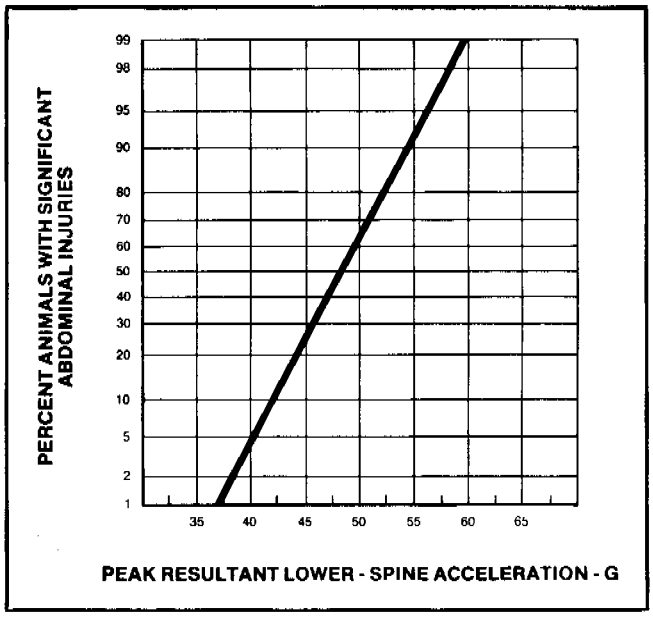

Figure 13. Percent of animals experiencing a significant abdominal injury (TL greater than 2) as a function of child dummy peak lower-spine resultant acceleration.

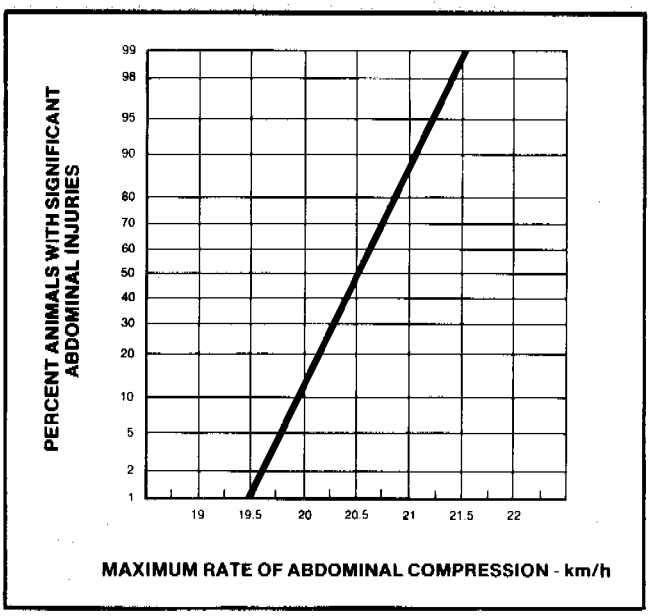

Figure 14. Percent of animals experiencing a significant abdominal injury (TL greater than 2) as a function of child dummy maximum rate of abdominal compression.

is desired are curves giving estimates of the probable occurrence of significant child injuries for various levels of measured child dummy responses. One approach to developing such relationships is to infer the probabilities of significant child injuries from the probable occurrence of animal injuries given by the curves of Figures 8-14. To develop such inferences, a comparison of the geometric, inertial and strength characteristics of the child and the animal must be made.

Animal Species Selection Rationale

The primary considerations used in selecting an animal species for the test program (4) were that its weight and size be comparable to a 3-year-old child, which was the size of the child dummy being used by GM to evaluate various passenger inflatable restraint system concepts. It was reasoned that animal surrogates that had overall geometric and inertial characteristics that were similar to the child would experience similar cushion-collision interaction forces as the child. Three animal species, the chimpanzee, the baboon and the pig, were considered as animal models. Based on comparable size and shape, the chimpanzee was the logical choice. However, chimpanzees could not to be obtained in sufficient quantities to carry out the proposed number of tests. Consequently, only the baboon and the pig were considered as possible child surrogates. While testing was done with both animal species, the majority of the tests were conducted using anesthetized pigs for the following reasons:

1. The pig's thoracic and abdominal breadths compared more favorable to the child's (Table 1). The implication of this consideration is that the thoracic-abdominal cushion interaction would be more comparable to those of the child.
2. The state of physical development of a 15 kg pig was estimated to be quite comparable to a 3-year-old child based on a comparison of human versus pig puberty ages (Table 1). The equivalent child age of the 15 kg pig was estimated to be 4.2 years while that of the baboon was 16.3 years. The implication is that the strength of the anesthetized pig would be similar to that of a child.
3. Based on a limited test program (4) where pigs and baboons were subjected to similar deploying cushion-collision environments, the pig experienced similar, but in some tests, more severe injuries than the baboon. This result is consistent with the previous implication that the physical development of the 15 kg pig is not as advanced as the 15 kg baboon. Using the apparently more injury prone pig would provide a more conservative estimate of the expectation of significant injuries.

Animal Model Deficiencies

There are a number of geometric and response differences between the pig and the baboon, and more importantly between either animal and the child. These differences can influence the interactions between the deploying cushion and the subject, and consequently, affect the resulting injury pattern.

Table 1. Typical size, shape and mass measurements for 15 kg pigs, baboons and children (4).

MEASUREMENT	AVERAGE OF 5 PIGS	AVERAGE OF 4 BABOONS	3-YEAR-OLD MALE CHILD	
			VALUE	REF.*
AGE (YEARS)	0.19	4.3	3	-
EQUIVALENT CHILD AGE (YEARS)**	4.2	16.3	3	-
MASS (kg)	14.9	15.2	14.9	6
SEATED HEIGHT (mm)	746	641	592	6
HEAD-NECK LENGTH (mm)	241	147	226	6
HEAD WIDTH (mm)	111	110	136	6
FORE-AFT HEAD MOTION (DEG)	45	110	105	7
NECK CIRCUMFERENCE (mm)	421	271	243	6
CHEST CIRCUMFERENCE (mm)	529	509	516	6
CHEST BREADTH (mm)	138	110	165	6
CHEST DEPTH TO BREADTH RATIO	1.33	1.44	0.67	6
ABDOMINAL CIRCUMFERENCE AT UMBILICUS (mm)	580	392	486	6
ABDOMINAL BREADTH AT UMBILICUS (mm)	147	125	165	6

NOTES:

* NUMBERS REFER TO PAPERS IN LIST OF REFERENCES.

** EQUIVALENT CHILD AGE = $\frac{\text{HUMAN PUBERTY AGE}}{\text{ANIMAL PUBERTY AGE}}$ x (ANIMAL TEST AGE)

Neither animal's head is geometrically similar to the child's. The pig's head size is comparable to a child's; however, its shape is not due to its snout. The baboon's head is much smaller than a child's, and is characterized by a pronounced muzzle, similar to a dog's head. These characteristics will influence how their heads interact with deploying cushions.

The brain sizes of both animals are much smaller than the child's. Consequently, neither animal is considered a good model for predicting the potential for child brain injury due to direct head impact. However, such impacts were rare events in the test program. The significant head injuries that were produced in the program were massive subdural hemorrhages that appeared to be related to rapid rearward displacement of the animal's head relative to its torso and not to direct head impacts.

For assessing the potential for child neck injuries, the pig has an advantage over the baboon since its head-neck length compares more favorably to the child's. However, both species have a number of major deficiencies as neck injury models. The pig has no chin protuberance for interacting with the deploying cushion since its neck attaches to the rear of its skull resulting in its snout being somewhat aligned with its cervical spine. In contrast, the baboon's neck attaches to the base of the skull similar to the human. However, its long muzzle provides an accentuated, simulated chin protuberance. The fore-aft range of motion of the pig's head-neck structure is much less than the child's, resulting in a smaller degree of rearward motion required to produce a hyperextension neck injury. The baboon can undergo a greater degree of hyperextension than the child. The pig's neck circumference is twice as large as the child's due to its large dorsal neck muscles. However, these muscles had little influence on its head-neck kinematics since the animal was anesthetized. The cervical vertebrae of the pig and child are of similar size.

The pig has a major anthropometric deficiency as a child thoracic injury model in that its chest depth to width ratio is the inverse of the child's (Table 1). Because of this geometric difference, the pig's fore-aft chest stiffness is greater than the child's resulting in greater force levels required to produce compression type injuries to the thoracic organs. This geometric difference could result in the pig underestimating the possibility of the child experiencing thoracic organ injuries due to chest compression. The baboon also has this geometric deficiency.

An in-depth study of the influences of all these various deficiencies is beyond the scope of this paper. A study was undertaken to investigate the influences of the neck deficiencies since significant neck injuries were the most frequent animal injury (Figure 3). The results of that study, when completed, will be the subject of a separate paper.

Interpretations of Measured Child Dummy Responses Relative to Child Injury Potential

The approach used to estimate the possibility of child injuries for GM second-generation, passenger inflatable restraint development program was to assume that a 3-year-old child would experience similar injury types and severities as the anesthetized animals. The curves shown in Figures 8-14 were used to provide a preliminary estimate of the probability of significant child injury based on measured child dummy responses. The final estimates were based on these preliminary estimates, tempered by the knowledge of the various animal model deficiencies discussed previously.

SUMMARY

A technique is given for estimating the potential for significant child injury due to deploying cushion-collision interactions forces based on measurements made with a specially instrumented, child dummy. These estimates should be tempered by the various geometric and response deficiencies noted for the animals that were used as child injury models. This approach proved quite useful in evaluating various concepts of a second-generation, passenger inflatable restraint system that were being developed by GM. The use of this approach should reduce the need for animal testing in any future inflatable restraint development program.

REFERENCES

1. Wolanin, M. J., Mertz, H. J., Nyznyk, R. S., and Vincent, J. H., "Description and Basis of a Three-Year-Old Child Dummy for Evaluating Passenger Inflatable Restraint Concepts", Proceedings of the Ninth International Technical Conference on Experimental Safety Vehicles, Kyoto, Japan, Nov. 1-4, 1982.
2. Patrick, L. M. and Nyquist, G. W., "Airbag Effects on the Out-of-Position Child", SAE 720442, May 1972.
3. Aldman, B., Anderson, A., and Saxmark, O., "Possible Effects of Air Bag Inflation on a Standing Child", Proceedings of the International Meeting on Biomechanics of Trauma in Children, Lyon, France, Sept. 17-19, 1974.
4. Mertz, H. J., Driscoll, G. D., Lenox, J. B., Nyquist, G. W., and Weber, D. A., "Responses of Animals Exposed to Deployment of Various Passenger Inflatable Restraint System Concepts for a Variety of Collision Severities and Animal Positions", Proceedings of the Ninth International Technical Conference on Experimental Safety Vehicles, Kyoto, Japan, Nov. 1-4, 1982.
5. Lipson, C. and Narendra, S. J., *Statistical Design and Analysis of Engineering Experiments*, McGraw-Hill, N.Y., 1973.
6. Snyder, R. G., Schneider, L. W., Owings, C. L., Reynolds, H. M., Golomb, D. H., and Schork, M. A., *Anthropometry of Infants, Children, and Youths to Age 18 for Product Safety Design*, SP 450, SAE, Warrendale, PA, 1977.
7. Diffrient, N., Tilley, A. R., Bradagjy, J. C., "Design Requirements for Infants and Children", *Human Scale (TM) 1/2/3*, MIT Press, Cambridge, 1974.

Clinical and Experimental Studies on Leg Injuries in Car-Pedestrian Accidents

O. BUNKETORP, B. ALDMAN, and L. THORNGREN
Department of Traffic Safety, Chalmers University of Technology, Göteborg, Sweden

B. ROMANUS
Department of Orthopaedic Surgery II, University of Göteborg.

ABSTRACT

Leg injuries in car-pedestrian accidents were analysed and correlated to the speed, the bumper level and the inclination of the car front. The injury mechanisms, not always obvious in these accidents, were studied experimentally with a biomechanical impact system using human leg specimens and a mechanical leg model.

The results from these studies showed a high injury potential of a bumper impacting at or just below the knee level and of a prominent bonnet edge. The experimental studies indicated a possible way to mitigate the injury severity of the impacted lower extremity.

A smooth, compliant, force-limiting and energy-absorbing impact zone with the vertex of the front profile at 35 cm above the ground and a 60 degrees maximum front inclination angle are proposed to lower the risk for serious leg injuries and permanent walking impairment in pedestrians in this type of accident.

INTRODUCTION

The aggressiveness of the vehicle front is an important safety problem in car-pedestrian accidents. Data from real accidents as well as from experimental testing using mechanical or mathematical simulations of the car and the human body have been used to evaluate an optimal car exterior. The bumper and bonnet edge have been shown to be important injury-producing structures (1-15). The majority of the car-pedestrian accidents occur in urban areas and at comparatively low speed. This leads to the assumption that it may well be possible to influence the severity and frequency of pedestrian injuries by rather moderate changes of the front structures of motor cars.

Accident investigations of car-pedestrian collisions have revealed that severe injuries occur in two main areas of the human body: the lower extremity and the head. Of these two types of injuries the head injuries have been considered to be the more important ones to prevent because they are thought to represent a higher risk of having a fatal outcome. The clinical studies referred to in this respect usually describe the short term effects of these injuries as are given by the AIS numbers (16-18). The bumper impacts often cause fractures to the lower extremities. The presence of soft tissue injuries is seldom reported even if this will influence the healing time and final outcome of the injuries. Delayed union of lower leg fractures is known to occur after these injuries.

Leg injuries often prolong the period of hospitalization and rehabilitation because of the difficulties to mobilize

these patients on crutches and different types of knee fixations. The leg injuries may also cause severe social and individual problems. Intraarticular fractures leading to osteoarthrosis are probably more frequent in the knee joint than in the ankle joint and are also more serious than fractures of the tibia diaphysis which usually heal without sequels.

Injuries to the knee joint were seen in only 1.5% in patients injured in car-pedestrian accidents as shown by Weinreich (19). However, knee ligament injuries may occur even at near zero impact velocity and they are easily overlooked during the first period after the accident which may lead to an underestimation of these injuries in accident studies. Intraarticular fractures and extraarticular fractures near the knee joint which influence the joint function in adults and the joint or the epiphyseal growth plates near the knee joint in children may lead to degenerative changes of the joint and permanent impairment. This may also be the result of ligament injuries. Gissane et al. (20) showed that 21% of surviving pedestrian inpatients suffered permanent disability and Baker et al. (21) stressed the importance to create rating systems to classify the injured patient before and after admission and to measure his outcome in all types of accidents. The long-term effects of specific injuries in car-pedestrian accidents remain unknown and have to be studied before final judgments can be made of the aggressiveness of the impact area of the car front.

The injury mechanisms in real car-pedestrian accidents are sometimes obvious: lower leg and knee injuries may be caused by the bumper impact, injuries in the hip and pelvic area by the bonnet edge, and head injuries by the head impact to the bonnet or in the windscreen area. Other details of the impact kinematics are less obvious and this has perpetuated the discussion of how to mitigate the injuries in this type of accident. The first impact of the car influences the kinematics of the body during the later part of the collision and thus also the injuries caused by secondary impacts.

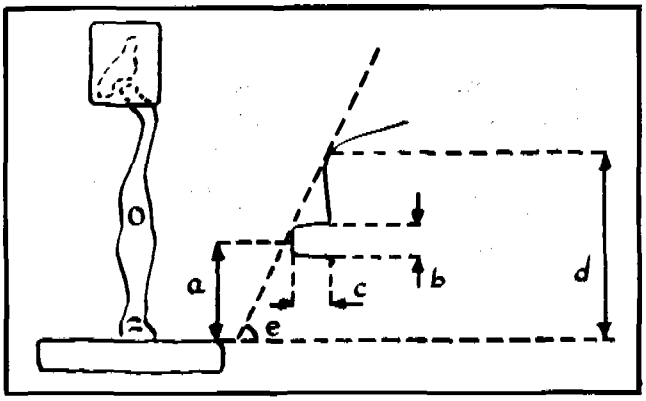

a=bumper level
b=bumper width
c=bumper lead distance
d=bonnet edge height
e=bumper lead angle (front inclination angle)

Figure 1. The experimental set up with a human leg specimen.

The connections between head injuries and the bumper level, the bumper lead angle and the bonnet edge height are not conclusive. Theoretically the car front parameters which determine the body rotation after the primary impact should be the bumper level, the bumper lead angle, and the bonnet edge height. A low mounting of the bumper and a short bumper lead distance, thus, have been recommended to minimize the injuries to the lower leg and knee. On the other hand a low leading edge of the car front may lead to a higher impact velocity of the head against the bonnet. In a mathematical simulation of the body kinematics in a car-pedestrian accident Lestrelin et al. (22) showed a somewhat higher impact velocity of the head if the bumper level was lowered from 50 to 40-35 cm. The same was obtained if the bumper lead angle was diminished. However, the higher risk for head injuries with a lower bumper level and a less steep front inclination has not been verified in any clinical study.

SCOPE

The aim of this paper is to put together the results of the studies undertaken by us so far to correlate the type and severity of leg injuries to the shape and mechanical properties of the vehicle front structures in car-pedestrian accidents. The results refer to adults and are based on a combined clinical and experimental analysis.

METHOD AND MATERIAL

The clinical part of this analysis is based on a retrospective study of 34 adult pedestrians injured by cars and treated at an orthopaedic department in Göteborg, 1975-1976 (23). Information in medical records, interviews with patients and witnesses as well as police reports were used to analyse the accidents and to correlate the injuries to the impact area of the vehicles. Follow-up medical examinations and interviews were made 1-3 years after the accidents. Special interest was focussed on the knee injuries and the walking impairment caused by the impact of the bumper and the car front.

The experimental parts of this research project performed at Chalmers University of Technology were accomplished with a biomechanical leg model system using a human leg specimen and a mechanical leg model impacted by a simulated car front (Fig. 1). The experimental equipment and the test method has been described earlier (24-26).

Two test series were made with human leg specimens. In the first series the specimens were amputated at the mid femur and in the other whole leg specimens including the hip joint were used. One test series was made with the mechanical leg model in which the direct and indirect impact forces in the lower leg and knee could be measured (25).

The injuries produced in these test series were compared with those seen in the real accident study. The possibility to mitigate the leg injuries in this type of accident was estimated.

RESULTS

The descriptions of the different parts of this research program have been presented earlier (23-26). The most important and conclusive results of the studies are synthesized in the following.

The Clinical Study

Injury Distribution and Severity (Table 1). The injuries were multiple in most of the accidents. Half of the injured had two or more fractures. Almost 90% sustained injuries to the lower extremities. In 7 cases (21%) both legs were injured. All head injuries were noted. Minor injuries (AIS = 1) were omitted in the other body regions.

Injuries Related to the Shape of the Car Front. In 33 accidents the injuries to the lower extremity were caused by a direct blow of the vehicle. One pedestrian sustained a knee cap fracture as a result of the fall on the ground after the collision. In another case the victim was overrun by the car after the collision which resulted in several severe injuries. In 28 cases the impact sequence could be reconstructed. In 23 of these the impact was caused by the centre of the car front and in 5 by the front corners.

In these frontal impacts, the bumper level and the bumper lead angle were used as test parameters for injuries in the different body regions. Thus, injuries caused by bumpers below the 40 cm level were compared to injuries caused by bumpers at or above the 40 cm level. In the same way injuries were compared for bumper lead angles below 70° and equal to or above 70°. The bumper level is defined as the "static bumper level," i.e., the distance between the ground to the midpoint of the bumper width when the car is not braking.

Fractures or ligament injuries to the lower extremities were noted in 30 accidents (88%). In 29 of these the injuries were caused by the impact of the car and in 28 accidents injuries were noted at or below the knee level. The bumper was the most important cause of these injuries. The bonnet edge caused injuries to the thigh and hip. Fractures of the femur diaphysis or the hip were noted in four accidents. In some accidents the bonnet edge may have contributed to the injuries to the knee joint.

Knee condylar fractures or knee ligament injuries were observed if the bumper impacted close to or at the knee level at lower speeds (< 30 km/h). The same type of injuries but more serious ones were seen at higher velocities at the same level of impact. Above 30 km/h very comminuted lower leg fractures also occurred. Impacts by bumpers mounted below 40 cm static level caused low tibia shaft fractures or ankle joint injuries.

Thirteen pedestrians (38%) sustained knee injuries. Seven of these (21%) were intraarticular fractures. If any of these were combined with ligament injuries was not noted in the medical records. In all 7 cases the lateral joint compartment was injured and 5 of these were fractures of the tibial condyle.

In 6 patients (18%) isolated knee ligament injuries were noted including avulsion fractures of the ligament attachments.

The mechanism of the leg injuries caused by the car impact were studied in 27 frontal collisions. The knee injuries (fractures and ligament injuries) related to the static bumper levels and the bumper lead angles are illustrated in Table 2.

Diaphyseal fractures of the tibia and the fibula were seen in 14 accidents (41%). Twelve of these were comminuted and dislocated and 4 were open. The tibia fractures were located 0-13 cm below the static bumper level of the involved car. Severe (AIS = 3) knee injuries were not observed with the bumper level below 40 cm.

Ankle joint injuries were noted in 6 patients (18%). Four of these were fractures. In one of them the fracture was combined with a lower leg fracture on the same side.

Healing Time of Leg Injuries. The healing time in 12 cases that survived with tibia shaft fractures were determined. The variation was 4-34 months. Half of the fractures healed within 8 months. In three of these the impact velocity was below 30 km/h. Fractures of the upper, middle and lower third of the tibia shaft had approximately the same healing time. There was no difference between the healing time of tibia shaft fractures caused

Table 1. Injuries in the different body regions.

Body region	Number of patients with injuries in this body region	Percent injured in this region	AIS-range
Head	20	59	1-5
Trunk incl. pelvis	13	38	2-4
Upper extremities	14	41	2-3
Lower extremities	30	88	2-3

Table 2. Knee injuries (fractures and ligament injuries), static bumper level and bumper lead angle.

Knee injury AIS	Static bumper level		Bumper lead angle	
	< 40 cm	≥ 40 cm	< 70°	≥ 70°
< 2	6	9	1	13
≥ 2	1	11	2	4
p(χ^2)	0.14		> 0.4	

by bumpers above or below 40 cm level. The healing time of the knee and ankle joint injuries were 2-7 months.

Walking Impairment. Four patients who died within one year from the accident as well as 3 patients with injuries only to the upper extremities were excluded from this part of the study. Twenty-two patients with leg injuries were re-examined 1-3 years after the accident when the fractures were healed. Of these 17 had leg injuries caused by car front impacts. The walking impairments of these patients were estimated in relation to their walking capacity before the accident. The following complaints were noted:

A Limited walking range
B Limited staircase climbing
C Limp at walking
D Use of walking aid (stick or crutches)
E Feeling of leg instability.

The patients were divided into two classes, those who complained of 0-2 impairments (I) and those who complained of 3 or more (II). The influence of the bumper level and the impact velocity on the walking impairment is illustrated in Table 3.

Fifteen patients had no complaints from their knee joints. Seven patients had walking impairment caused by knee injuries. In 6 of these the injuries were caused by bumpers at or above the 40 cm level above the ground.

Conclusions. Even if the material is small and the follow-up time is short the following conclusions could be made:

Old pedestrians were more severely injured than younger ones in car-pedestrian accidents.

The main cause of the long time of hospitalization were the leg injuries.

Knee injuries were caused by the bumpers as well as the bonnet edges.

Walking impairment seemed to be correlated to static bumper levels above 40 cm.

The long-term effect of leg injuries in car-pedestrian accidents was not well correlated to the primary injury severity or the impact speed. Further investigations of the long-term effect of leg injuries are needed.

The Experimental Studies

I. The Femur-Amputated Leg Model. During the first part of this project the experimental set up was checked for accuracy and repeatability and a preliminary comparison was made with the injuries seen in the real accidents. Thirty-six experiments were made with a primary leg model using human leg specimens amputated at the femur (24).

Table 3. Walking Impairment, Bumper Level and Impact Velocity.

Impairment Class	Bumper level		Impact velocity	
	< 40 cm	≥ 40 cm	< 30 km/h	≥ 30 km/h
I	4	4	5	3
II	1	8	3	6
$p(\chi^2)$	0.2		> 0.5	

Table 4. Bumper deformation values.

Bumper No.	Type	Impact width cm	Deformation mm	Force kN
A I	Semi-rigid SAAB 99	10	25	1.00
A II	Rigid SAAB 96	3	0	> 1.00
A III	Rigid SAAB 96 + 5 cm plastic foam layer	25	45	0.25

A 10 cm wide semi-rigid standard bumper (SAAB 99) was used in 16 experiments and a 3 cm wide rigid standard bumper (SAAB 96) was used in 17. The bumper lead distance was 15 cm. The bumper lead angle was 60 degrees. The bonnet height was 50 cm above the bumper level. A 5 cm layer of plastic foam covered the front. In three experiments one similar layer also covered the rigid bumper and two such layers were used on the front to reduce the bumper lead to zero. The static deformation characteristics of these front structures is presented in Table 4.

The test cart was accelerated to a constant speed before the collision. Its mass was approximately 300 kg. A low (16-17 km/h) or a moderate (23-24 km/h) impact velocity and a low (25 cm) or a high (45 cm) bumper level above the ground were chosen.

Injuries occurred in 31 experiments. In two experiments with legs from people 15 and 16 years of age epiphyseal fractures near the knee were obtained. Some other typical injuries were seen for example: undisplaced malleolar fractures or ankle ligament ruptures associated with a violent tilting of the ankle joint when the leg was hit by the bumper at the lower level and at the lower velocity, comminuted tibia and/or fibula fractures at the impact level when the leg was hit at the lower level and at the higher velocity, ligament ruptures of the knee joint opposite the impact side when the leg was hit at the higher level and at the lower or the higher speed, fractures of the tibial or femoral condyles when the leg was hit by the bumper at the higher level and at the higher velocity. No knee injuries occurred when the leg was hit at the lower level.

The type of injury was not clearly related to the age or sex of the specimens. In three tests in which the smooth and compliant front modification was used (A III) lower bumper forces were recorded, 0.7 kN in all three tests as compared to a mean value of 1.2 kN (0.9-1.7 kN) in the corresponding nine experiments with the two production bumpers. Even if the differences in body weights are taken

Table 5. AIS vs. velocity.

AIS	Velocity (km/h) 17	24	Total
≤2	7	6	13
=3	3	13	16
	10	19	29

$\chi^2 = 3.91$

into account this discrepancy remains. No obvious correlations were noted between the bumper forces, ground friction forces, the accelerations of the foot and leg recorded and the injury ratings in the other experiments, nor did the impact angle seem to matter.

Impact Level, Impact Speed, and Injury Severity. The injury ratings at the two velocities and bumper mounting levels used differed significantly in a X^2-test on the 5% level. This is shown in Tables 5 and 6 for the standard bumper types.

In all three experiments with the smooth and compliant front surface (A III) moderate injuries were noted: undisplaced malleolar fractures and in one case also a partial ligament injury of the knee. All these injuries were given the AIS rating of 2. The difference in AIS rating for this front modification as compared to the production bumpers was not statistically significant when comparing the lower bumper level but it was when comparing both bumper levels.

Conclusions. A bumper impacting at 45 cm level above the ground, which corresponds to the knee level in most adults, caused knee injuries. A bumper impacting at 25 cm level above the ground, which corresponds to the adult mid-tibia level, did not cause knee injuries. At this level the bumper, however, may cause injuries to the lower leg or the ankle joint.

A bumper impacting at the knee level caused severe leg injuries (AIS = 3) more often than a bumper impacting at the mid-tibia level.

The severity of the injuries caused by a rigid metal bumper and a semirigid plastic bumper did not differ significantly. However, by restricting the bumper lead and by making the impact area smooth and compliant the severity rating of the leg injuries was limited to AIS 2 when the impact area was centered to the mid-tibia level and the impact speed was below 25 km/h.

II. The Whole Leg Model. A modified leg model was used in the same type of impact tests between 20 and 30 km/h (25). The leg specimens then also included the hip joint and the lower part of the iliac bone. In most cases the specimens were placed vertically with the knee extended and loaded by a simulated body mass. In some cases the load was reduced to study the influence of the ground reaction forces.

Table 6. AIS vs. bumper level.

AIS	Bumper level (cm) 25	45	Total
≤2	9	4	13
=3	5	11	16
	14	15	29

$\chi^2 = 4.14$

The impact level was 42 or 23 cm above the ground plate, i.e., 2-3 cm below the impact levels used in the earlier tests. A 3 cm wide rigid metal bumper and a specially made 10 cm wide force-limiting bumper was used in these experiments (Fig. 2).

The force-limiting element of this bumper consists of an aluminium tube. This element was mounted between two wooden plates and a 2.5 cm thick polyurethane plastic foam layer covered the front plate. During impact the aluminium tube deformed plastically at a force of about 1 kN. The maximal deformation distance of the tube was 10 cm. The coefficient of restitution of the polyurethane foam layer is 0.4. The mass of the original metal bumper was three times higher than the deformable one. In order to study the influence of the bumper impact separately the bonnet structure was removed in some of the tests.

Nineteen leg specimens were used in 24 experiments. They originated from individuals 47-92 years of age. The influence of the bumper level, the bumper type, the bumper lead angle, and the bonnet edge height was studied.

Rigid Bumper at the 42 cm Level and a Prominent Bonnet Edge. The rigid bumper was used in 5 experiments at the 42 cm level. This corresponds to 6-9 cm below the knee joint. The bumper lead angle was 85 degrees, the bonnet edge height 71 cm, i.e., approximately at the mid-femur level and the impact velocity 20-28 km/h. The specimens were impacted at the anterolateral aspects. In all these cases severe knee injuries were noted. The body mass did not influence the type and severity of the injuries. The injury mechanisms with the bumper and the bonnet edge from one of the experiments in this set up are illustrated in Figure 3.

The probable injury sequence in this case was

1—A transverse fracture below the tibial condyle at

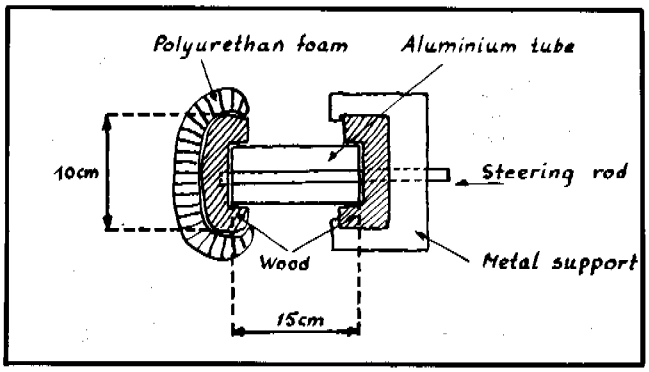

Figure 2. The force-limiting bumper.

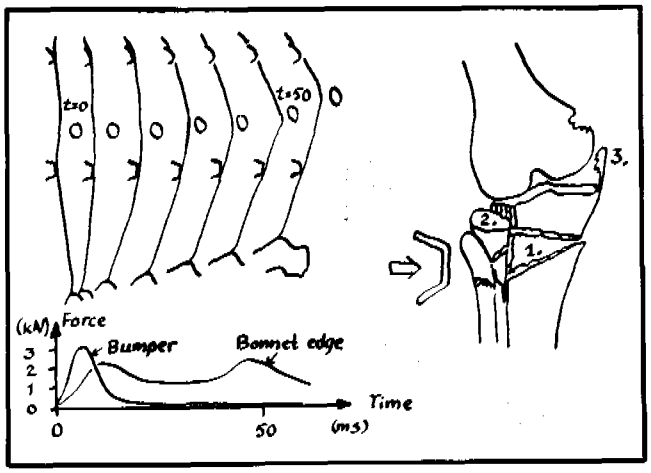

Figure 3. Kinematics and injuries in one of the experiments at 28 km/h with a 42 cm bumper level and a prominent bonnet edge.

the impact level caused by the rigid bumper at 5 ms.

2—A split and depression fracture of the lateral tibial plateau caused by the bumper and/or the bonnet edge at 10 ms

3—An avulsion of the femoral attachment of the medial collateral ligament caused by the bonnet edge at 45 ms.

The injuries 2 and 3 might have occurred in the opposite order but in that case the cruciate ligaments would have been more strained than was seen at the dissection.

Deformable Bumper at 42 cm Level Combined with Less Prominent Bonnet Edge. In 3 experiments the deformable bumper was used at 42 cm level. The bonnet edge height was the same as in the earlier experiments. The bumper lead angle was 60°/75°, i.e., 60 degrees with the tube intact and approximately 75 degrees with the tube compressed. The specimens were loaded with 26 or 45 kg simulated body weight. In these cases somewhat less severe knee injuries were noted compared to the experiments described above. However, the maximum AIS ratings were 3 in all these cases. The injuries in these cases were caused by the bumper but the bonnet edge contributed probably to the outcome.

Deformable Bumper at 23 cm Level Combined with Different Bumper Lead Angles and Bonnet Edge Heights. In 6 experiments the deformable bumper was used at the 23 cm level. The body mass was 45 kg. The bumper lead angle and the bonnet edge height varied. In 2 tests these parameters were 75°/90° and 71 cm, respectively. The knee injuries in these cases were severe (AIS = 3) and caused by the bonnet edge. In 2 other tests a lower bonnet edge (52 cm) and a smaller bumper lead angle (60°/75°) were used. In one of these severe knee injuries occurred. In the other a moderate knee injury was caused. The injury cause in these two cases was shown to be the bonnet edge. In 2 tests the bumper lead angle was 45°/50° and

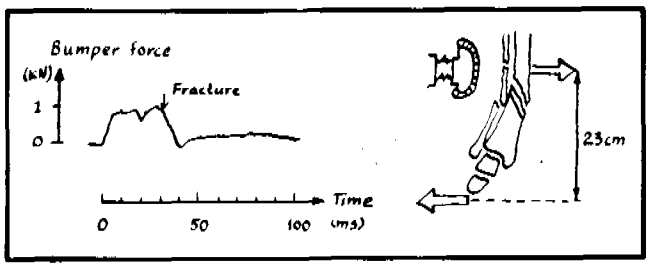

Figure 4. Bumper force and injury in a test with a deformable bumper and a fully loaded leg.

the bumper height 82 cm. No injuries were noted in these cases.

Deformable Bumper at the 23 cm Level and no Bonnet. In 4 experiments the deformable bumper was mounted at 23 cm and the simulated bonnet was removed. The body mass was 71 kg but in one test the load on the platform was reduced to 0.45 kN by lifting the leg. In two of the tests with full load similar types of lower leg fractures were seen. In one other test an undisplaced fracture of the medial malleolus was noted. In the other there was no injury at all. The force-limiting effect of this bumper and the lower leg fracture type is illustrated in Figure 4.

Injuries AIS Related to Bumper Level, Bumper Lead Angle and Bumper Type. For anterolateral impacts the influence of the bumper level, the bumper lead angle and bumper types are illustrated in Table 7.

In three experiments the AIS = 3 injuries were located to the knee joint. They were caused by the bonnet edge and not by the bumper as could been seen on the films. These cases were omitted in this analysis. The 23 cm bumper level caused less severe injuries than the 42 cm level. A deformable bumper and a bumper lead angle below 60°/75° also seemed to cause less severe injuries.

Injuries Related to the Bonnet Edge. The bonnet edge impacted the femur at different levels. The impact tolerance of the femur is greater than that of the lower leg. The highest bonnet edge forces, 4.0 – 7.3 kN, were noted for bonnet edge heights of 71 and 82 cm. Still no injury occurred to the hip or to the femur diaphysis in these tests. In 2 experiments knee injuries were caused during the later part of the impact by the prominent bonnet edge. No injuries were noted with a bumper level of 23 cm and a bumper lead angle of 45°/50°.

Leg Rotation after Impact. The angular velocity of the specimen at 200 ms after impact and the maximal rotation angle were analysed for different bumper levels and bonnet heights. The maximal leg rotation angle caused by the deformable bumper and bonnet edge was compared for the 23 and 42 cm bumper levels. It was greater at the higher bumper level but the difference was not statistically significant. The influence of the bonnet edge height and the bumper lead angle on the leg rotation could not be clearly assessed.

Table 7. Leg injury severity related to bumper level, bumper lead angle, and bumper type.

Injuries max AIS	Bumper level (cm) 23	42	Bumper lead angle (degrees) <60/75	≥60/75	Bumper type Deformable	Rigid
2	3	1	4	2	6	0
3	2	10	2	10	7	5
$P(\chi^2)$	<0.05		<0.15		<0.20	

Conclusions. This improved biological leg model system was found to be able to simulate the kinematics and disclose the injury mechanisms of the lower extremity impacted by a vehicle front in real car-pedestrian accidents.

Fractures of the femur diaphysis and the hip joint were unusual below 30 km/h impact velocity.

High ground friction increased the fracture risk during the simulated stance phase of walking when the leg was impacted at lower bumper levels. The fracture tolerance limit may be below 1 kN in these cases.

A bumper located at or just below the knee level and a prominent bonnet edge were both correlated with increased risk of knee injuries.

A force limiting and energy-absorbing bumper impacting at the lower half of the tibia and a bumper lead angle below 60 degrees reduced the risk of knee injuries.

Lowering of the impact level from 42 to 23 cm reduced the severity of the leg injuries and did not increase the leg rotation after impact.

III. The Mechanical Leg Model. A mechanical model of the adult human leg and knee was constructed (Figs. 5a and b). The description of this model and of the results from the tests with the model has been published earlier (25). The following is a summary of those results.

The following bumper types were used:

B I Metal bumper; no padding; 3 cm impact width

B II Metal bumper; 5 cm polyurethane padding; 5 cm impact width

B III Metal bumper; 10 cm polyurethane padding; 5 cm impact width

The mean bumper forces for different impact levels and paddings at 12 km/h are illustrated in Figure 6.

The peak "ligament" forces for pure bending and for varying impact levels and paddings at 12 km/h are illustrated in Figure 7.

The knee distortion angles for varying impact levels and paddings are illustrated in Figure 8.

The leg angular velocities after impact for various impact levels and paddings at 12 km/h are shown in Figure 9.

Conclusions. The direct impact forces caused by the bumper-leg contact had a maximum when the impact was made near the center of gravity of the lower leg.

The knee reaction forces had a minimum when the impact occurred near the center of gravity of the lower leg.

The knee ligament forces had a maximum for impacts at the knee level.

A padding on a rigid bumper reduced the direct impact bumper force but not the bending forces in the knee.

DISCUSSION

Injury Mechanisms and Clinical Relevance

Impacts on the lower extremity may cause injuries to the ankle joint, the lower leg, the knee, the thigh or the hip. Judging the injury potential of a car front one has to take into account the vulnerability of the impacted parts of the human body as well as the outcome of different types of injuries. Most fractures of the diaphyseal parts of the femur and lower leg heal without permanent impairment although in some cases delayed union and pseudarthrosis occur.

Intraarticular fractures or juxtaarticular fractures or ligament injuries interfering with the joint function should be prevented especially in the knee as these injuries are more difficult to treat and may lead to impaired joint function and osteoarthroses.

The injury mechanisms in real accidents are difficult to determine. In many cases similar injuries were produced in the experiments and a combined analysis of the results from these parts has made it possible to evaluate the injury potential of different car front geometries.

Ankle Joint. Malleolar fractures and ligament injuries of the ankle joint are usually caused by bumper impacts

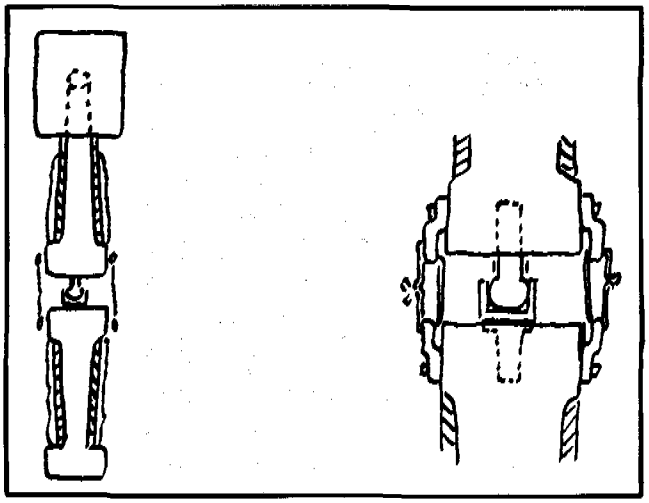

Figure 5a. The whole leg. Figure 5b. The knee joint

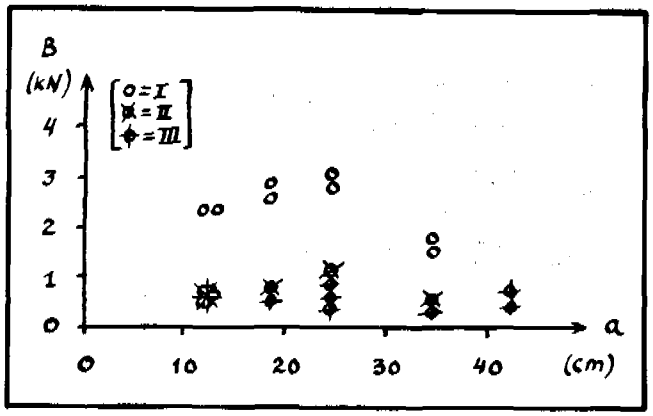

Figure 6. Mean bumper forces B for different impact levels a and paddings at 12 km/h.

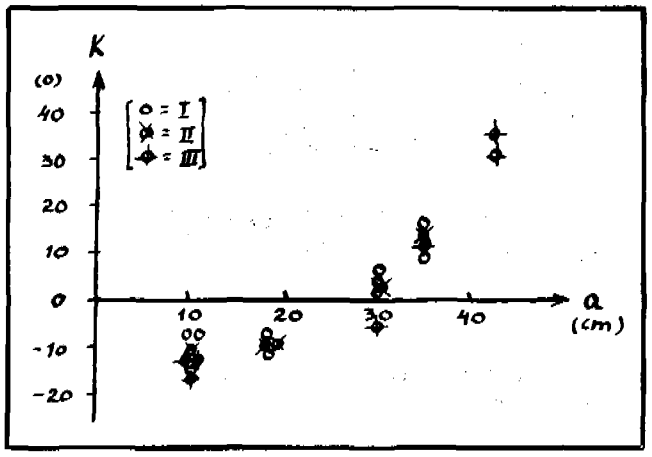

Figure 8. The knee distortion angles K for varying impact levels a and paddings at 12 km/h.

at mid-tibia level. The injury mechanisms are probably a combined action of the shearing force of the distal part of the tibia and the inertia force of the accelerating foot. The severity of these injuries in the experimental investigations were all moderate (AIS = 2) and the fractures should be easily stabilized with a lower leg cast in most real cases.

Lower Leg. The lower leg injuries mostly caused by bumper impacts are soft tissue injuries and fractures at the impact level. A rigid and narrow impact surface concentrates the blow on the leg to a shorter time and a smaller area and what could be called a "high impact speed" fracture may occur. The skin and muscular injuries adjacent to a lower leg fracture are significant and the healing time is longer for this type of injury compared to a "low impact speed" fracture (27). The results obtained in the first experimental study indicated 15 km/h as a lower speed limit below which serious injuries (AIS = 3) would not occur if the bumper impacted at mid-tibia level. The lowest speed for avoiding severe injuries at other impact levels could not be assessed.

Knee. Knee injuries are usually caused by the bumper and sometimes by a prominent bonnet edge. They are seen even at low velocities (< 15 km/h) if the bumper impacts near the knee level. Knee injuries are caused by direct or indirect forces. Hypothetically the impact reaction forces will increase with increased ground friction. This could not be verified with the bumper impacting near the knee level. In this case there was a bending of the leg around the bumper. Although the body mass loaded the leg the impact velocity was high enough to lift the foot from the ground very early in the impact sequence. The conclusion is that the ground friction could have little influence upon the occurrence of injuries compared to the inertia of the leg if the leg is hit at the knee level at above 15 km/h impact speed.

A lower bending stiffness of the leg in the impact direction at the knee level will reduce the bumper impact force and the knee shear force. If the extended leg is hit from the anterior side not far below the knee level the posterior capsule and the posterior cruciate ligament of the knee are most heavily loaded (28). If the lower leg is

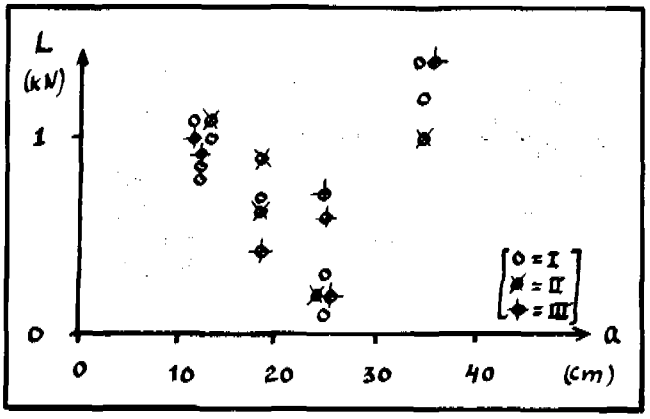

Figure 7. Peak knee ligament forces L for varying impact levels a and paddings at 12 km/h.

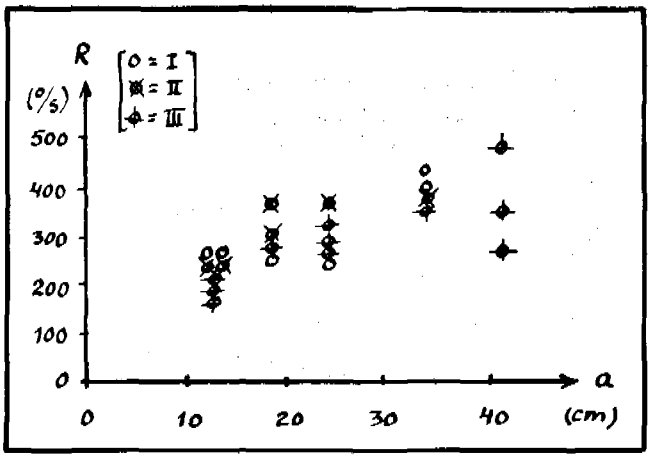

Figure 9. Leg angular velocities R after impact for varying impact levels a and paddings at 12 km/h.

hit in the opposite direction the anterior cruciate ligament is maximally strained. For intermediate impact directions mixed ligamentous and menisceal injuries are possible (28).

The knee joint surface compression force also depends on the parameters mentioned above. A flexed knee seems to be more vulnerable to compression forces as compared to an extended knee according to a biomechanical study by Hirsch and Sullivan (30). Blow fractures of the tibial or femoral condyles combined with injuries in the knee joint caused by bending, shearing and compressive forces are severe as they may lead to permanent instability and osteoarthrosis.

Thigh and Hip. Injuries to the thigh and hip were noted in 4 cases (12%) in the clinical study but not in the experimental one. Fractures of the proximal part of the femur and hip are frequently caused by a fall to the ground in adults. The injury mechanisms may be different in car-pedestrian accidents. The impact velocity must probably exceed 30 km/h for these injuries to occur.

Ground Friction. The ground friction force is important at low impact speeds. Severe ligament ruptures or condyle compression fractures can easily be produced even near zero impact velocities if the force is applicated at the knee level and the foot is pressed against the ground. The friction force may also be important if the impact occurs at mid-tibia level due to the smaller distance between the impact and friction force in this case and to the higher bending stiffness of the leg at this level.

Theoretical Analysis

A theoretical analysis has been made of the bumper-leg impact sequence (31). In this analysis a compound pendulum model was used. The mass and dimensions of this pendulum correspond to an adult human leg. The model was based on the results from the earlier experiments on human leg specimens. The relative values of the mean bumper force at the impact point and the ligament force in the knee joint and the sum of these forces calculated on the basis of this model are illustrated in Figure 10.

The knee reaction forces can be considered as a combination of a shear force component and a bending force couple consisting of a ligament tension force and a joint surface compression force. An axial rotation force and an axial tensile force of the ligaments can also appear as a result of the impact. The total ligament force approximately equals the bending force plus the axial tensile and rotational forces. The axial tensile force will lower the surface compression force.

This theoretical analysis indicates the possibility of minimizing the reaction forces in certain parts of the lower extremity during lateral impacts by choosing suitable impact level. The bending force at the knee joint level of this model has a well-defined minimum when the impact

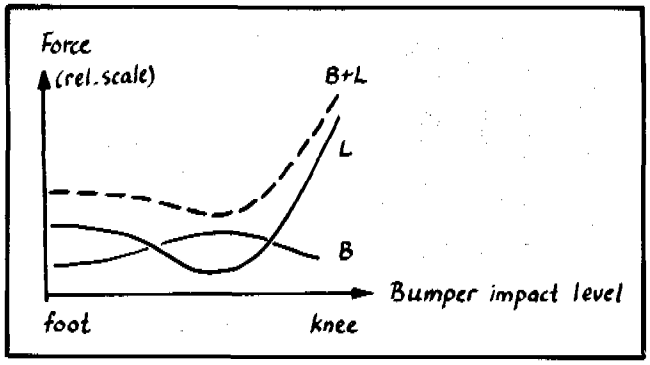

Figure 10. Relative values of the mean bumper force B, the mean ligament force L and the sum of these forces for various impact levels.

occurs near the center of gravity of the lower leg. On the other hand the direct impact force would be higher at this level than at the knee joint level. The sum of the direct impact force and the knee reaction forces probably has a minimum value somewhere between the mid-tibia and the knee joint level. This minimum will be just above the center of gravity of the lower leg.

Proposals for Injury Mitigation in Car-Pedestrian Accidents

The bumper and the bonnet edge are both correlated with severe injuries to the lower extremity in adults as has been shown in these studies. The car front design should be determined by protection criteria against serious injuries at the time of accident as well as against injuries causing permanent impairment. A static bumper level above 40 cm and a bumper lead angle greater than 60 degrees should be avoided. An optimal impact level between 25 and 30 cm for minimal knee and lower leg injuries was suggested in the theoretical analysis of leg impacts and has been shown to lower the risk for severe injuries in the lower extremity compared to a bumper impacting at the knee level. The static bumper level was 0 — 13 cm above the fracture centres in the clinical study. Thus, the optimal static bumper level should be 35 cm for adult pedestrians. This is in good agreement with Stürtz (18).

The impact force can be sufficiently reduced by incorporating deformable material in the impact area. However, this does not significantly lower the risk for knee injuries if the impact is at the knee level. Besides, a higher angular velocity of the body rotation after the primary impact may follow as well, if the elasticity of the impact area is high. An increased risk for head injuries has been feared if the bumper level is lowered (22). However, in the mechanical leg model study an increased leg rotational velocity has not been verified for the 34 cm impact level compared to the 42 cm level. Quite the contrary at impact

levels below 34 cm the angular velocity of the leg seems to diminish. This was also noted in the other test series. A lower bumper level was not correlated with a higher incidence of head impacts in the clinical study either. The body rotation after the primary impact to the car front is probably not governed by the bumper level as much as by the bumper lead distance and the bonnet edge height. Further investigations are needed to answer these questions. There is also a high risk of head and trunk injuries in children impacted by the bonnet edge and thus this parameter should not primarily be evaluated out of leg injury protection criteria in adults only.

Based on the results in these investigations and on the studies presented by Ashton and Mackay (32) and by Pritz (33) the principles for injury mitigating in car-pedestrian accidents are illustrated in Figure 11.

In the model a "pedestrian bumper" with a smooth and soft impact area is mounted on a force-limiting element which can deform plastically below 1 kN. The bonnet edge is not prominent and made deformable for loads below the injury tolerance limit of the body parts impacted by this element, that is the femur and pelvis of adults and the head and trunk of children.

SUMMARY AND FINAL CONCLUSIONS

The results from these clinical and experimental studies are in good accordance with each other. The number of cases in the clinical study is small but the conclusions should be quite reliable as they are not contradicted by any results in the experimental parts.

Based on these studies the following conclusions and recommendations are made:

1) Old pedestrians are more severely hurt than younger ones in car-pedestrian accidents.
2) Leg injuries are the main cause of the long time of hospitalization for adults in car-pedestrian accidents.
3) Fractures of the femur diaphysis or the hip joint are unusual below 30 km/h impact velocity.
4) The bumper is the main cause of injuries to the ankle joint, the lower leg, and the knee in adult pedestrians.
5) Also a prominent bonnet edge may cause knee injuries.
6) A bumper impact at or just below the knee level is correlated with a high risk of serious knee injuries.
7) High ground friction increase the fracture risk during the stance phase of walking if the leg is impacted at lower levels. The fracture tolerance limit may be below 1 kN in these cases.
8) A force-limiting and energy-absorbing bumper impacting at the lower half of the tibia and a bumper lead angle below 60 degrees will reduce the injury severity of the lower extremity in car-pedestrian accidents.
9) Lowering the static bumper level from 45 cm to 35 cm above the ground will reduce the severity of the leg injuries in adults in car-pedestrian accidents.
10) The biomechanical leg model system which has been developed and used in this research program can simulate the kinematics and disclose the injury mechanisms of the bumper and bonnet edge impacts on the lower extremity in car-pedestrian accidents. The equipment can be used as an instrument for rating car front aggressiveness in this type of accidents.

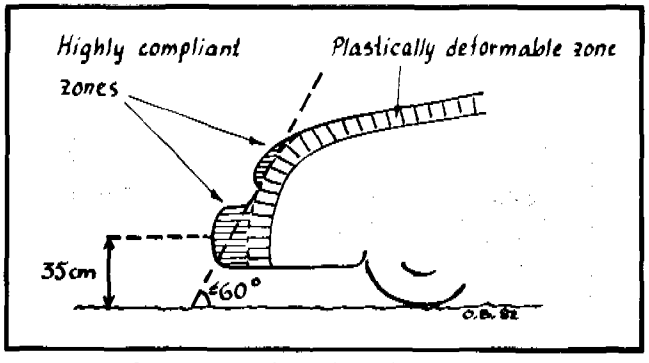

Figure 11. Pedestrian adapted car front.

REFERENCES

1. Fisher, A. J., Hall, R. (1972): The influence of car frontal design on pedestrian accident trauma. Accid. Anal & Prev 4: 47-58.
2. McLean, A. J. (1972): Car shape and pedestrian injury. Proc of the National Road Safety Symposium. Canberra, March 1972.
3. Kramer, M., Burow, K., Heger, A. (1973): Fracture mechanism of lower legs under impact load. Proc of the 17th Stapp Car Crash Conference, Oklahoma, November 1973, pp 81-100.
4. Schneider, H., Beier, G. (1974): Experiment and accident: Comparison of Dummy Test Results and Real Pedestrian Accidents. Proc of the 18th Stapp Car Crash Conf. Ann Arbor, December 1974. pp 26-29.
5. Appel, H., Stürtz, G., Gotzen, L. (1975): Influence of impact speed and vehicle parameter on injuries of children and adults in pedestrian accidents. Proc of the 2nd IRCOBI Conference on the Biomechanics of Serious Trauma, Birmingham, September 1975. pp 83-100.
6. Ashton, S. J., Pedder, J. B., Mackay, G. M. (1976): A review of riders and pedestrians in traffic collisions. Proc of the IRCOBI-meeting on Biomechanics of Injury to Pedestrians, Cyclists and Motorcyclists. Amsterdam, September 1976. pp 129-162.
7. Bacon, D. G. C., Wilson, M. R. (1976): Bumper characteristics for improved pedestrian safety. Proc of the 20th Stapp Car Crash Conf., Michigan, October 1976. pp 389-428.

8. Krieger, K. W., Padgaonkar, A. J., King, A. I. (1976): Full scale experimental simulation of pedestrian-vehicle impacts. Proc of the 20th Stapp Car Crash Conf., Michigan, October 1976. pp 429-464.
9. Kramer, M. (1977): Bestimmungen der äquivalenten Verletzungsschwere in experimentellen Fussgänger-Fahrzeug-Unfällen. Vortschrittberichte der VDI Zeitschriften, Reihe 17, Nr 3, Mai 1977.
10. Weiss, Jr., E., Pritz, H. B., Hassler, C. R. (1977): Experimental automobile-pedestrian injuries. The Journal of Trauma. Vol 17, No 11, 1977. pp 823-828.
11. Padgaonkar, A. J., Krieger, K. W., King, A. I. (1977): A three-dimensional mathematical simulation of pedestrian-vehicle impact with experimental verification. J of Biomechanical Engineering, May 1977.
12. Twigg, D. W., Tocher, J. L., Eppinger, R. H. (1977): Optimal design of automobiles for pedestrian protection. Society of Automotive Engineers, 770094.
13. Ashton, S. J., Pedder, J. B., Mackay, G. M. (1977): Pedestrian leg injuries, the bumper and other front structures. Proc of the 1977 IRCOBI Conference on Impact Trauma, Berlin, Sept., 1977, pp 33-51.
14. Kühnel, A., Rau, H. (1978): The fidelity of dummies in pedestrian collisions. Proc of the 3rd IRCOBI meeting on the Simulation and Reconstruction of Impacts in Collisions. Lyon, September 1978. pp 183-194.
15. Lucchini, E., Weissner, R. (1978): Influence of bumper adjustment on the kinematics of an impacted pedestrian. Proc of the 3rd IRCOBI meeting on the Simulation and Reconstruction of Impacts in Collisions. Lyon, September 1978. pp 172-182.
16. Gotzen, L., Flory, P. J., Otte, D. (1980): Der Fussgängerunfall-Seine Verletzungssituation und Kollisionsmechanik. Unfallheilkunde Vol 83, pp 306-314.
17. Langwieder, K., Danner, M., Wachter, W., Hummel, Th. (1980): Patterns of multi-traumatisation in pedestrian accidents in relation to injury combination and car shape. Eighth International Technical Conference on Experimental Safety Vehicles (ESV), Wolfsburg, October 1980.
18. Stürtz, G. (1981): Das Kind in Verkehrsunfall: Biomechanik, Anforderungen an die äussere und innere Sicherheit von Kraftwagen. VDI-Verlag, Düsseldorf.
19. Weinreich, M. (1979): Der Verkehrsunfall des Fussgängers. Unfallheilkunde Vol 135.
20. Gissane, W., Bull, J., Roberts, B. (1970): Sequele of road injuries. Injury Vol 1, No 3, pp 195-203.
21. Baker, S. P., O'Neill, B., Haddon, W., Long, W. B. (1974): The injury severity score: A method for describing patients with multiple injuries and evaluating emergency care. The Journal of Trauma Vol 14, No 3. pp 187-196.
22. Lestrelin, D., Brun-Cassan, F., Fayon, A., Tarrière, C., Castan, F. (1980): "Prakimod": Mathematical simulation of accident victims. Validation and application to car-pedestrian collisions. Presented at the 8th ESV-Conference, Wolfsburg, October 1980.
23. Bunketorp, O., Romanus, B. (1981): Clinical studies on leg injuries in car-pedestrian accidents. Proc of the 1981 IRCOBI Conference on the Biomechanics of Impacts, Salon de Provence, September 1981. pp 235-242.
24. Aldman, B., Lundell, B., Thorngren, L., Bunketorp, O., Romanus, B. (1979): Physical simulation of human leg-bumper impacts. Proc of the 1979 IRCOBI Conference on the Biomechanics of Trauma, Göteborg September 1979, pp 232-242.
25. Aldman, B., Thorngren, L., Bunketorp, O., Romanus, B. (1980): An Experimental Model for the Study of Lower Leg and Knee Injuries in Car-Pedestrian Accidents. Proc of the 1980 IRCOBI Conference on the Biomechanics of Impacts, Birmingham, September 1980. pp 180-193.
26. Bunketorp, O., Aldman, B., Jonson, R., Romanus, B., Roos, B., Thorngren, L. (1981): Experimental studies on leg injuries in car-pedestrian accidents. Proc of the 1981 IRCOBI Conference, Salon de Provence, September 1981. pp 243-255.
27. Bauer, G. C. H., Edwards, P. (1965): Fractures of the shaft of the tibia. Acta Orthopaedica Scandinavica 36, 1965. pp 95-103.
28. Kennedy, J. C., Grainger, R. W., (1967): The posterior cruciate ligament. The Journal of Trauma, Vol 7, No 3. pp 367-377.
29. Kennedy, J. C., Weinberg, H. W., Wilson, A. S. (1974): The anatomy and function of the anterior cruciate ligament. The Journal of Bone and Joint Surgery. Vol 56-A, No 2, March 1974.
30. Hirsch, G., Sullivan, L. (1965): Experimental knee joint fractures. Acta Orthopaedica Scandinavica 36, 1965. pp 391-399.
31. Bunketorp, O. (1979): Theoretical studies on leg injuries in car-pedestrian accidents. (Unpublished)
32. Ashton, S. J., Mackay, G. M. (1979): Car design for pedestrian injury minimization. 7th Int Techn Conference on Experimental Safety Vehicle, Paris, June 1979. pp 630-640.
33. Pritz, H. B. (1979): Vehicle design for pedestrian protection. 7th Int Technical Conf on Experimental Safety Vehicles. Paris, June 5-8, 1979.

ACKNOWLEDGEMENTS

The clinical studies of this project have been supported by grants by